NASA-CR-173083

SEVENTH SEMIANNUAL STATUS REPORT
VOLUME II - APPENDIX A

1 April 1981 - 30 September 1981

ENERGY EFFICIENT ENGINE
COMPONENT DEVELOPMENT AND INTEGRATION PROGRAM

30 October 1981

Contract NAS3-20646

Prepared for

NATIONAL AERONAUTICS AND SPACE ADMINISTRATION
Lewis Research Center
Cleveland, Ohio

PWA-5594-179

UNITED TECHNOLOGIES
PRATT&WHITNEY
AIRCRAFT

Commercial Products Division
400 Main St.
East Hartford, Connecticut 06108

ER-8050-F

ENERGY EFFICIENT ENGINE HOLLOW FAN BLADES

D. J. Moracz
C. R. Cook

FINAL TECHNICAL REPORT

July 15, 1981

For:

United Technologies Corporation
Pratt & Whitney Aircraft Group
Commercial Products Division
East Hartford, Connecticut

TRW Materials Technology
TRW Inc.
23555 Euclid Avenue
Cleveland, Ohio 44117

FOREWORD

This final technical report covers the work performed under United Technologies Purchase Order 20646-9 for the period November 1, 1978 through June 30, 1981.

This contract with TRW Inc., Cleveland, Ohio is being monitored and coordinated with Pratt & Whitney Aircraft Group by Mr. C. J. Michael of P&WA Commercial Products Division. At TRW this program is the responsibility of Mr. C. R. Cook who reports to Dr. I. J. Toth, Manager of Materials Development. Mr. D. J. Moracz is the principal investigator. Contributors in the early tasks of this effort include Dr. I. A. Martorell, Mr. G. Friedman, Mr. J. M. Marder and Mr. J. N. Fleck. Dr. J. L. Frater and Dr. B. L. Ferguson assisted in areas of ply development and manufacture respectively. Mr. R. D. Pryatel was responsible for the computer aided design activities in M.I.S. for the die, core and ply definitions. The assistance of Messrs, F. N. Lake, F. J. Hlad, J. F. Ivancic, and E. J. Stachura in the area of die design and die finishing is acknowledged. Others making significant contributions to the program are Messrs. E. Thomas, R. L. Nussel, J. B. Bell, J. W. Sweeney, and R. R. Ebert.

This program is being conducted under internal Project No. 512-004098-88. This report has been assigned internal number ER-8050-F.

TRW Publication Review

Approved by: _____
I. J. Toth
Materials Development Dept.

Table of Contents

		Page No.
I	INTRODUCTION	1
II	PROGRAM PLAN	2
	A. Task I - Critical Experiments	2
	1. Elements of Processing	2
	2. Specimen Fabrication	2
	B. Task II - Blade Process Development	2
	1. Tooling	2
	2. Process Development	3
	3. Prototype Blade	3
III	EXPERIMENTAL PROGRAM	4
	A. Program Material	4
	1. Titanium Alloy Sheet Materials - Plies	4
	2. Core Materials	4
	3. Canning Materials	4
	B. Task I - Critical Experiments	6
	1. Diamond Specimen Ply Definition	6
	2. Diamond Specimen Core Design	13
	3. Can Design and Fabrication	13
	4. Diamond Specimen Fabrication	17
	5. Machining of Diamond Specimens	33
	C. Task II - Blade Process Development	33
	1. Tooling	33
	2. Ply Design and Manufacture for Hollow Fan Blade	42
	3. Core Design and Manufacture for Hollow Fan Blades	45
	4. HIP Cans for Hollow Fan Blades	48
	5. Fabrication of Hollow Fan Blades	48
	6. Post-HIP Processing of Hollow Fan Blades	57
IV	RESULTS AND DISCUSSION	65

Table of Contents (continued)

		Page No.
A.	Task I - Critical Experiments	65
1.	Diamond Specimen Fabrication	65
2.	Machining of Diamond Specimens	115
B.	Task III - Blade Process Development	115
1.	Hollow Blade Fabrication	115
2.	Post-HIP Processing of Hollow Fan Blades	127
V	CONCLUSIONS AND RECOMMENDATIONS	157
VI	REFERENCES	160
	APPENDIX A - PLY DESIGN	161
	APPENDIX B - TEXTURE	186

LIST OF TABLES

Table		Page No.
I	Typical Core Material Chemistry	4
II	Summary of Diamond Specimen Fabrication Parameters	8
III	Processing Procedures for Hollow Fan Blades	62
IV	Summary Evaluation of Ten Diamond Specimens	114
V	Dimensional Measurements of Canned Blades	126
VI	Pitch Thickness Measurements of Blade 4	135
VII	Pitch Thickness Measurements of Blade 6	136
VIII	Pitch Thickness Measurements of Blade 9	137
IX	Dimensional Analyses of Blade 7 and 8	138
X	Core Length Changes for Blades 7 and 8	143
XI	Wall Thickness Measurements for Section AG-AG - Blade 4	146

LIST OF FIGURES

Figure		Page
1.	Typical Microstructures for Ti 6Al-4V Sheet Material Purchased for Tasks I and II.	5
2.	TRW Test Specimen Design	7
3.	Outermost Titanium Laminates for Hollow Diamond Specimen	10
4.	Innermost Titanium Laminates for Hollow Diamond Specimens	11
5.	Miscellaneous Hollow Diamond Specimen Laminates Used to Fill in Void at Ply Endings	12
6.	Steel Cores to be Used to Produce Cavity in Hollow Diamond Blade Specimen	14
7.	Typical 0.062-Inch Radius Cores Showing Differences in End Detail	15
8.	Steel Can Half Made by Pressing a Flat 0.060-Inch Thick Low Carbon Steel Sheet Into a Die Using a Pad of Rubber	16
9.	Solid Diamond Specimen (DS1) Before Hot Isostatic Pressing	18
10.	Sketch of Hole Detail for Ultrasonic Test Standard	19
11.	Stainless Steel Fixture Used to Hold the Diamond Specimens During Ultrasonic Nondestructive Evaluation	20
12.	Steel-Titanium Fitted Insert Used in Specimen DS3	22
13.	An Example of a Diamond Can Half Sprayed With Graphite	23
14.	Core Plies	26
15.	Fourteen Plies Required for Diamond Cover Per Half	27
16.	Twenty-Two Plies Required for Root Per Half. Shown Unassembled and Assembled	28
17.	X-Ray of Core Location in DS 14	31
18.	Sketch of P&WA's Hollow Fan Blade Design for Energy Efficient Engine Program.	34

LIST OF FIGURES (cont'd)

Figure		Page
19.	Wood Patterns Used to Produce IN-100 Isothermal Forging Dies	36
20.	IN-100 Isothermal Forging Die Castings	37
21.	IN-100 Isothermal Forging Tooling	38
22.	Camber Tooling	40
23.	Schematic Illustration of Camber Tooling	41
24.	Twist Tooling	43
25.	Blade Inspection Fixture and Templates	44
26.	Example of Ply Generation by Computer for Section A-A	46
27.	NC Machined 1045 Steel Cores for Hollow Fan Blade	47
28.	Airfoil-Root Assembly Configuration	49
29.	Hand Cut Titanium Alloy Plies Used in First HIP Blade Iteration	52
30.	One-Half of a Typical Hollow Blade Assembly (15 Plies)	54
31.	Surface Condition of Canning Sheet Welded to Root Block	56
32.	Camber Tooling Shown Installed in 1500 Ton Hydraulic Press	58
33.	Twist Tooling Shown Installed in Ajax Crank Press Twister. Root and Center Section Dies Shown	60
34.	Isothermal Forge Tooling Shown Installed in 2500 Ton Hydraulic Press	61
35.	Solid Diamond Specimen (DS1) After Hot Isostatic Pressing	66
36.	Ultrasonic Through-Transmission C-Scan of Both Halves of Specimen DS1	67
37.	Microstructure of a Portion of Section AA of Specimen DS1	68
38.	Microstructure of a Portion of Section BB of Specimen DS1	69

LIST OF FIGURES (cont'd)

Figure		Page
39.	Microstructure of a Portion of Section CC of Specimen DS1	69
40.	Microstructure of a Portion of Section DD of Specimen DS1	70
41.	Ultrasonic Test Standard Prepared From DS1 Material	71
42.	Ultrasonic C-Scan of Test Standard for Two Different Sensitivity Levels	72
43.	X-Ray of DS2	74
44.	Ultrasonic C-Scan of Diamond Specimen Two	75
45.	Typical Microstructures in DS2 at Several Areas	76
46.	Ultrasonic Through-Transmission C-Scan for Specimen DS3	77
47.	Representative Microstructures of Sections AA, BB and CC of Specimen DS3	78
48.	Surface Condition of Titanium After HIP Using Can Surface Treatment or Interfaces as Noted	80
49.	Interface Between Valve Steel Core (TRW VMS-478) and the Titanium Laminates	81
50.	Macro of Trailing Edge Definition for 0.015-Inch Radius Core	82
51.	Typical Microstructure and Bond Line for DS 4	83
52.	Typical As-HIP Microstructure in DS3 Given a Heavy Etch to Delineate Bond Lines	85
53.	Typical Microstructures After Heat Treatment at 1750°F	86
54.	Edge View of Sectioned Core That Was Twisted	87
55.	Diamond Specimen 7 After HIP	88
56.	Step Root in Diamond Specimen 7	89
57.	Typical Microstructure in DS 7 at Several Areas.	91

LIST OF FIGURES (cont'd)

Figure		Page
58.	Diamond Specimen 8 After HIP	92
59.	Diamond Specimen 9 After HIP	93
60.	Diamond Specimen 10 After HIP	94
61.	Ultrasonic C-Scan of Diamond Specimen 8	95
62.	Ultrasonic C-Scan of Diamond Specimen 10	96
63.	Microstructure in DS 8 at Several Areas	97
64.	Microstructures in DS 8 at Several Areas	98
65.	Typical Microstructure in DS 9 at Several Areas	99
66.	Typical Microstructures in DS10 at Several Areas	100
67.	Temperature-Pressure Cycle Used for HIP	101
68.	X-Ray of DS 13 After HIP	103
69.	X-Ray of DS 15 After HIP	104
70.	Ultrasonic C-Scan of Diamond Specimen 15	105
71.	X-Ray of DS 25 After HIP	106
72.	Ultrasonic C-Scan of DS 25	107
73.	Typical Microstructure Along Edge in DS 25	108
74.	SEM Photomicrographs Depicting What Appears to be Preferential Etching at Bond Lines in DS 25	110
75.	SEM Photomicrographs Illustrating That the Preferential Etching Leaves Voids in DS 25	111
76.	X-Ray of DS 24 After HIP, Machining and Core Leaching	112
77.	Ultrasonic C-Scan of DS 24	113

LIST OF FIGURES (cont'd)

Figure		Page
78.	Six Machined and Core Leached Diamond Specimens	116
79.	First iteration Blades After HIP	117
80.	Closeup of Root End of HIP Blade Illustrating Location of Weld Failures	118
81.	As-HIP Blade 3	119
82.	Typical Microstructure and Bonding Conditions Found in Blade 3	121
83.	AS-HIP Blade 4	122
84.	AS-HIP Blade 5	123
85.	X-Ray of Tip Area of Blade 4	124
86.	Blades 6 Through 9 Shown After HIP	125
87.	Blade 2 After Cambering	128
88.	Shear Area as a Result of Cambering for Blade 4	129
89.	Blades 6 Through 9 After Cambering	130
90.	Blades 6 Through 9 After Twisting on Ajax Crankpress Twister	131
91.(a)	Blades 6 Through 9 Are Shown After Isothermal Forging	133
91.(b)	Blades 7 and 8 Are Shown After Isothermal Forging	134
92.	Blade 9 Shown Immediately After Removal From Isothermal Forging Die	138
93.	Tip Section of Blade 7 After Isothermal Forging Showing Lack of Contact During Forging in This Area as Indicated by Ply Endings Present on Surface	140
94.	X-Ray Showing Lateral Core Movement Due to Isothermal Forging	141
95.	Section AM-AM of Blade 4	144
96.	Section AG-AG of Blade 4	145

LIST OF FIGURES (cont'd)

Figure		Page
97.	Section AF-AF of Blade 4 With Core Removed and Typical Internal Wall Surface Condition	147
98.	Typical Longitudinal Sections From Blade 6	148
99.	Photomacrographs and Photomicrographs Illustrating Various Surface Conditions at the Core Edges for Blade 4	149
100.	Microstructure Observed for Blade 4	153
101.	Racetrack Holes in Blade Tip	155
102.	Blades 7, 8 and 9 After Finish Machining and Core Leaching	156
103.	Ply Designs	163

1 INTRODUCTION

The NASA Energy Efficient Engine project is a cooperative government-industry effort aimed at advancing the technology base for large turbofan engines for civil aircraft transports. Major objectives were to significantly lower fuel consumption (10 to 15%) and to improve environmental and economic considerations (1) over present engines. Pratt & Whitney Aircraft, as a major participant in this project, was interested in developing an engine having a fan with a single stage of shroudless hollow titanium blades. TRW was selected by P&WA to develop the manufacturing technology for the production of these blades.

The large size and the requirement for precise lightening cavities in a considerable portion of the titanium fan blades necessitated the development of a new manufacturing method. The approach which was selected for development incorporated several technologies including HIP diffusion bonding of titanium sheet laminates containing removable cores and isothermal forging of the blade form. The technology bases established in HIP/DB for composite blades and in isothermal forging for fan blades were applicable for development of the manufacturing process.

The program conducted was divided into two tasks at TRW. The first task was an experimental study to establish the process techniques and parameters for producing and inspecting the cored diffusion bonded titanium laminate blade preform. The method was demonstrated with the production of twelve hollow simulated blade shapes for P&WA evaluation. The second task was the blade process development. The techniques established in Task I were extended to the processing of full size fan blades and the isothermal forging method for finish forming the blade was demonstrated. One blade airfoil processed by the established method was furnished to P&WA for evaluation.

Initially a third task, fan blade fabrication, was planned to produce twenty-two hollow fan blades for P&WA; however, during the course of this program this effort was cancelled because Pratt and Whitney's analysis did not show an economic advantage for the shroudless hollow blade as designed. Therefore, the program effort was redirected to demonstrate only the technology under development.

The results of the program effort are summarized in this final report. Evaluations of the critical experiments conducted to establish procedures to produce hollow structures by a laminate/core/diffusion bonding approach are included. In addition the transfer of this technology to produce a hollow fan blade is discussed.

II PROGRAM PLAN

The overall program objective was to develop a viable process for manufacturing hollow titanium fan blades for P&WA's Energy Efficient Engine and to produce blades for P&WA evaluation. The method selected for development was a full lamination/diffusion bonding and isothermal forging approach. To achieve the program goal, a two-task program was conducted.

A. Task I - Critical Experiments

The objective of this task was to establish the elements of blade design and processing to fabricate hollow structures. The fabrication process to be developed was intended for use in the manufacture of large hollow titanium fan blades.

1. Elements of Processing

Key experiments were planned to develop a technology base for use in fabricating large hollow fan blades. Elements considered were as follows: 1) laminate thickness considering flow characteristics and cost; 2) ply cutting approaches that are cost effective; 3) core design, manufacture and materials; 4) can fabrication and welding considerations; 5) establishment of fixturing techniques to assure proper registry of cores and laminates; and 6) the applicability of ultrasonic and radiographic NDE for blade inspection.

2. Specimen Fabrication

The evaluation of the key elements of processing were established by the fabrication of a diamond shaped, fully laminated and cored test specimen. All specimens fabricated were bonded by hot isostatic pressing (HIP). Radiographic, ultrasonic, and metallographic evaluations of the diamond test specimens were performed.

B. Task II - Blade Process Development

The Task II objective was to demonstrate the technology developed in Task I for the fabrication of a large hollow titanium fan blade. This objective was achieved by utilizing the Task I process parameters in fabricating a fully laminated, titanium alloy hollow blade.

1. Tooling

TRW designed and built tooling necessary to produce the fully laminated hollow blade. Tooling and/or methods selected for each element of the process sequence included:

- NC machining of mild steel cores.
- NC machining of airfoil plies.
- Blade assembly fixtures.

- o Seam welding for HIP cans.
- o Camber tooling.
- o Twist tooling.
- o Isothermal forging tooling.

2. Process Development

Based on Task I results, TRW developed the technology for a fully laminated and cored blade consolidated and diffusion bonded by HIP. Final forming of the airfoil contour was achieved through successive deformation on camber, twist and isothermal forge tooling. The hollow internal cavities of the blade were achieved by utilizing a leachable core material.

3. Prototype Blade

One prototype blade produced by the laminate/core/HIP diffusion bonded approach was delivered to P&WA.

III EXPERIMENTAL PROGRAM

A. Program Materials

1. Titanium Alloy Sheet Materials - Plies

Ti 6Al-4V sheet material was procured in 0.010, 0.030, 0.062 and 0.125-inch thicknesses. Initial material procurement was to meet AMS 4911 and P&WA Supplement S4928 chemical restrictions; however the material does not necessarily meet Rotating Quality Material Requirement per P&WA 1217. The material initially was procured from TIMET (0.030, 0.062 and 0.125-inch thick sheet) and Lawrence Aviation (0.010-inch thick sheet). This material was double melted with at least one cycle being vacuum melted, but a review of the material certification test sheets indicate that possibly only one heat would meet the Rotating Quality Material Requirements.

A microstructural evaluation was performed on all heats purchased. The microstructures were determined to consist of primary alpha in a transformed beta matrix. Grain size was equivalent for each heat within a given size range. Examples of the microstructures are shown in Figure 1. All heats evaluated meet P&WA Material Specification E72 for acceptable microstructures.

Rotating Quality Material in the form of 0.030-inch thick sheet was purchased from RMI for the blade fabrication task.

2. Core Materials

Two types of core materials were procured, AISI 1045 steel and TRW VMS-478 valve steel. The chemistry for both of these materials is shown below in Table I.

Table I

Typical Core Material Chemistry

Alloy	C	Mn	Cr	Ni	Si	P	S	N	Fe
1045	.43-.50	.60-.90				.040 max.	.050 max.		Bal.
TRW VMS-478	.50-.60	7.00-9.50	19.25-21.50	1.50-2.75	.25 max.	.05 max.	.06 max.	.02-.04	Bal.

3. Canning Materials

Canning materials selected for use in this program were 0.060-inch DQAK carbon steel, 0.025-inch IN-744 and 0.030 and 0.060-inch Ti 6Al-4V. DQAK carbon steel is essentially equivalent to AISI 1006/1008, that is very low in carbon. IN-744 (Fe-26Cr-

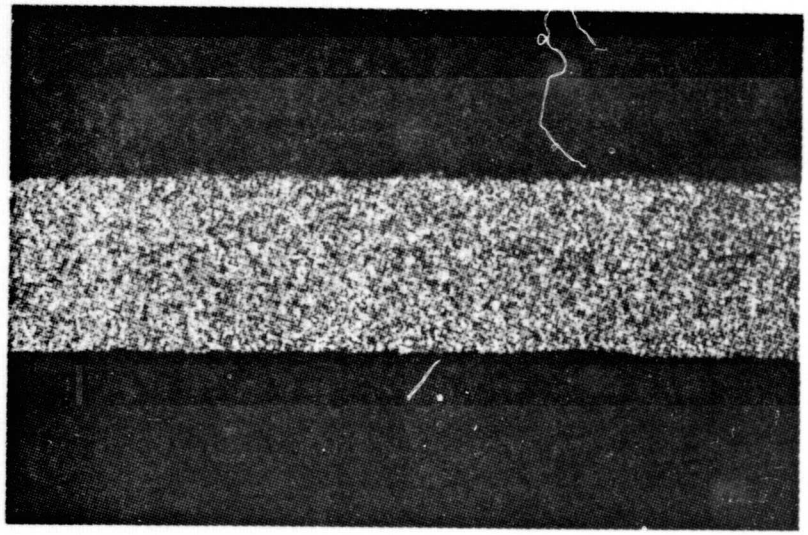

0.010-Inch Heat 295555

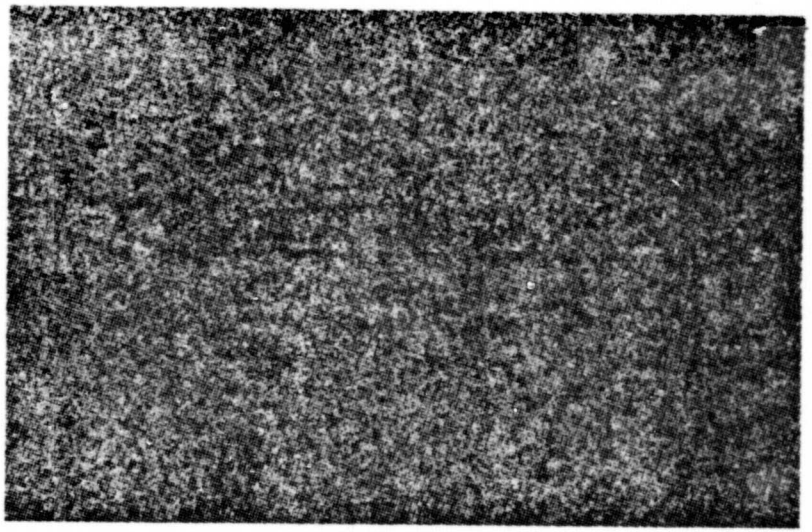

0.030-Inch Heat P-3909

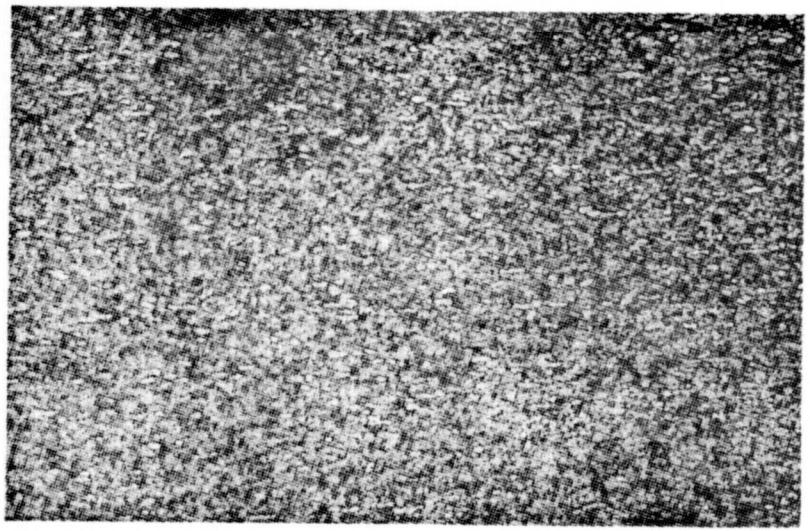

0.062-Inch Heat N-8490

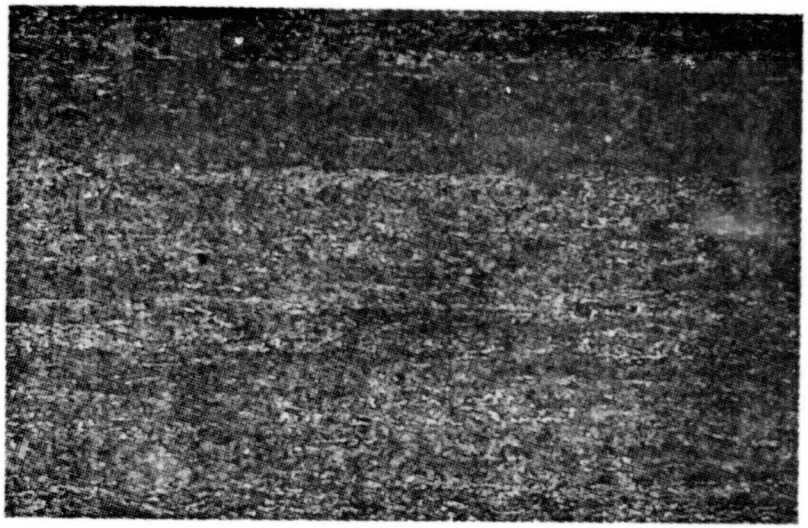

0.125-Inch Heat P-3392

Figure 1. Typical Microstructures for Ti 6Al-4V Sheet Material Purchased for Tasks I and II. 100X

6.5Ni-.5Ti) is an INCO product that behaves superplastically at temperatures in the range 950-1000°C (1742-1832°F). The Ti 6Al-4V sheet used for canning was the material also procured for plies.

B. Task I - Critical Experiments

The critical experiment task was conducted by evaluating various process parameters on fabricated diamond test specimens shown schematically in Figure 2. A total of twenty-five diamond specimens were fabricated during the performance of this task. The twenty-five diamond specimens are described in Table II. The specimens were processed in various size lots and are discussed in this section as such. Presentation of the experimental work for each lot better illustrates how the conduct of this task evolved. Prior to discussing specimen fabrication the elements required for fabrication including ply definition, core design and can design and fabrication are presented.

1. Diamond Specimen Ply Definition

There were essentially two types of ply designs considered for the fabrication of the diamond specimens, depending upon whether the diamond specimens were solid or hollow. The plies used in the solid specimen were all parallel to the outside surfaces. The dimensions of these laminates were defined by the intersection of the ply with the mid-plane of the specimen and/or with the planes limiting specimen's length and width. A total of sixteen primary laminates were used to make up the specimen. Eight of the laminates were 0.030-inch thick, whereas the remainder were 0.010-inch thick. An additional laminate through the midplane was used to control the volume of the specimen. With this configuration the titanium laminates in a hollow specimen would intersect the steel cores at an angle. Irregular cavity surface could result from indentation of the sharp titanium edges into the steel or from the flow of the steel into the voids at ply edges during the HIP cycle. To minimize the possibility of the indentation occurring and to have better ply definition, the laminates for the hollow specimens were redesigned.

The ten outermost layers (Figure 3) are parallel to the outside surfaces. The dimensions of these are defined by the intersection of the laminates with a 0.010 thick ply (Ply Number 5.2, 5.803 wide and 12.500 long) that lays in contact with the plane of cores and/or with the planes defining the specimen's width and length. The central portion of the specimen half consists of 10 laminates (Figure 4). These are parallel to the plane of both cores and are defined by their intersection with the mid-plane of the specimen and with the two planes that limit the specimen's length.

These 21 laminates (Figure 3 and 4, and Ply 5.2, not shown) form one-half of the specimen. Additional miscellaneous pieces (shown in Figure 5) are needed to fill the voids at the edges of these 21 laminates. Initially the core cavities were formed by cutting each individual ply along AA (Figure 4), along BB, along the leading/trailing edges of the cores and along the length of the cores at the center. The core cavities in most of the plies were cut by a stamping die, a very inexpensive, high volume production approach. In addition plunge electrical discharge machining (EDM) was also evaluated where the core plies were layed up for each half and machined as an assembly with a graphite electode shape similar to one-half of the core. The advantage of this approach is that the edges of

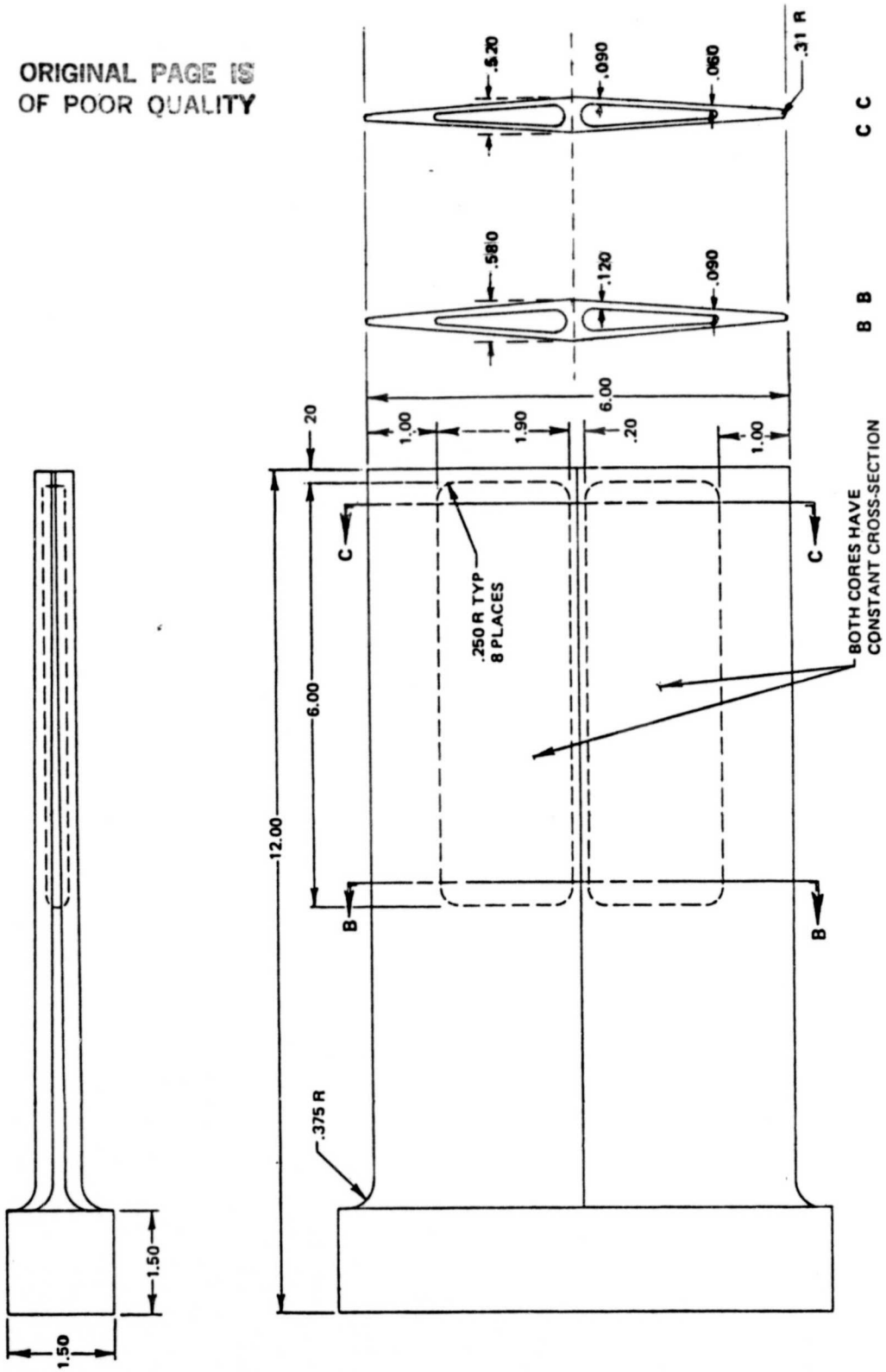

Figure 2. TRW Test Specimen Design.

TABLE II

Summary of Diamond Specimen Fabrication Parameters

Specimen Number	Core Material	Core Edge Radius	Ply Cavity	Root Layup	Covers	Other Comments
DS1	Solid	No Core	-	No Root	Titanium Sheet	-
DS2	1045 1045 (2 pcs)	0.062	Hand Cut	Straight	Carburized Can	One core Ti 6Al-4V foil wrapped. Second core cut in half - one piece polished.
DS3	1045	0.062	Hand Cut	No Root	Titanium Sheet	Special titanium inserts around cores.
DS4	VMS-478 1045	0.062 0.015	EDM Hand Cut	Step	Carburized Steel Graphoil	Stainless steel overcan
DS5	1045 1045 Polished	0.062 0.062	EDM Hand Cut	Insert	Carburized Foil Graphite Spray	Stainless steel overcan
DS6	1045 1045	0.062 0.062	EDM Hand Cut	Straight	Carburized Can	Stainless steel overcan
DS7	1045	0.062	EDM Hand Cut	Insert	Graphite Spray	-
DS8	1045	0.062	Stampings	Step	Graphite Spray	-
DS9	1045	0.062	Stampings	Step	Graphite Spray	TIG in helium.
DS10	1045	0.062	Stampings	Step	Graphite Spray	TIG in air under argon blanket.
DS11	1045	0.062	Stampings	Step	Graphite Spray	-
DS12	1045	0.062	Stampings	Step	Graphite Spray	IN-744 overcan.
DS13	1045	0.062	Stampings	Step	Graphite Spray	
DS14	1045	0.062	Stampings	Step	Graphite Spray	-
DS15	1045	0.062	Stampings	Step	Graphite Spray	-
DS16	1045	0.062	Stampings	Step	Graphite Spray	-

TABLE II (CONTINUED)

Specimen Number	Core Material	Core Edge Radius	Ply Cavity	Root Layup	Covers	Other Comments
DS17	1045	0.062	Stampings	Step	Graphite Spray	-
DS18	1045	0.062	Stampings	Step	Graphite Spray	-
DS19	1045	0.062	Stampings	Step	Graphite Spray	Ti 6Al-4V overcan.
DS20	1045	0.062	Stampings	Step	Graphite Spray	-
DS21	1045	0.062	Stampings	Step	Graphite Spray	-
DS22	1045	0.062	Stampings	Step	Graphite Spray	-
DS23	1045	0.062	Stampings	Step	Graphite Spray	-
DS24	1045	0.062	Stampings	Step	Graphite Spray	-
DS25	1045	0.062	Stampings	Step	Graphite Spray	-

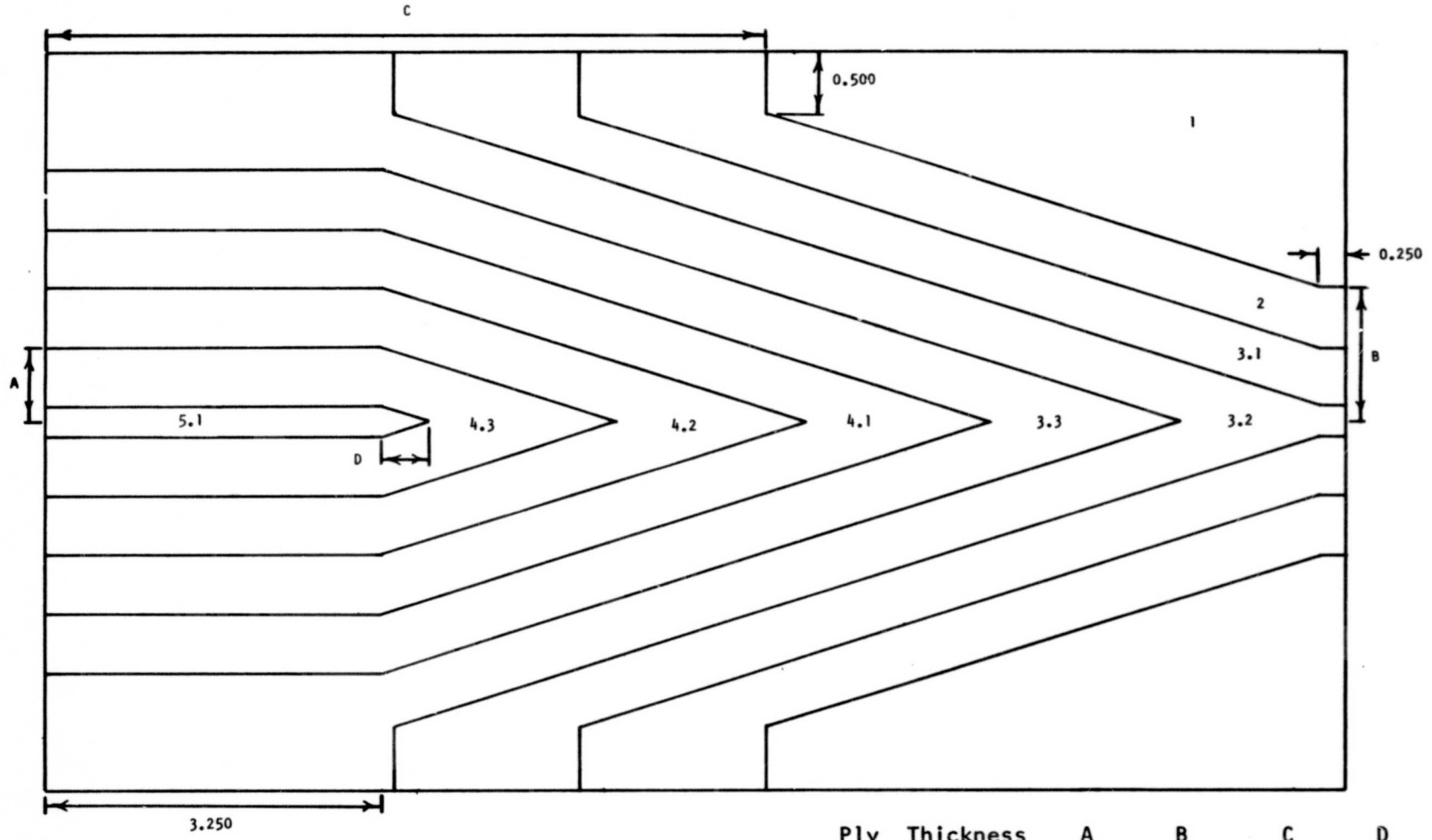

Ply	Thickness	A	B	C	D
1	0.030	3.5	3.5	12.500	-
2	0.030	3.5	1.257	6.964	-
3.1	0.010	3.5	0.699	5.165	-
3.2	0.010	3.5	0.140	3.364	-
3.3	0.010	2.373	-	-	7.653
4.1	0.010	1.815	-	-	5.854
4.2	0.010	1.257	-	-	4.054
4.3	0.010	0.699	-	-	2.254
5.1	0.010	0.141	-	-	0.454

Figure 3. **Outermost Titanium Laminates for Hollow Diamond Specimen.**

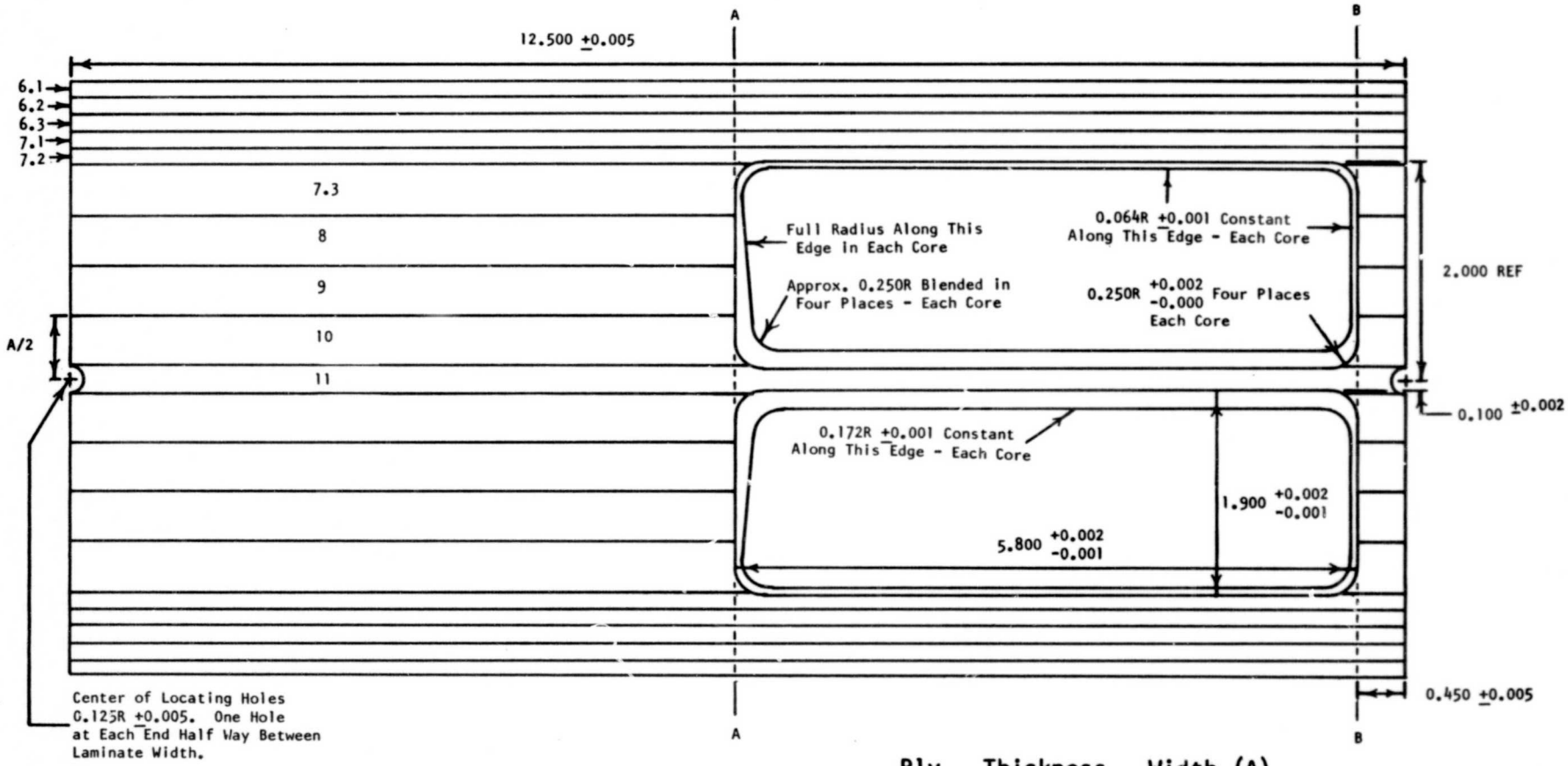

Ply	Thickness	Width (A)
6.1	0.010	5.494
6.2	0.010	5.184
6.3	0.010	4.875
7.1	0.010	4.565
7.2	0.010	4.256
7.3	0.010	3.946
8	0.030	3.017
9	0.030	2.089
10	0.030	1.160
11	0.030	0.232

Figure 4. Innermost Titanium Laminates for Hollow Diamond Specimens.

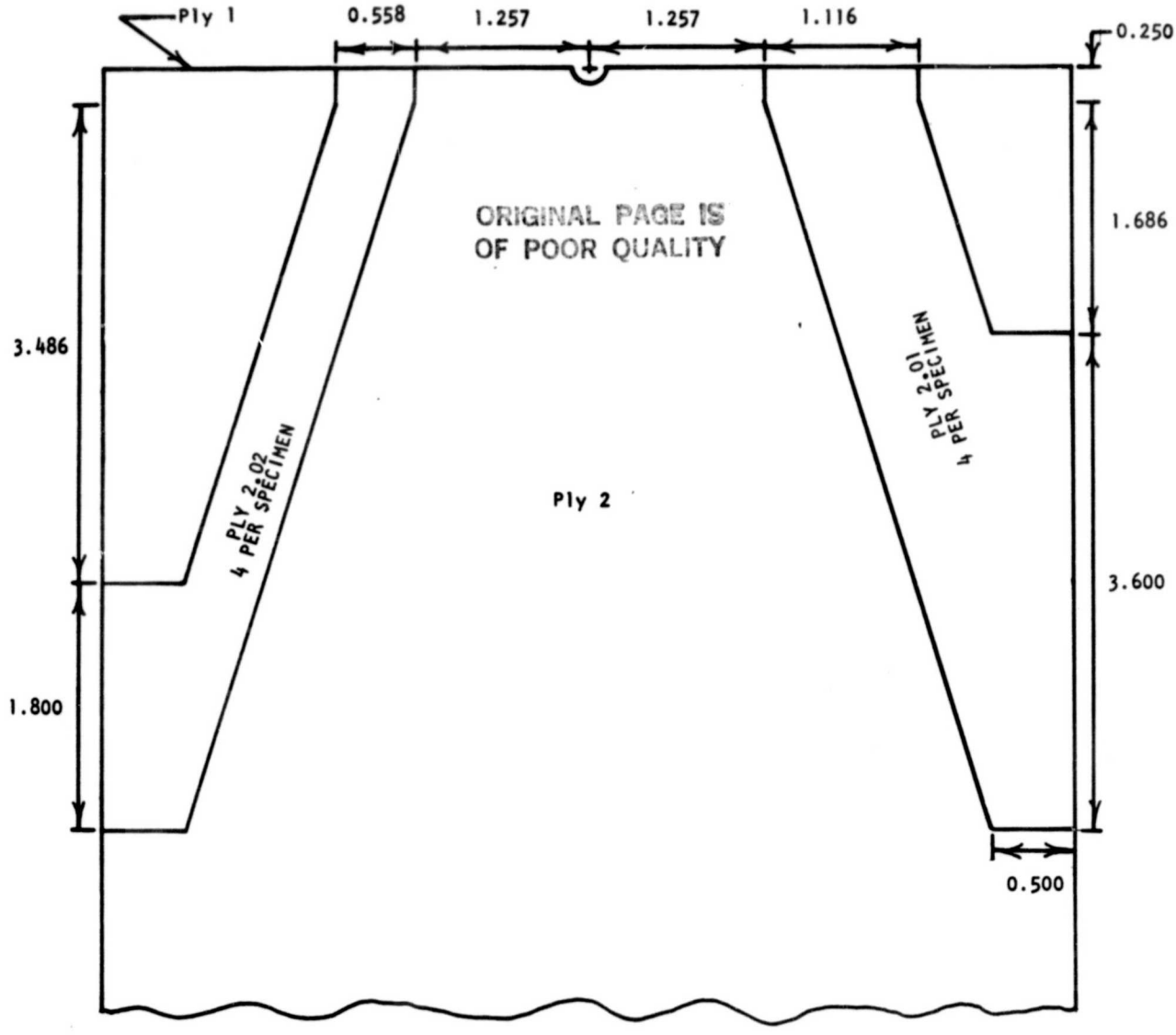

Figure 5. **Miscellaneous Hollow Diamond Specimen Laminates Used to Fill in Void at Ply Endings.**

the holes were angled and/or radiused to accept the core such that the contact surfaces between the plies and cores were parallel at all points. Hand cut or stamped plies have straight edges and the plies intersect the edges of the radiused ends of the cores at an angle. Wire EDM was also considered for cutting the plies, but because this method could only cut one ply at a time it was not selected.

There were some minor modifications to the ply design for the hollow specimens, basically some material addition which will be discussed for the appropriate diamond specimen fabrication.

In addition to the laminate designs for the "airfoil" section of the diamond specimens three root designs were evaluated. The first layup, a step root, consisted of sixteen laminates per half. The eight laminates closest to the airfoil surface were stepped in width, each laminate being 0.030-inch wider than the previous. The eight remaining laminates were 1.5-inches wide. The first seven laminates were 7.0-inches in length while the remaining nine laminates were two-piece with the length varying as a function of the diamond angle. The root layup edge which when assembled would form the root/airfoil radius. The remaining root laminates (twelve) were similar to the step root laminates except all were 1.5-inches wide. The third root layup was the straight design, all 1.5-inch wide laminates.

2. Diamond Specimen Core Design

Several variations of a basic core design were evaluated. All cores machined were 5.8-inches long and 1.9-inch-inches wide. One core design had a 0.062-inch radius at the leading/trailing edges and a full 0.170-inch radius at the centerline. A second core design had a 0.015-inch radius and 0.155-inch radius at leading/trailing edge and centerline respectively. In addition the core ends at the specimen end were either machined square with the breaking of the sharp corners or machined with a full radius. Examples of some of these cores are shown in Figures 6 and 7.

3. Can Design and Fabrication

Cans for HIP were designed to be made by the Guerin forming method (rubber pad forming) because this method was considered quite expedient and cost effective in the manufacture of cans. Cans were produced to a 12.5-inch length by a 7.0-inch width and having the ability to accept the tapered diamond specimen design shown in Figure 2. Cans were fabricated both with and without a root cavity. Although the can fabrication was achieved quite easily with the DQAK low carbon steel complete root cavity detail was never really achieved. A typical rubber pad formed can half is shown in Figure 8. The flanges of the cans were used to achieve a weld between the two can halves after assembly. The IN-744 and Ti 6Al-4V material were used exclusively for overcanning which will be discussed later in the text.

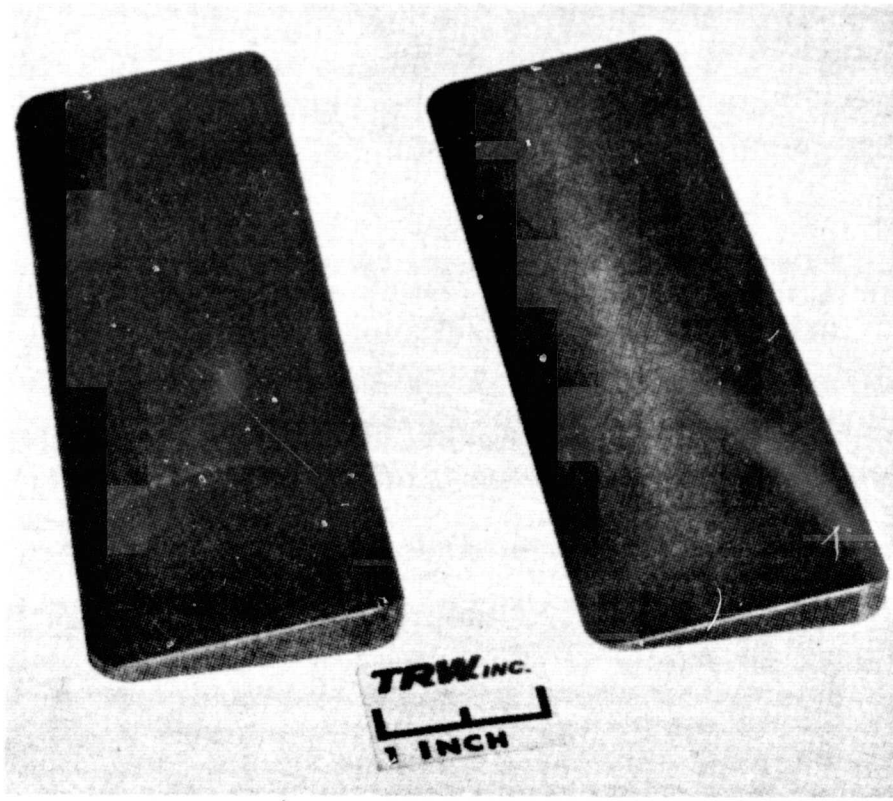

Figure 6. Steel Cores to be Used to Produce Cavity in Hollow Diamond Blade Specimen (1.900 Wide, 5.800 Long. Radii: Left 0.062/0.170, Right 0.015/0.155).

Figure 7. Typical 0.062-Inch Radius Cores Showing Differences in End Detail.

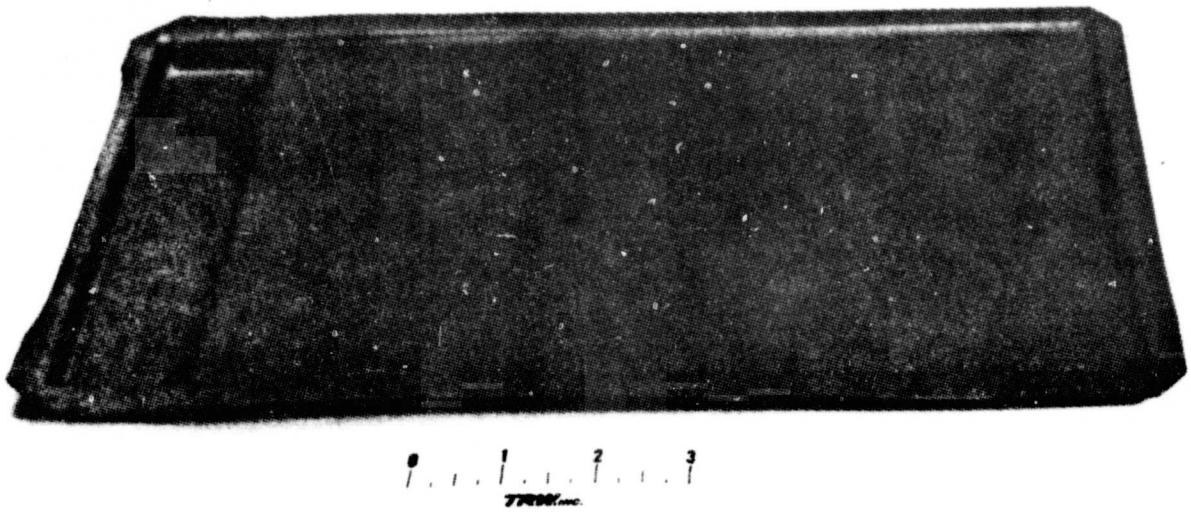

Figure 8. Steel Can Half Made by Pressing a Flat 0.060-Inch Thick Low Carbon Steel Sheet Into a Die Using a Pad of Rubber.

4. Diamond Specimen Fabrication

a. Diamond Specimen 1

The first diamond specimen (DS1) assembled was solid (i.e. it had no steel cores) with no root blocks. The plies used for this specimen were all parallel to the outside surface and as previously discussed consisted of sixteen plies (8 - 0.030-inch and 8 - 0.010-inch). The outer laminates were used to form a can by TIG welding in an argon atmosphere, these outer laminates along the length with each other and with diamond shaped end plates along the width.

The can was fitted with an evacuation pipe, pressurized with helium and "sniffed" using a mass spectrometer to check the can, especially the welds, for leaks. After the leak check, the evacuation pipe was removed and the can was placed in an EB weld chamber, evacuated for a minimum of six hours, and sealed. Changes in thickness before and after EB welding were used to insure that the specimen was properly evacuated and sealed. The specimen was HIP at 1750°F/2.5 hours/15 ksi at IMT, Woburn, Massachuetts (all specimens in this program were HIP at IMT). Specimen DS1 is shown in Figure 9 before hot isostatic pressing.

Plans were to use specimen DS1 to establish the ultrasonic nondestructive evaluation (UNDE) procedures and to correlate indications with the metallographic results. For this purpose, four flat-bottom holes were machined in the specimen as a standard defect reference after HIP. Two holes were 0.010-inch in diameter and two were 0.020-inch diameter. One of each was 0.160-inch deep, the remaining two were 0.270-inch deep. Because of "noise" problems which will be discussed later, a second standard was prepared from DS1 material. Flat bottom holes were drilled in the size range of 2/64 to 7/64-inch diameter at two different depths as shown in Figure 10.

In addition, a fixture was used to hold the specimen during inspection. The fixture permits inspection of the entire specimen at one time as well as tilting of the specimen to change the angle of the incidence of the sound wave. The tilt adjustment is necessary since the transmitted sound signal is affected by thickness and incidence angle, and it was necessary at times to make tilt adjustments. The fixture is shown in Figure 11.

b. Diamond Specimens 2 and 3

DS2 was the first hollow diamond specimen fabricated. The laminates for this and all succeeding specimens were those that were designed to be parallel to the core surface as discussed previously. The plies, including the core plies, were hand cut. Both cores were made from AISI 1045 steel with the 0.062-inch LE/TE radius. One core had a full radius along the width at the root end and was wrapped in two layers of 0.002-inch thick Ti 6Al-4V foil for 5.3-inches of its length. The second core was cut into two parts, each of which was 2.75-inches long. One half was polished on abrasive paper (through 600 grit) and the other half had the as-machined surface. Neither half had a radius at the end nor were they wrapped in foil. The DS2 specimen was expected to

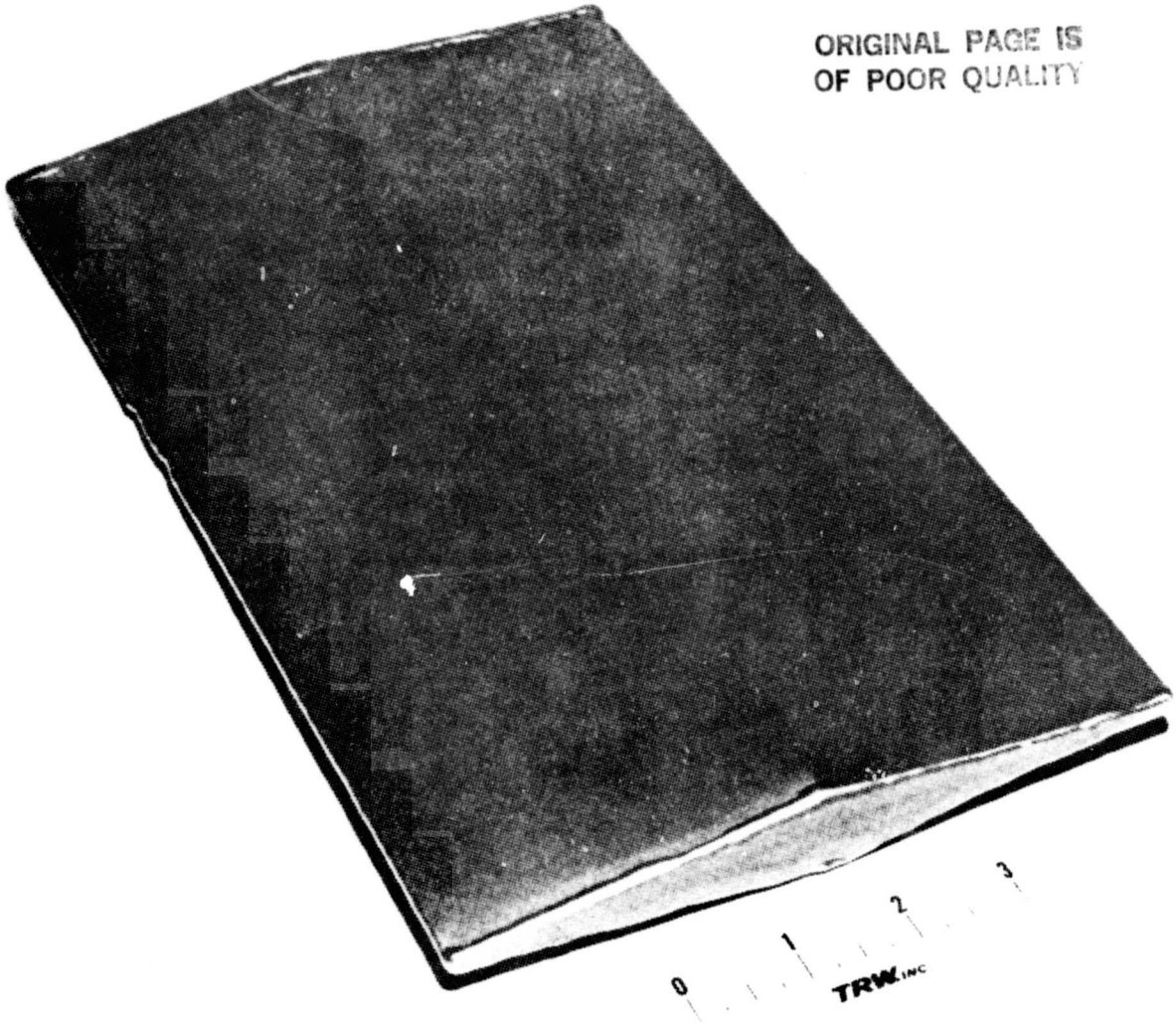

Figure 9. Solid Diamond Specimen (DS1) Before Hot Isostatic Pressing.

TRW

DEPT. NDE
SUBJECT: ULTRASONIC STANDARD

PROJECT NO. 512-024098-BB PAGE: 1
PREPARED BY: JOHN TOUHALISKY DATE: 8-10-79
CHECKED BY: D. J. MORACZ DATE: 8-10-79

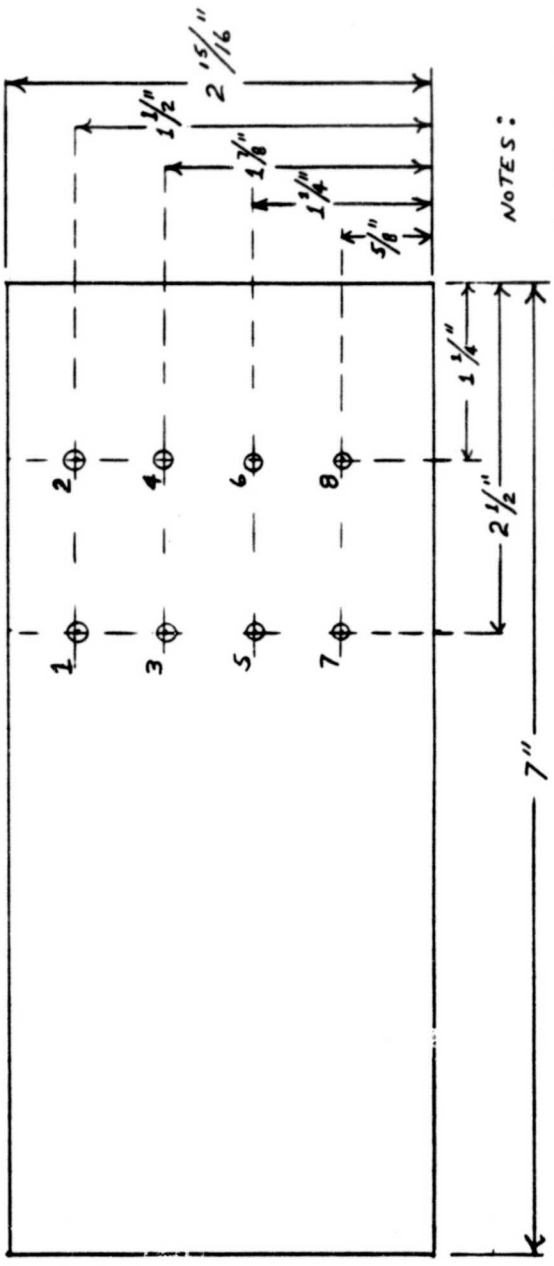

NOTES:
1. ALL HOLES FLAT BOTTOM
2. HOLES #1, 2, 3, 4 — 2/64" DIA.
HOLES #3 & 5 — 3/64" DIA.
HOLES #5 & 6, — 5/64" DIA.
HOLES #7 & 8, — 7/64" DIA.
3) HOLD ALL LOCATION DIMENSIONS ± 1/64"

Figure 10. Sketch of Hole Detail for Ultrasonic Test Standard.

PROJECT ANALYSIS SHEET TPFC-423A REV.2 PRINTED IN U.S.A.

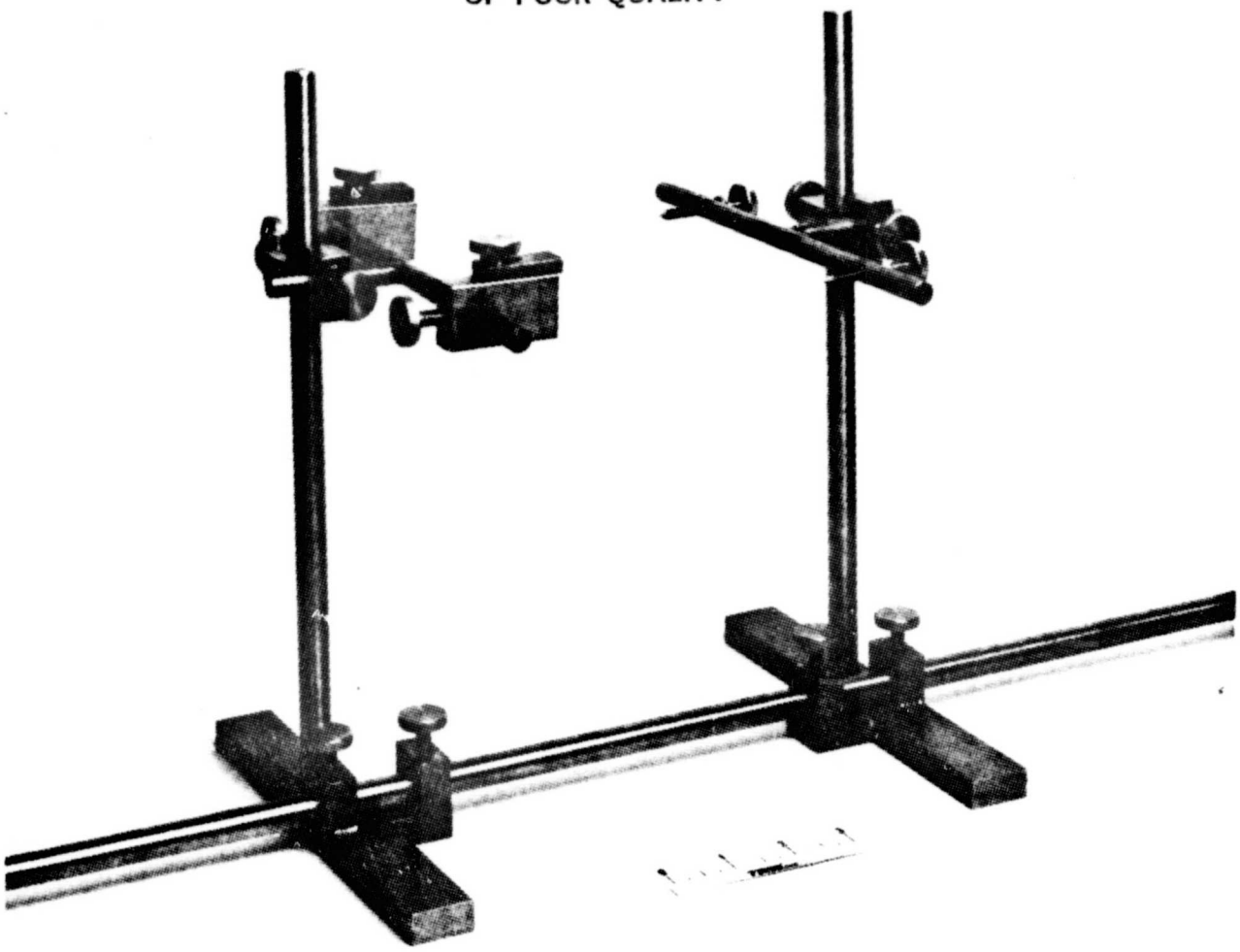

Figure 11. Stainless Steel Fixture Used to Hold the Diamond Specimens During Ultrasonic Nondestructive Evaluation.

provide some information on the flow of the steel cores with respect to the titanium laminates at the HIP conditions. Specimen DS2 also had laminated root blocks consisting of sixteen laminates for each root half but without an airfoil-to-root radius. This specimen was encapsulated in a carburized (0.7% carbon) steel can by TIG welding in argon. Carbon levels in the area of 0.030-0.040 w/o minimum are required at the steel can-titanium laminate interface to prevent a diffusion reaction during HIP.

The second hollow diamond specimen (DS3) used the same basic laminate configuration as for DS2 and shown in Figures 3, 4 and 5. This specimen had two carbon steel cores cut to 5.3-inches long. The cores are separated by a matching titanium insert. Two additional titanium inserts match the cores' leading and trailing edges. The cavity of this titanium-steel core insert (Figure 12) was also produced by cutting each individual laminate widthwise at the core root and tip and lengthwise at the edge of the insert.

This specimen was originally encapsulated in a carburized steel can. However, during welding, cracking occurred both in the heat-affected zone and at areas previously subjected to very high strains during can fabrication. It was subsequently found that this can had been carburized to 1.08% (as opposed to 0.7% in DS2). The carbon steel container and root-block plies were removed and the specimen was encapsulated in titanium sheet similar to DS1. After leak checking using a mass spectrometer, DS2 and DS3 were HIP at 1750°F/2.5 hours/15 ksi. DS2 had a can leak during HIP and was recanned at TRW and again HIP under the identical conditions.

c. Diamond Specimens 4, 5 and 6

Specimens DS4, DS5 and DS6 were the next group to be assembled for HIP. A summary of the assembly parameters is presented in Table II. Ply designs used were those shown in Figures 3 through 5 and plies were either hand cut or the holes for the cores were machined by EDM as discussed in an earlier section. Two types of core materials were evaluated: AISI-1045 and TRW VMS-478 high strength valve steel. Cores with both 0.062 and 0.015-inch LE/TE radius were considered with all cores having a full radius on the tip end. Root layups included a step laminate layup to help form the radius between the diamond surface and root, a solid insert and a straight laminate. Alternative approaches to can carburization included using graphoil (a sheet of graphite), carburized steel foil and graphite spray. The graphoil and carburized foil were placed between the can and the titanium laminates during assembly. The graphite was applied simply by spraying. An example of the graphite sprayed can is shown in Figure 13.

Leak checking of DS4, 5 and 6 indicated small leaks in two of the three cans after TIG welding. The cans were TIG welded in argon with mild steel weld rod material. Tests conducted afterwards indicated that welding with a stainless steel rod would yield a better weld and eliminate weld porosity. Future cans were welded in this manner. To provide "insurance" against leaks during the HIP run all diamond specimens were double-canned. The second can was made from flat stainless steel sheet welded at the edges. After welding all cans were again leak checked using helium and a mass spectrometer and sealed. The assemblies were then HIP at IMT.

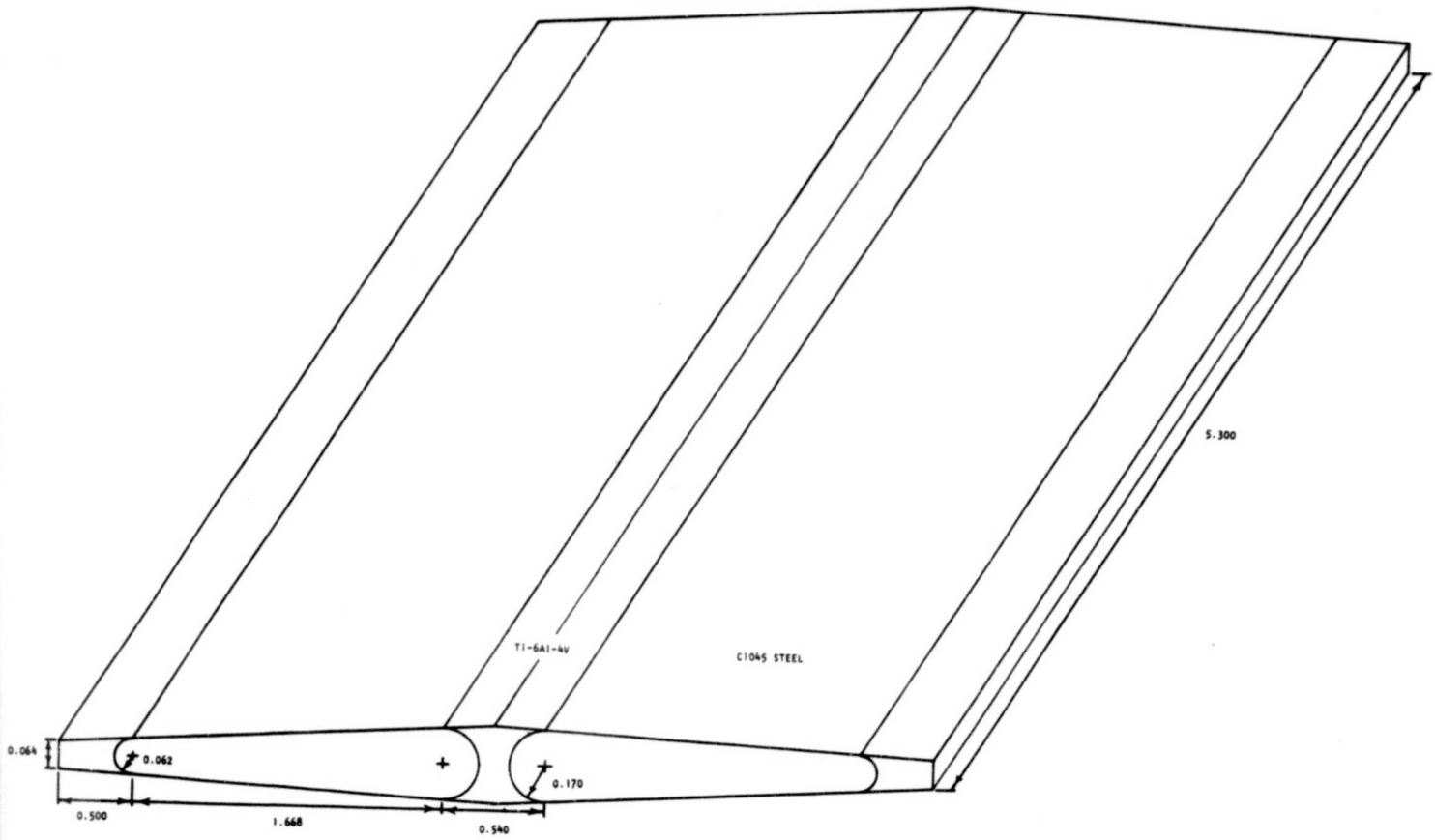

Figure 12. Steel-Titanium Fitted Insert Used in Specimen DS3.

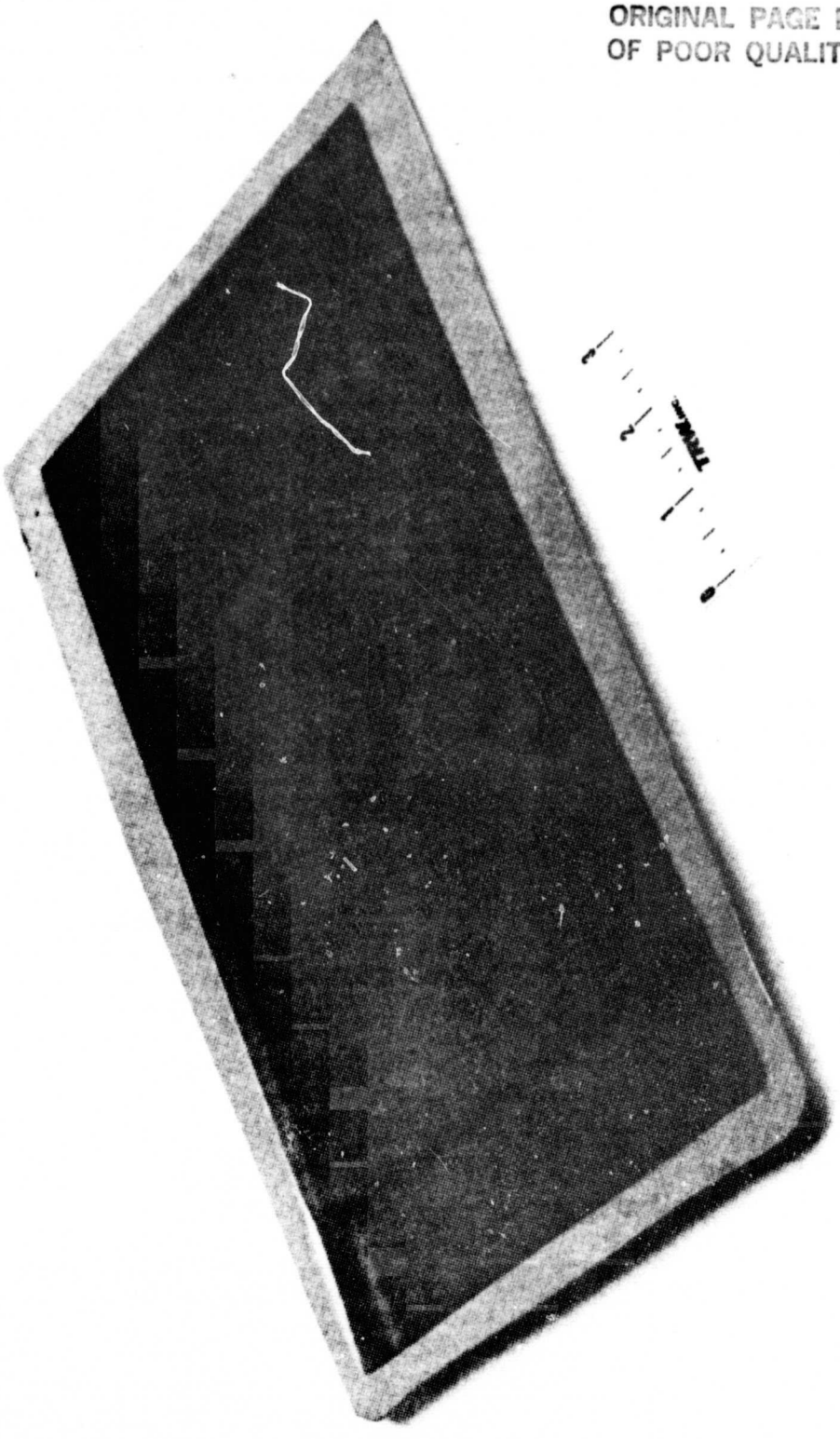

Figure 13. An Example of a Diamond Can Half Sprayed With Graphite.

One of the questions to be answered prior to fabricating blades was the approach to be taken in assembly of the blade plies, that is, should the blade be assembled flat or cambered and/or twisted. The obvious advantage of a flat layup is ease of assembly and core registry. There are advantages and disadvantages for both approaches but it is believed that a flat layup will result in greater accuracy in the core location for the finish part and lower overall cost. A question to be answered, also, was the ability to twist after HIP. A trial twisting study was planned for DS6 to observe the behavior of the core with respect to the laminate. Twisting was accomplished by heating the part to 1750°F, removing the part from the furnace and placing in a vise, and then twisting the airfoil section in the area of the cores using specially fabricated diamond shaped wrenches.

d. Diamond Specimen 7

Results of the HIP run for DS4, 5 and 6 which will be presented in Section IV discussed the "flattened" appearance of these specimens after HIP. This flattened appearance was attributed at this time to the double canning. Results of the studies at this point in the evaluations led to the selection of 1045 steel can as a core material and sprayed graphite an an interface to prevent reactions between the can material and laminates. In an effort to verify that double canning caused non-uniform pressure distribution and flattening of the diamond shape as observed in DS4, 5 and 6, DS7 was assembled similar to DS5 except that graphite spray was used for both can halves and it was sealed in a single low carbon steel can. After TIG welding in argon, leak checking and sealing the specimen was HIP. The standard HIP cycle 1750°F/2.5 hours/15 ksi, was used.

e. Diamond Specimens 8, 9 and 10

The metallographic results, discussed in detail in Section IV for DS7, indicated that a problem still existed at the bond interface. Consideration was given to several approaches to eliminate this problem. Obviously one approach was to change the method of welding if adsorbed argon was considered a potential source for the "voids" at the interface. TIG welding in helium, TIG welding in air with an argon blanket, electron beam welding and resistance welding were considered. Electron beam welding was not feasible for two reasons: (1) a virtual perfect matchup of the "lips" of the can halves was required and (2) the can material was mild steel (1008) and quite "gassy" which leads to welding problems. Resistance welding was considered the best approach; however, baffles or changes in the "lip" configuration may be required to prevent iron (can material) from spalling onto the titanium laminates during welding.

Three alternate methods for welding and sealing were proposed for evaluation for DS8, 9 and 10 prior to producing the twelve deliverable diamond specimens for P&WA. The methods selected were:

a) TIG weld in argon as before, leak check using helium, outgas in vacuum at 800° to 1000°F, and seal outgassing port by EB.

b) Same as (a) but TIG weld in helium.

c) Same as (a) but TIG weld in air under an argon blanket.

The vacuum outgas cycle was added at this time to remove any adsorbed gases.

A modification to the diamond assembly was to add more material. To allow for the debulking at the center of the specimen, a 0.03-inch thick by 0.444-inch wide ply was added in the center of each half. In addition a 0.010-inch sheet full size was added to each half to compensate for some of the undersize areas at the trailing edges.

In an effort to improve the uniformity of the pressure during the initial stages of HIP and eliminate the extrusion of material from the edge to cause a buildup at the 0.062-inch radius the HIP cycle was modified to the following:

> Heat diamond specimens to 1750°F with lowest pressure compatible with facility operation. Apply pressure gradually at 1750°F to 15 ksi and hold for 2.5 hours.

The difference between this HIP cycle and the earlier procedure was that the application of full pressure was previously initiated at 1000°F.

Diamond Specimens 8, 9 and 10 were assembled using the modifications discussed above. These were the first diamond specimens that utilized core plies produced by stamping. Figures 14 through 16 illustrate these plies along with the remaining plies required to produce one-half of the diamond. There are twenty plies required for the core, twenty-eight plies required for the cover, and forty-four plies necessary for the root for each diamond or a total of ninety-two plies. Every other DS9 ply was given a beta anneal in order to obtain a transformed beta phase microstructure. This treatment was applied to delineate each ply to show the metal flow and how voids were being filled during HIP. After assembly, welding, leak checking, hot outgassing and sealing the can assemblies were HIP using the modified cycle.

f. Deliverable Diamond Specimens for P&WA Evaluation

After evaluation of the last series of diamond specimens assembly for deliverable diamond specimens to P&WA was initiated. The diamond specimens were all assembled initially under the same conditions. Basically the plies were those shown in Figures 14 through 16 produced by hand cutting and stamping (core plies only). The root was a laminated step assembly (Figure 16). AISI-1045 cores with a 0.062-inch LE/TE radius was used. The cans were all sprayed with graphite to prevent bonding between the titanium laminates and the cans.

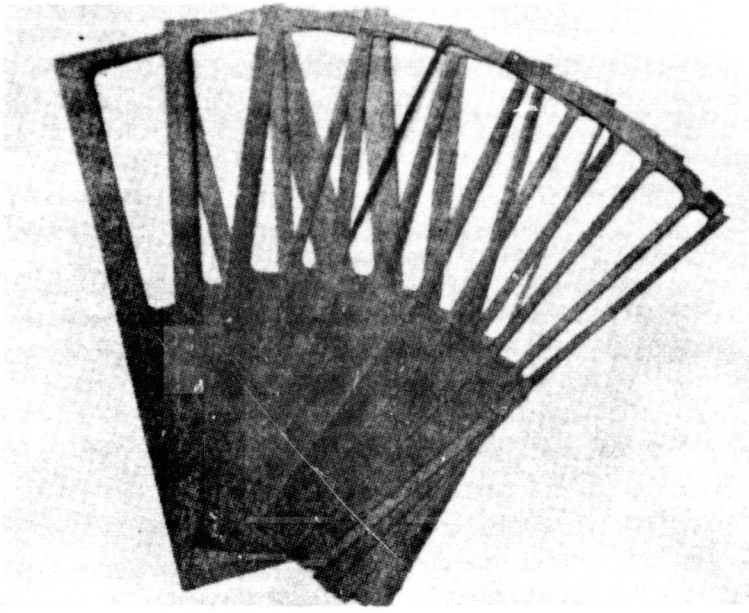

a. Ten Core Plies Required Per Half of Specimen.

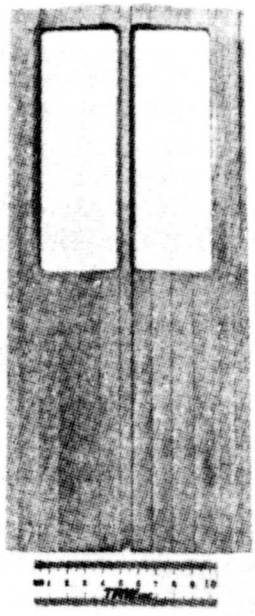

b. Core Plies Assembled.

Figure 14. Core Plies.

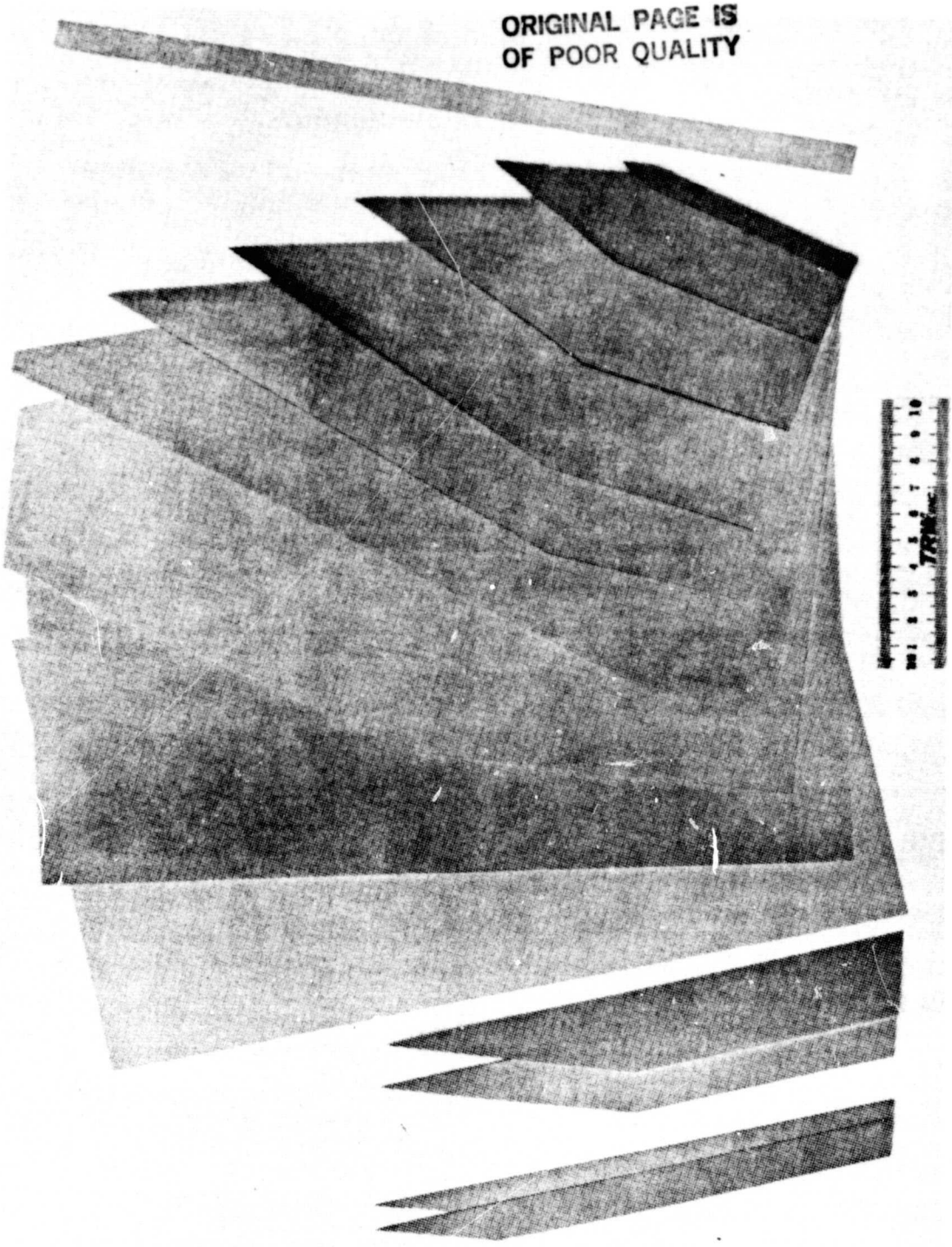

Figure 15. Fourteen Plies Required for Diamond Cover Per Half.

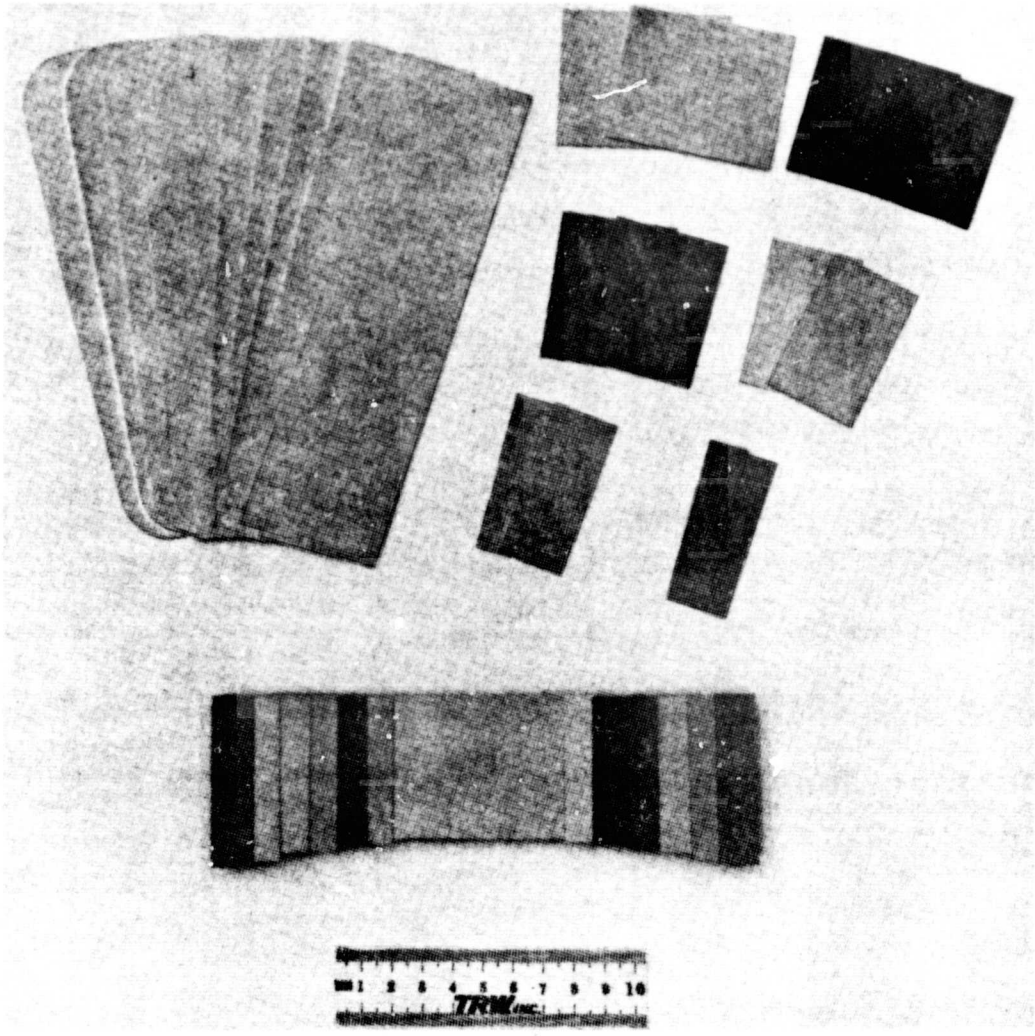

Figure 16. Twenty-Two Plies Required for Root Per Half. Shown Unassembled and Assembled.

A total of fifteen diamond specimens, nine with longitudinal and six with transverse grain orientation (with respect to the sheet rolling direction) were assembled. Previously all other diamond specimens had longitudinal grain direction. Procedures for assembly were as follows:

a) Clean all plies in an acid bath - $50H_2O$-48 HNO_3-2HF (by volume).

b) Water rinse.

c) Alcohol rinse and dry.

d) Assemble plies and tack weld (two core ply, two cover ply, and two root ply assemblies per blade).

e) Degrease cores.

f) Place assembled plies and cores in graphite coated steel cans.

g) TIG weld cans in helium (one can, DS25, was resistance seam welded).

h) Mass spectrometer leak check using helium.

i) Hot outgas in vacuum furnace (10^{-6}-10^{-7} microns) at 900-1000°F for 18 hours.

j) Seal can by electron beam (EB) welding.

k) X-ray.

Several comments should be made with regard to the above assembly procedure. The assembled package of plies consists of six subassemblies, two halves of the following: core, cover and root plies. They are final assembled in a diamond can half. The can, cores and notches in the core plies align the specimen. Permanent alignment was achieved in the resistance seam welded specimen by heli-arc welding all plies at the ends where the alignment notch is present, prior to placing in the cans. All cores were used in the as-machined and degreased (acetone plus alochol rinse) condition.

Modification of the evacuation tube was accomplished by cutting the tube to approximatley a 1/4-inch length and inserting in the tube a mild steel rod. Insertion of the rod prevents collapse of the tube during HIP and minimizes shear stress at the tube-can interface.

Prior to HIP all cans were X-rayed to look for core shift. Core shift had occurred in nine of the fifteen diamond specimens. This shift apparently occurs during handling in final assembly or welding. This problem has been attributed to the lack of a positive placement of the cores in the holes of the core plies. The fit is too tight. This

problem was alleviated in the fabrication of the blade by allowing a fit such that the core falls snugly in place. The core-ply hole was previously designed to a zero gap; however, the acid stock removal was to provide a gap of 0.002-0.003-inch per side. The gap would be acceptable if all the cores were machined to the same width within this tolerance. Shifting the cores back in place was accomplished by an inertial type blow to the side edge of the diamond can. An example of core location for diamond Specimen 14 before and after correction is shown in Figure 17. X-rays were used to verify that this method forced the cores back into proper registry.

i. Diamond Specimens 13 and 15

Initially only DS13 and 15 were shipped for HIP. The HIP cycle used was the cycle that allowed for application of full pressure to be initiated at 1000°F. Both specimens were heat treated (1750°F/1 Hour/FAC + 1300°F/2 Hours/AC) after HIP while in the mild steel can. This heat treatment was performed at the request of P&WA as an approach to improve the overall microstructure after HIP.

ii. Diamond Specimens 12, 19 and 25

Evaluations of both DS13 and 15 (see Section IV) had shown that both cans leaked during the HIP cycle. Several approaches were considered to improve the reliability of the HIP diamond specimens including making new cans, overcanning, coating the present can in a ceramic and other approaches. The leak problems were attributed to two areas: the lack of a wide flange near the root to improve weld reliability and the evacuation tube area undergoing shear stresses during HIP. Preparation of new cans having wide flanges was the desired solution, but required additional tooling that would cause a long delay in delivery of the diamond specimens. To improve the yield after HIP it was decided to overcan the diamond specimens. IN-744, a superplastic iron-base alloy, and Ti 6Al-4V were used as overcan materials. The IN-744 material was 0.025-inch thick and the Ti 6Al-4V material was 0.030-inch thick. Overcanning was accomplished with some difficulty because of the lack of room temperature formability (the material was "stiff"). The overcan material was TIG welded at the edges and then was sealed in an EB chamber. To provide more adherent form to the overcan material around the sealed diamond specimen, the packages were heated to 1600°F and 1650°F for the IN-744 and Ti 6Al-4V, respectively, in an autoclave. The objective was to insure true isostatic pressure during the HIP cycle. The diamond specimen with the IN-744 overcan (DS12) was held at temperature for about one hour. The material was found to be so superplastic that atmospheric pressure formed the IN-744 overcan over DS12. The diamond specimen with the Ti 6Al-4V overcan (DS19) was heated to 1650°F and pressure was applied gradually until 200 psi was reached. The total cycle was about one hour. The Ti 6Al-4V material also formed quite well around the diamond shape. These two overcanned diamond specimens along with the diamond specimen that was seam welded (DS25) were HIP. After receipt of the diamond specimens after HIP only DS25 was heat treated. DS12 and 19 had leaked during the HIP run.

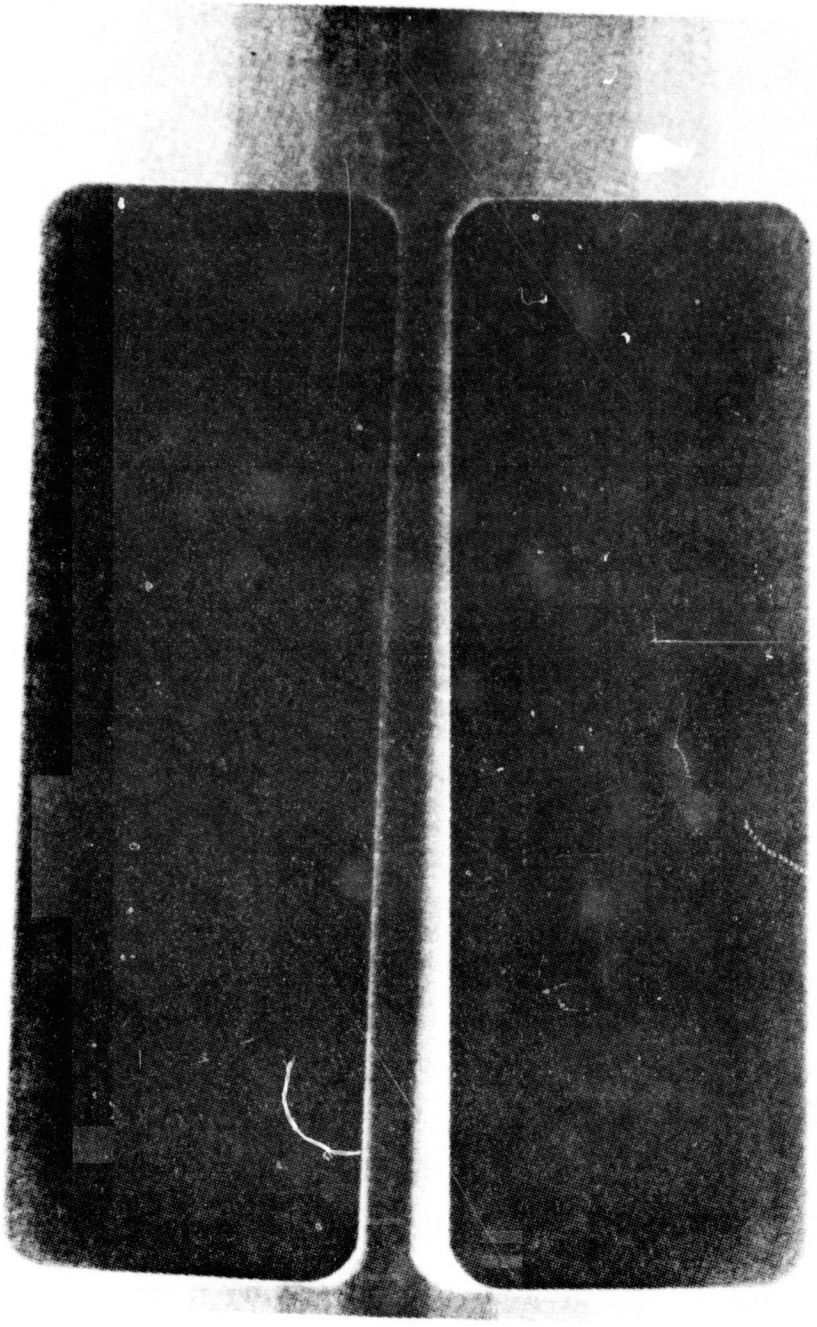

a. After Assembly

Figure 17. X-Ray of Core Location in DS 14.

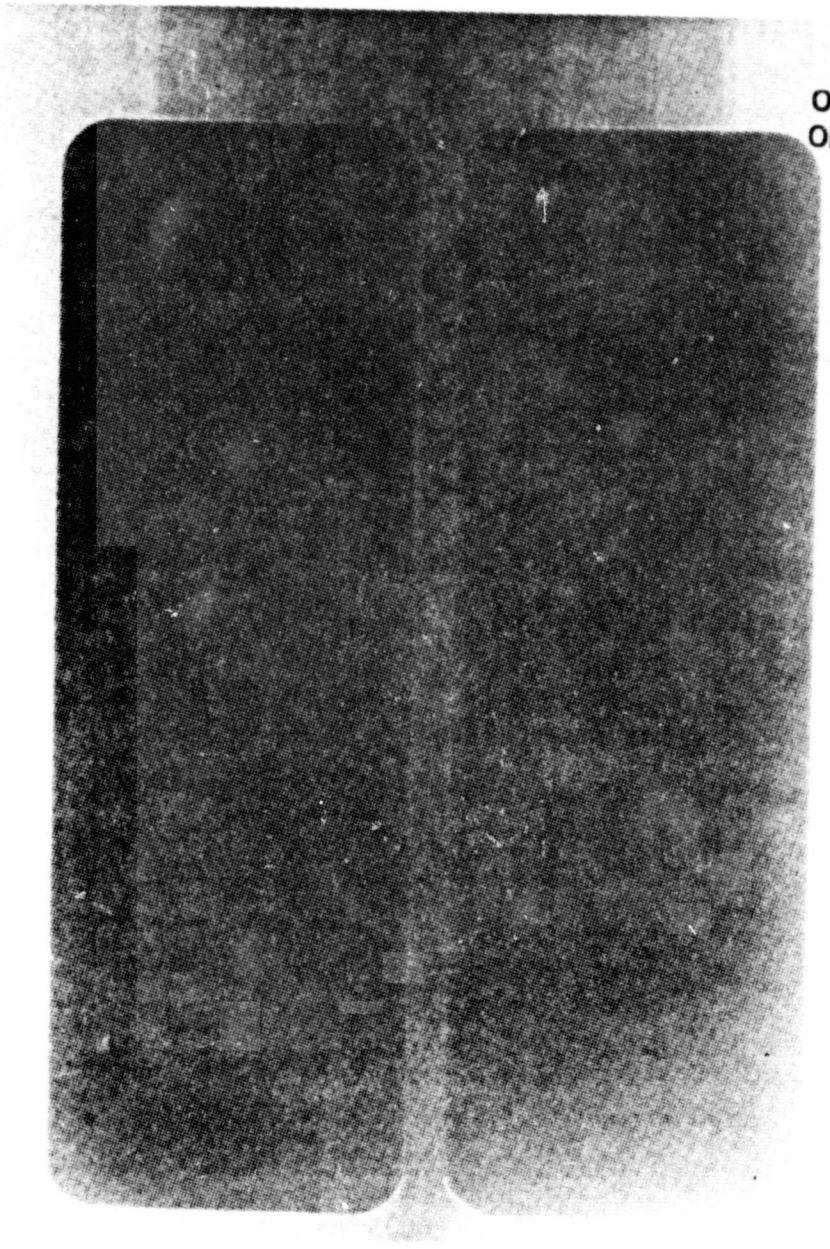

b. After Inertia Correction

Figure 17. (cont'd) X-Ray of Core Location in DS 14.

iii. Diamond Specimens 11, 14, 16, 17, 18, 20, 21, 22, 23 and 24

Just prior to shipping the remaining ten diamond specimens for HIP, Pratt and Whitney completed an analysis of the diamond specimen design. Their results indicated that, if the specimen was tested, failure of the specimen would always occur in the root area not in the hollowed portion of the specimen as was required. Based on this analysis, TRW rubber pad formed new mild steel cans without a root. The ten diamond specimens were decanned and then recanned in the new rootless cans. The can halves were seam welded based on the success of DS25, leak checked using a mass spectrometer, hot outgassed ($1000^{\circ}F$/18 hours/better than 10^{-6} microns vacuum), and electron beam sealed in a vacuum better than 10^{-4} microns. The specimens were then X-rayed to assure proper core registry and corrections were made to core location if required by an inertial type blow on the side of the diamond. These last ten diamond specimens were HIP using the previously established HIP cycle ($1750^{\circ}F$/2.5 hours/15 ksi). After HIP four of the ten specimens appeared suspicious and were again leak checked by drilling a small hole into the can material and using a mass spectrometer. All ten specimens were heat treated with the cans on.

5. Machining of Diamond Specimens

The last steps to be conducted in this task were the machining and leaching of the diamond specimens. DS8 and DS25 were machined to length and width and the surface was abrasive belt polished. DS11, 14, 16, 17, 21 and 24 were machined to length and width only. All eight specimens had the cores removed by hot acid leaching in a water/nitric acid bath (ratio of about 2:1) at a temperature of at least $150^{\circ}F$. Two 0.125-inch diameter holes were drilled in the end for each core for leaching. After leaching the interior cavities were chemically milled with a 5HF-35 HNO_3-60 H_2O solution. Chemical milling was accomplished by pumping cold acid through the cavities for a period of thirty minutes. Twelve diamond specimens were shipped to P&WA (DS8, 11, 14, 16, 17, 18, 20, 21, 22, 23, 24 and 25).

C. Task II - Blade Process Development

The blade process development task objective was to take advantage of the process data generated in Task I and apply the data to produce a hollow fan blade. Much of the effort in Task II was performed concurrently with Task I in the area of tooling, ply design and core manufacture. These topics are discussed initially followed by the fabrication efforts to produce the hollow fan blade. A total of nine blades were fabricated in this task. A schematic of the blade is shown in Figure 18.

1. Tooling

a. Isothermal Forge Tooling

A computer aided design approach was used for the blade forging die design. P&WA initially supplied a magnetic tape which gave the blade airfoil section description per P&WA specification 390. A preliminary layout (L-111013) was also

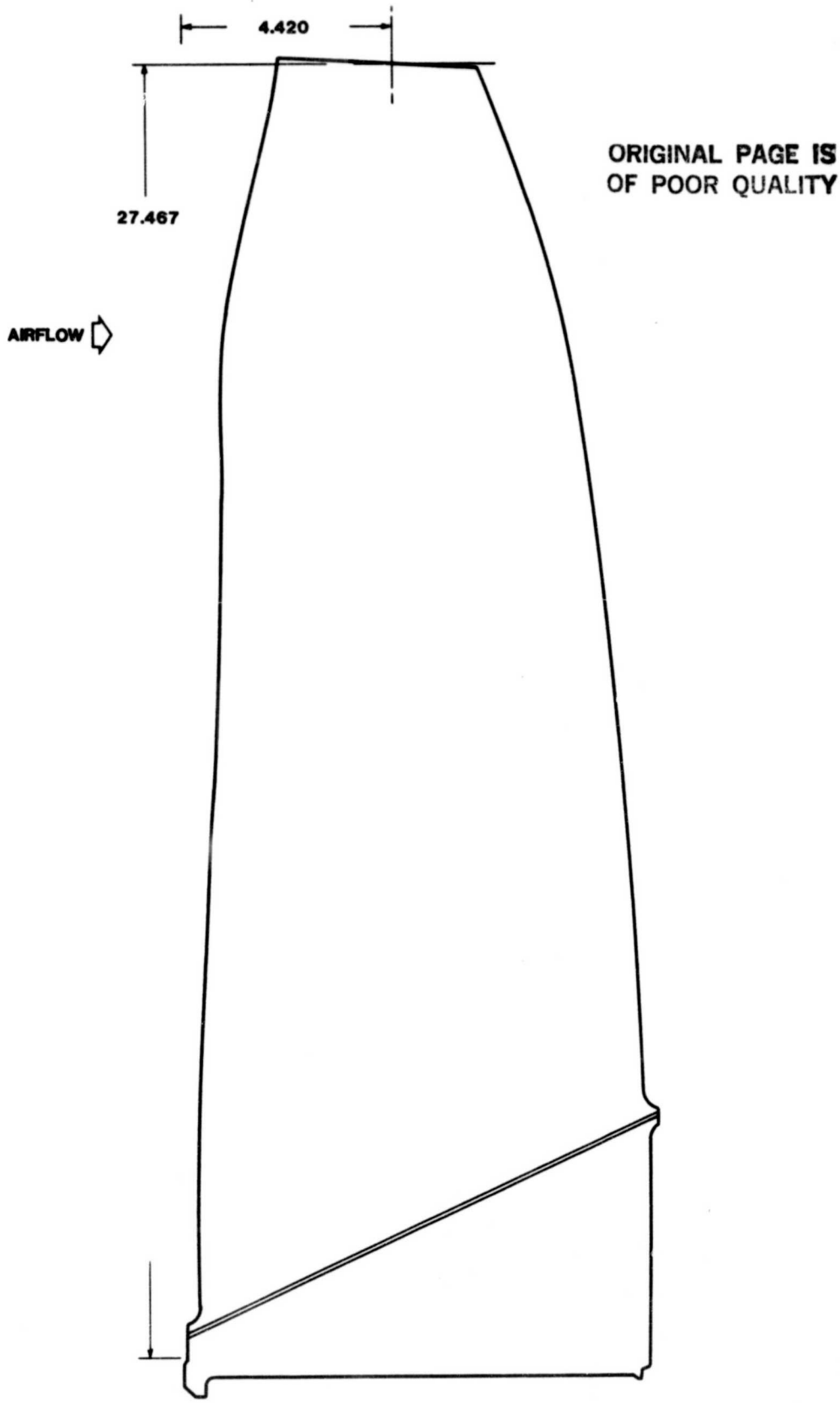

Figure 18. Sketch of P&WA's Hollow Fan Blade Design for Energy Efficient Engine Program.

supplied. The design represented the blade description to within ±0.25-inch of the final design. This design information was sufficient to prepare die and punch casting drawings and order IN-100 material for the die block castings. Based on this information a forging plane was selected.

A final hollow fan blade layout L-111052 and CA file were received after P&WA completed their design of the blade. This file was given to the TRW computer center for conversion from P&WA coordinate system to TRW coordinate system. It was found that due to an anomaly with the TRW software that produces digitized data used for preparing NC tapes for EDM electrodes, the forging plane (42°) originally selected had to be changed to 27°. The die and punch casting design drawings were revised and again sent to the casting vendor. The casting vendor prepared wooden model patterns from the design drawings and from cross-section plots of the airfoil. These models were reviewed and approved by TRW personnel and released for use in casting the die and punch. The die and punch wood models and castings are shown in Figures 19 and 20. These castings were the largest IN-100 die blocks ever produced for isothermal forging blades.

The CA file also was used to establish coordinate data required for the NC tapes to produce electrical discharge machining (EDM) electrodes. TRW added data for flash extensions and gutters. P&WA notified TRW shortly after this work was completed that there were some problems with the radii on the external blade CA file and a new file would have to be supplied. The radii change would have no impact on the IN-100 die and punch castings, but were important for the finish machining of the die and the inspection tooling. A new blade CA file and one set of fan blade EMD's were received from P&WA. This CA file was used to again establish the coordinate data required for the NC tapes.

Utilizing the final P&WA design information finished machined die and punch and die nest tooling design drawings were prepared. Design drawings for EDM electrodes for the airfoil, airfoil gutters and root and root gutters were prepared. NC tapes produced from the P&WA supplied design data were used to produce EDM electrodes for machining the airfoil and airfoil gutters. EDM electrodes required to machine the root cavity were produced from duplicating wooden models of the root based on root design requirement.

The airfoil electrodes used to EDM the airfoil were inspected on TRW's Cordax and found to be acceptable. These electrodes were then released to the tool vendor for EDM of the airfoil surface. The airfoil surfaces for both die and punch were Cordax inspected at TRW after EDM. Cordax inspection results after airfoil machining indicated that the dies were within an acceptable tolerance band (0.010-inch) after EDM. The dies were returned to the vendor for final machining of all surfaces, root pockets and heating element holes (prepared by gun drilling). The finish machined IN-100 isothermal forging dies were again Cordax inspected. The inspection results indicated a tolerance band of about 0.010-inch was observed except for selected areas of steep climb at the leading and trailing edges. Inspection probe deflection due to the severe camber and twist in these areas limits accurate inspection. Since a certain degree of die rework is necessary due to die deflection and thermal expansion, the dies were found to be satisfactory for the first forging trials. The finish machined dies are shown in Figure 21.

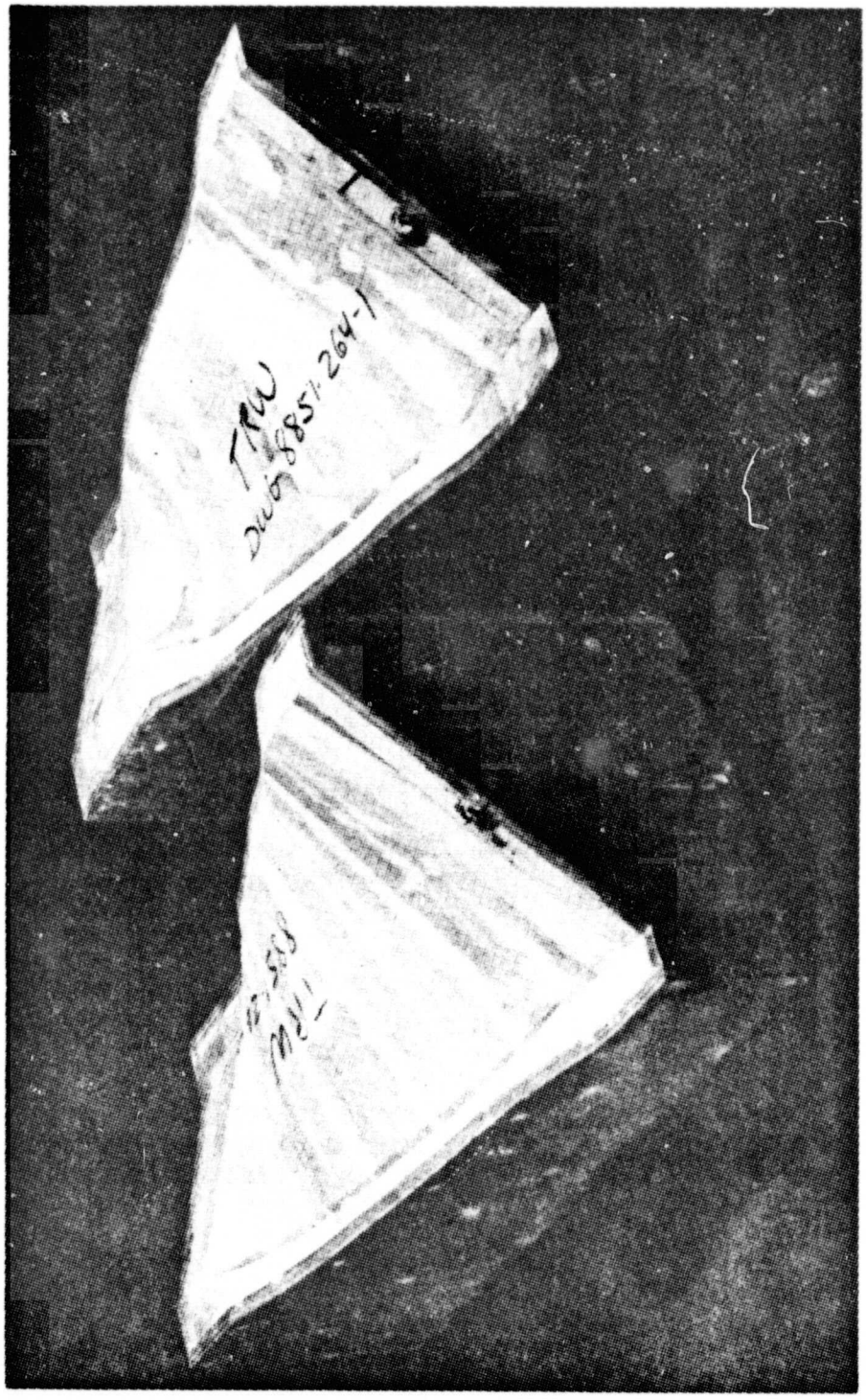

Figure 19. Wood Patterns Used to Produce IN-100 Isothermal Forging Dies.

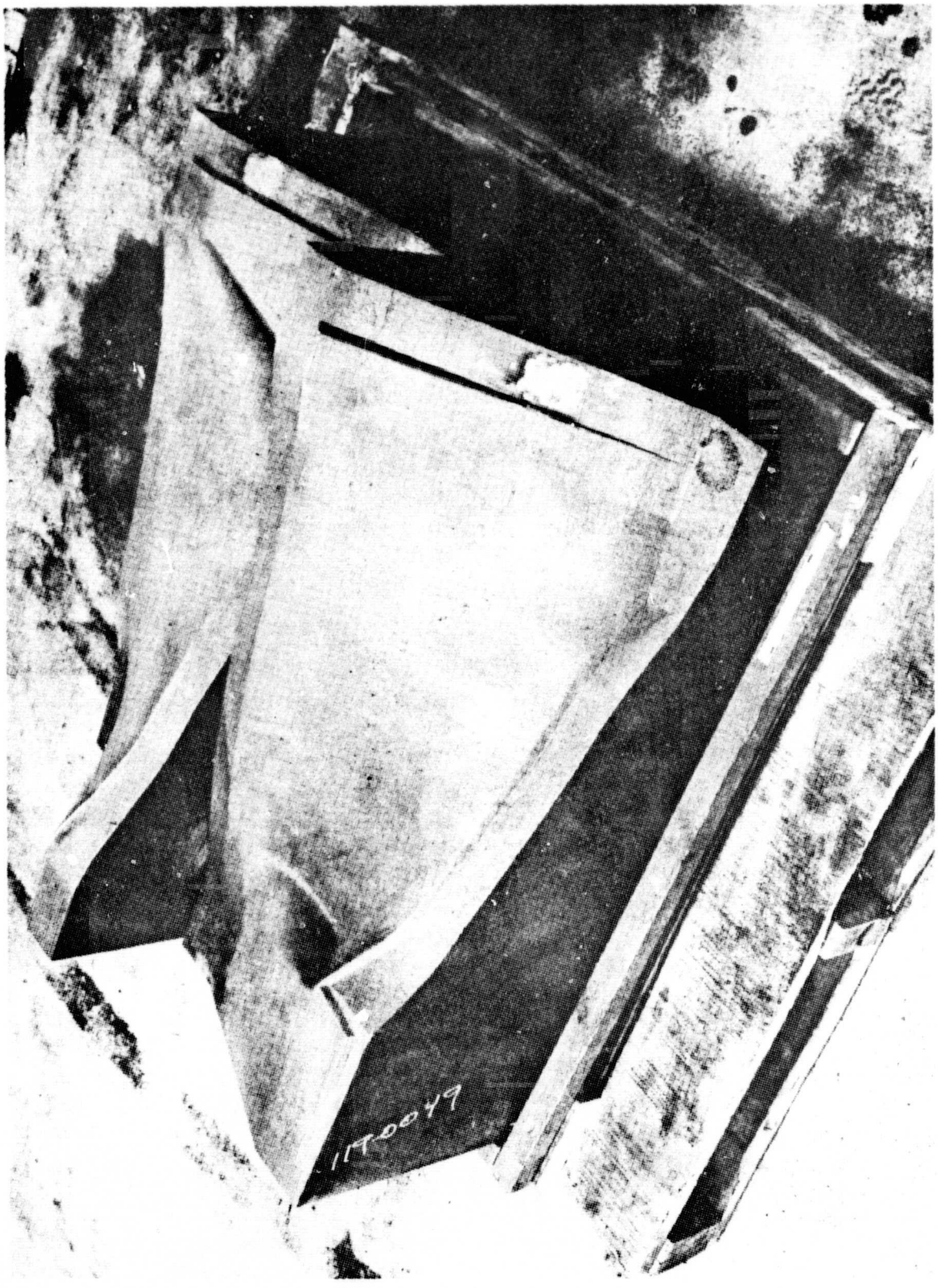

Figure 20. IN-100 Isothermal Forging Die Castings.

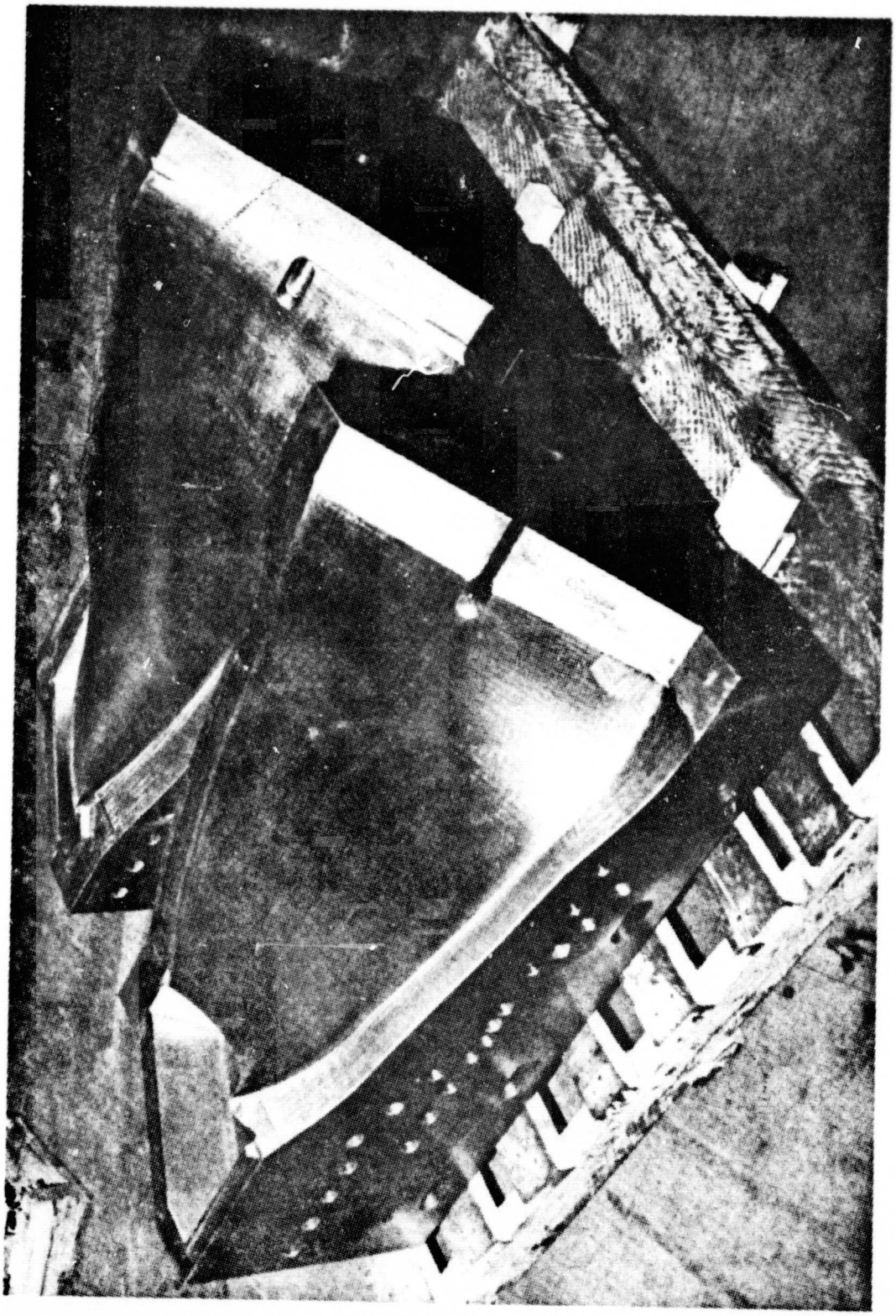

Figure 21. IN-100 Isothermal Forging Tooling.

b. Die Nest, Heating Elements, Insulation and Thermocouples

Using the design information for the isothermal forging dies, a four post die nest was built. Some of the features of this die nest include water cooled platens and locator inserts which provide a positive location of the die and punch with respect to each other and minimizes any chance for movement of the tooling during forging.

Other items that were part of the tooling system included heating elements and insulation. Cartridge heating elements specified in design by TRW were manufactured by Watlow. Ceramic plate insulation, 1-1/2-inches thick, was used between the die and punch bottom surface and the water cooled platens. Ceramic blanket insulation encapsulated in stainless steel was placed around the periphery of the die and punch to minimize heat loss. Thermocouples were used to monitor temperature at twenty locations within the IN-100 tooling.

c. Ply-Core Assembly Tooling

TRW designed and built ply-core assembly tooling. The fixture was a flat wooden block that had provisions for two locators at the root end. The position of the plies during assembly was maintained by two 3/8-inch diameter holes which were pinned with 3/8-inch diameter bar. The holes were located 1/4-inch from the root end in an area that will be machined. The position of one hole was along the blade stacking axis while the second hole was located 2-inches from the stacking axis along the root end. Initially, the holes were 3-inches apart, but final ply design dictated that the holes be placed closer together to maximize the number of plies that were double pinned. In addition, a single pin was located at the blade tip along the stacking axis to help in alignment of the full length plies.

Alignment of the root/cover skin welded assembly was maintained with the airfoil ply assembly by two blind holes drilled in the cover skin sheet and root block to a depth of about 1-inch. In addition, the holes were also required to allow outgassing in the area between the cover skin and root blocks after seam welding of the entire package. This approach was used only for blades assembled with roots.

d. Camber Tooling

The blade layup approach selected was uncambered, and untwisted. Tool steel camber tooling was designed and built by TRW to camber the HIP bonded blade in one operation. TRW's computer was used to draw untwisted versions of the cross-sections of the airfoil. These drawings were used to produce wooden models from which EDM electrodes could be machined. The finish tooling is shown in Figure 22. The concept of the tooling is relatively simple. A sketch of the camber tooling is shown in Figure 23. The tip of the blade is held by a fixture. A 1-1/2-inch diameter pin extends beyond the tip and is located along the stacking axis of the blade. The alignment at the root is maintained by the sides of the root block. The blade was placed hot (1600-1750^{o}F) in the die and "squeezed" to camber the root and airfoil. There was excess material in the root which was to be machined after cambering. The camber dies were operated at about 400-600^{o}F and cambering was performed in a 1500 ton hydraulic press.

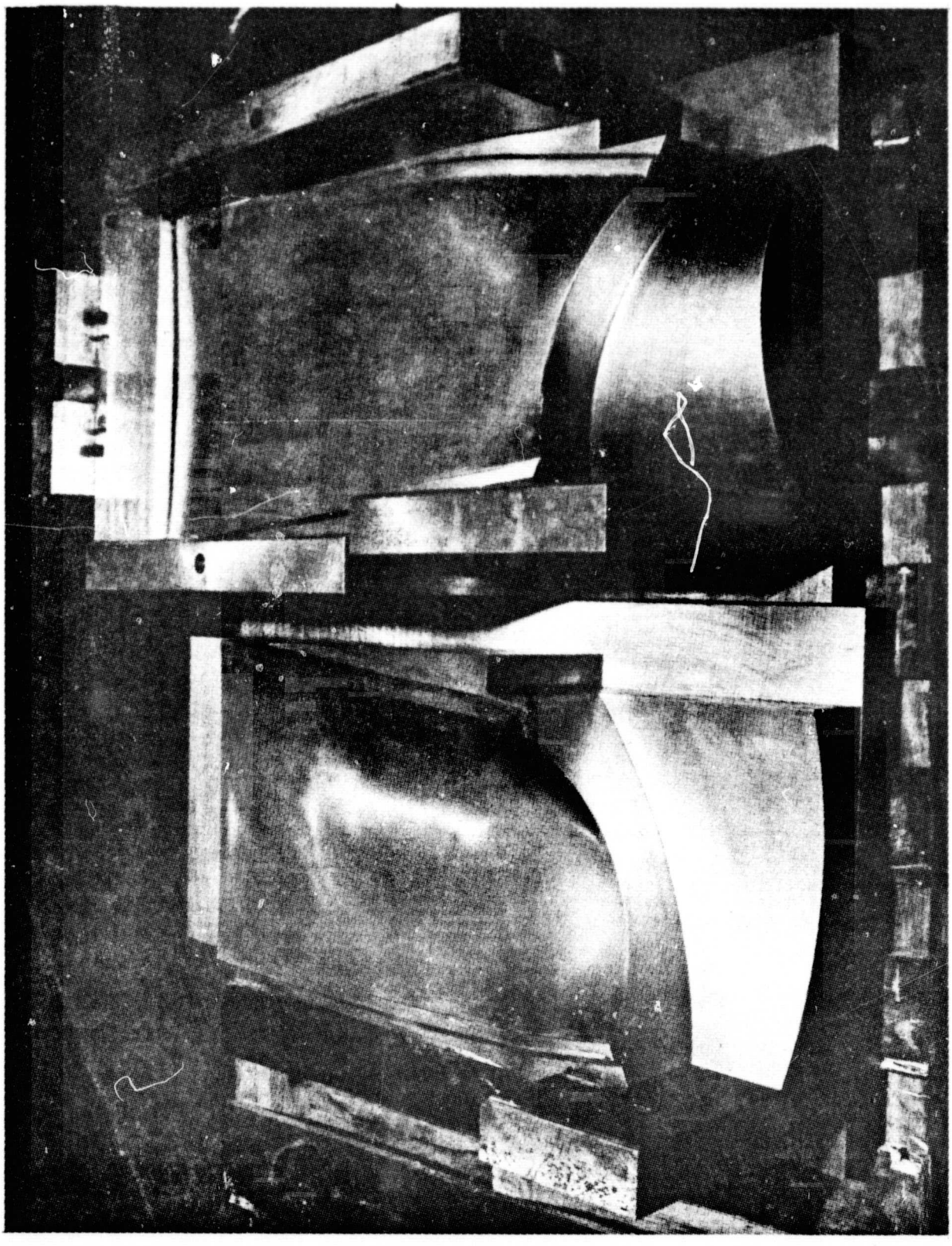

Figure 22. Camber Tooling.

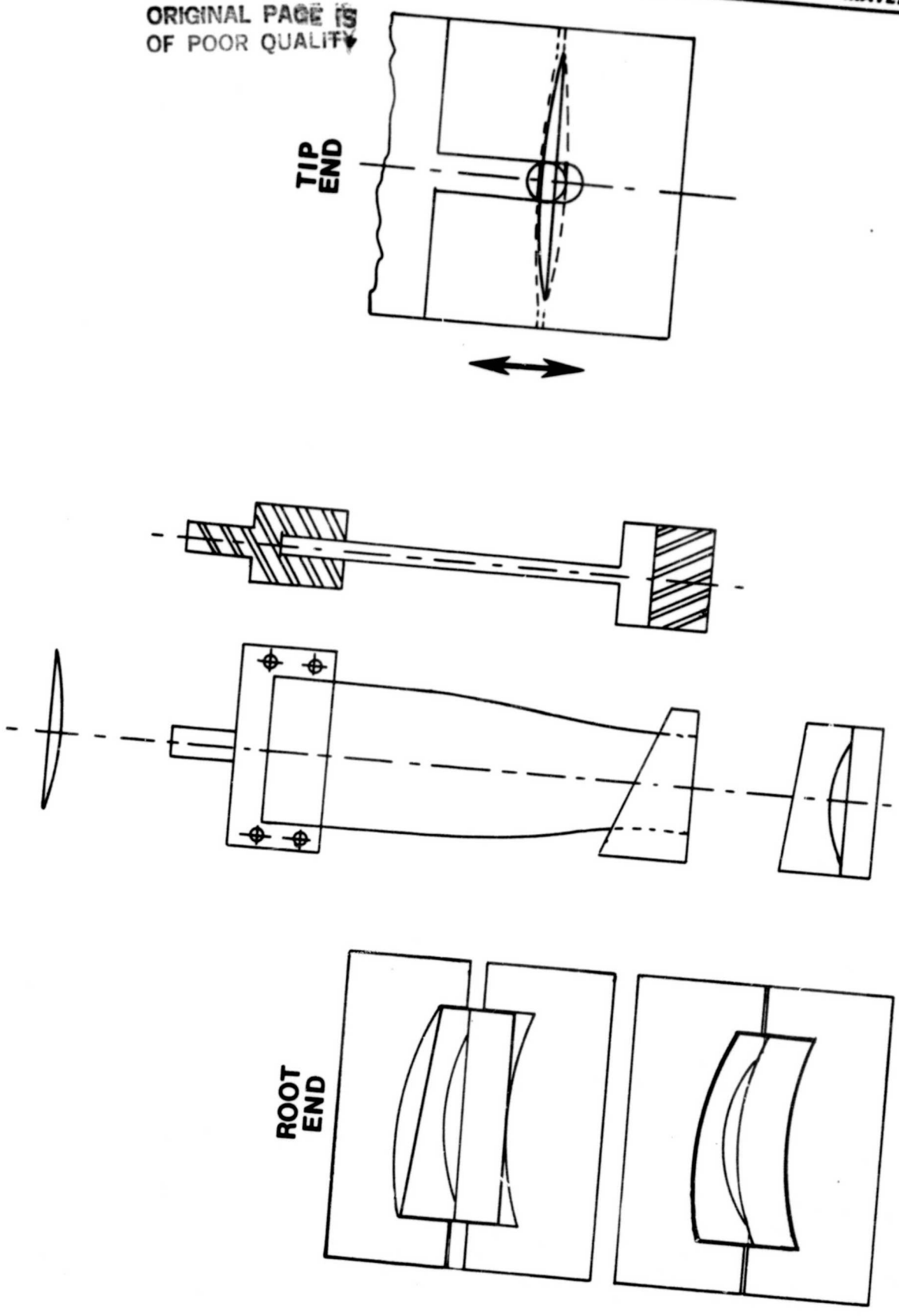

Figure 23. Schematic Illustration of Camber Tooling.

e. Twist Tooling

TRW had available an Ajax crank press twister designed for use in twisting crankshafts but adaptable to twisting blades. Tool steel twist dies were designed and built for twisting nine cambered HIP blades. TRW had the support tooling available for use on this program. An earlier internal study study showed that this approach was very successful in twisting large fan blades; therefore this approach was considered low risk because of the previous development and success.

The blade was twisted by a two-step approach. There were three sets of dies: root, center of airfoil, and tip as shown in Figure 24. Initially, the airfoil was clamped with the dies at the center of the blade. Then the dies at the tip were clamped together. The clamping action at the tip allowed some twist to be put into the blade. The remaining twist in the center-to-tip section was accomplished by the rotation of a large bull gear to which the center dies were mounted. Similarly, for the root-to-blade center section, the process were repeated. When twisting, only the center set of dies and either the root or tip dies were used at one time. The twisting was performed hot - 1600 to 1750°F. The tool steel dies were at ambient temperature.

f. Blade Inspection Fixture

TRW designed and built a blade inspection fixture. The fixture shown in Figure 25 locates off the root and tip locator of the final isothermally forged blade. The fixture allows inspection of the blade at six sections.

2. Ply Design and Manufacture for Hollow Fan Blade

Ply design required the use of P&WA supplied CA files for both the blade and cores. Extensive modifications were made to current TRW software programs for ply generation to better define ply ends and to plot plies with core cutouts. Each core that was defined was essentially a new airfoil that had to be generated.

Prior to initiation of ply design (and isothermal die design) TRW tested the transformation of P&WA supplied coordinates to TRW coordinates. To test the transformation of P&WA coordinates to TRW coordinates, plots of the airfoil sections using the new TRW coordinate system were compared to the EMD's of the sections received from P&WA. A problem was encountered when comparing airfoil section plots drawn using TRW's airfoil design system and the EMD's supplied by P&WA. The differences observed were as large as .020-inch in airfoil thickness. The source of this problem was determined to be that the point spacing used to define the airfoil section was too sparse in the high camber areas for the E^3 blade. In particular, points at 85 to 95% of the chord length were not provided. The differences between TRW's plot and the EMD's reflect the difference between the Aitken-Lagrange interpolation algorithm that was used by TRW and the cubic spline algorithm used by P&WA. To solve this problem TRW used a cubic spline interpolation program to add points at approximately 55, 65, 75, 85 and 95% of the chord length. A comparison plot using this new data set demonstrated excellent agreement with the EMD's.

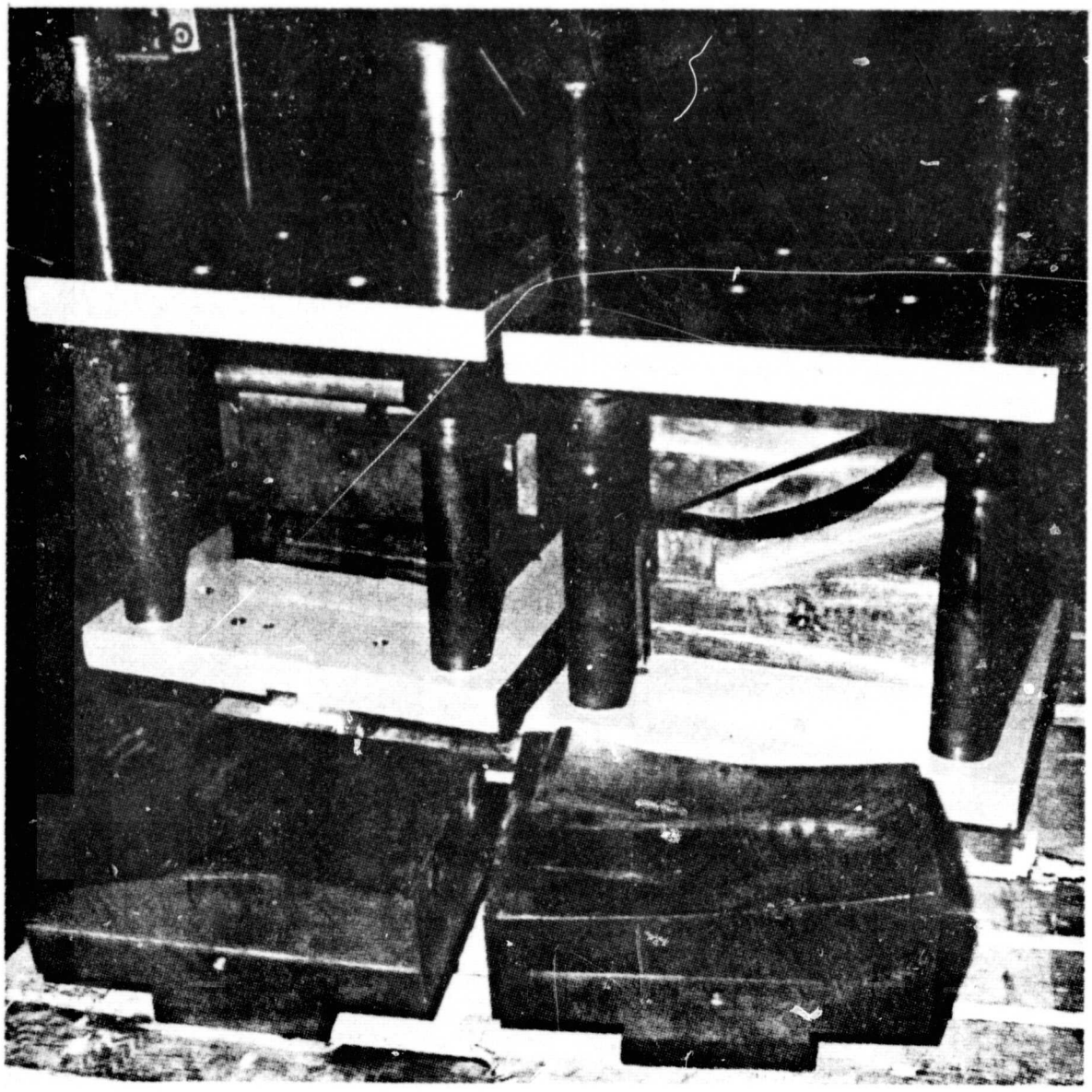

Figure 24. Twist Tooling.

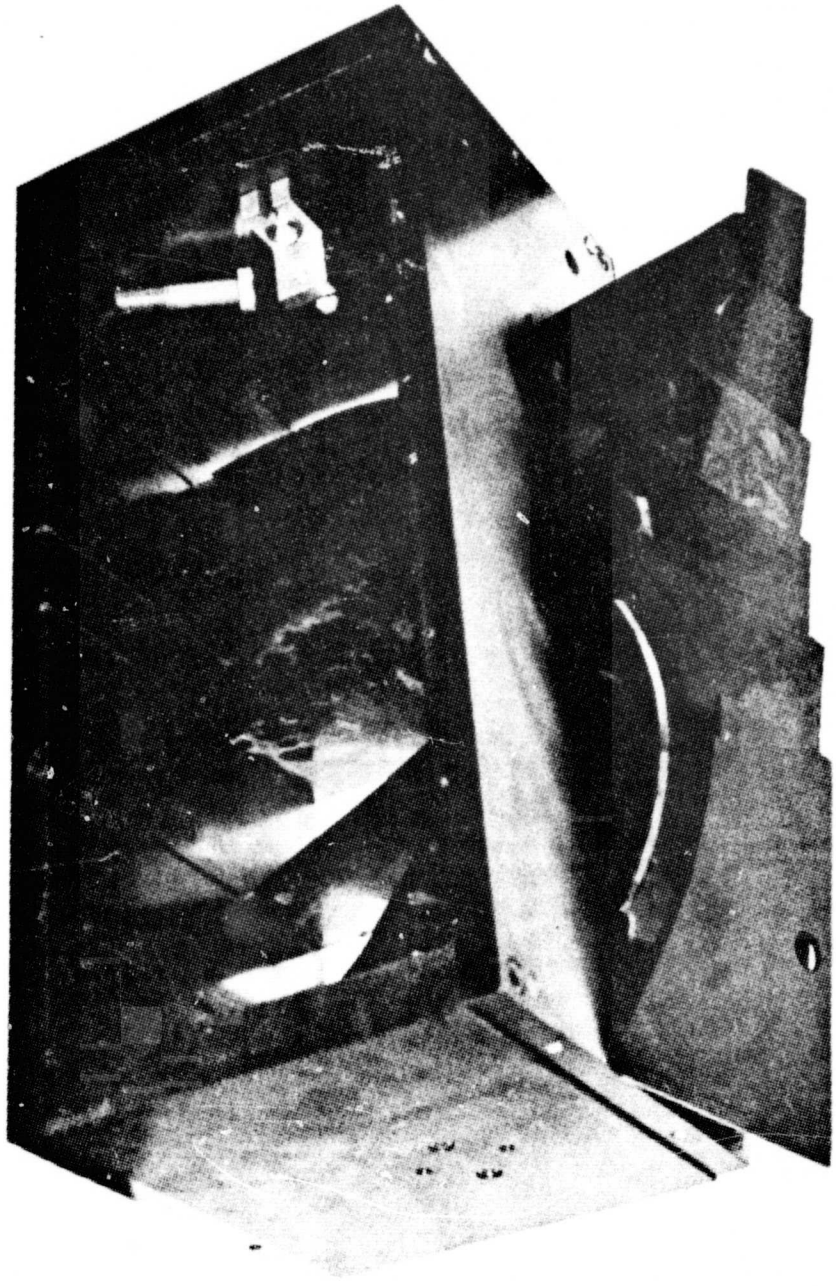

Figure 25. Blade Inspection Fixture and Templates.

Some of the assumptions used in the ply generation were as follows: the plies were to be 0.030-inch thick; there was a full ply located along the mean camber line; there were full plies on the concave and convex surfaces of the airfoil; a maximum of 10% deformation by isothermal forging was planned; and a chemical milling envelope of 0.0025-inch was added. There were a total of thirty-one plies that define the airfoil. These ply designs with the core cavity definitions were quite complex as expected because of the core geometry. The computer, although defining the core cavity geometry in the ply, did not define the radii of core corners in the ply. This was accomplished manually because definition by computer could have taken several months. In addition, the computer plots were modified for additional stock in the root and in the tip (for the eleven full length plies only) Ply designs are shown in Appendix A along with a more detailed discussion of the ply generation program. An example of ply generation is shown in Figure 26 for Section AA.

Three methods of producing plies were considered: tape controlled punch press (Wiedematic), stamping and NC milling. The initial quote from the NC punch press vendor was very high because the vendor considered the purchase of many specialized punch tools. A requote using conventional punch tools was received and was less than one-third the previous quote. Some hand-working of the plies would be necessary using the conventional punch tools if this approach had been selected. The stamping vendor no-quoted the request. An order was placed with the NC milling vendor because of lower cost and delivery. The vendor was asked to machine twelve extra pieces of the center ply. Based on the results of the diamond specimens, material for debulking between cores was needed. To supply this material, a portion of the center ply that surrounds the cores was added for debulking in addition to the full length center ply. Twelve total sets of 0.030-inch Ti 6Al-4V plies were manufactured. All plies were machined such that the primary working direction of the sheet was perpendicular to the stacking axis of the blade.

3. Core Design and Manufacture for Hollow Fan Blades

Core designs, of which there are four, were supplied by P&WA. Based on the results of the critical experiments task the cores were made from AISI-1045 steel. Many manufacturing approaches were considered to fabricate the cores including casting, powder metallurgy, forging and tracer mill machining from masters. All of the above approaches were found to be either too costly or not applicable because of the complexity and length of the cores. The least costly and most direct approach was NC machining. The vendor developed NC tapes to produce cores without any twist using TRW supplied NC tapes. The NC tapes were initially checked out on machining plexiglass and were found to be acceptable. Twelve sets of cores were NC machined, one of which is shown in Figure 27. Figure 27 depicts the core passages between the upper and lower sections of the cores. The core passage design selected allowed for a width of 0.250-inch by the pitch thickness of the core at the location of the passage. The distance between passages for each core was 1.00-inch. The core passages by the edges were allowed to be machined similarly with the edge. Reduced core passage sections, that is less than pitch thickness and recessed from an edge, were avoided to minimize the core costs.

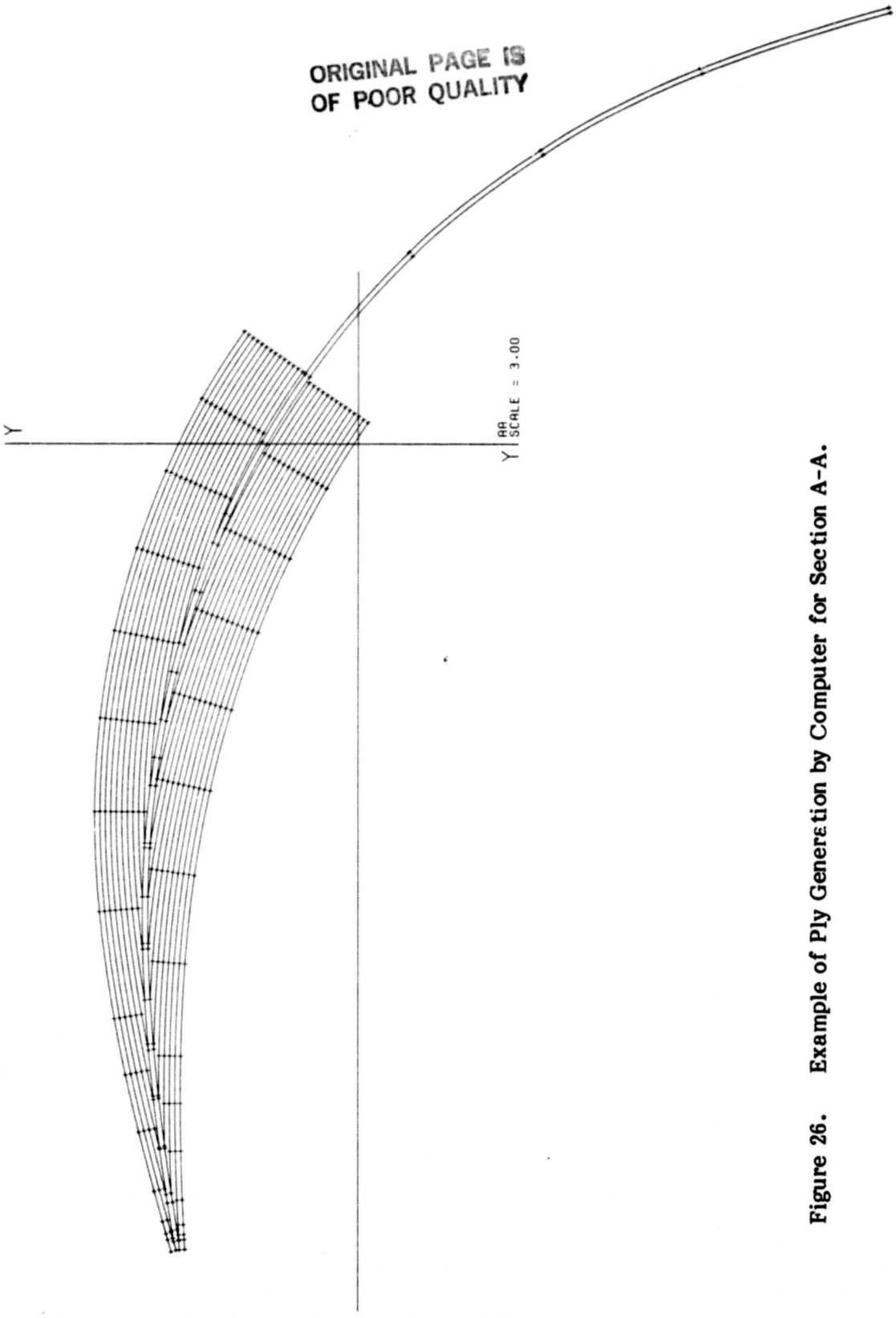

Figure 26. Example of Ply Generation by Computer for Section A-A.

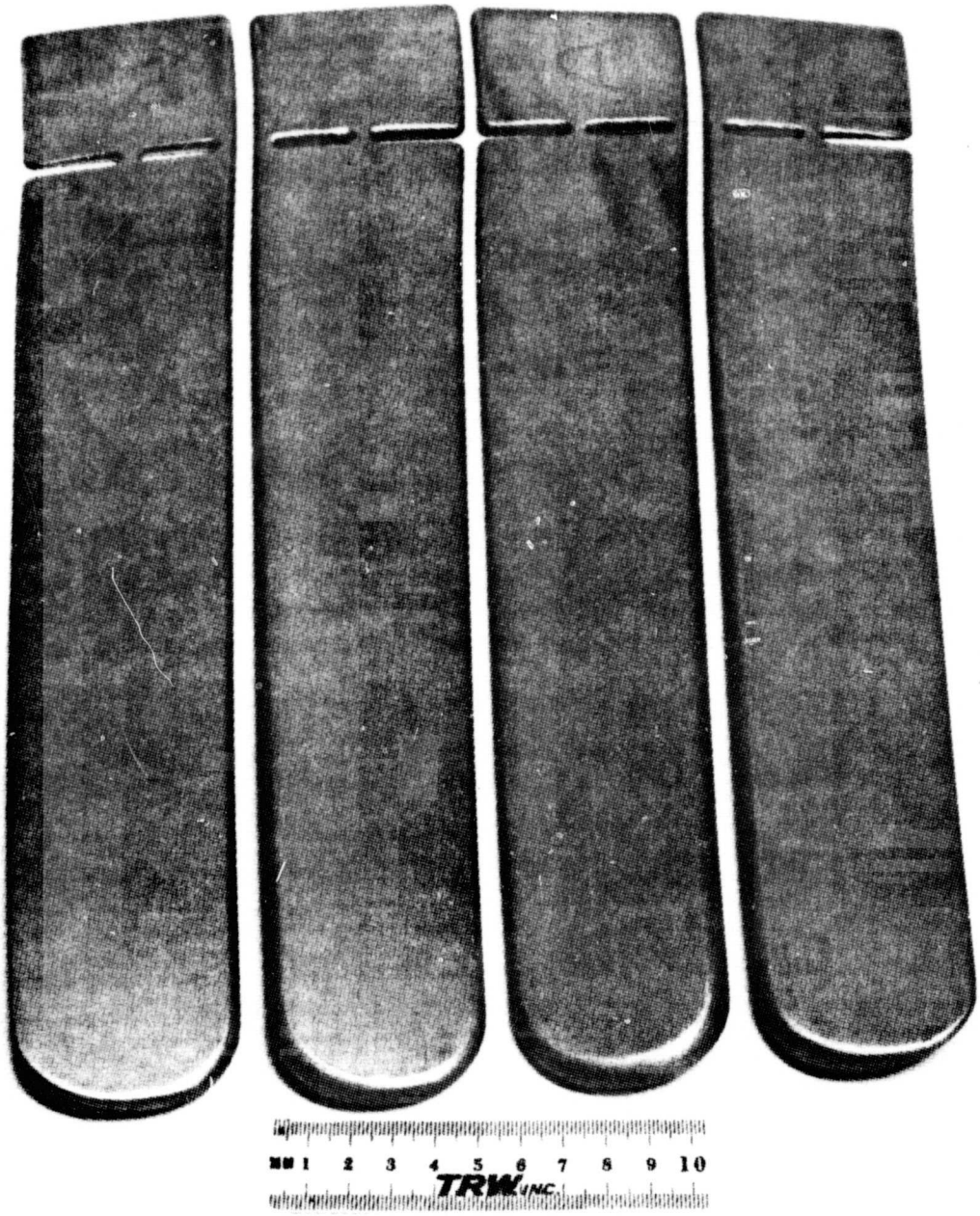

Figure 27. NC Machined 1045 Steel Cores for Hollow Fan Blade.

4. HIP Cans for Hollow Fan Blades

The initial approach to encapsulating the blade for HIP was to use a DQAK steel can that was either deep drawn or hydroformed. The TRW designed can included provisions for seam welding and a gutter to prevent iron vapors that may arise during welding from contaminating the titanium alloy plies. Quotes received from two deep draw vendors indicated a reasonable cost for the cans; however, the tooling costs were excessive since the deep draw on the root area required two sets of tooling. Due to the large size of the cans, the hydroform vendor no-quoted the job even if they were allowed to make two-piece halves.

Because of the high costs and the inability to use a hydroform vendor, TRW decided to use a 0.030-inch titanium skin for the can material. Figure 28 is an illustration of the blade root design and airfoil. The titanium cover sheet was approximately 1-inch wider on each side and end than the maximum width and length dimensions. Because of the difficulty and cost of forming the sheet around the root, the root block was TIG welded to the sheet cover skin. Solid root blocks were selected because of this alternate approach. Previously the root was to be made by a lamination approach. The root blocks were welded to the cover skins prior to any assembly. After assembly which is discussed in the next section, the oversized cover skins were seam welded together. This design allows for removal of sufficient material to assure that no weld heat-affected zone is present.

This approach was also used to make rootless blades in the blade fabrication task. Titanium alloy cover sheets, either 0.030- or 0.060-inch thick were used. The sheets were designed to be oversize to allow for seam welding. The assembly of these blades is discussed in the next section.

5. Fabrication of Hollow Fan Blades

Processing parameters selected for fabrication of the hollow fan blades were based on the information gained in conducting the first task of this effort. In the blade process development task a total of nine blades were assembled and HIP. For discussion purposes a simplified routing is presented below:

- Clean plies per P&WA procedures.
- Degrease cores.
- Uncambered, flat ply and core assembly (either with or without titanium alloy root blocks).
- Weld solid root blocks to titanium alloy sheet (0.030-inch) cover skin.
- Assemble plies and cores - registry maintained by two steel pins in root area and one steel pin in tip area.
- Place assembled package between root/cover skin or cover skin. Steel pins in root area of plies extend into the solid root block.

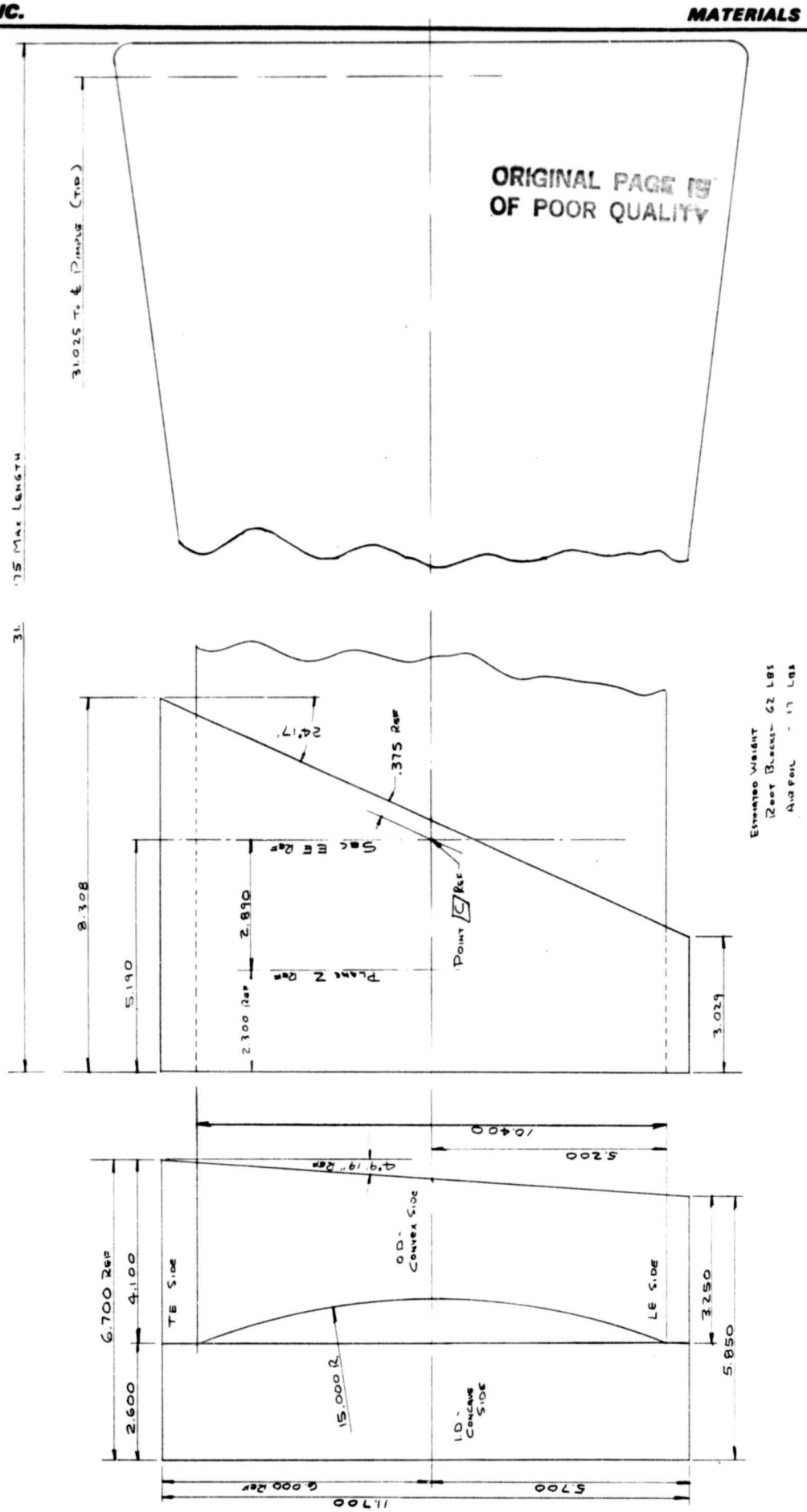

Figure 28. Airfoil-Root Assembly Configuration.

- o Seam weld periphery.
- o Leak check using a mass spectrometer.
- o Hot outgas and anneal at 1550°F.
- o Sealed in EB chamber.
- o X-ray for core location.
- o HIP.
- o X-ray.
- o Trim excess can material.
- o Camber in camber tooling.
- o Twist in twist tooling.
- o Forge in isothermal forge tooling.
- o Finish machine.
- o Leach out cores.
- o X-ray.

Obviously the above is a simplified routing of the blade manufacture, but is presented as an introduction to discussing the effort directed at producing the hollow fan blade.

As noted above the blade layup was an uncambered, no twist condition. This approach was selected for several reasons. It was TRW's belief that core registry could be better maintained during assembly and subsequent handling. Earlier data indicated that the core would easily camber and twist. Cambering and/or twisting plies prior to assembly would require extensive tooling commitments, and when HIP cans were being considered, cans would be even more difficult to form.

Four iterations of blade assembly were performed in the conduct of this task. The experimental procedures used for each iteration are discussed in detail below.

a. First Iteration

The first iteration to produce the hollow fan blades was directed at fabricating one solid blade and one blade with simplified cores. Titanium cover (can) sheets were TIG welded in argon to the root halves. Two sets of titanium plies were hand cut by band sawing to the external contour designs described by the computer. NC

machined plies and cores were not available at this stage of the program. One-half of the blade as defined by these plies is shown in Figure 29. This figure also indicates the cavity in five plies per half that defined the core. Basically, the core was similar to the cores used for the diamond specimens. The addition of cores in one blade assembly was for the purpose of learning more about core movement during HIP, camber, twist and forge. The hole in the plies was stamped using one of the stamping dies used for the diamond specimens. Core design was simplified, basically a flat plate five plies thick (0.150-inch) by width and length of the diamond core. The cores were machined from AISI O-1 steel plate stock (0.9% carbon level). The plies were assembled using the ID root block (flat block). OD root block (contoured block) was placed onto the pins and pressed down (arbor press) onto the ply-ID root block assembly. The package was spot welded together along the periphery to secure the assembly for handling. The package was then seam welded together in air except for an area at the root end saved for insertion of an evacuation tube.

A 5/8-inch diameter by 0.028-inch wall thickness CP titanium tube was placed between the cover sheets at the root end where there is a natural gap due to the total ply thickness. The tube was flattened slightly and a 3/8-inch diameter AISI O-1 steel bar was placed inside the tube in the back of the root area to prevent the tube from total collapse during HIP. The tube was TIG welded in argon to the cover sheets. Some filler sheets of titanium were tack welded together to form a step wedge and placed in the back of the root block between the sheets to minimize shear forces in the back area of the root during hot isostatic pressing. These sheets were added prior to seam welding. The blade assembly was leak checked using a mass spectrometer, vacuum hot out-gassed at 950-1000°F for a minimum of six hours and sealed by hot forging the evacuation tube. Dimensional measurements before and after sealing indicated that the hot forged seal was effective. The end of the tube was TIG welded as a precautionary measure after hot forging.

Several problems were encountered during the assembly of these first two blades. Welding of the 0.030-inch thick cover sheet (can) to the root block was time consuming due to problems associated with fitup and restrictions in manipulating the large blocks within the welding chamber. Procedures established with the first blade resulted in efficient welding of the second blade (root block-sheet). Although considerable care was taken in drilling the pinholes in the root portion of the plies, the pin hole location was not accurate enough. Some correction by hand filing was required. The NC machined plies will not have this inaccuracy problem. On the plus side, blade assembly took less than an hour. Tack welding of the two outer sheets prior to seam welding was easily accomplished. Seam welding of the blade periphery required thirty-five minutes and the weld quality appeared to be excellent. As noted earlier, no leaks were evident in the assembly inspection.

The two blade assemblies were sent to IMT for HIP. The HIP cycle was altered to allow a total time of 4.5 hours at 1750°F (compared to 2.5 hours used for the diamond specimens) because of the massive size of the root blocks. The special pressure delay cycle that was used for the diamond specimen in Task I was employed.

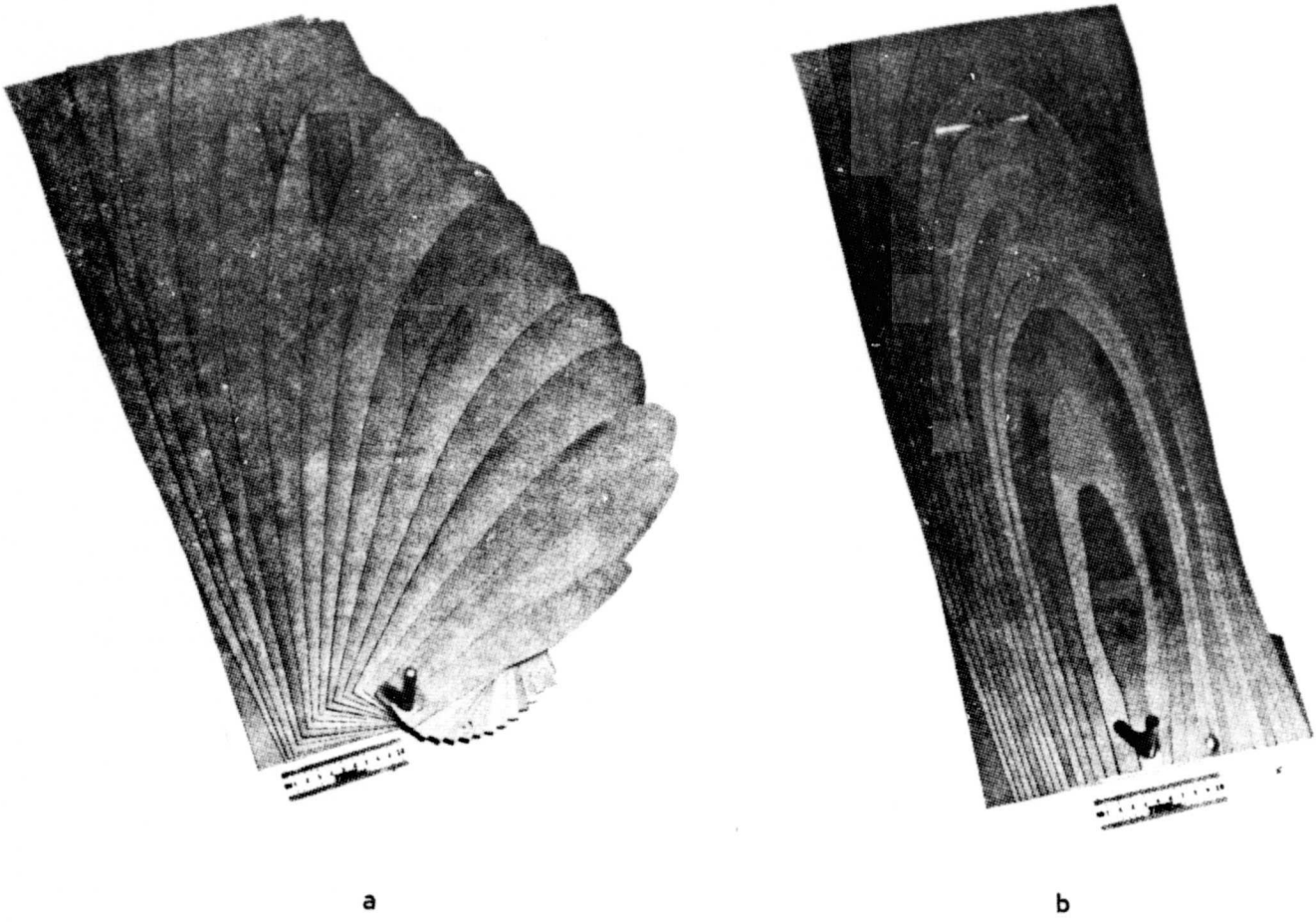

a b

Figure 29. Hand Cut Titanium Alloy Plies Used in First HIP Blade Iteration.
a. Fifteen Plies for One-Half Airfoil.
b. One-Half Airfoil Assembled.

b. Second Iteration

The second iteration to produce a Task II blade evaluated the re-HIP of blade 2 and assembly and HIP of a rootless cored blade (blade 3). Blade 2 leaked initially during HIP due to a TIG failure near the evacuation tube at the root end of the blade. Based on IMT's suggestions and a review of the welding in this area at TRW, a different sealing approach at the root end was evaluated. A 3/4-inch diameter titanium bar with a 3/16-inch diameter hole drilled through the center was used as the evacuation tube. A 1/2-inch thick plate of titanium with a 3/4 diameter hole drilled through the plate to accept the heavy walled evacuation tube was machined. The tube was TIG welded to both sides of the plate and the plate was TIG welded to the back of the root blocks. The blade was leak checked using a mass spectrometer, hot out-gassed and annealed at 1550^{O}F for one hour, leak checked again, and sealed by forging the evacuation tube. The higher hot outgassing temperature was selected to help anneal any residual stress due to welds.

The rootless blade was assembled with the NC machined plies and cores. One half of an assembled airfoil (plies only) is shown in Figure 30. Assembly was accomplished without any problems. To insure core location, the edge cores were held in place by a strip of Ti 6Al-4V 2.5 mil foil wrapped around the two central plies and tack welded to the core surface. This approach was easily accomplished and currently appears to be a good solution to avoiding core displacement. At the root end of the blade, a series of rectangular plies (filler material) was layed up and welded together to form a wedge shape. The intent was to minimize sheet metal (can) deformation in this area during HIP. After assembly the package was seam welded along the periphery. Leak checking and evacuation for sealing were accomplished through a 0.095-inch diameter hole drilled through the cover sheet at the root end. The assembly was leak checked through the drilled hole using a mass spectrometer, evacuated in an electron beam (EB) chamber, and sealed by EB welding. Assurance of a sealed package was gained by measuring the blade assembly before and after sealing. The sealed package was X-rayed prior to shipping for HIP to assure proper core location. No core movement was noted. Both blades were HIP at IMT using the delayed pressurization and a 4.5 hours at 1750^{O}F HIP cycle.

c. Third Iteration

After can leakage in the first three blades, several process modifications to prevent failures in future HIP iterations were considered. For the rootless blade, filler material should be welded to the root end of the blade and a strip of material should be placed over this joint to prevent flow between the root end and filler material. It was also decided that a can sheet thickness of 0.060-inch would be more desireable than 0.030-inch. It appeared that TIG welding leads to problems with leaks during HIP. Instead of TIG welding the can sheet to the root blocks for blades with roots, the welding was to be accomplished by a combination of seam welding and overlapping spot welding. A simple fixture was built to accomodate the curvature of one root block for spot welding.

Figure 30. One-Half of a Typical Hollow Blade Assembly (15 Plies).

The third iteration included the assembly and HIP of a rootless blade (blade 4) and a blade with a root (blade 5). Assembly, welding and sealing of blade 4 were performed as described earlier for blade 3. There were, however, two significant differences. The filler material was attached to the root end by a 0.030-inch sheet of titanium that overlapped and was welded to the filler material and airfoil plies. Secondly, a 0.060-inch thickness of titanium can material was used. The blade was X-rayed prior to HIP to verify core locations.

The assembly of the blade with the root incorporated one significant change, the can material was seam welded to the flat root block half and overlapping spot welded to the curved root block half. The welded areas are shown for comparison in Figure 31. The welds were leak checked by drilling a hole into the sheet (shown in Figure 31) in the area where the locating pins were used and the root-cover assembly was leak checked by examining with a mass spectrometer. The remainder of the blade assembly was identical to blade 2 including the redesigned evacuation tube-plate at the root end described for the blade 2 re-HIP. The blade was seam welded along the periphery, leak checked, hot outgassed at 1550°F for one hour, leak checked, and sealed. After the hot outgas a considerable amount of can collapse was observed because the interior of the can was under vacuum during hot outgassing and the atomospheric pressure was exerted on the exterior of the can. The collapse accentuated areas containng the cores and some ply endings. The can collapse, however, did not cause any leaks. After total assembly some leaks were found at the corner of the root-cover sheet-back plate interface. These leaks were repaired by TIG welding prior to hot outgassing and shipment for HIP. The same HIP cycle used in the previous iteration was employed.

d. Fourth Iteration

Based on the results of blade 4, blades 6 through 9 were assembled without a root and sealed in a 0.060-inch thick cover skin Ti 6Al-4V can. The decision to assemble rootless blades was based on a decision between P&WA, NASA-Lewis and TRW engineering personnel. Tooling costs for shaped cans were too high for this current effort, and welding a thin structure (can) to a heavy root block and expecting the weld to withstand high shear stresses under HIP seemed implausible. The decision was made to produce only airfoils. In the future a root section could be press diffusion bonded to the airfoil section, a technology that is well understood. Four blades were assembled, placed in the titanium cans (0.060-inch thick), seam welded, leak checked, sealed by electron beam welding, X-rayed, and shipped to IMT for HIP. The only difference in assembly between blade 4 and these four blades was that some material was removed in the area where the pins connect the tip of the core. This material was removed to eliminate "bumps" on the surface that were observed after HIP for blade 4 (see Section IV). Dimensional measurements were made of each blade at eight locations to measure the amount of collapse due to sealing and HIP.

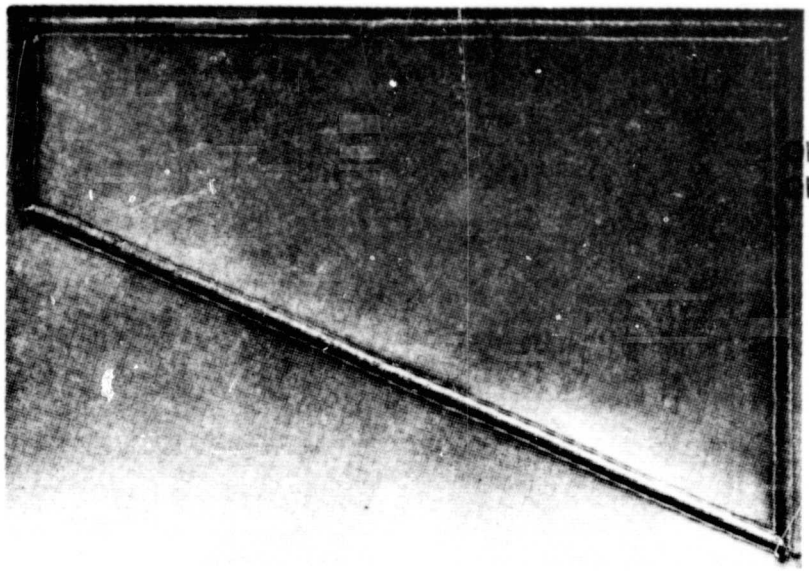

a. Flat Block - Seam Weld

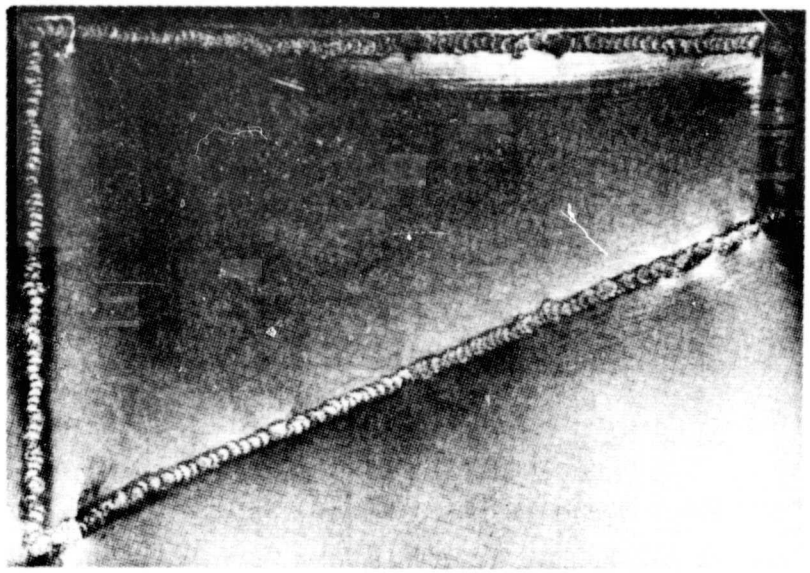

b. Curved block - Overlapping Spot Weld

Figure 31. Surface Condition of Canning Sheet Welded to Root Block.

6. Post-HIP Processing of Hollow Fan Blades

This section discusses the camber, twist, isothermal forging, machining and leaching of blades 4 and 6 through 9. Prior to any post processing root and tip locators were welded to the blades. Placement of these locators was based on the steel pin placement used for assembly.

a. Camber Trials

Prior to cambering blades some tooling trials were conducted with blade 2, the incompletely bonded blade with root. The camber tooling was installed in a 1500-ton hydraulic press (see Figure 32). The tooling was gas torch heated to about 400°F. For the initial tryout blade 2 was band saw trimmed to remove excess canning material along the periphery, protective glass coated, and heated in an air furnace to 1700°F for 2-1/2 hours. Because of the blade weight (~ 90 lb.), the blade was transferred from the furnace to the press with a fork lift. The transfer operation was accomplished easily and the cambering operation was performed in the press. Load requirements appeared to be about 500-600 tons although the load was increased to nearly 1000 tons before removing the blade. Very little if any additional cambering was observed being accomplished on the root area above 600 tons. Most of the tooling was already making full contact with the airfoil.

Based on the results of the first camber trial die rework at the root/airfoil interface was performed. Camber trials were initiated with blade 4. The blade was coated with a protective glass coating and heated to 1750°F for 35-45 minutes. Transfer of the blade to the press was accomplished by using a fork lift. Cambering was conducted similarly to blade 2. Cambering of blades 2 and 4 were performed with the tip locator illustrated in Figure 23.

As discussed in Section IV blade 4 experienced severe tearing near the leading and trailing edges at the intended root/airfoil interface area. The upper camber die was removed from the press for rework to alleviate the shearing problem. Cambering was then planned to be a two-sequence approach. During the first sequence the blade was cambered by placing the blade extended about eight inches beyond the root, cambering, pushing the blade about four inches more into the die and again cambering with no tip locator. The blade was then reheated and again cambered with the blade located by the tip locator in the proper position. For both cambering operations, the blade was coated with a protective coating and heated to 1750°F for 35-45 minutes. Transfer of the blade from the furnace to the press was carried out manually to improve transfer times. The first cambering sequence required less than twenty seconds and the second cambering sequence required less than ten seconds transfer time. The approach described above was used to camber blades 6 through 9.

b. Twist Trials

After cambering and prior to twisting, blades 4 and 6 through 9 were chemically milled. Approximately 0.010-inch per side was removed at this time. Twisting of the blades was planned such that the tip section was twisted first and the near root section of the airfoil last. Initially, the center dies were preset for a counterclockwise

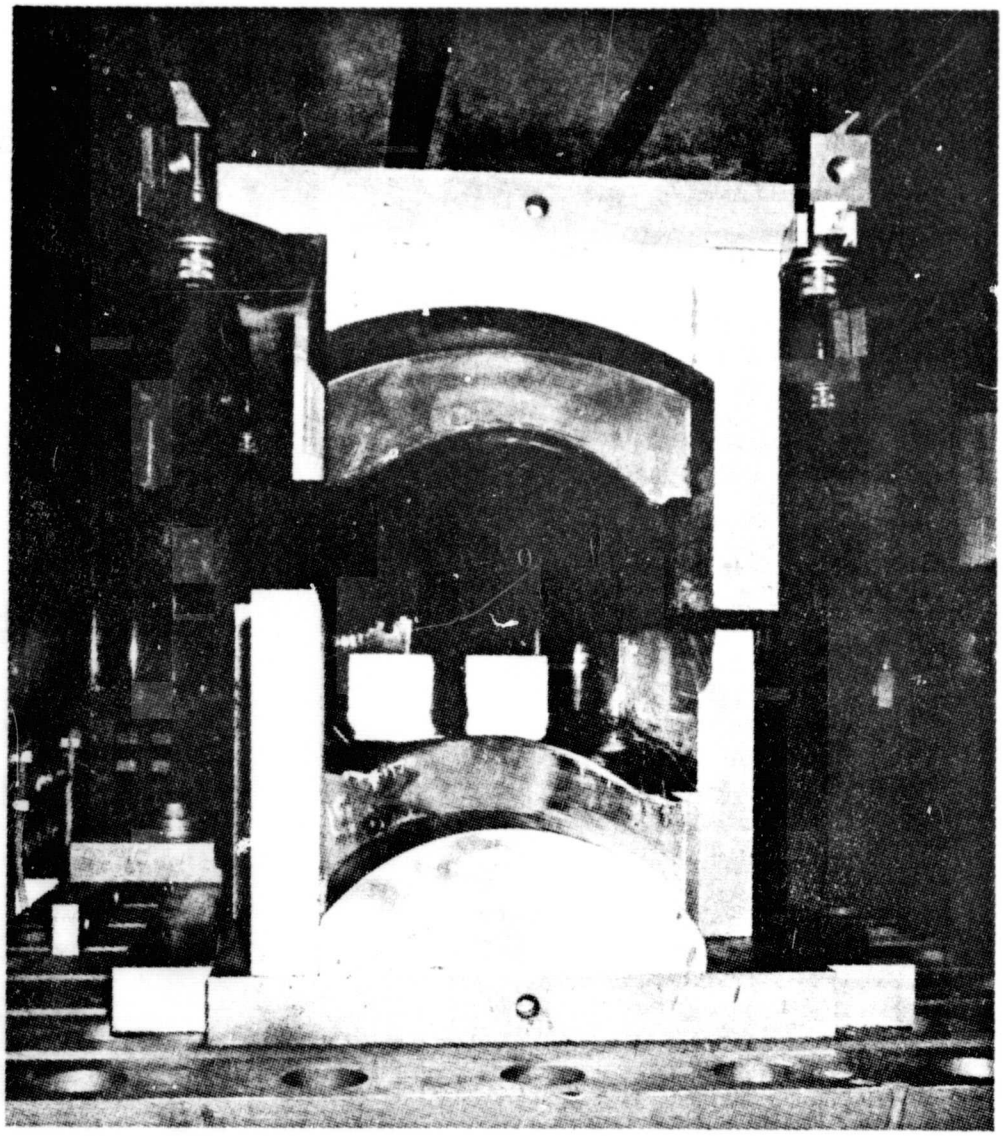

Figure 32. Camber Tooling Shown Installed in 1500 Ton Hydraulic Press.

7.5° twist. For the twisting operations, the tip or root end of the blades was coated with a protective coating and heated to 1750°F for about 30 minutes. The procedure for twisting the tip end was as follows:

- Place heated blade in dies (dies were cold).
- Clamp center section dies.
- Clamp tip section dies.
- Continue twisting by rotating center dies counterclockwise until a 10.5° position of the center dies is reached.
- Release both dies and remove part.

The twist dies are shown installed in the crank press twister in Figure 33.

Only visual inspection of the blades was performed after twisting.

c. Isothermal Forging

Dimensional inspection of the blades after twisting indicated that approximately 0.07-inch of material (0.035-inch per side) should be removed prior to isothermal forging. The removal of this excess material was performed in TRW's production acid stock removal (ASR) facilities. The ASR of the blades was performed within a total tolerance of 0.001-inch.

The isothermal forging dies and die set were installed in a 2500 ton hydraulic press in the TRW Compressor Components Division hydraulic press area. The tooling is shown installed in the press in Figure 34.

One of the problems initially encountered was to determine how to maintain location of the blade when loading in the die. The location initially was to be provided by the root block and a tip pimple locator; however, these blades did not have a root block. Location of the blade within the die was accomplished with a machined stainless steel root segment having holes drilled in the exact location as the locator holes in the root end of the block. The stainless steel root segment was bolted to the blade. When placed in the bottom die, no lateral or longitudinal movement can occur because of the nature of the root segment design with respect to the cavity design.

The procedure for isothermal forging the five blades (blades 4 and 6 through 9) was relatively straightforward. Prior to forging all blades were spray coated with a lubricant which also acted as a protective coating. The stainless steel root segment was bolted to the blade prior to each preheat operation. The forging procedure simply required preheating the part in a furnace, loading the part in the die and holding until temperature equilibrium was reached between part and die, ramp pressure up over a period of about five minutes and then hold under pressure. Table III lists the procedures used for each blade. Blades 4, 6 and 9 were forged three times in an effort to achieve

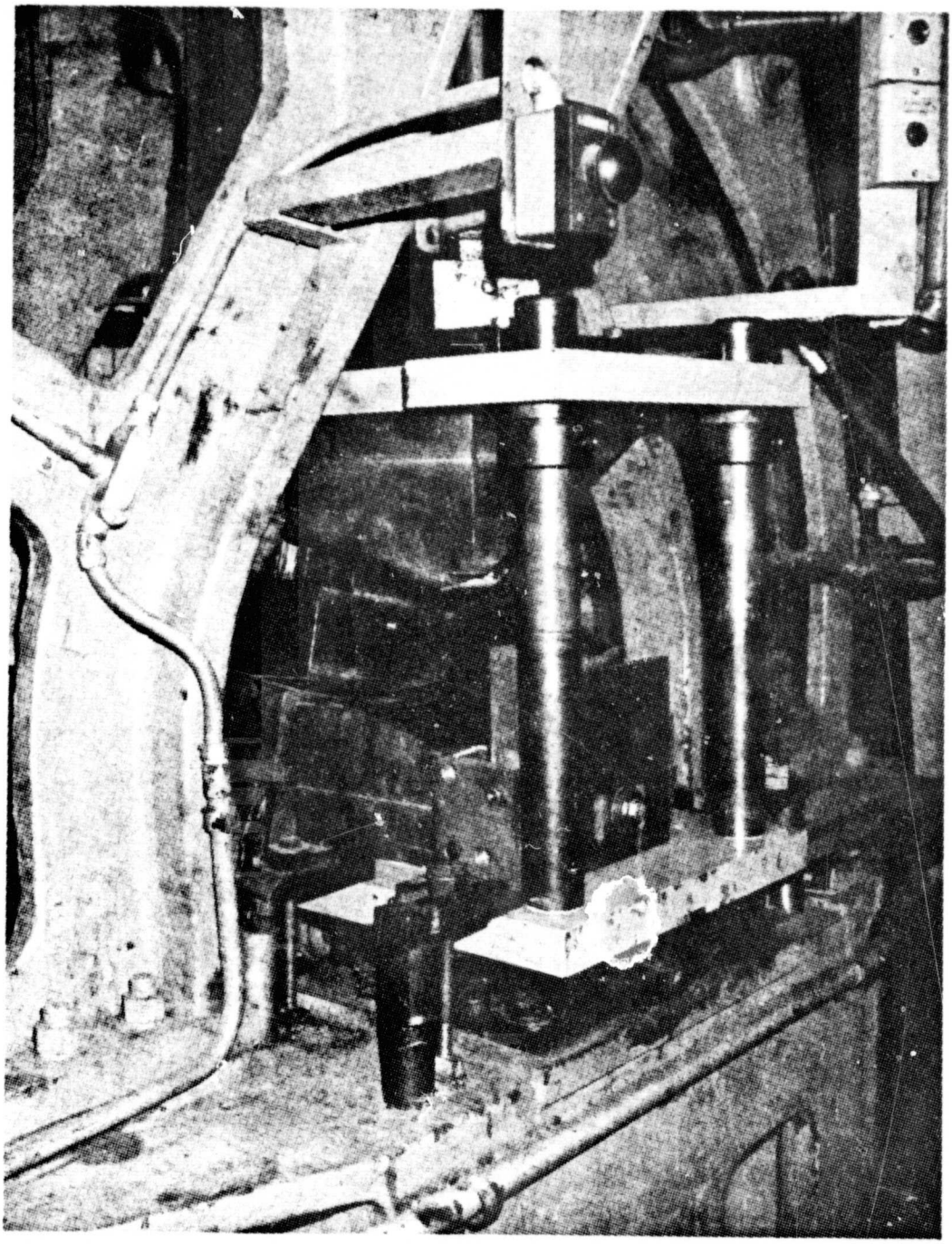

Figure 33. Twist Tooling Shown Installed in Ajax Crank Press Twister. Root and Center Section Dies Shown.

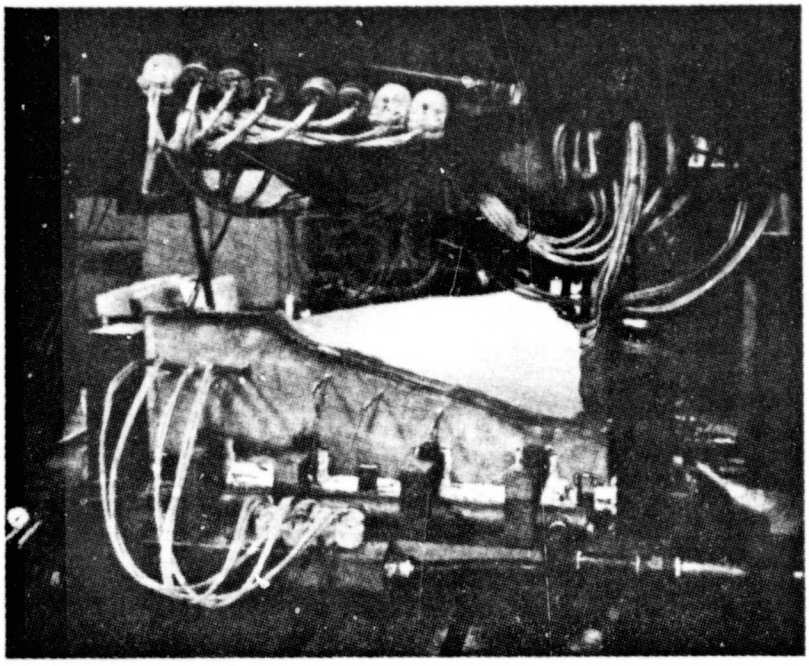

Figure 34. Isothermal Forge Tooling Shown Installed in 2500 Ton Hydraulic Press.

TABLE III

Processing Procedures for Hollow Fan Blades

Blade 4	Blade 9*	Blade 6*	Blades 7 & 8*
Spray Coat	Spray Coat	Spray Coat	Spray Coat
Preheat: 1100°F/10 Min.	Preheat: 1100°F/10 Min.	Preheat: 1100°F/10 Min.	Preheat: 1100°F/10 Min.
Load in Die, Hold 10 Min. (Shim: R-.620, T-.620)	Load in Die, Hold 15 Min. (Shim: R-.760, T-.300)	Load in Die, Hold 10 Min. (Shim: R-.940, T-.300)	Load in Die, Hold 10 Min. (Shim: R-1.00, T-.300)
Apply 1500 Tons/10 Min.	Apply 2000 Tons/10 Min.	Apply 1800 Tons/10 Min.	Apply 1800 Tons/10 Min.
Remove Part	Remove Part	Remove Part	Remove Part
Repeat Above for Two Restrikes Except	Repeat Above for Two Restrikes Except	Repeat Above for Two Restrikes Except	
Restrike #1 (Shim: R-.620, T-.540)	Restrike #1 (Shim: R-.860, T-.220)	Restrike #1 (Shim: R-.940, T-.240)	
Restrike #2 (Shim: R-.700, T-.460)	Restrike #2 (Rework Flash Land and Shift Die .125-Inch Tip to Root)	Restrike #2 (Shim: R-.945, T-.300; Shift Tip .125)	
	Rework Flash Land Prior to Blade 6		

* Blades 6, 7 8, and 9 hot formed prior to isothermal forging.

desired thickness dimensions. After forging blade 4 the first time it was noticed that although the blade fit the die reasonably well it would be desireable if a better fit could be achieved. A better fit on the first hit minimizes transfer time and prevents die temperature losses. Blades 6 through 9 were given a hot form operation in the isothermal forging dies. This simply means that spray coated blades were placed in the die cold, die heated for five minutes, and the dies were then clamped tight together (required about 100-200 tons). The pieces were held under pressure for not more than 30 seconds and then removed from the die. After recoating the pieces were ready for isothermal forging. Blades were measured between each restrike. Because of problems of trying to obtain full blade contact at the tip end, the die was reworked three times in the press to relieve flash land areas. In addition, the die was "cocked" by using external shim blocks and plates a maximum of 0.700-inch from root to tip. The external shim blocks and plates can be seen on the press bed in Figure 34. Die temperatures were 1700°F nominal. The final forging procedures selected for blades 7 and 8 which were struck only once were as follows:

- o External shims: Root 1.000-inch - tip 0.300-inch
- o Spray coat blade
- o Attach root block locator
- o Preheat in furnace, 1100°F/10 minutes
- o Load in die, hold for 10 minutes
- o Ramp pressure up to 1800 tons in a period of 5 minutes
- o Hold under pressure 10 minutes
- o Release pressure, remove part

After forging the blades were routed through kolene and inspected. Inspection included X-ray, pitch thickness, leading and trailing edge thicknesses, core length changes, and wall thickness of sectioned blade. Blades 4 and 6 were sectioned for metallography, internal cavity evaluations and cavity surface evaluations. Blades 7, 8 and 9 were finish machined and cores were leached.

d. Blade Machining and Leaching

Machining of the blades essentially consisted of cutting excess chord stock off, radiusing the leading and trailing edges, and cutting to length. No attempt was made to bring thickness dimensions into blueprint because of the lack of suitable gauge equipment.

After machining two racetrack holes for leaching were machined in the ends of the blades for each core. Hole dimensions for edge cores were 0.100-inch by 0.250-inch and for central cores were 0.125-inch by 0.250-inch. Cores were removed by leaching in a hot (180°F) water-nitric acid (2:1 ratio) bath. Assurance of complete core removal was made by X-ray analysis.

Final blade preparations were an ASR treatment to remove about 0.001-inch per side and vapor blast of the airfoil surface.

IV RESULTS AND DISCUSSION

The results of the diamond specimen and hollow blade fabrication trials are presented and discussed.

A. Task I - Critical Experiments

1. Diamond Specimen Fabrication

a. Diamond Specimen 1

DS1 is shown in Figure 35 after HIP. Visual examination indicated a well bonded specimen. Evaluations of the specimens included ultrasonic C-scan and metallography. At the time specimen DS1 was scanned, the fixture shown in Figure 11, required to hold the specimen, had not been completed; therefore specimen DS1 was scanned in two halves. For this reason, the scans will not match across the transition line. Both ultrasonic through-transmission C-scans are shown in Figure 36. Metallographic portions of the sections indicated in Figure 36 showed no evidence of disbonding. (See Figures 37, 38, 39 and 40). The shadows shown in the C-scans (Figure 36) are not caused by "flaws" but are believed to be caused by a combination of factors, such as the surface waviness resulting from the laminate endings, thickness variations or surface angle and microstructural variations through the thickness of the specimen.

The "noise" evidenced in Figure 36 prevented detection of the 0.010 and 0.020-inch flat bottom diameter standard holes. As previously mentioned a second standard was prepared utilizing material from DS1. Flat bottom holes were drilled in the size range 2/64 to 7/64-inch diameter at two different depths as shown in Figure 10 with the ultrasonic test standard shown after drilling in Figure 41. The dark circular areas on the surface are the drilled holes filled with an epoxy material. Ultrasonic inspection of the standard indicated that depending upon the sensitivity used holes as small as 2/64-inch could be found; however if the location of this hole was not known prior to inspection differences in thickness and ply edges would be considered to be defects. This effect is shown in the Figure 42(a) C-scan. Reducing the sensitivity to eliminate ultrasonic pickup of surface undulations, ply endings and thickness differences is shown in Figure 42(b). The 2/64-inch flat bottom hole is not shown. Basically these results indicate that defects as small as 3/64-inch can be found in the diamond specimens using currently developed ultrasonic inspection methods. The detection of smaller defects may be confused with surface undulations, ply ending thickness differences or other features of the test specimen.

b. Diamond Specimens 2 and 3

As was previously noted DS2 had leaked during HIP. The leak was attributed to the embrittlement of the carburized can. The DS2 canned package was placed in a second can of mild steel, welds were leak checked using helium and a mass spectrometer, sealed and sent for HIP.

Figure 35. Solid Diamond Specimen (DS1) After Hot Isostatic Pressing. The Collapse of the Outer Ply Over the Ply Step Can Be Clearly Noticed. The Stain in the Right Hand Side is Probably Due to Some Contaminants in the Hot Gases During HIP.

ORIGINAL PAGE IS
OF POOR QUALITY

Figure 36. **Ultrasonic Through-Transmission C-Scan of Both Halves of Specimen DS1. The Shadows Shown Are Believed Caused by a Combination of Factors and Not by Delamination. The Sections Used for Metallography Are Indicated.**

79-250

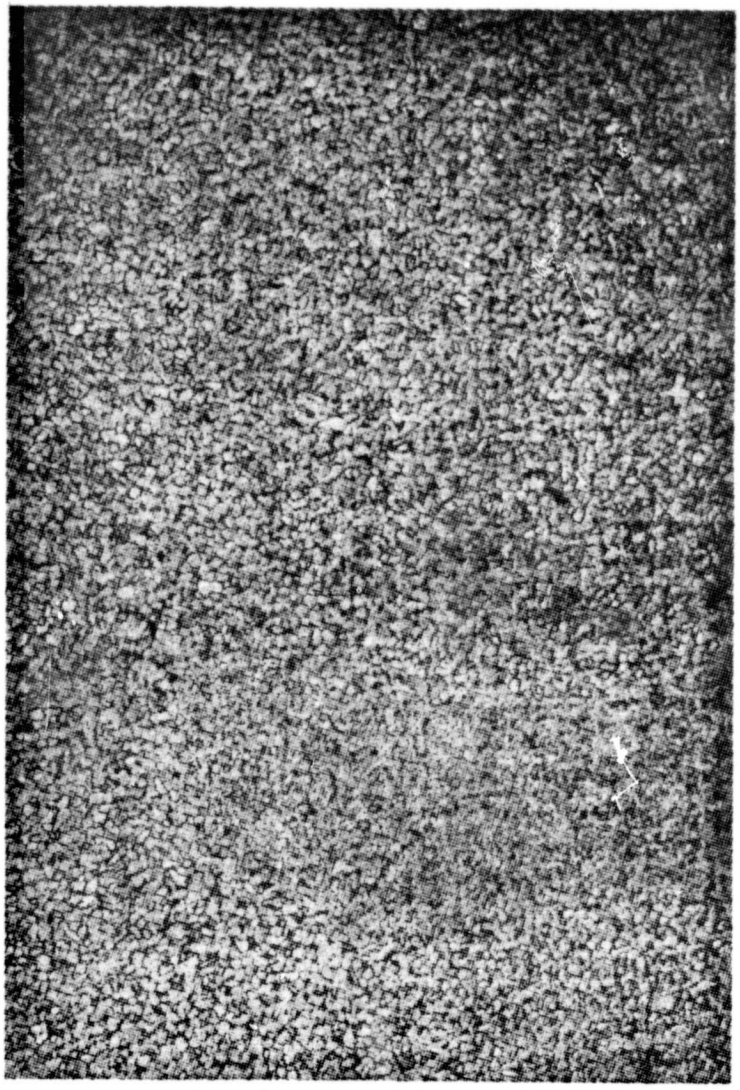

Figure 37. Microstructure of a Portion of Section AA (See Figure 36) of Specimen DS1. The Area of Noticeable Difference in Microstructure Seen in the Lower Portion represents What Used to be a Filler Strip at the End of a Ply. Such Variations in Microstructure Are One Possible Cause for the Shadows in the Ultrasonic C-Scan. Other Areas of Microstructure Variation Are Also Shown in Figures 38, 39 and 40.

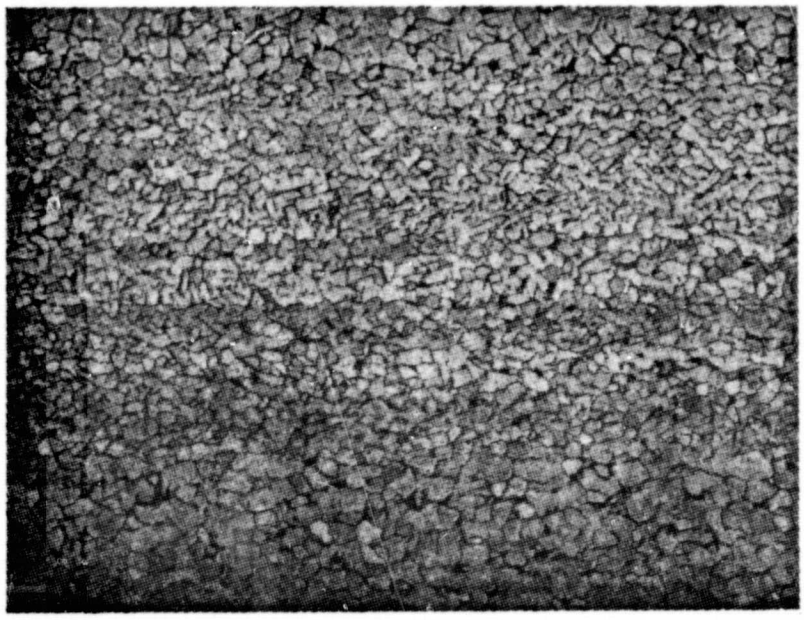

Figure 38. Microstructure of a Portion of Section BB (See Figure 36) of Specimen DS1. See the Caption of Figure 37. 200X

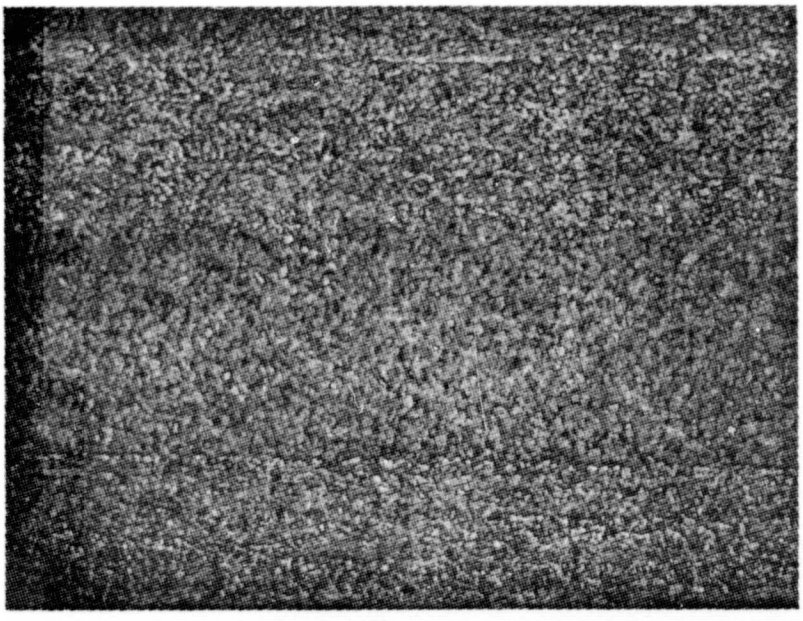

Figure 39. Microstructure of a Portion of Section CC (See Figure 36) of Specimen DS1. See the Caption of Figure 37. 100X

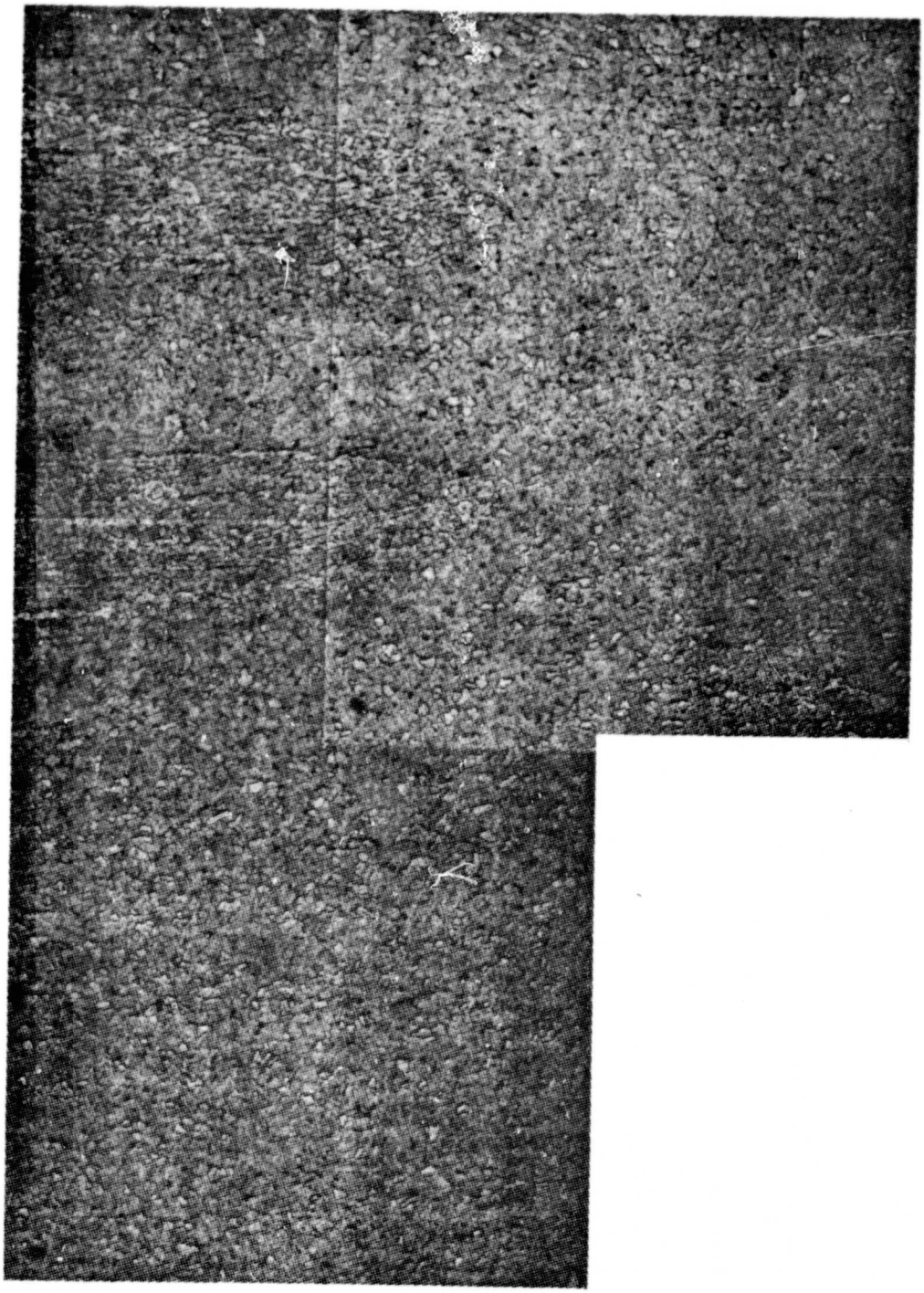

Figure 40. Microstructure of a Portion of Section DD of Specimen DS1. See the Caption of Figure 37. 100X

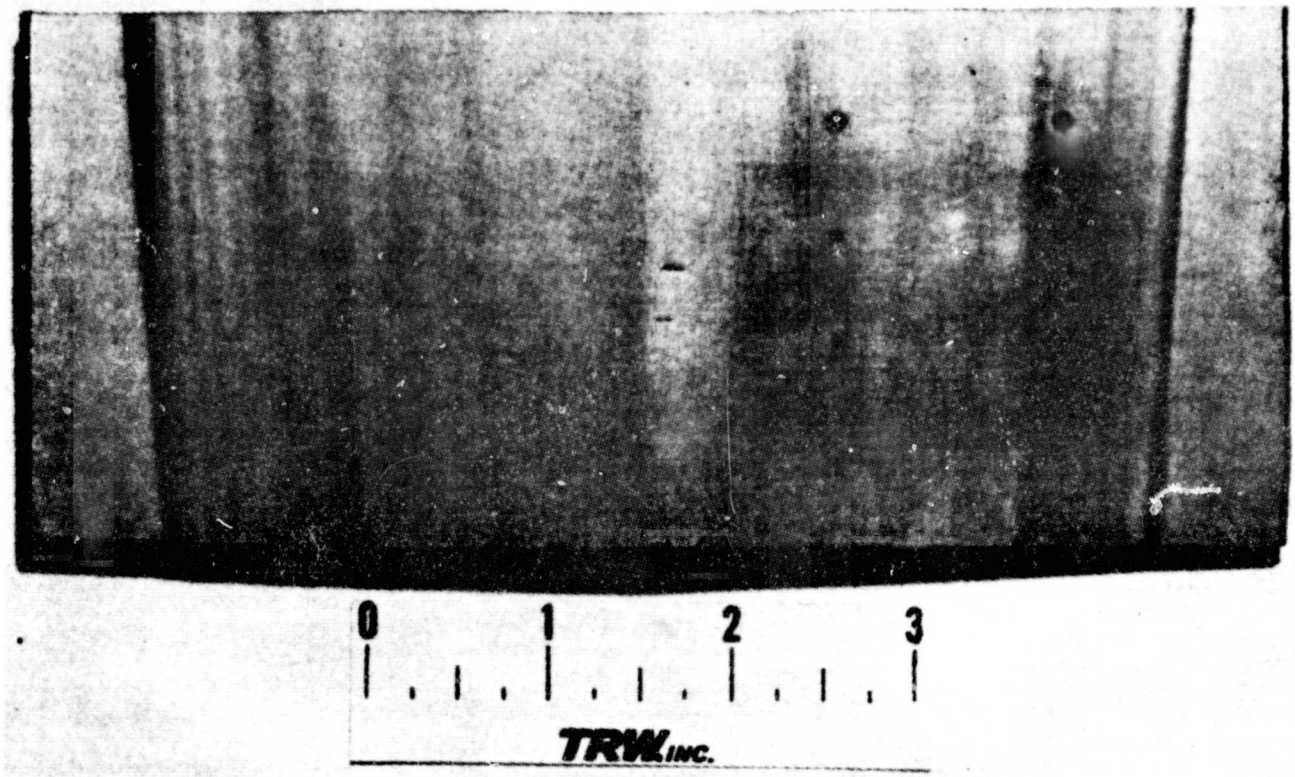

Figure 41. Ultrasonic Test Standard Prepared From DS1 Material.

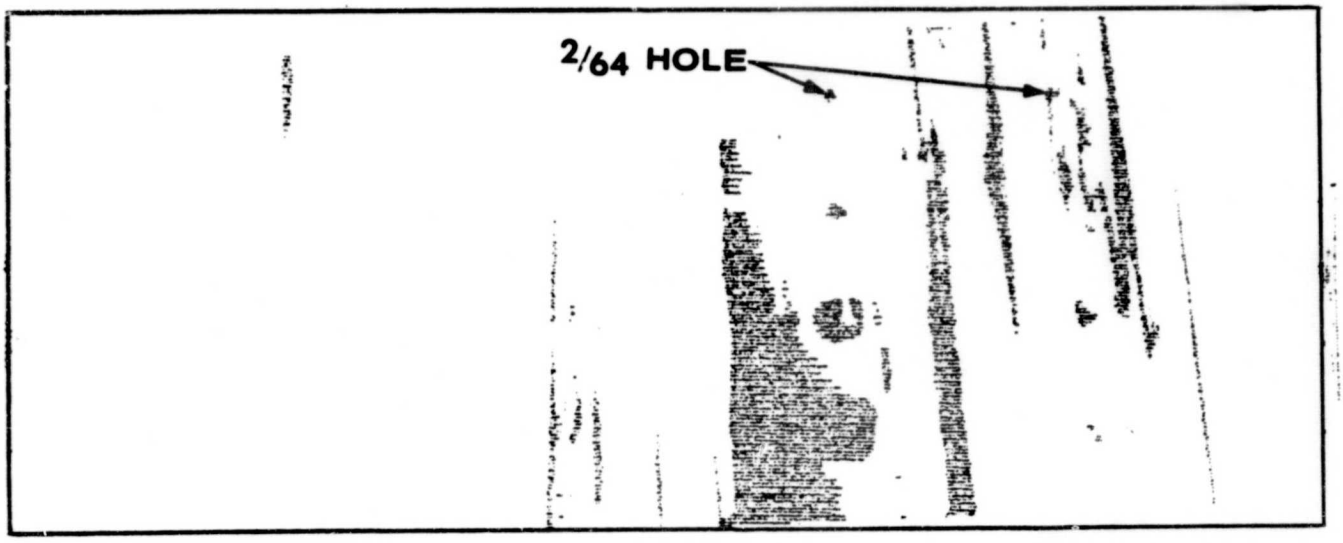

a. ~ 70% Gate Level

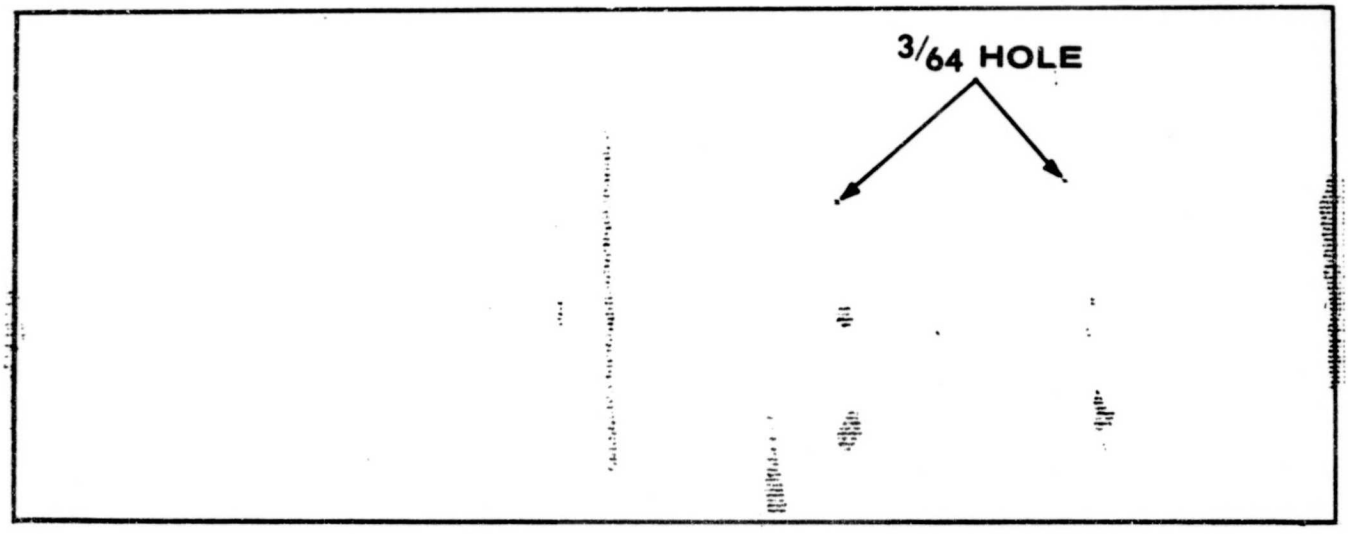

b. 50% Gate Level

Figure 42. Ultrasonic C-Scan of Test Stanard for Two Different Sensitivity Levels.

After re-HIP, which visually appeared good based on can deformation, DS2 was decanned, X-rayed and C-scanned. X-rays indicated a lack of fill and/or bond at the core/titanium interface at the root end. This area is visible in the X-rays shown in Figure 43. Ultrasonic inspection, C-scan, indicated a lack of bond in the area between one of the cores and the root. This defective area is shown in Figure 44. Based on the results to-date with ultrasonics the C-scan should be a mirror image along the centerline of the diamond specimen. Other dark areas in the C-scan are attributed to either cores, differences in material thickness, or surface irregularities.

The lack of a total bond in the specimen is related to the can failure (leak) during the first HIP run. Apparently some bonding was achieved between the laminates, but the leak caused the entrapment of argon gas used in HIP. The argon remained during the second HIP run causing the poor bonds. An example of voids at the bond lines of the laminates is shown in Figure 45(a). This section corresponds to the defective area noted in the Figure 44 (C-scan). Other areas of the diamond specimens also had voids present at the bond lines, but in most cases not as many as shown in Figure 45(a).

Several observations were to be made from this diamond specimen. The specimen was expected to provide information on the flow of the steel cores with respect to the titanium laminate at the hot isostatic pressing conditions. Specimen DS2 also had laminated root blocks, but without an airfoil-to-root radius. The surface condition of the cores was also to be evaluated as machined, polished on abrasive paper, or wrapped in 0.002-inch Ti 6Al-4V foil. Due to the lack of bonding at the core/laminate interface conclusions with respect to the effects of different core surface conditions could not be made. Figures 45(b) and 45(c) indicate that straight cut titanium core plies flow and form around the mild steel cores without causing core deformation. The radius at the root/airfoil interface was also found to be quite smooth conforming to the can radius as shown in Figure 45(d). In the initial layup a ninety degree angle was present at the root/airfoil interface.

Visual inspection of DS3 indicated a successful HIP. The specimen was inspected using ultrasonic evaluation techniques, primarily to establish inspection criteria for the steel cores. DS3 had been evaluated prior to DS2 due to re-HIP of DS2. The C-scan is shown in Figure 46. Also shown in the scan are the sections used for metallography. Typical microstructures of these sections are shown in Figure 47. The C-scan did not indicate any areas of concern.

Metallographic examination of samples of Sections AA, BB and CC revealed no evidence of any unbonded area. Figure 47(a) shows a representative portion of Section AA. Some difference in the microstructure believed to represent a 0.010-inch thick ply is noticeable in the center of the field. Figure 47(b) shows a portion of the interface between the 1045 steel core plane and a titanium laminate. An estimate of the thickness of the diffusion zone is on the order of a few microns (2 to 3 μm). Figure 47(c) shows a portion of the interface where the titanium insert, titanium laminates and steel core meet. Some distortion of the interface can be seen. This distortion is caused by movement of titanium and/or steel core into a void area at the laminate-insert-core interface.

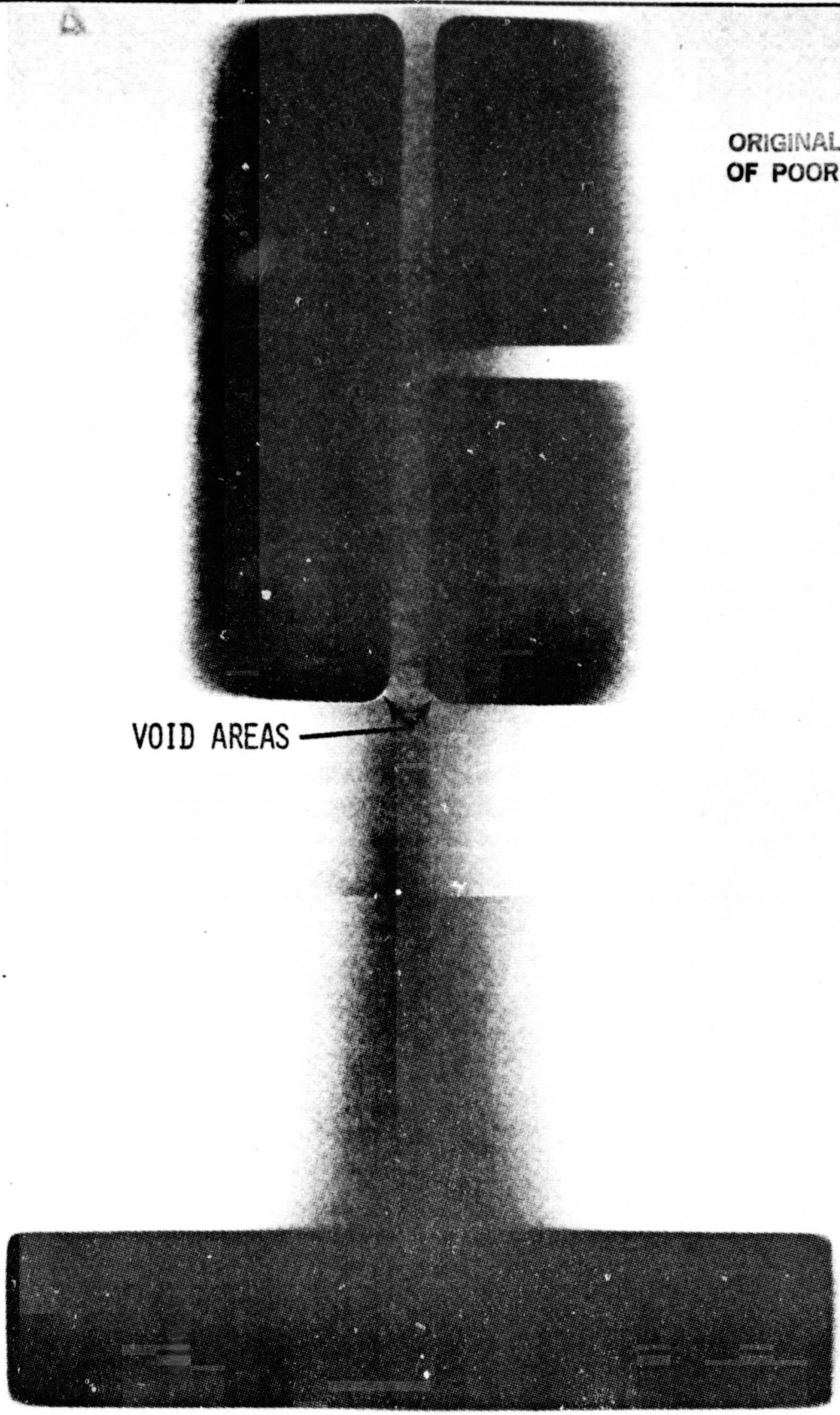

Figure 43. X-Ray of DS2. Note Lack of Fill at Core Ends.

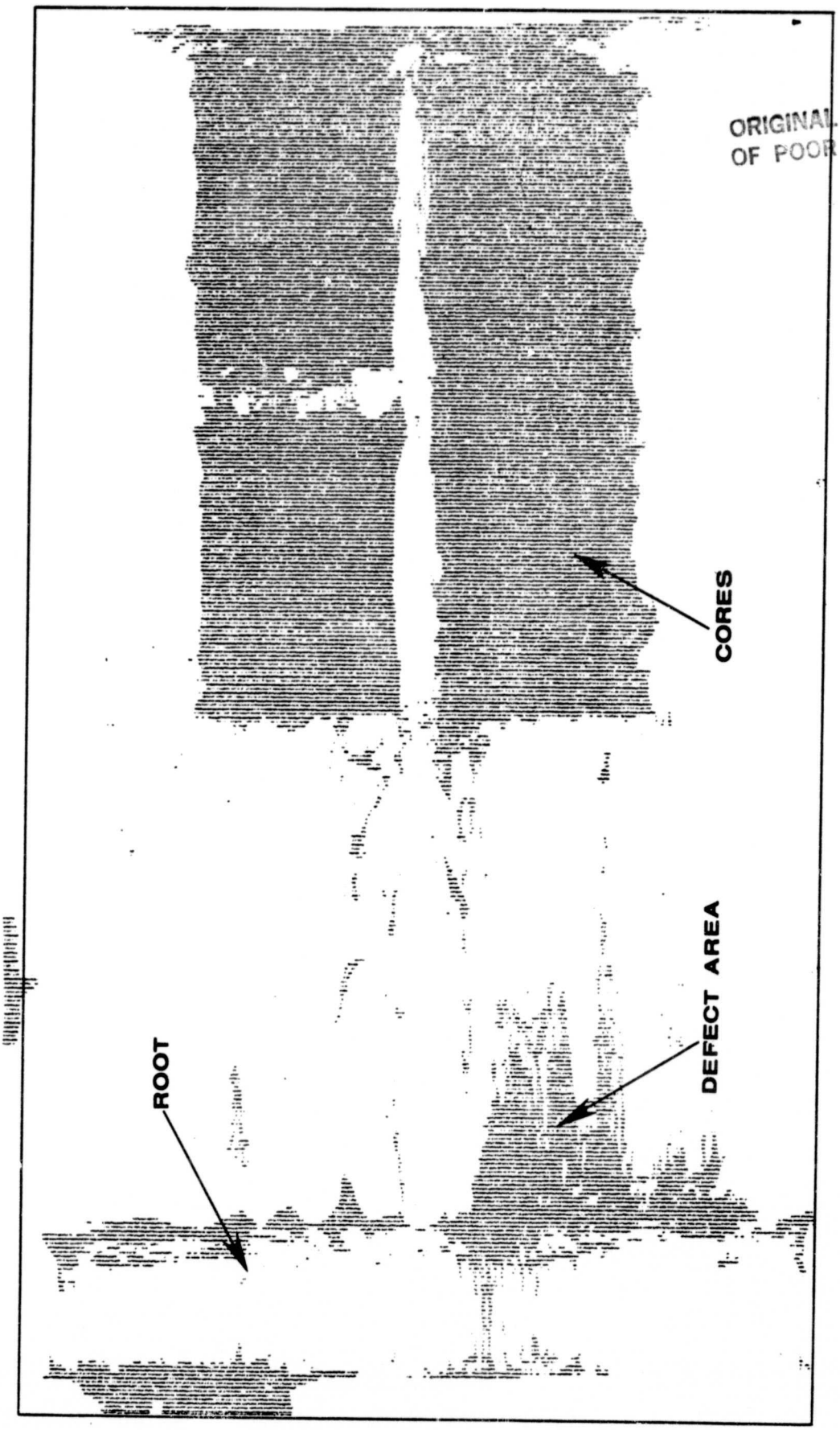

Figure 44. Ultrasonic C-Scan of Diamond Specimen Two.

a. Typical 100X

b. TE Radius 30X

c. Core End 30X

d. Root Radius 30X

Figure 45. Typical Microstructures in DS2 at Several Areas.

Figure 46. Ultrasonic Through-Transmission C-Scan for Specimen DS3. Sections Cut for Metallography Are Shown.

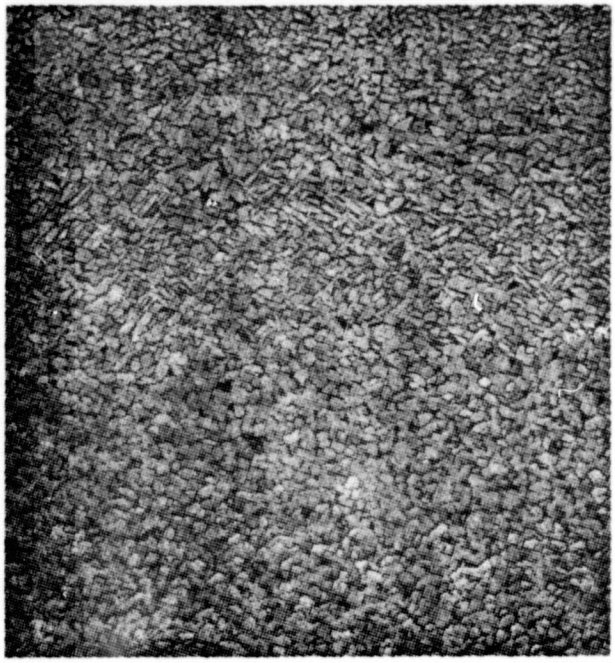

a) 100X

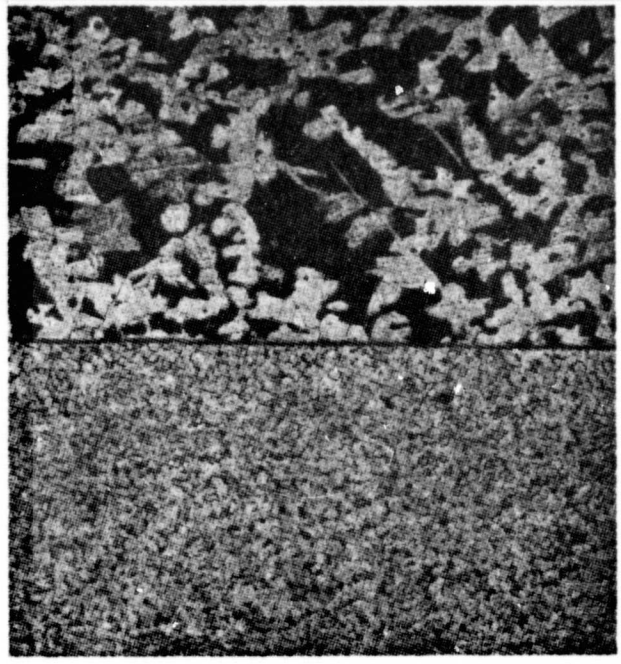

b) 100X

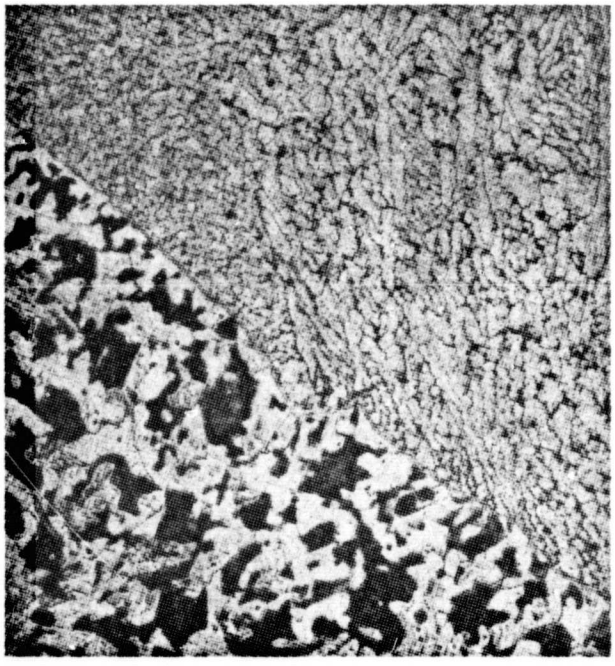

c) 100X

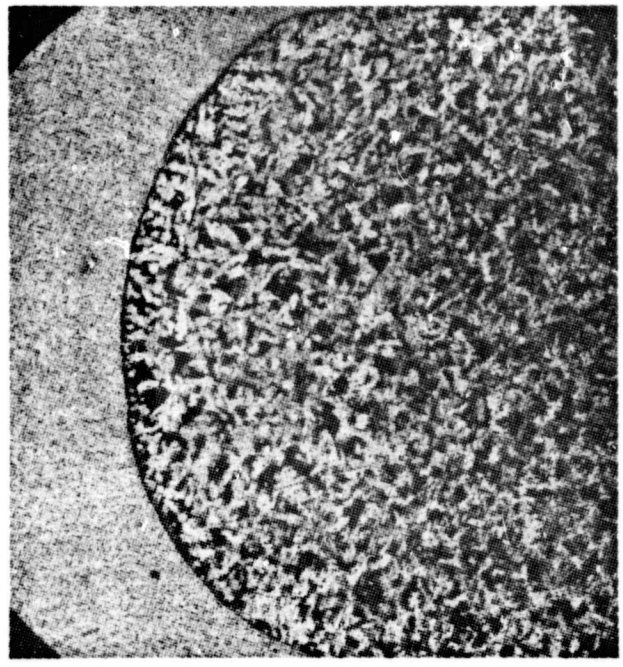

d) 30X

Figure 47. Representative Microstructures of Sections AA, BB and CC (Figure 46) of Specimen DS3. a) A Portion of Section AA- A 0.010 Thick Ply is Seen in the Center; b) A Portion of the Steel Core - Titanium Interface, Representative of Sections BB and CC. Another Portion of the Interface is Shown in c; d) The 0.062 Radius of the Steel Core.

c. Diamond Specimens 4, 5 and 6

Visual examination of the third lot of diamond specimens (DS4, 5 and 6) indicated that DS4 and DS5 were successfully HIP while DS6 showed evidence of a leak. All cans stripped easily from the specimens with no evidence of bonding. The diamond specimens appeared to be flat at the center in some areas and thinner than designed. The deformation of the diamond specimens was attributed to the second stainless can. It appears that the stronger stainless can applied non-uniform pressure to the mild steel can thus causing a "flattened" diamond specimen. Visual observations of the root/airfoil radius indicate that the step radius and the insert are approaches which could give sufficient radius detail and require only a simple machining operation or possibly could be formed further to a net surface during isothermal forging. X-ray evaluations indicated complete fill around the cores with some core shift found for specimen 4. The core shift could have occurred during handling after assembly or could have been due to the double canning which prohibited true hydrostatic conditions. Ultrasonic C-scan evaluations of the diamond specimens showed no delaminations larger than 3/64-inch.

Metallographic evaluations of the titanium-can interface have shown that all four methods of can surface treatment-carburizing, carburized foil, graphite and graphoil - were successful in preventing a reaction between the can material and titanium laminates during HIP. Microstructures of the titanium-can interfaces are shown in Figure 48.

Three different cores and/or core materials were evaluated: TRW VMS-478 valve steel with a 0.062-inch trailing edge radius and 1045 steel with either a 0.015-inch or a 0.062-inch trailing edge radius. Metallographic results indicated that the valve steel core gave better cavity definition than the mild steel cores; however, some cracks and a lack of debulking were observed in the laminates near the core. Examples are shown in Figure 49. The crack observed in the titanium at the leading edge of the core has been attributed to the larger difference in thermal expansion between the titanium and valve steel than between the titanium and mild steel. The mean coefficients of thermal expansion (inch/inch/^{o}F) from room temperature to 1200^{o}F for these materials are 9.90 for Ti 6Al-4V, 14.7 for 1045 steel and 18.2 for TRW VMS-478 steel. Cracks were not observed in diamond specimens previously fabricated with 1045 steel cores. In addition, a reaction zone (see Figure 49(d), which probably contributed to the crack initiation, was observed at the titanium-valve steel interface. Good definition of the trailing edge for both the 0.062 and 0.015-inch radius 1045 steel cores was observed. Examples of 0.062-inch radius have been shown previously; the 0.015-inch radius is shown in Figure 50. Some waviness at the interface was present due to some local core deformation. There also appeared to be some bending of the core at the trailing edge for the 0.015-inch radius core which has been attributed to the non-uniform pressure distribution caused by a double canning approach.

Typical bond lines for diamond specimens 4, 5 and 6 are shown in the photomicrographs for DS4 in Figure 51. There are indications present at the bond lines. These indications have been seen in previous specimens.

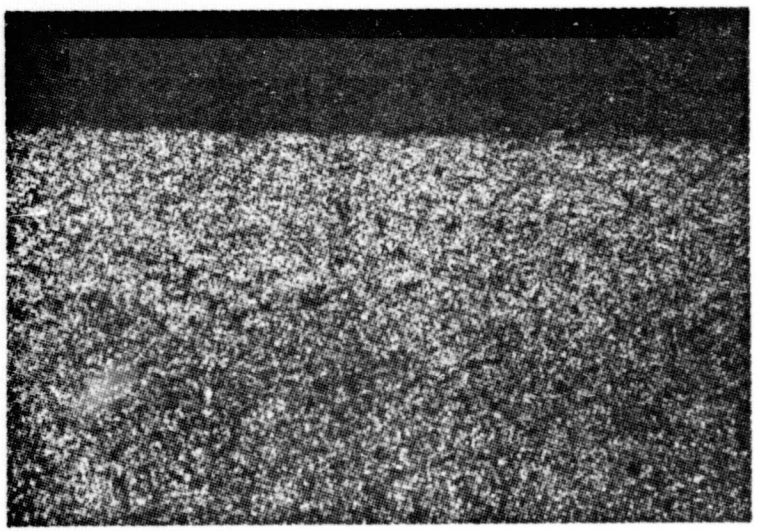

a. Carburized Can

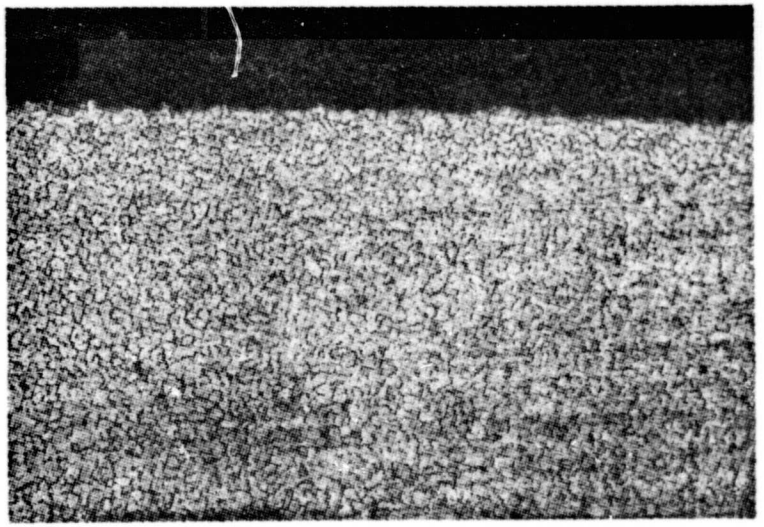

b. Carburized Foil

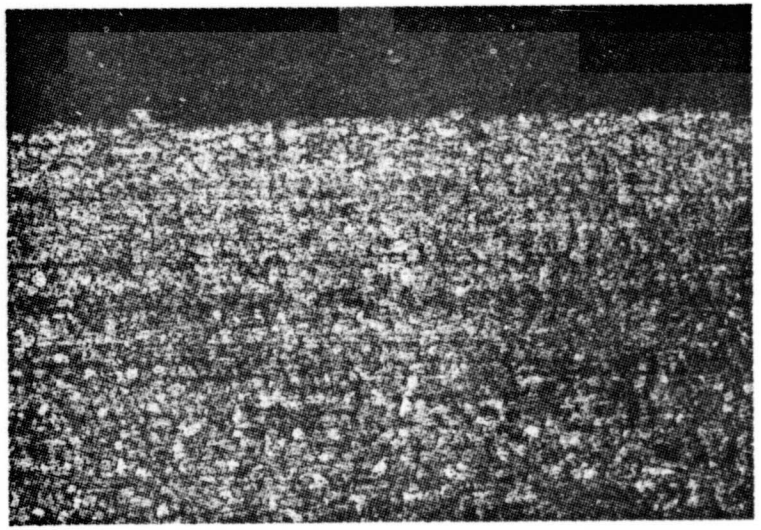

c. Graphite

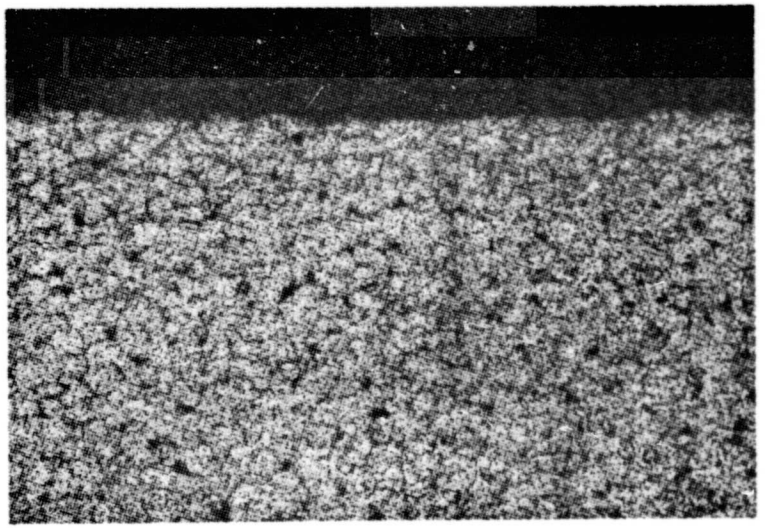

d. Graphoil

Figure 48. Surface Condition of Titanium After HIP Using Can Surface Treatment or Interfaces as Noted.

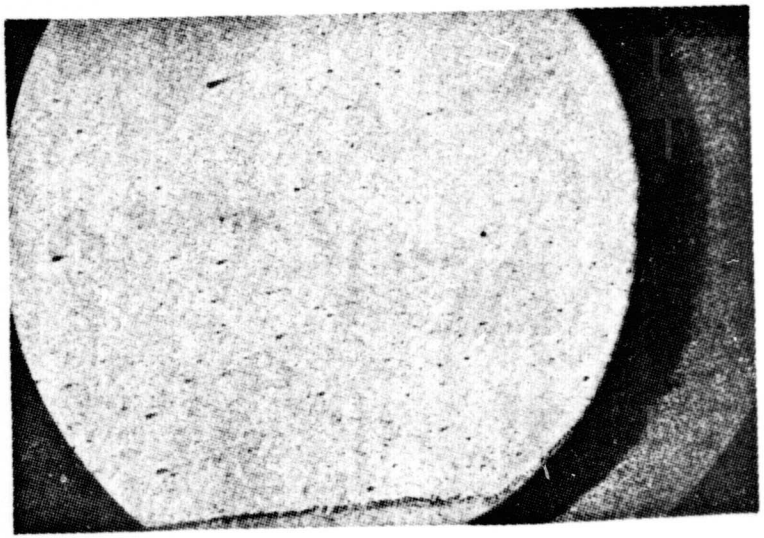

a. Trailing Edge (0.062-Inch Radius) 30X

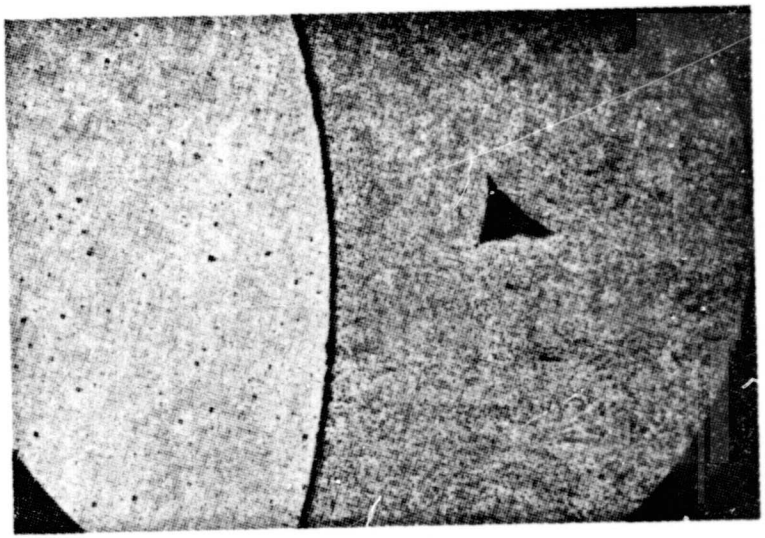

b. Void Present at Leading Edge 30X

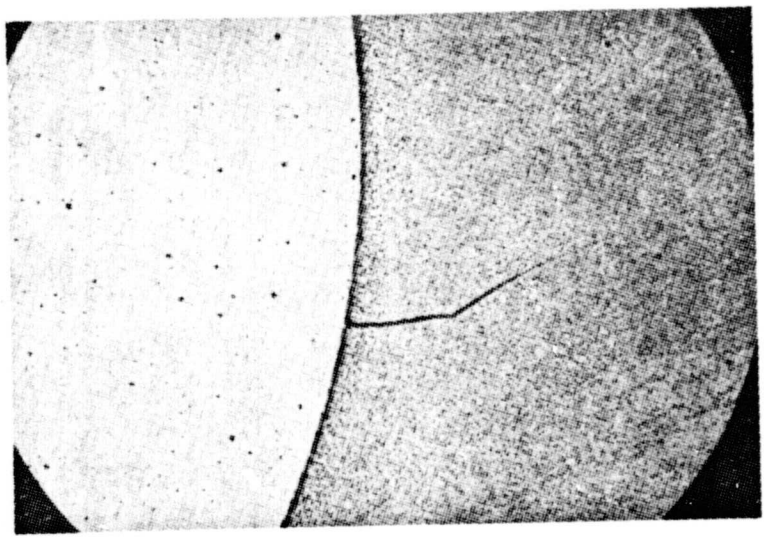

c. Crack Observed at Leading Edge 30X

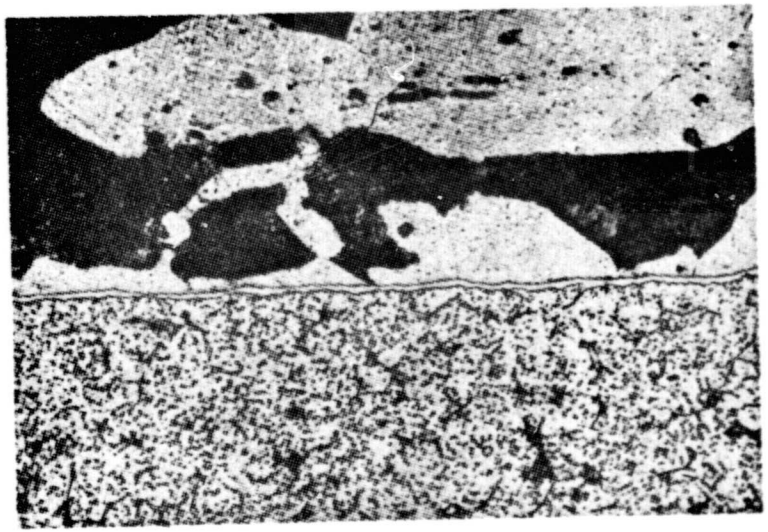

d. Reaction Zone 500X

Figure 49. Interface Between Valve Steel Core (TRW VMS-478) and the Titanium Laminates.

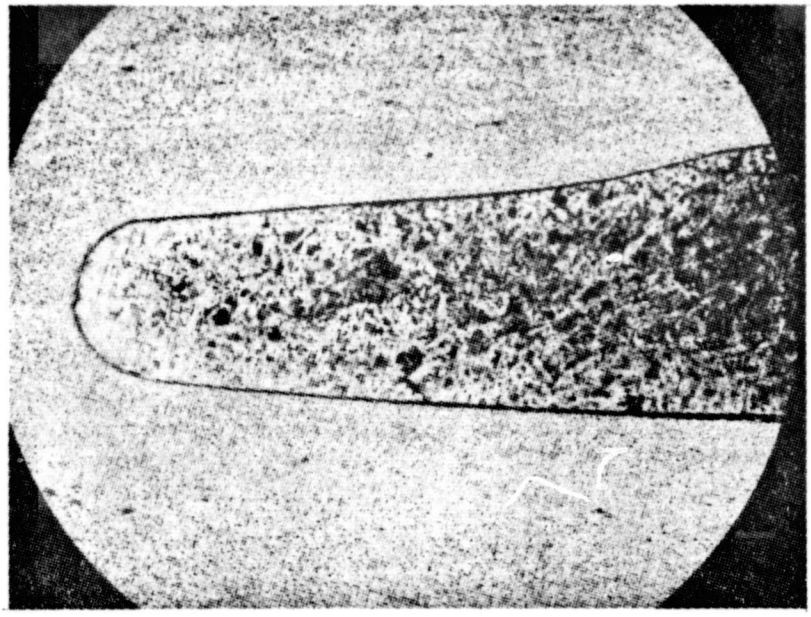

Figure 50. Macro of Trailing Edge Definition for 0.015-Inch Radius Core. 30X

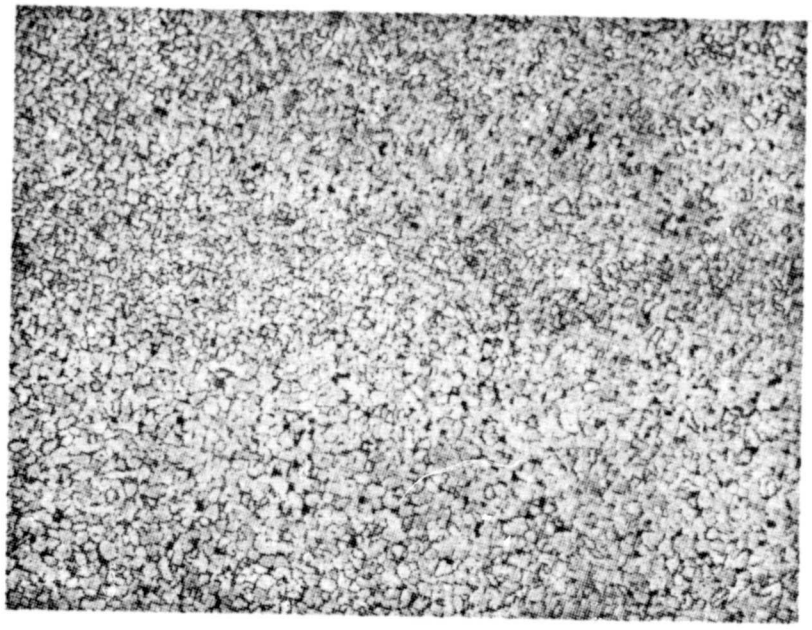

Bond Line

100X

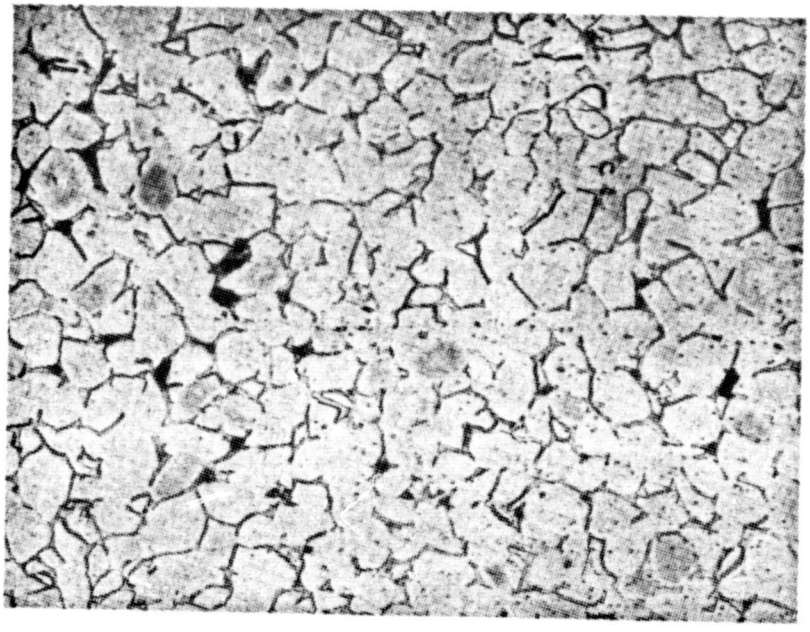

Bond Line

500X

Figure 51. Typical Microstructure and Bond Line for DS 4.

An anomaly occurs when bond lines in cross-sections of the diamond specimens are heavily macroetched. Conventional etching for microstructure usually does not delineate the bond line. A typical example is shown in Figure 52. Heat treatments at 1750°F, from 1/2 hour to 24 hours, had no effect on the macroetched evidence of the bond line (see Figure 53); however, the long time treatments caused some grain growth. The preferential etching may be due to the new grains and the energy at the interface. Also at the interface there appears to be a precipitate. Other potential causes could be adsorbed argon which is made available during the TIG welding operation or lack of cleanliness of the plies. This subject will be discussed later in this section of the report.

A preliminary trial twisting was made with DS6 to observe the behavior of the core with respect to the laminate. Twisting was accomplished by heating the part to 1750°F, removing the part from the furnace and placing in a vise, and then twisting the airfoil section in the area of the cores using specially fabricated diamond shaped wrenches. The specimen was twisted by hand. Measurement of the amount of twist at the edge of the diamond specimen was found to be about 1° per inch over a 6-inch length or about the same amount required for the area of the blade where there are cores. The core was removed from the diamond specimen and the amount of twist along the 0.062-inch radius was also found to be about 1° per inch (see Figure 54) while the edge of the core near the center of the diamond specimen is substantially less as would be expected. It appears that the core and titanium laminates behave isotropically when twisted which would indicate that the flat layup approach is even more promising. While DS6 had some disbond areas due to a leak during the HIP run, this trial was considered encouraging with regard to the feasibility of twisting a laminate plus core preform.

d. Diamond Specimen 7

DS7 was prepared similar to DS5 and verified that double canning will distort the diamond specimen. DS7 is shown after HIP with the can attached and after stripping the can in Figure 55(a) and (b) respectively. X-ray and C-scan evaluations indicated that the diamond specimen was successfully HIP with no evidence of voids or delaminations. A dimensional inspection of the diamond specimen has shown excessive debulking between the cores which results in a depressed area. A buildup of titanium along the 0.062-inch radius of the core was also observed. The buildup of titanium in this area has been attributed to non-uniform hydrostatic pressure applied to the laminates because the HIP can does not contact the laminates uniformly. Titanium at the edge of the diamond is flowing towards the 0.062-inch radius edge of the cores during the HIP. Dimensional inspection of the diamond specimen indicated that the dimensions were between 0.005 and 0.035-inch undersize in thickness in various sections (other than the center where the excessive debulking occurred). Double canning apparently does cause some flattening of the shape but does not account for titanium buildup in areas.

Stepping of the plies near the root was one approach to allow sufficient material for machining the radius (shelf radius on a blade). The results shown in Figure 56 for DS7 indicate that a step approach is a viable means of adding material to areas where radii are to be machined.

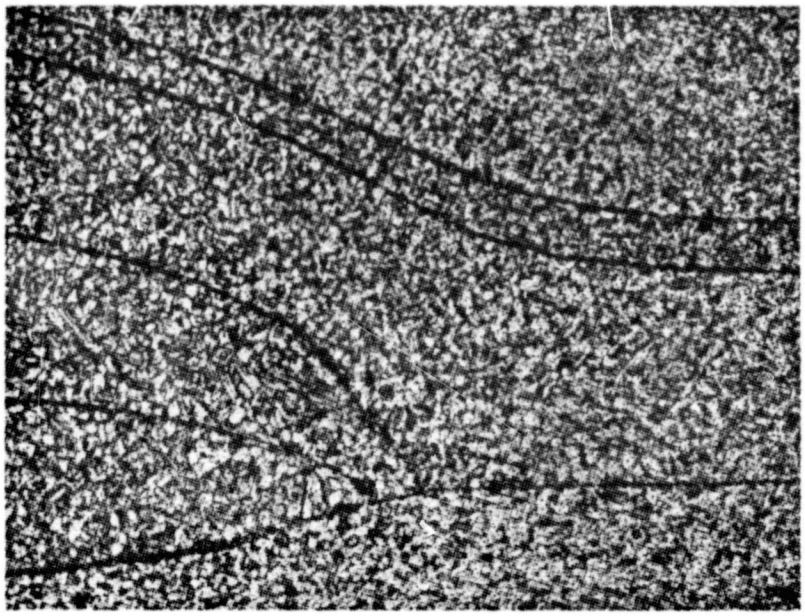

Macro Etch: 60cc H_2O
35cc HNO_3
5cc HF

Figure 52. Typical As-HIP Microstructure in DS3 Given a Heavy Etch to Delineate Bond Lines. 100X

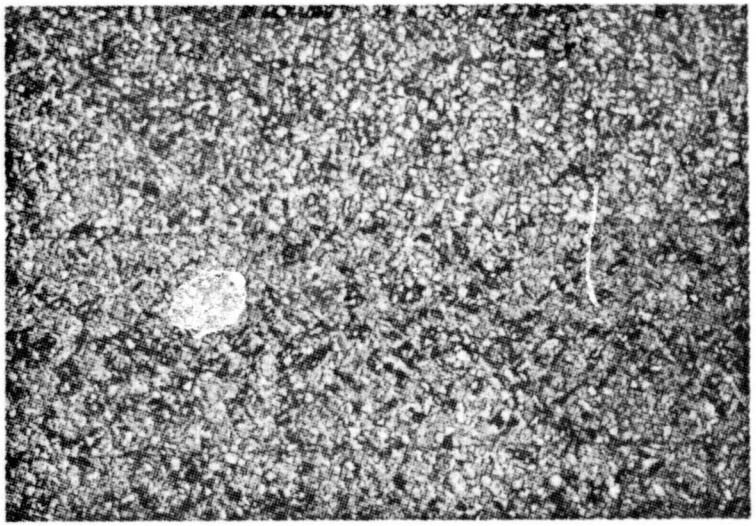

1/2 Hour/1750°F - Micro Etch

Micro Etch

96cc H_2O
2cc HNO_3
2cc HF

Macro Etch

60cc H_2O
35cc HNO_3
5cc HF

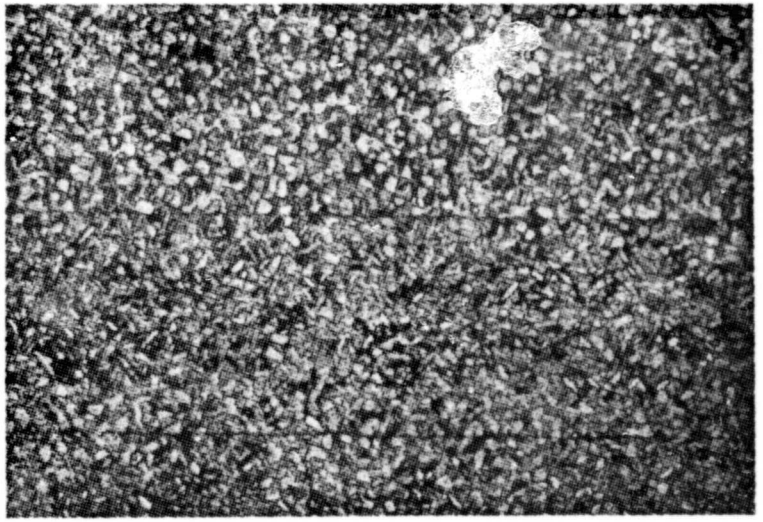

1/2 Hour/1750°F - Macro Etch

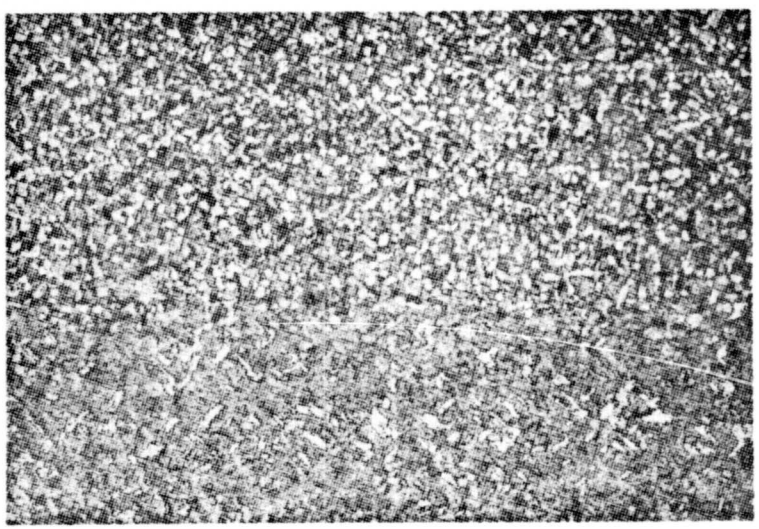

24 Hours/1750°F - Micro Etch

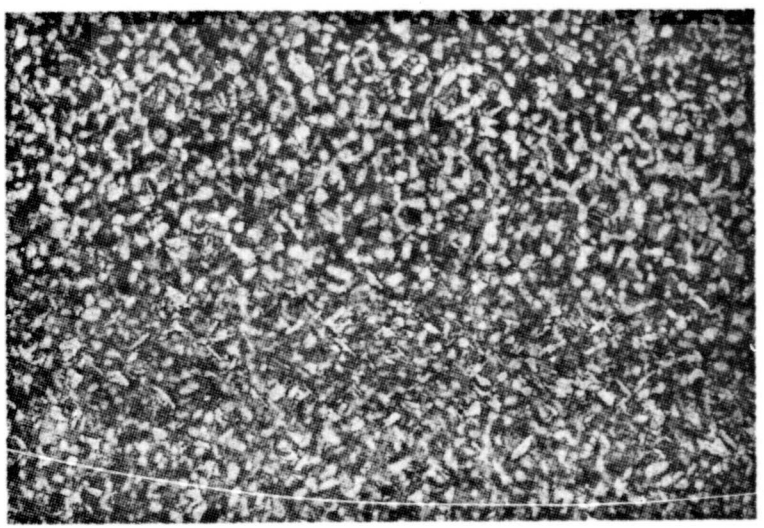

24 Hours/1750°F - Macro Etch

Figure 53. Typical Microstructures After Heat Treatment at 1750°F. Note Bond Line Delineation for Heavy Etch. 100X

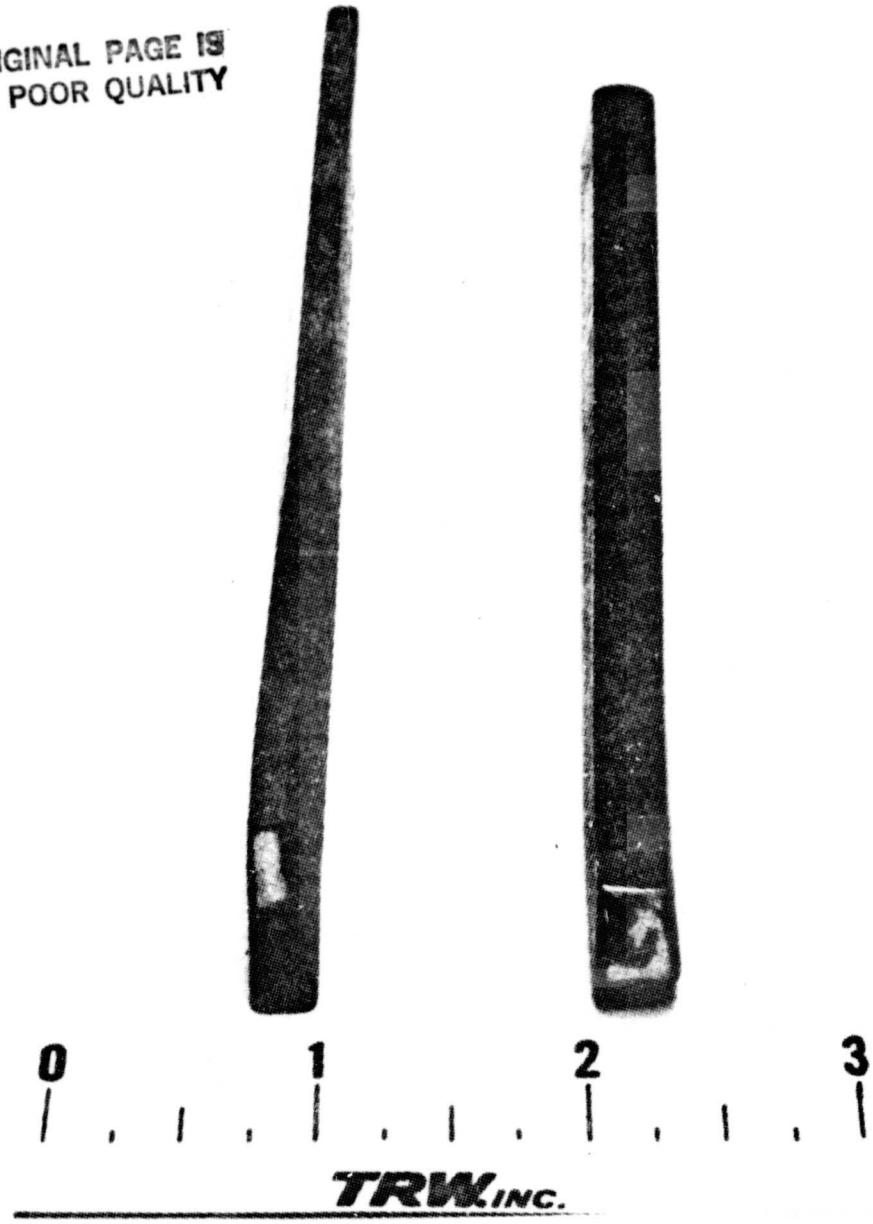

Figure 54. Edge View of Sectioned Core That Was Twisted. Twist Along Trailing Edge Radius Approximately 1°/Inch is Shown on the Left in Photograph.

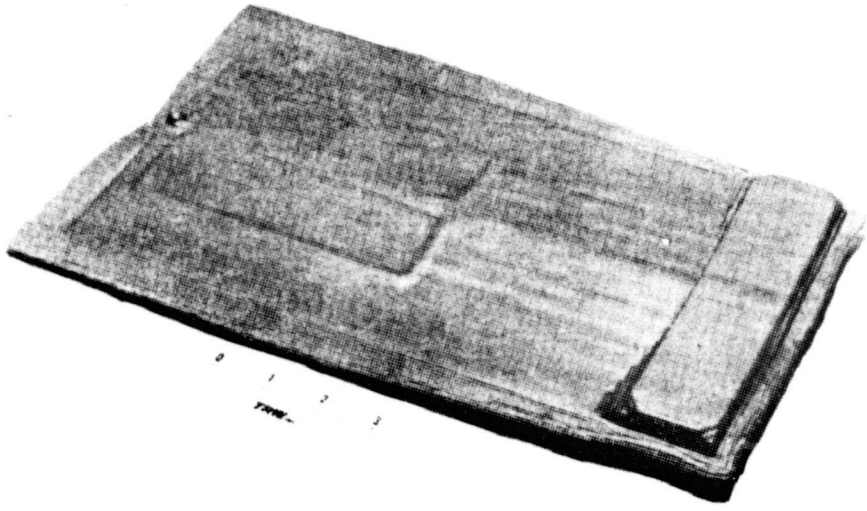

a. DS 7 in Can

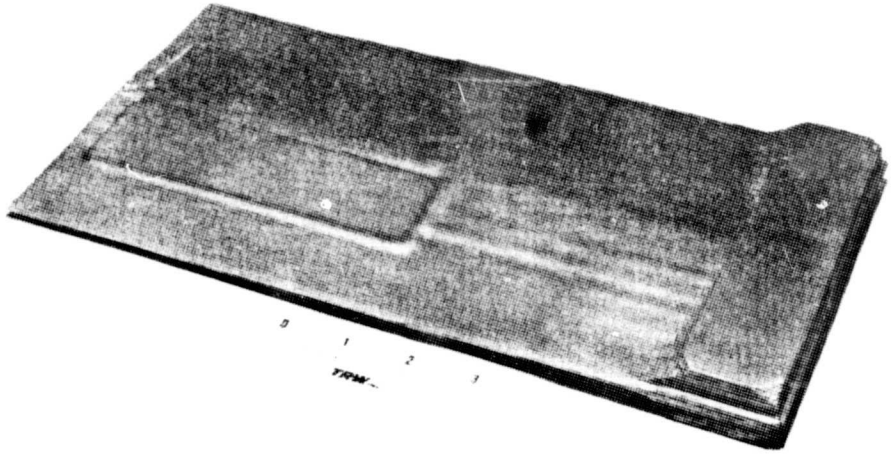

b. Can Removed

Figure 55. Diamond Specimen 7 After HIP.

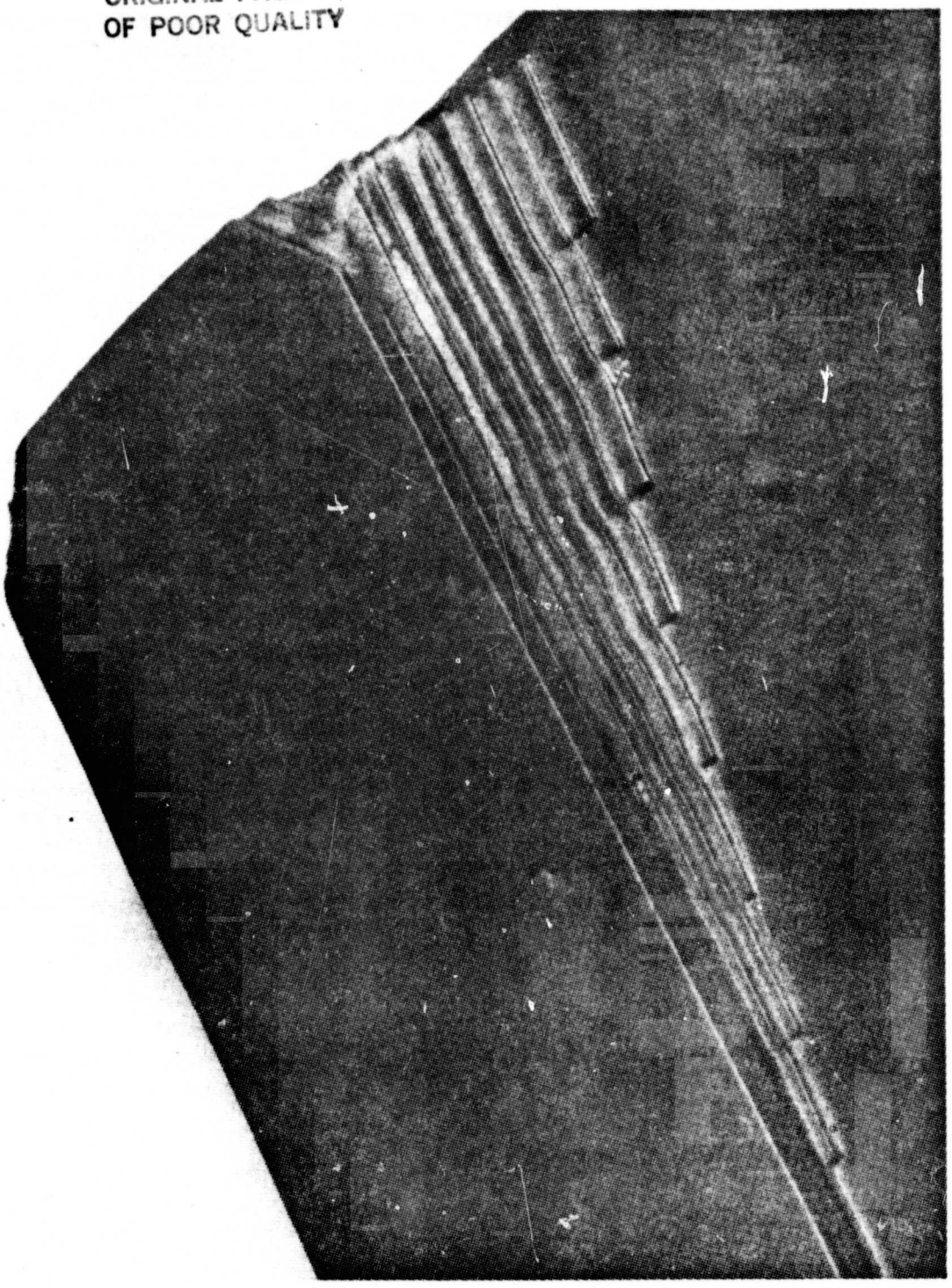

Figure 56. Step Root in Diamond Specimen 7. ~2X

Metallographic evaluations of DS7 indicated good bonds were achieved; however, there was still evidence of some indications at the bond lines (see Figure 57). SEM analysis at P&WA has indicated that these indications are very small voids which they believe are probably attributable to argon. At the same time TRW reviewed the entire procedure of diamond specimen assembly and compared this process with previous efforts in titanium bonding. The only difference noted was that previous bonding was conducted under a dynamic vacuum while the current HIP is done in a static vacuum (sealed can). Since the cans are TIG welded in an argon atmosphere and mass spectrometer leak checked using helium, some adsorption of these gases is possible. The final sealing by electron beam (EB) welding would not be expected to allow removal of all of these gases.

e. Diamond Specimens 8, 9 and 10

DS8, 9 and 10 after HIP using the modified cycle are shown in Figures 58 through 60. Visual examination indicated that the HIP run was successful except for a core shift in DS9. (An investigation of the core shifts was discussed for the assembly of the remaining diamond specimens.) The HIP diamonds were evaluated by X-ray and ultrasonic C-scan. Some differences in the radiographs were observed when comparing DS8 with DS9 and 10. It was observed that delineation of individual ply edges was particularly evident for DS10 and somewhat evident for DS9; however, ply edges for DS8 were not delineated and instead a blending of color or tone of the X-ray was observed. These differences are not illustrated herein because the radiographs do not reproduce well unless there are gross differences in color tone. C-scan inspection of the diamonds indicated no defects larger than 3/64-inch for DS8 but indications were present for DS9 and 10. An example is shown in Figures 61 and 62 when comparing DS8 and DS10.

Dimensional analyses indicated that the three diamonds met the required blueprint dimensions (see Figure 2) except for the core shift area in DS9. Selected areas were sectioned for metallography and evaluated. Metallographic evaluations confirmed that disbond areas were present in DS9 and 10. These disbonds were due to a can leak at some stage of the HIP cycle after the can had formed around the plies. Typical results are shown in Figures 63 through 66. For the diamond specimen TIG welded in argon (No. 8) the vacuum outgas appeared to remove most of the adsorbed gases. Figure 64 shows one area where voids at the bond line were observed after reviewing literally hundreds of bond lines. Delineation of bond lines due to gases from welding were not observed for DS9 or 10; however, disbonds and incomplete fill at ply endings were present due to the can leak. The questions as to where and/or why the cans leaked remained to be answered. The welds undergo a compressive force during HIP except where the evacuation tube is placed. The weld in this area may develop a shear stress. Modification of this tube area as discussed before was made for future HIP runs.

Modifications to the HIP cycle seemed to have no impact on the buildup of material at the 0.062-inch radius of the core. Since there is sufficient material in this area to meet blueprint dimensions no further modifications were planned for the diamond specimen plies. The differences in the HIP cycles are shown in Figure 67. The modified

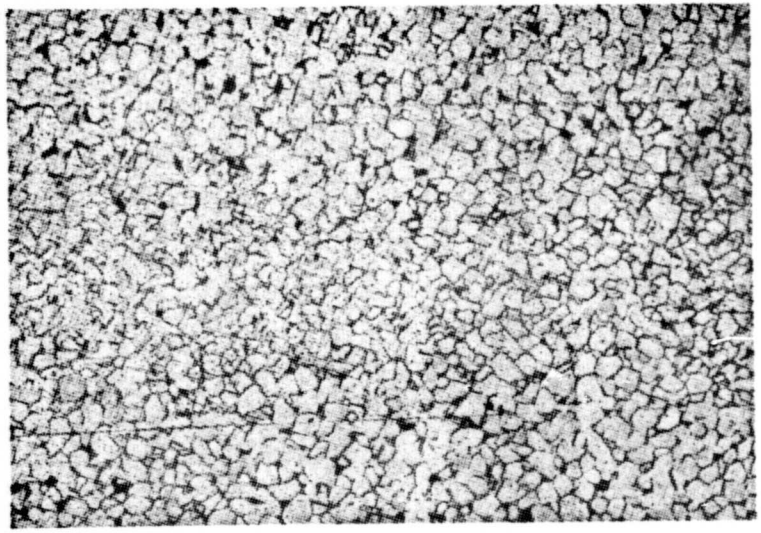

a. Near the Tip 200X

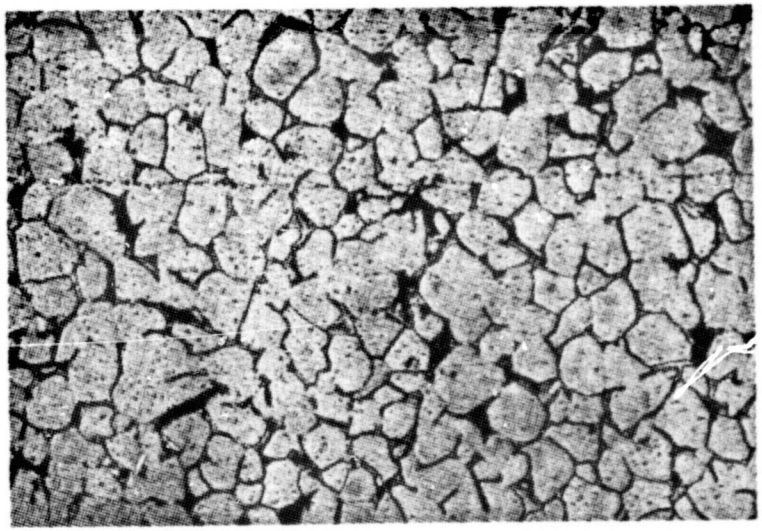

500X

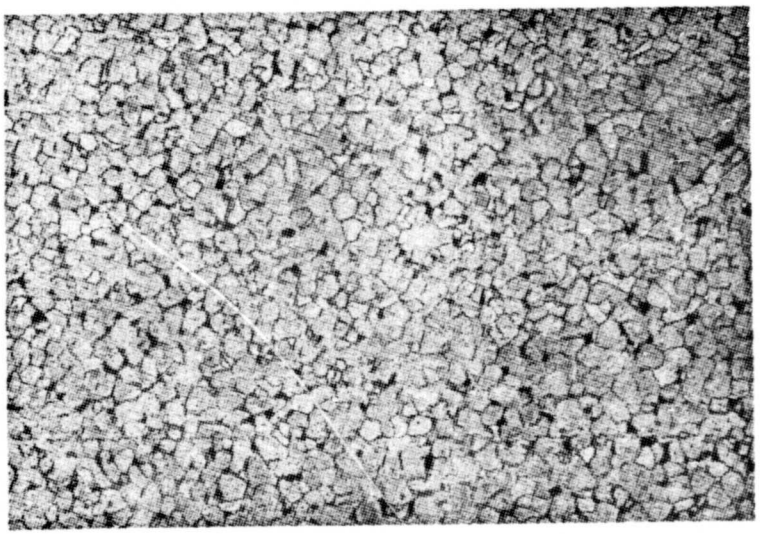

b. Root 200X

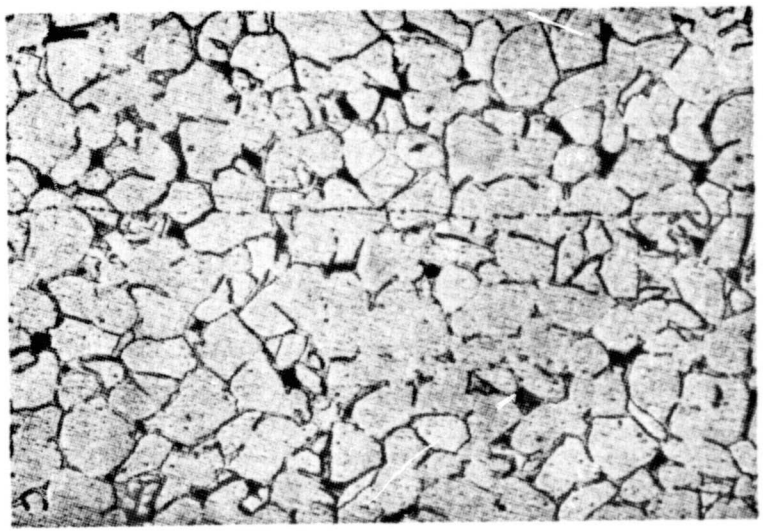

500X

Figure 57. Typical Microstructure in DS 7 at Several Areas. Bond Lines Are Evident.

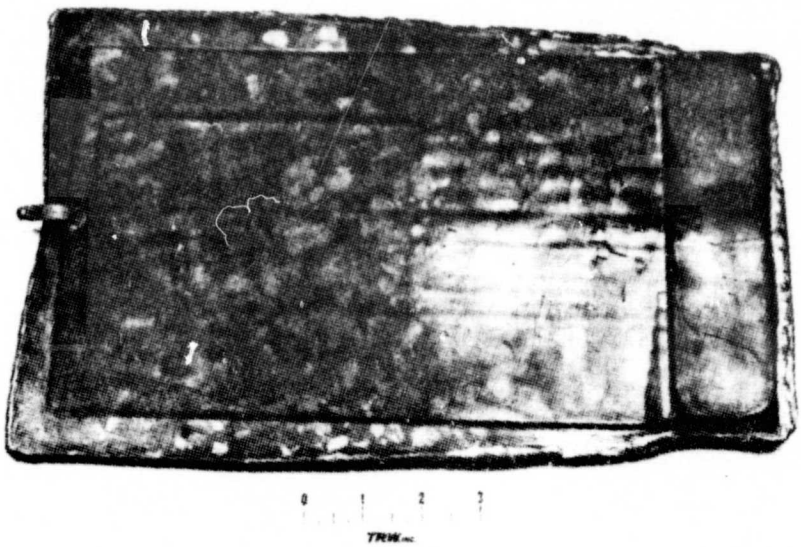

a. Can Intact

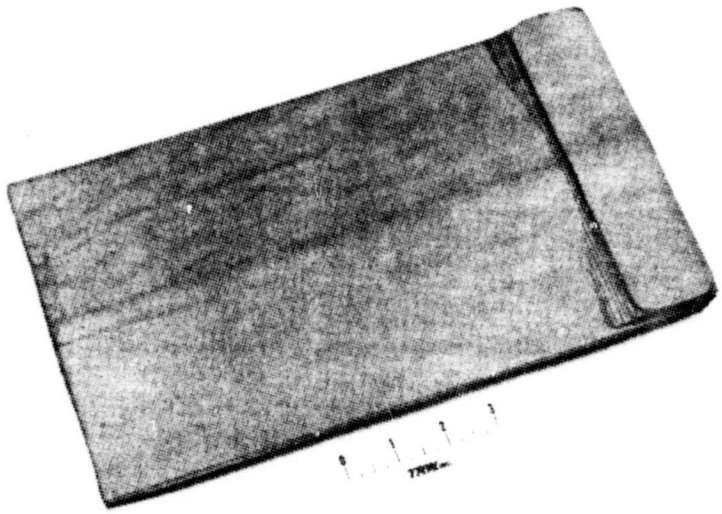

b. Can Removed

Figure 58. Diamond Specimen 8 After HIP.

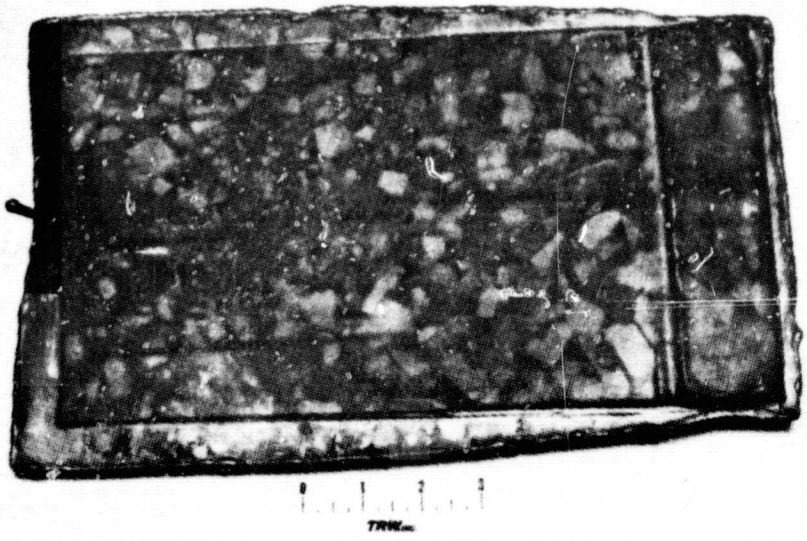

a. Can Intact

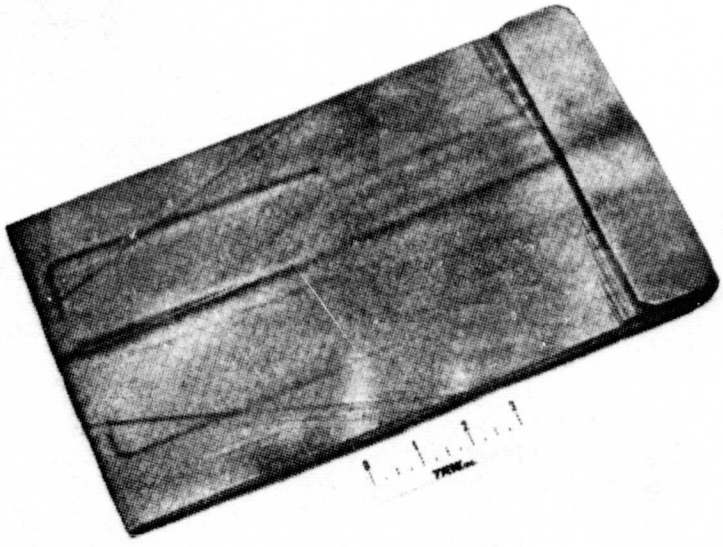

b. Can Removed

Figure 59. Diamond Specimen 9 After HIP.

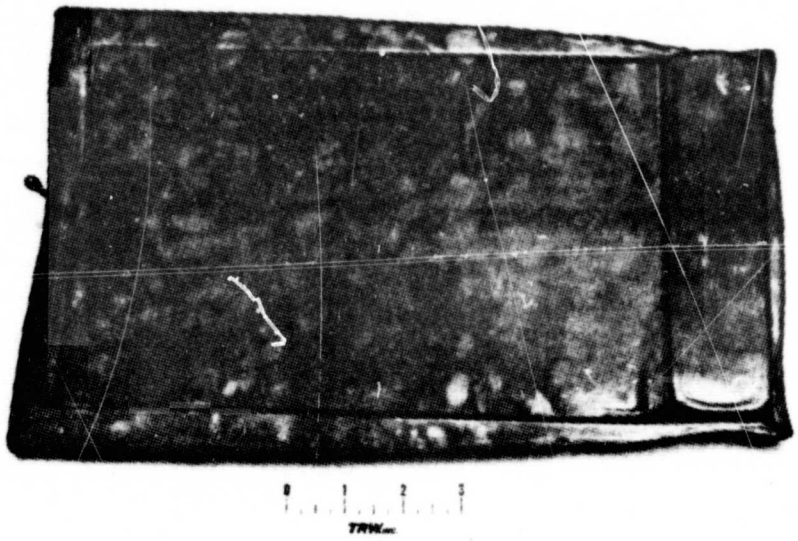

a. Can Intact

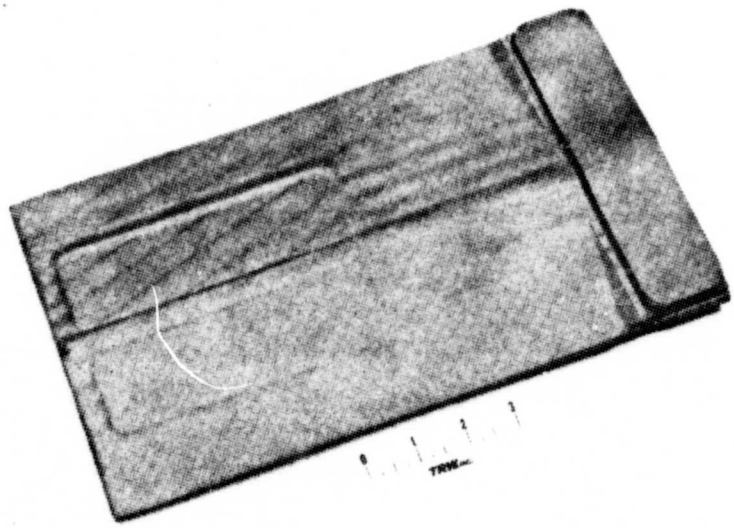

b. Can Removed

Figure 60. Diamond Specimen 10 After HIP.

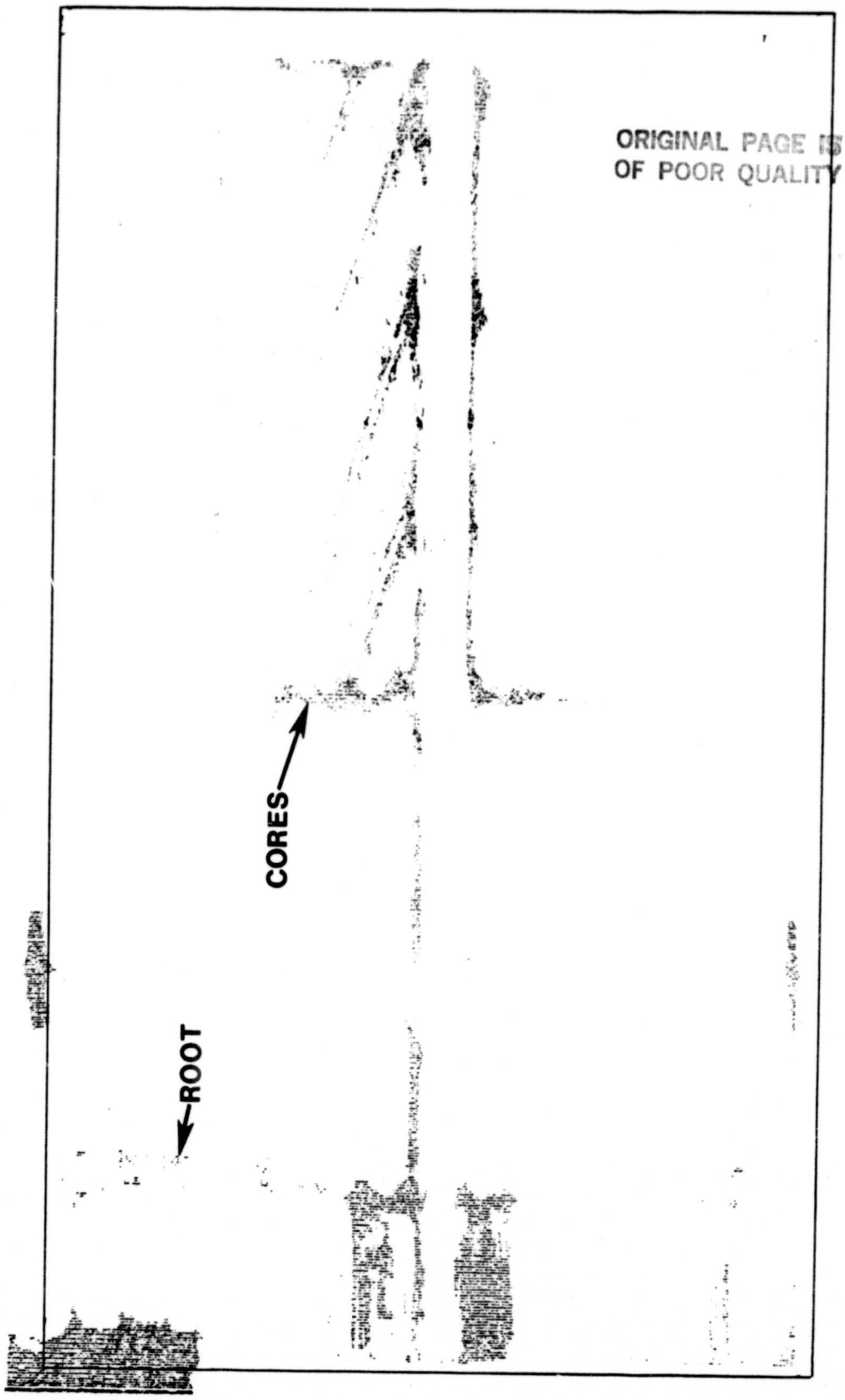

Figure 61. Ultrasonic C-Scan of Diamond Specimen 8.

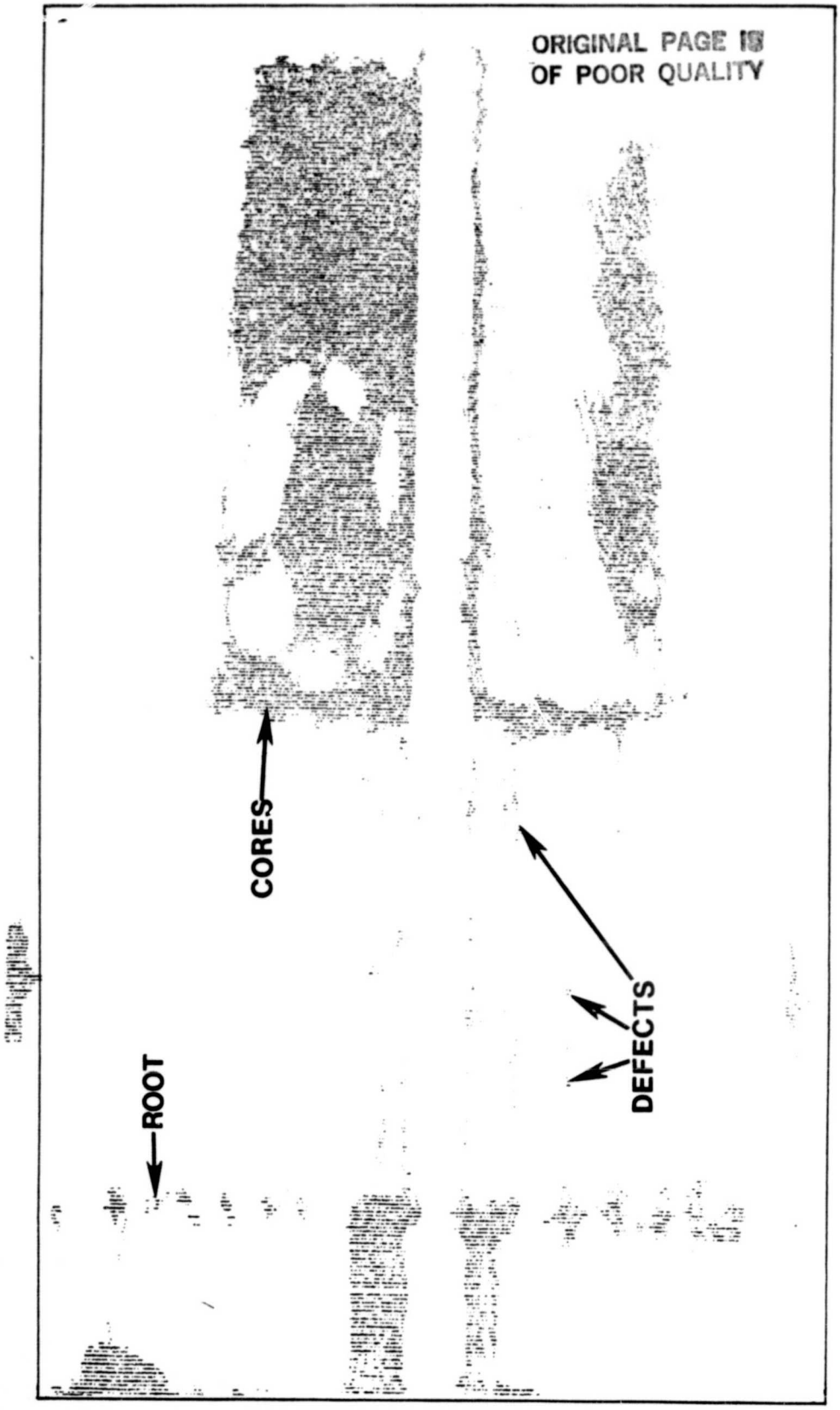

Figure 62. Ultrasonic C-Scan of Diamond Specimen 10.

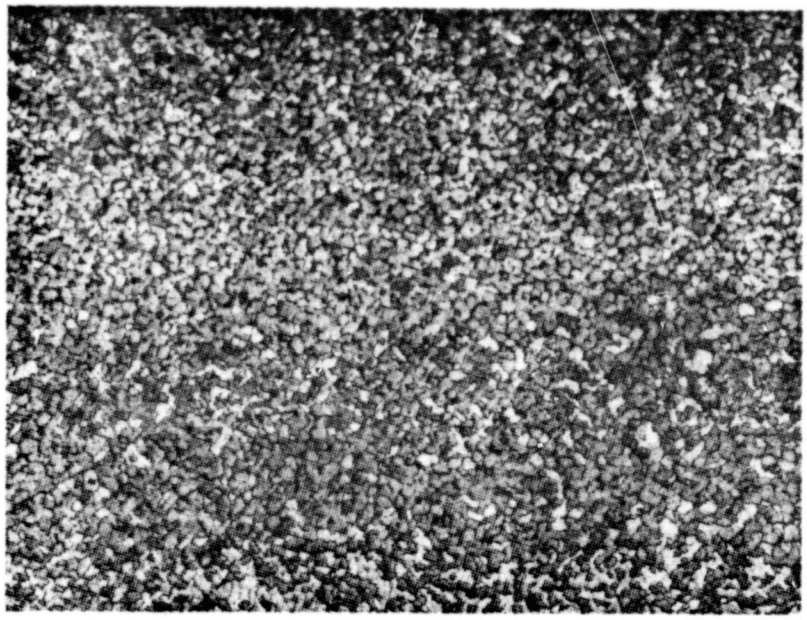

Bond Line

Bond Line

100X

Bond Line

500X

Figure 63. Microstructure in DS 8 at Several Areas. Etchant 96 H_2O-2HNO_3-2HF.

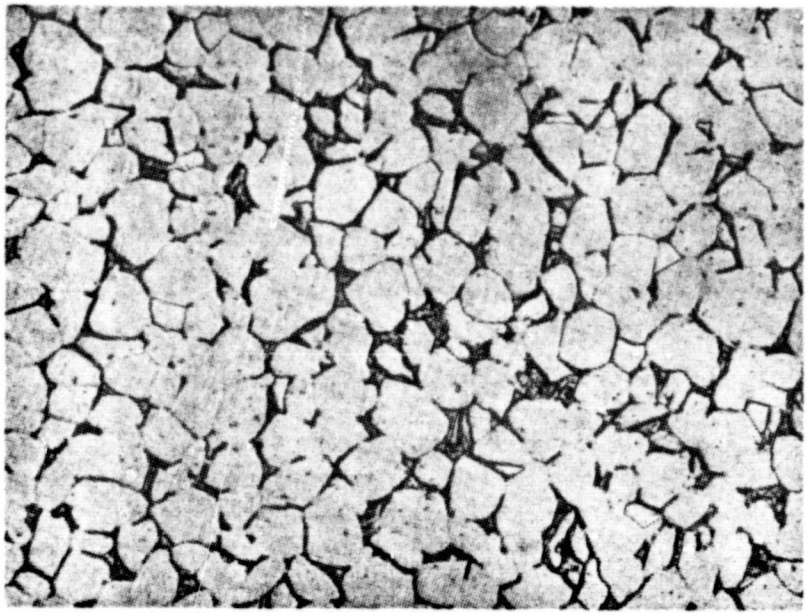

Bond Line

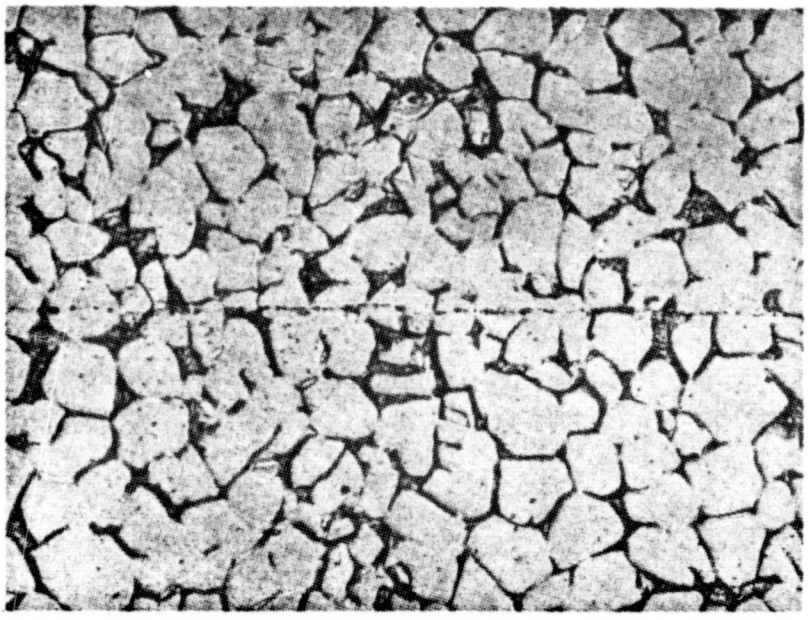

Bond Line

Figure 64. Microstructures in DS 8 at Several Areas. Etchant 60 H_2O-35HNO_3-5HF. 500X

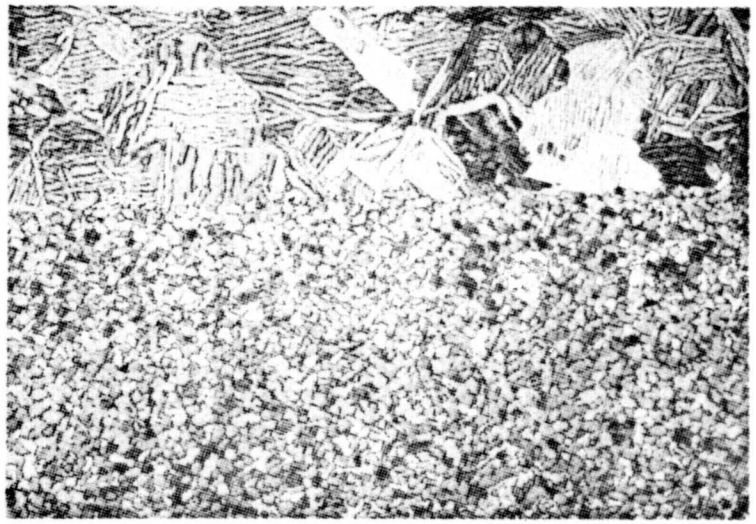

100X

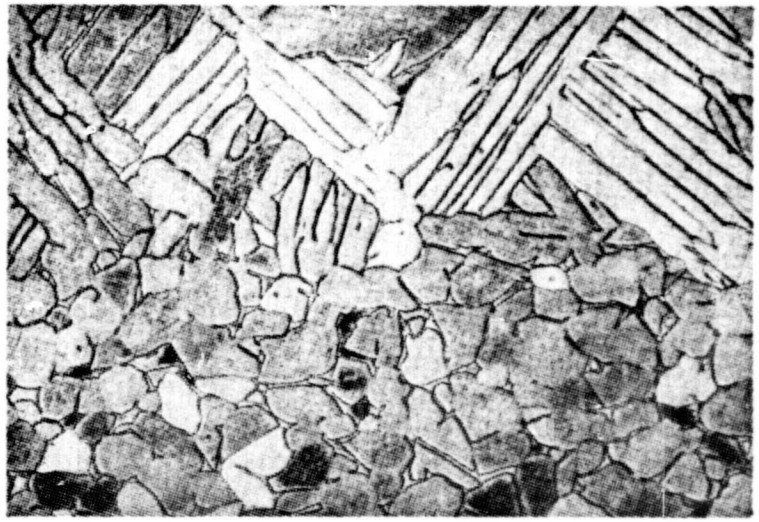

500X

Bond Line

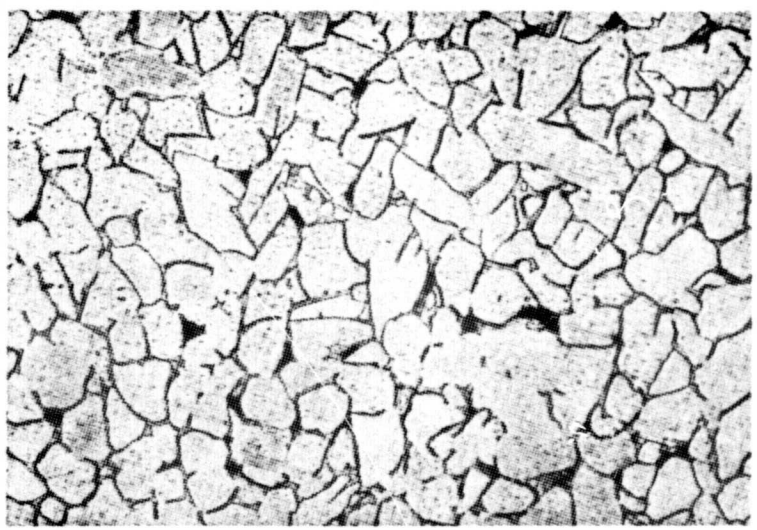

500X

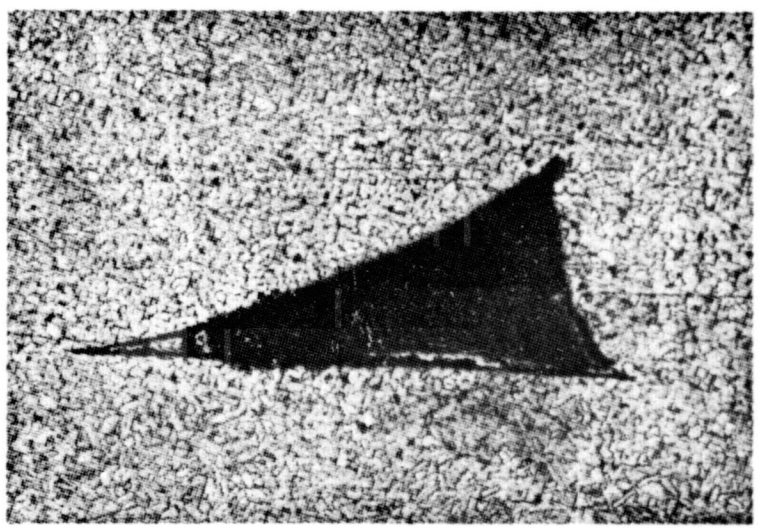

100X

Figure 65. Typical Microstructure in DS 9 at Several Areas.

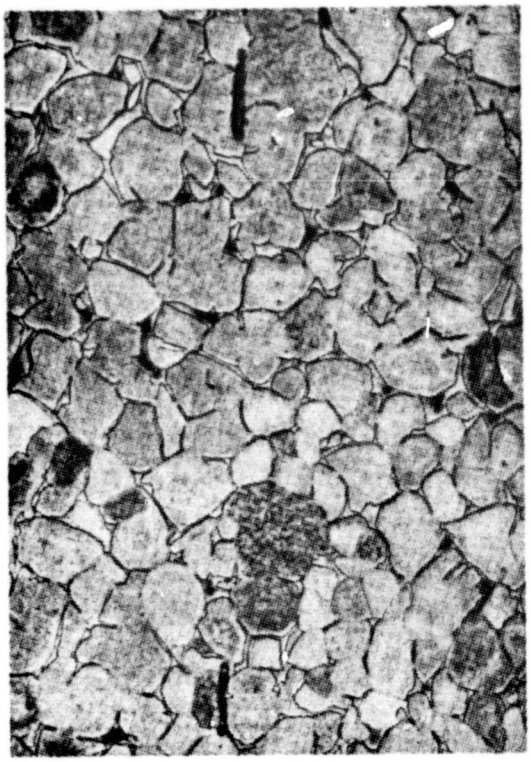

500X

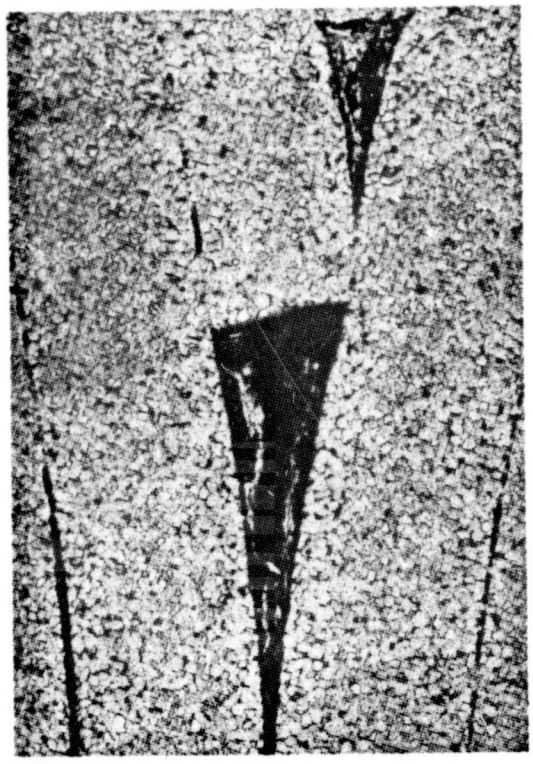

100X

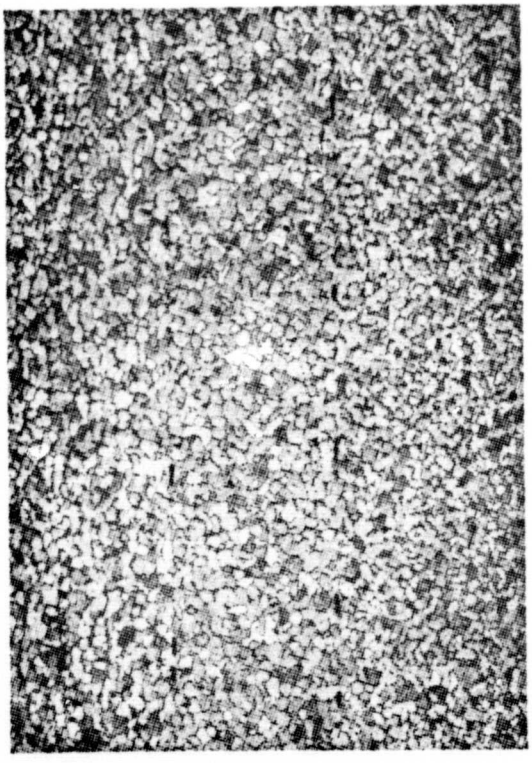

100X

Figure 66. Typical Microstructures in DS10 at Several Areas.

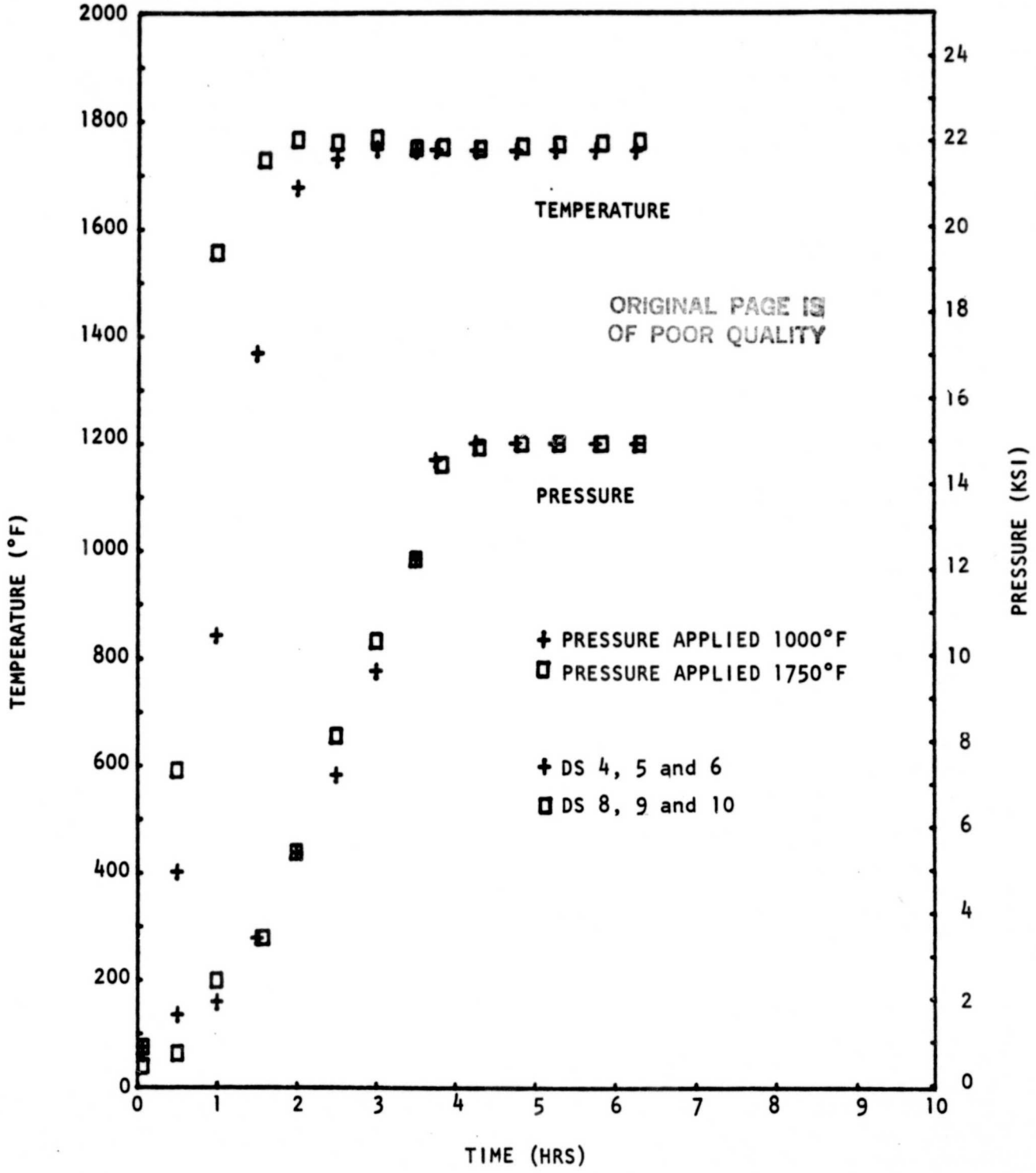

Figure 67. Temperature-Pressure Cycle Used for HIP.

cycle heats the specimens at a faster rate to 1750°F in order to initiate maximum pressure buildup. Since the HIP vendor has to continuously increase pressure in both cycles to operate the equipment efficiently the concept of minimum pressure to eliminate material buildup at the edges was not feasible with the current HIP vendor.

f. Deliverable Diamond Specimens for P&WA Evaluation

i. Diamond Specimens 13 and 15

The first two diamond specimens fabricated for delivery to P&WA were DS13 and 15. Visual examination of the diamond specimens after HIP indicated a successful run. Both specimens were heat treated (1750°F/1 hour/FAC + 1300°F/2 hours/AC) after HIP while in the mild steel can. After stripping the can it was observed that both cans were leakers with DS15 appearing to be better bonded in all areas except the root. The poor bond areas in DS13 were obvious after HIP because the surface was "bubbled." This feature was due to expansion during heat treating of the entrapped argon gas from the HIP run. X-rays of these specimens after HIP indicated that the cores remained in position during the HIP cycle (see Figures 68 and 69); however, DS13 cores were about 0.050-inch farther apart than blueprint requirements. DS15 was submitted for ultrasonic C-scan evaluation. Based on experience gained with interpreting the C-scans there appeared to be some indications (unbonded areas) present in DS15 as shown in Figure 70. The delineation of the plies in the Figure 68 X-rays has also been a good nondestructive evaluation of ply disbonds. In a well bonded part ply edges are not well delineated.

ii. Diamond Specimens 12, 19 and 25

The second lot of diamond specimens fabricated for delivery to P&WA were DS12 with an IN-744 overcan, DS19 with a Ti 6Al-4V overcan and DS25, which was sealed along the periphery by seam welding. After receipt of these three specimens back from the HIP vendor it was obvious that the diamond specimens that were overcanned, DS12 and DS19, leaked during HIP. Visually, DS25 appeared successful after HIP. DS25 was given the 1750°F/1 hour/FAC + 1300°F/2 hours/AC heat treatment and the can was stripped from the part. The specimen appeared well bonded with no visible voids at the ends of the specimen. Based on the appearance at the ends and the shape and bond of the plies at the root radius, TRW was confident that this diamond specimen was fully bonded.

DS25 was evaluated by X-ray, C-scan and metallography. X-ray and C-scan indicated a well-bonded specimen with the proper core registry. The results are shown in Figures 71 and 72. Metallographic evaluations of some edge material indicated excellent bonding (see Figure 73) when using the conventional $96H_2O$-$2HNO_3$-2HF etchant for titanium. A more aggressive etchant, $60H_2$-35 HNO_3-5HF, revealed the "microporosity" observed at the bond line in other specimens when this etchant was used. This "microporosity" previously was attributed to adsorbed argon; however, this diamond specimen was not exposed to argon since it was seam welded in air.

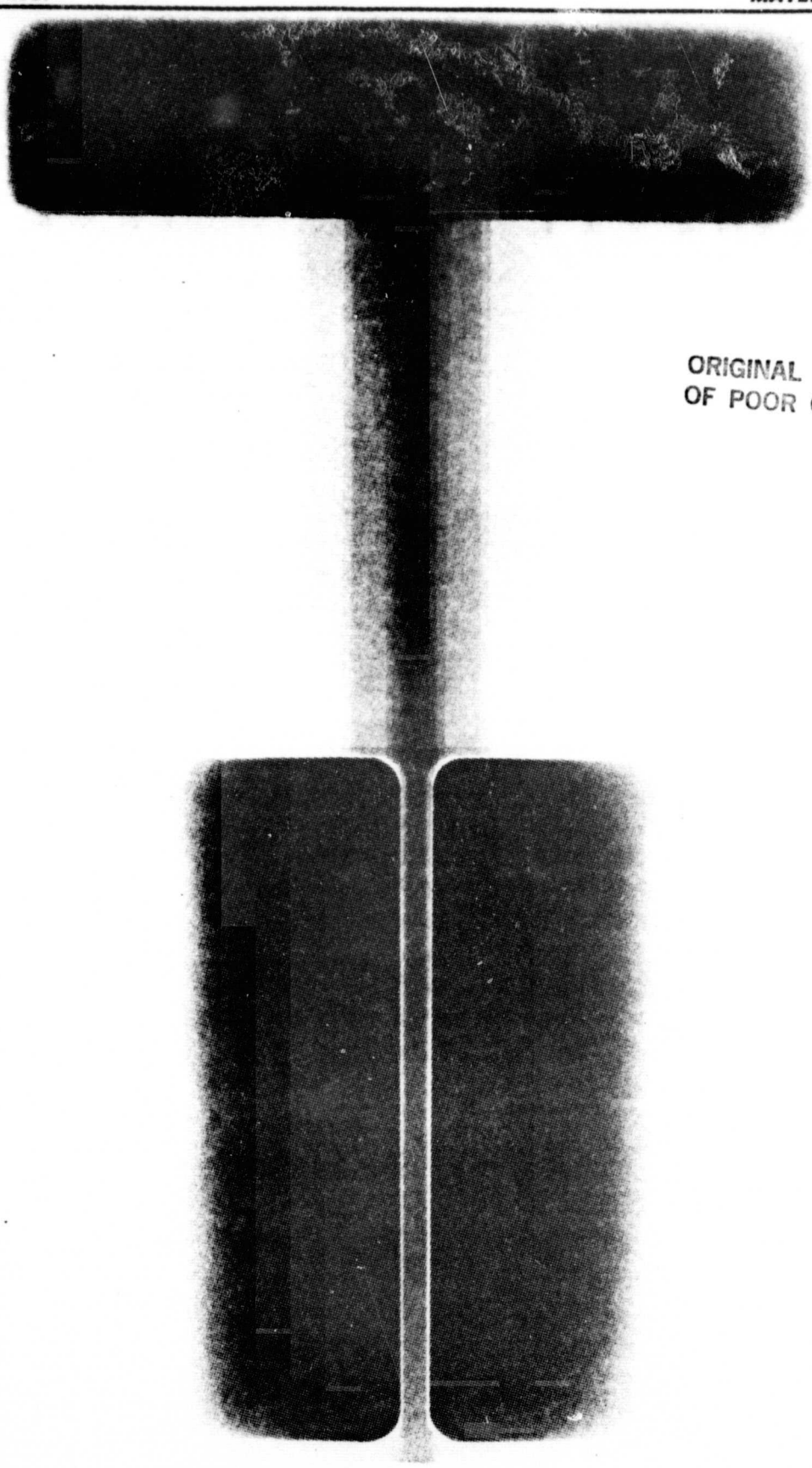

Figure 68. X-Ray of DS 13 After HIP.

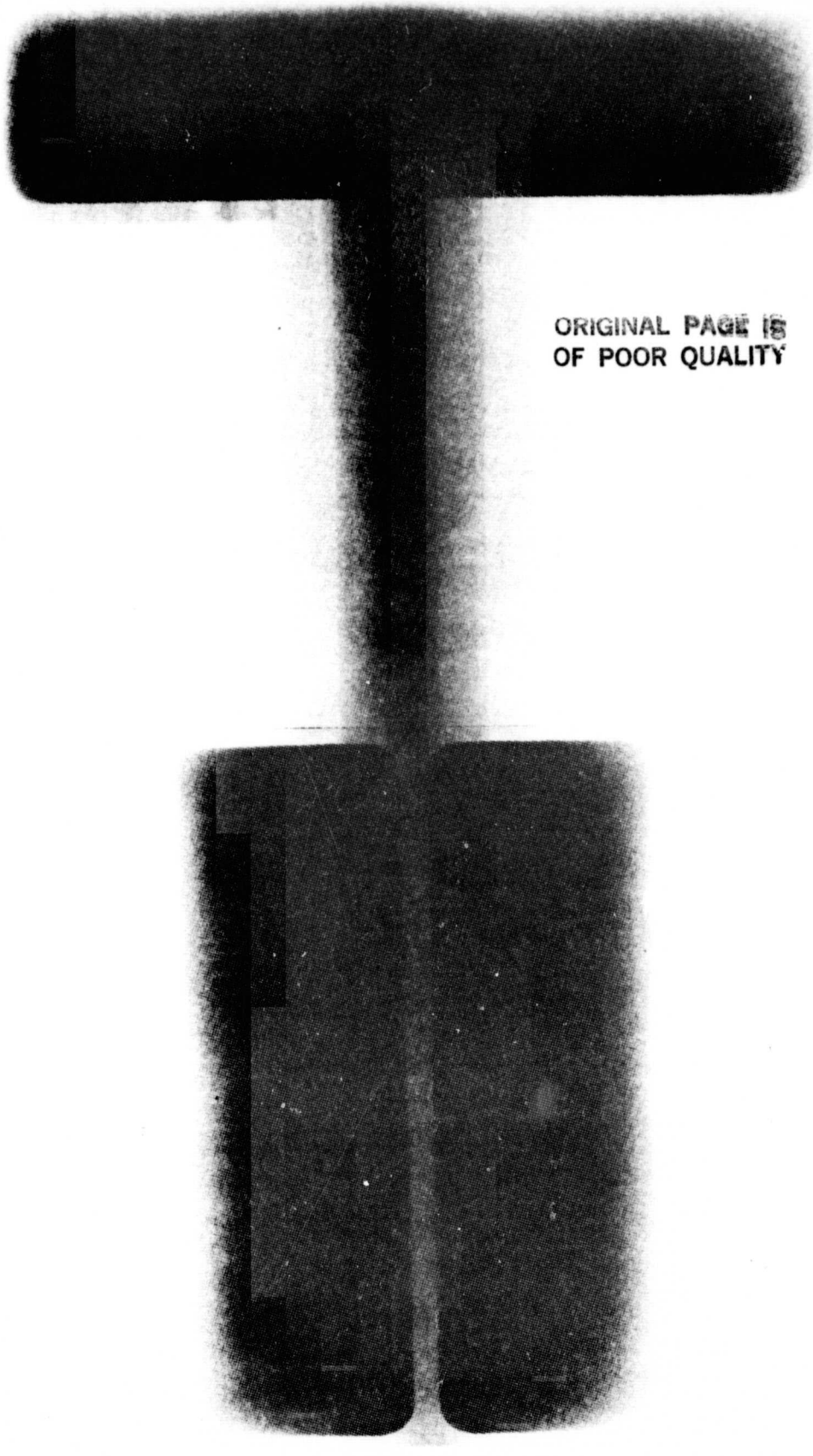

Figure 69. X-Ray of DS 15 After HIP.

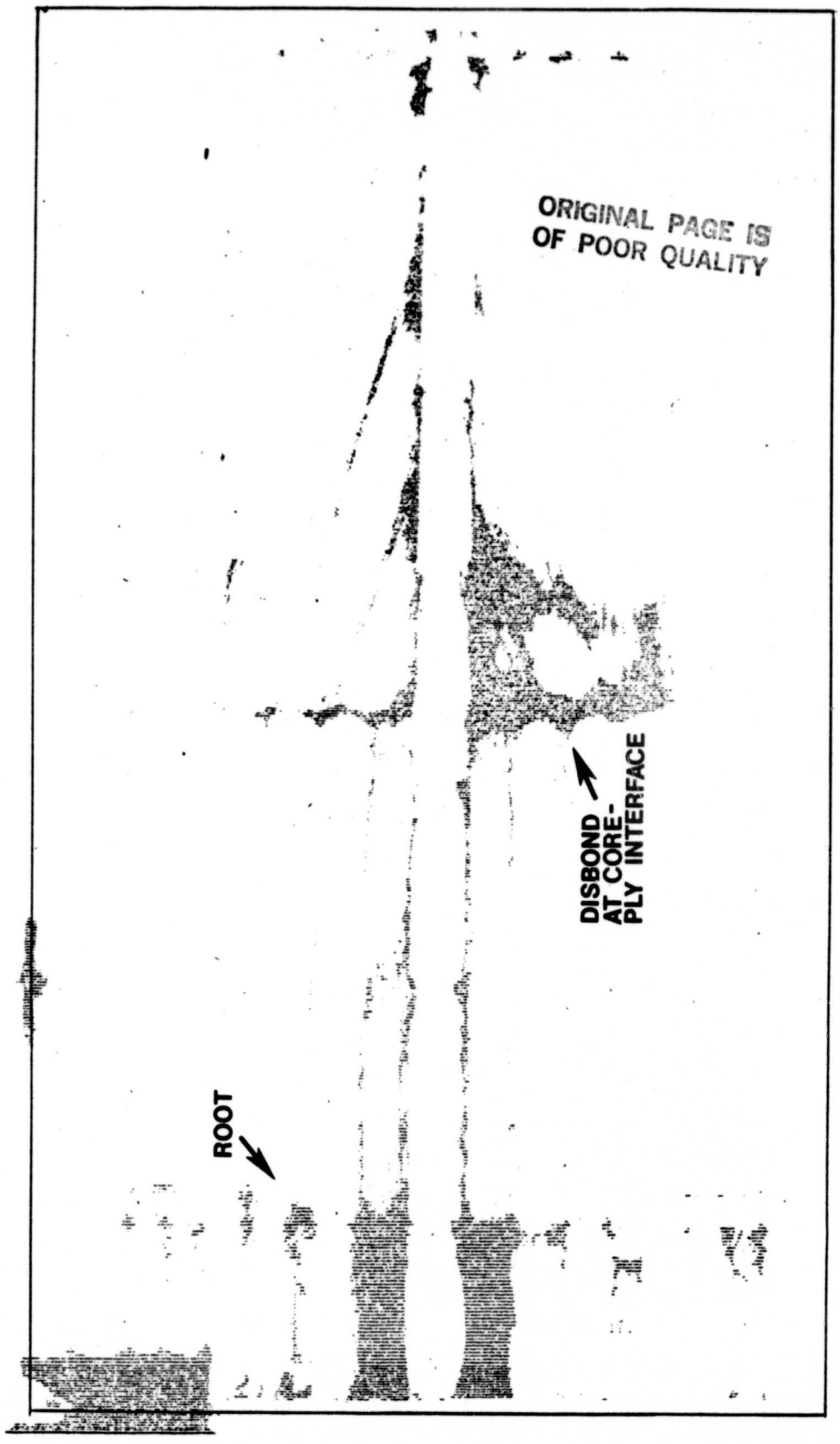

Figure 70. Ultrasonic C-Scan of Diamond Specimen 15.

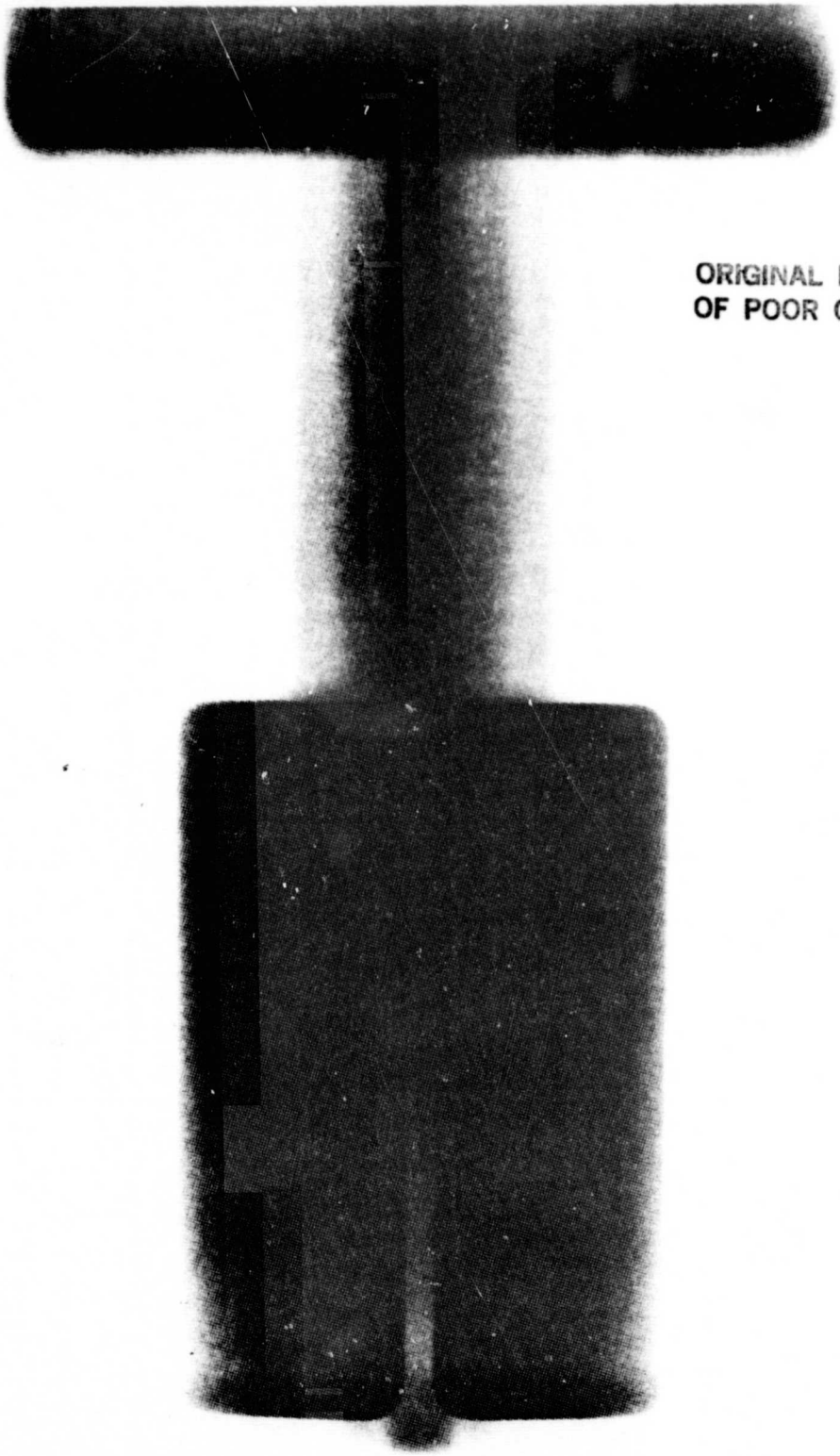

Figure 71. X-Ray of DS 25 After HIP.

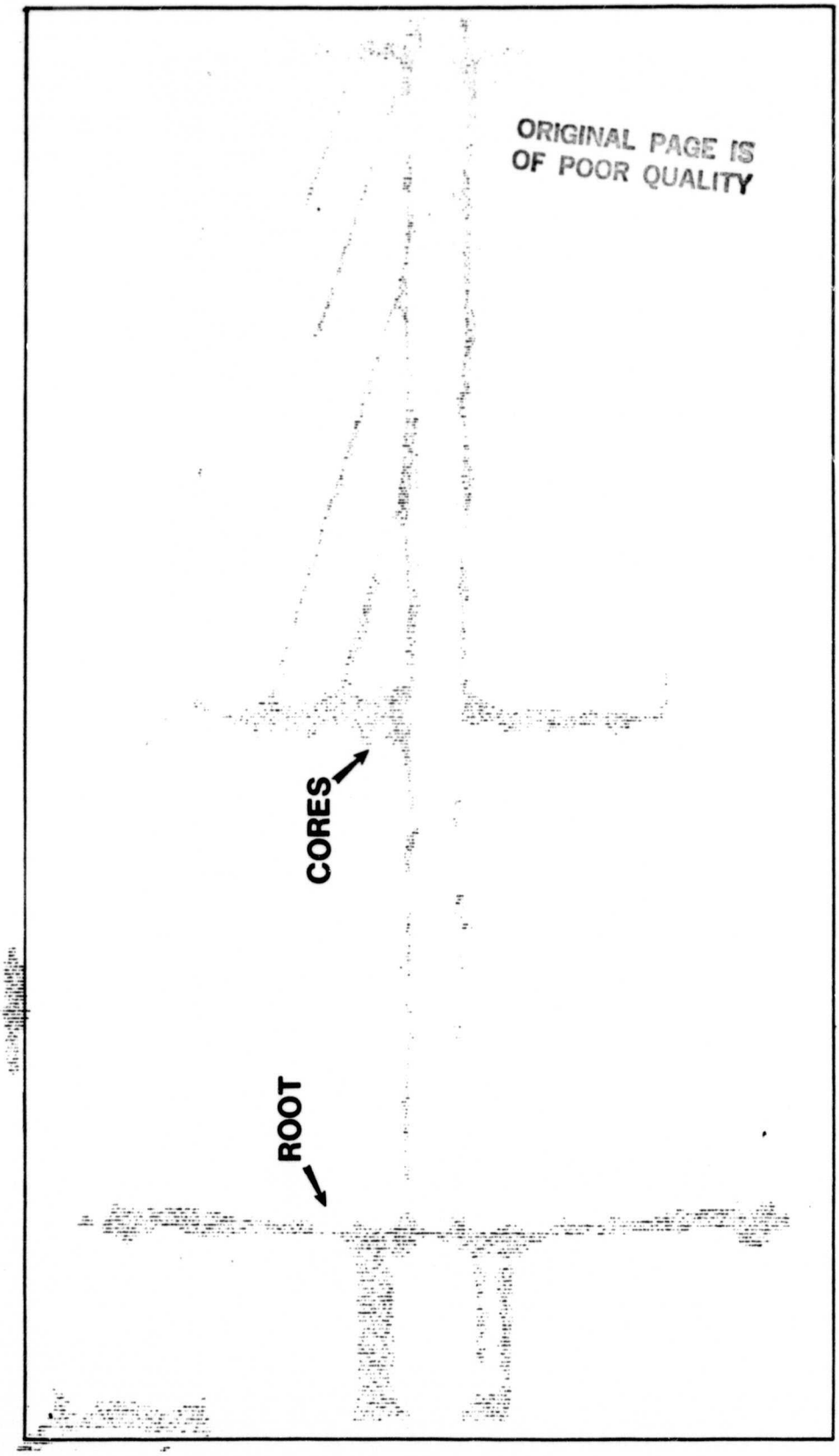

Figure 72. Ultrasonic C-Scan of DS 25.

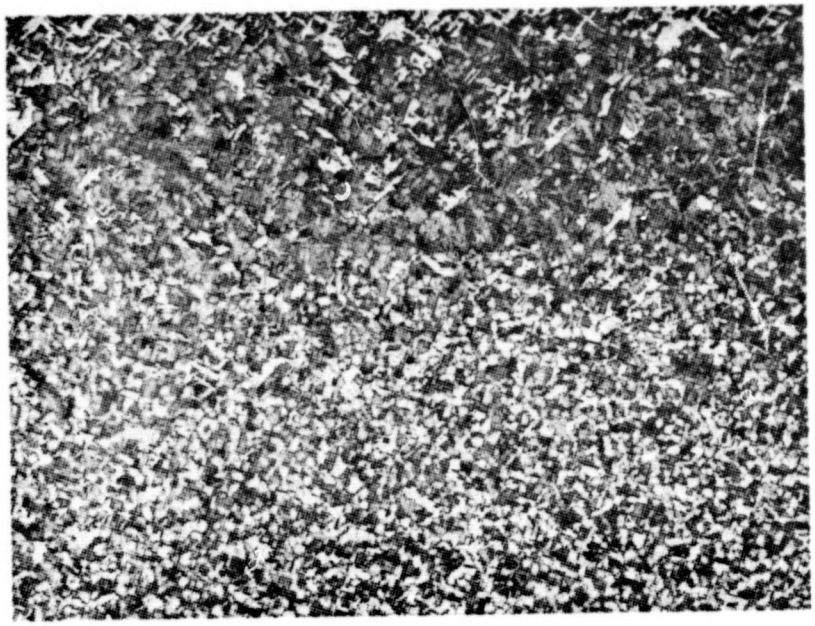

Bond
Line

100X

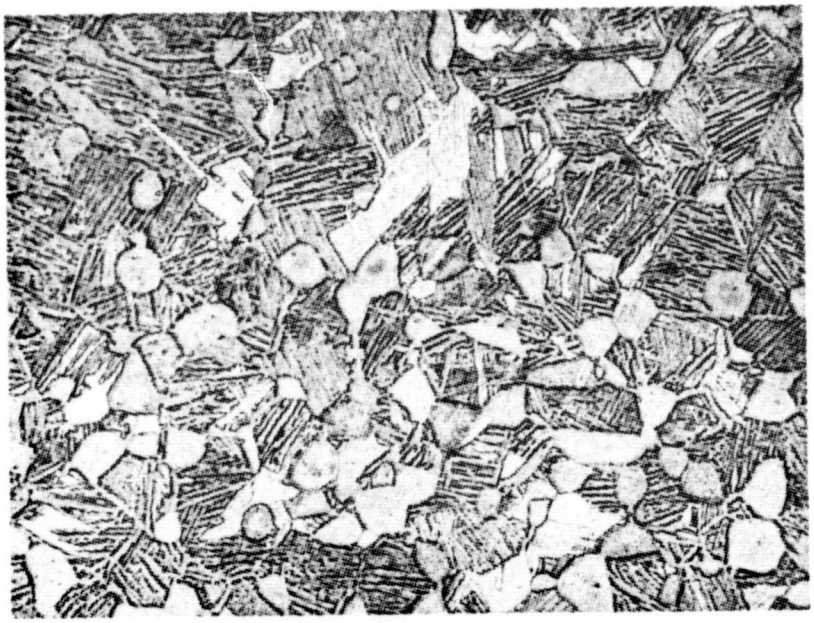

Bond
Line

500X

Figure 73. Typical Microstructure Along Edge in DS 25.
Etchant: $96H_2O$-$2HNO_3$-2HF.

A SEM analysis of these micropores was conducted at TRW on DS25. Figure 74(a) shows an area that was etched very lightly to just reveal some structure. No evidence of micropores was found at the bond lines. The light etch was also given as an attempt to remove any "smeared" material as a result of the polishing. The specimen then was given a heavy etch that usually reveals the micropores at the bond lines. SEM photomicrographs were again taken at the same areas (see Figure 74(b)). The micropores are now readily visible. Figure 75 better illustrates these indications at a higher magnification. It is TRW's belief that these pores could be the result of preferential etching.

An independent evaluation of the microscopic problem was conducted for TRW by the Air Force. Their conclusions was that SEM observation of the electropolished surface of the specimen along with electropolishing followed by etching, revealed that the pores are an etchpit effect, possibly due to contamination of the sheet surfaces prior to bonding.

iii. Diamond Specimens 11, 14, 16, 17, 18, 20, 21, 22, 23 and 24

The last lot of ten specimens were returned from the HIP vendor. Visual examination indicated that all ten cans HIP successfully; however, tapping the can to see if the cans "ring" suggested that four of the ten cans were not bonded. Small holes were drilled into these cans in order to leak check using the mass spectrometer. No leaks in the seam weld were found; however, there were some indications, particularly in DS18, that the can leaked at a 90° bend area at the root end of the specimen. After leak checking the four suspicious specimens, the ten diamond specimens were heat treated: 1750°F/1 hour/FAC + 1300°F/2 hours/AC. After heat treating the specimens were decanned. The four specimens that were suspicious were verified to be leakers during HIP. Examination of the cans after decanning showed tears in the areas where the leaks were detected. Although the decanning caused the tears, it was obvious that the material was weak in these areas compared to other perimeter areas. Metallography of these areas was inconclusive. The can material, although of drawing quality, may be "hot short" since the rupture appears to be occurring late in the HIP cycle in a high percentage of cans, at times in areas not requiring excessive deformation.

The six specimens that visually appeared bonded were further evaluated by X-ray and C-scan. Based on previous experience, the X-rays indicated that DS24 may not be entirely bonded as expected because of good ply delineation in the radiograph. The C-scan also is not as "clean" showing some indications. These observations are shown in Figures 76 and 77. Compare these results with those observed for DS25 (Figures 71 and 72) and the differences are obvious. The X-rays and C-scans for the remaining five diamond specimens are similar to DS25 and thus these specimens appear to be well bonded. Reviewing X-rays taken to verify core position before and after HIP, it was found that the cores remained in place during HIP; however, one of the diamond specimens (DS11) was found to have a core separation of 0.28-0.29-inch rather than the required 0.20-inch separation. This larger separation was also present prior to HIP based on the X-rays. A summary of the ten diamond specimens is given in Table IV.

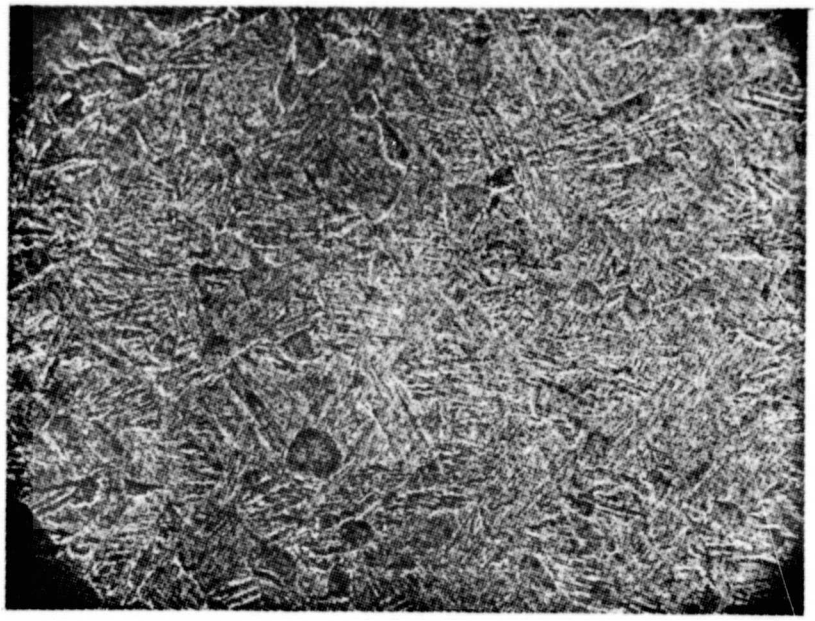

Bond
Line

a) Etchant: $96H_2O$-$2HNO_3$-2HF

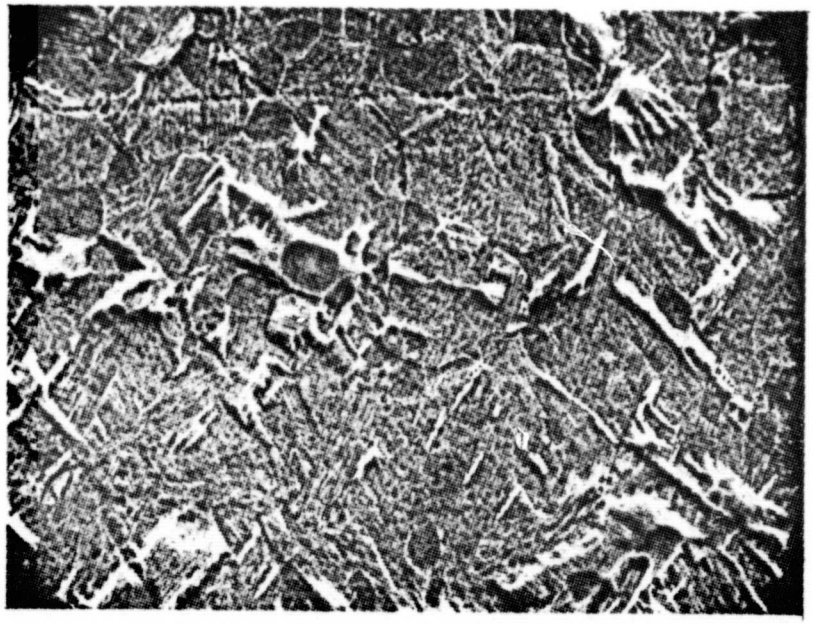

Bond
Line

b) Etchant: $60H_2O$-$35HNO_3$-5HF

Figure 74. SEM Photomicrographs Depicting What Appears to be Preferential Etching at Bond Lines in DS 25. 500X

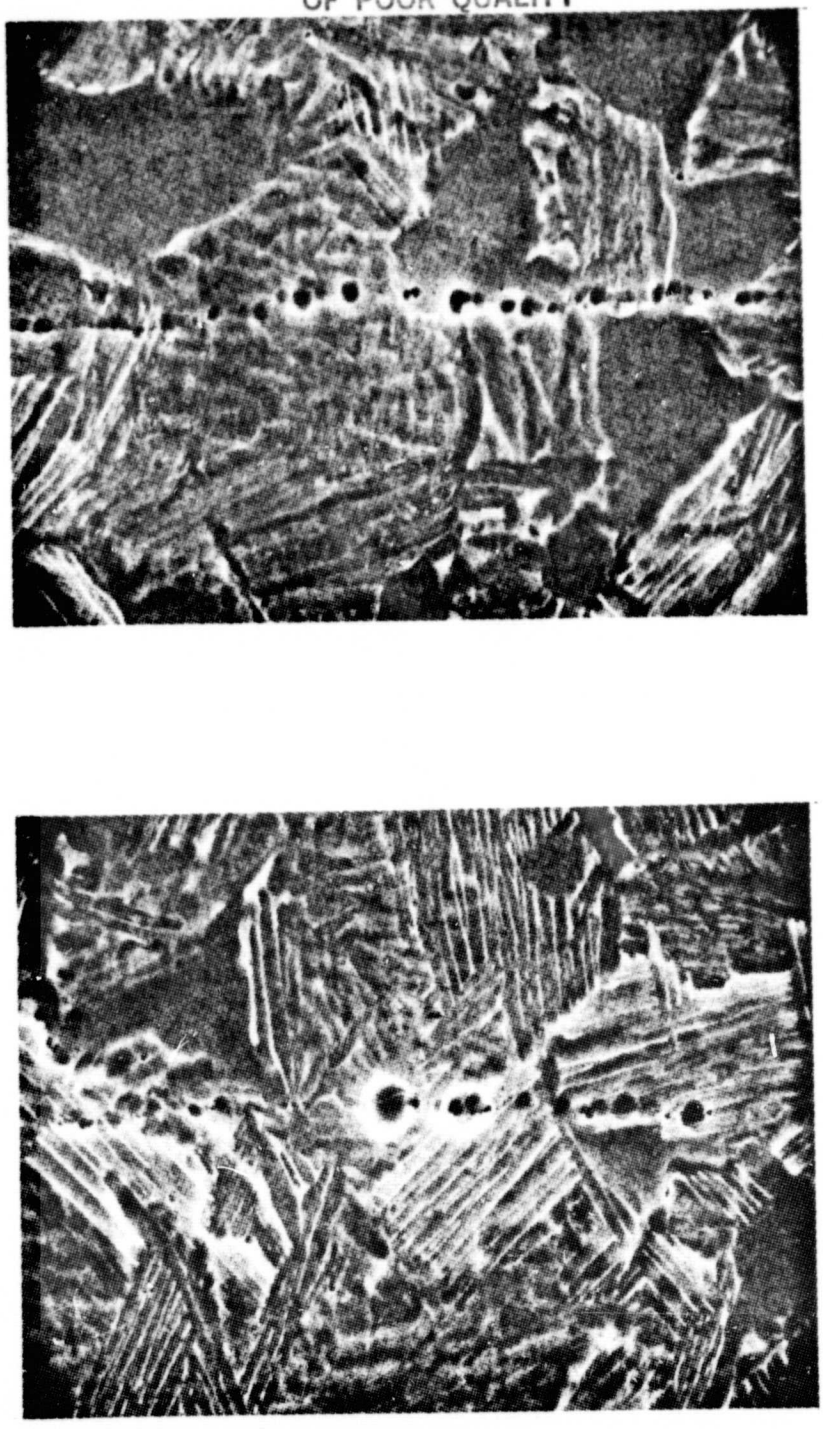

Figure 75. SEM Photomicrographs Illustrating That the Preferential Etching Leaves Voids in DS 25.
Etchant: 60 H_2O-35HNO_3-5HF 2000X

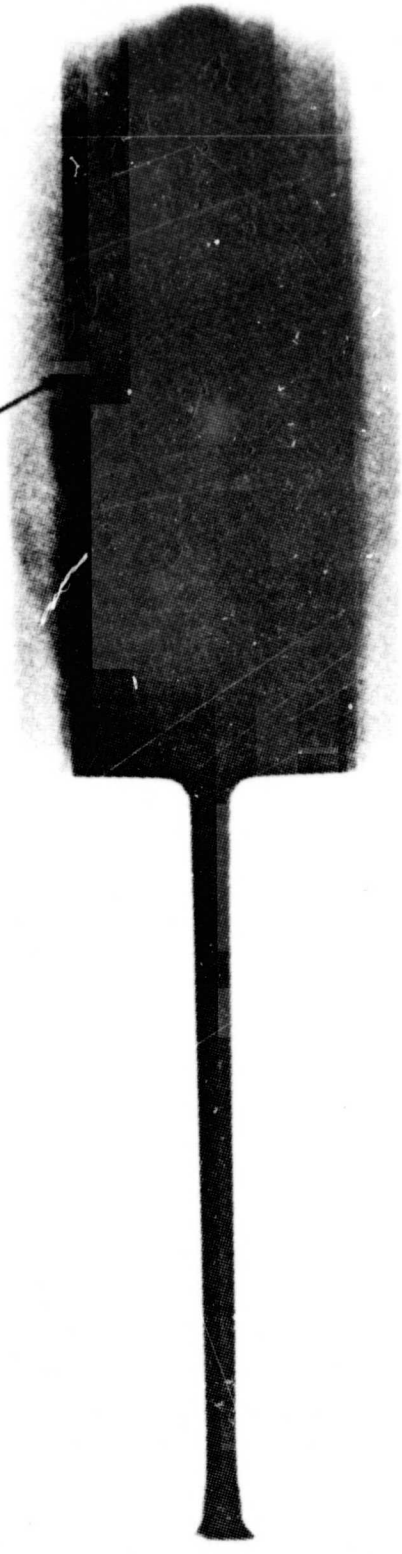

Figure 76. X-Ray of DS 24 After HIP, Machining and Core Leaching.

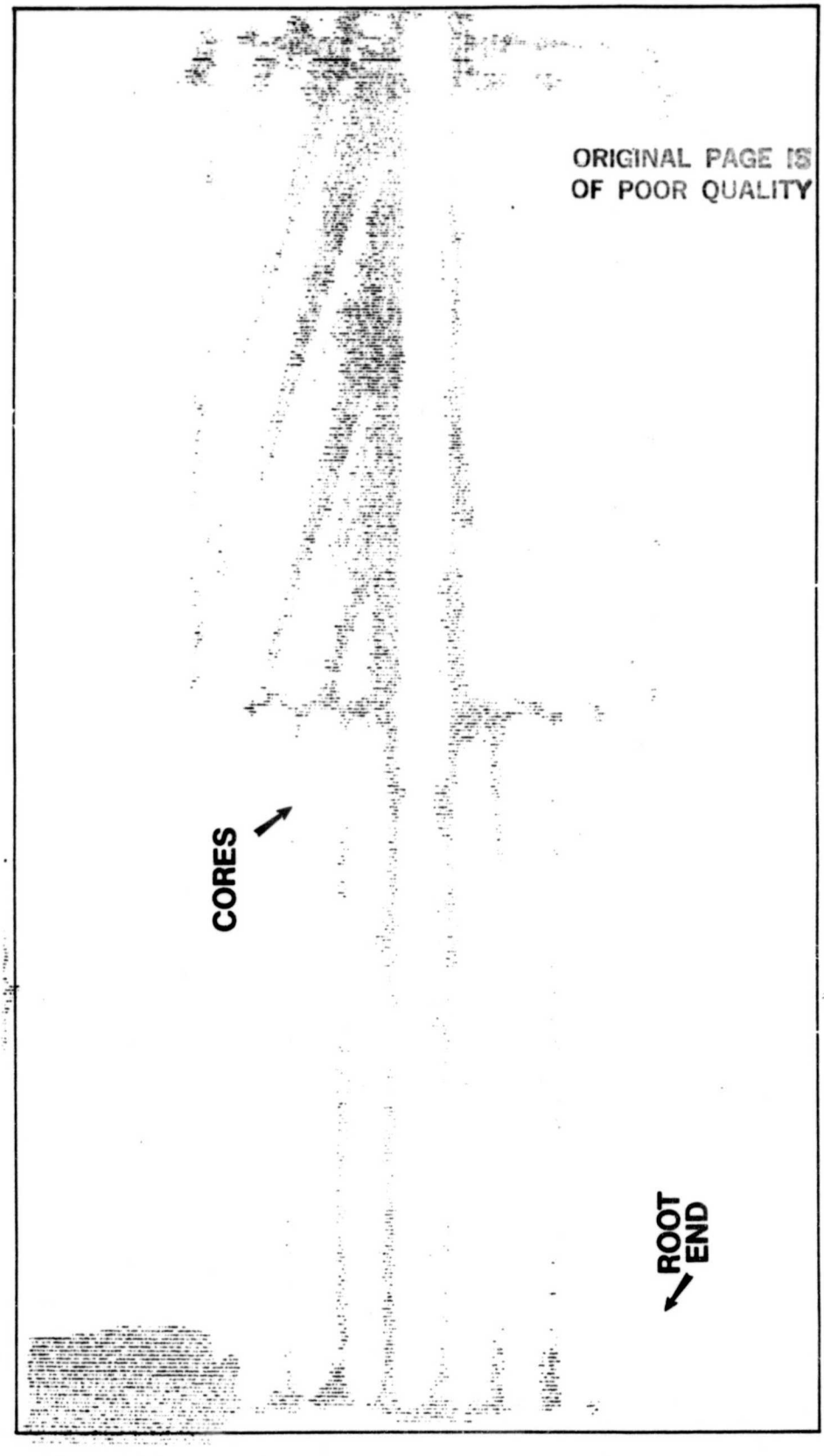

Figure 77. Ultrasonic C-Scan of DS 24. The Additional Pickup May Indicate a Lack of Bond.

TABLE IV

Summary Evaluation of Ten Diamond Specimens

Diamond Specimen	Material* Direction	Visual (Decanned)	X-ray	C-scan	Core Separation
11	L	Good	Good	Good	0.28-0.29
14	L	Good	Good	Good	0.23
16	L	Good	Good	Good	0.20-0.21
17	L	Good	Good	Good	0.22-0.25
18	L	Not Bonded	-	-	-
20	T	Not Bonded	-	-	-
21	T	Good	Good	Good	0.20
22	T	Not Bonded	-	-	-
23	T	Not Bonded	-	-	-
24	T	Good	Questionable	Questionable	0.19-0.20

* With respect to the material rolling direction.

2. Machining of Diamond Specimens

The last effort in this task was machining and leaching of the cores for the diamond specimens. DS8 and 25 not only were machined to length and width but also the surface was abrasive belt polished. Due to the thin wall design of the specimen and some shifting of the core in the short transverse direction, the surface was abrasive machined through the wall in one corner into the core. The original plan was to deliver these specimens as-HIP and the abrasive machining was an attempt to simulate the smoother surface to be produced on the blades after isothermal forging. The other six diamond specimens; DS11, 14, 16, 17, 21 and 24; were machined and leached successfully and are shown in Figure 78 prior to shipment to P&WA. Abrasive belt polishing of the surface was not performed for these six specimens.

B. Blade Process Development

1. Hollow Blade Fabrication

a. First Iteration

The blade assemblies after HIP are shown in Figure 79. Both assemblies leaked during HIP, probably early into the cycle. The HIP assemblies were again leak checked using a mass spectrometer. A hole was drilled at the root end and a vacuum was pulled on the assembly. Assembly was leak checked using helium. Both blades leaked at the root end but the leaks were large enough to prevent exact location using the mass spectrometer. The assembly was then pressurized with helium from the inside and a leak check solution (soap solution) was applied at all weld areas. This solution pinpointed two weld failures in each blade. Both blades failed along the TIG weld-base metal interface near the tube exit and also failed at a spot weld that was inside the seam welded area. Figure 80 illustrates typical locations of the two leak sources for both assemblies. These areas were sealed and the entire assembly was leak checked again using a mass spectrometer. No other leaks were found. Obviously, no spot welds should be within the seam welded perimeter. The few spot welds inside the seam welds on these initial assemblies were unintentional. The poor condition of the blades after HIP limited any other evaluations.

b. Second Iteration

Visual observation of the blades after HIP revealed that the outer can leaked during the HIP cycle. Blade 2 was re-HIP to evaluate 8he new evacuation tube procedure knowledgeable to the fact that a fully bonded blade would not be possible due to the entrapped argon from the first HIP run. Evaluations of this blade indicated that weld failures occurred at the can-root-TIG weld interface. The visual appearance of the blade remained the same as after the first run. Evaluations of the rootless blade indicated that the titanium can ruptured in several places at the junction of the root end and the filler plies due to excessive can movement during the initial stages of HIP. Blade 3 is shown in Figure 81. A considerable amount of can deformation occurred in the initial stages of HIP prior to occurrence of the leak. X-rays of the rootless blade after HIP indicated that the

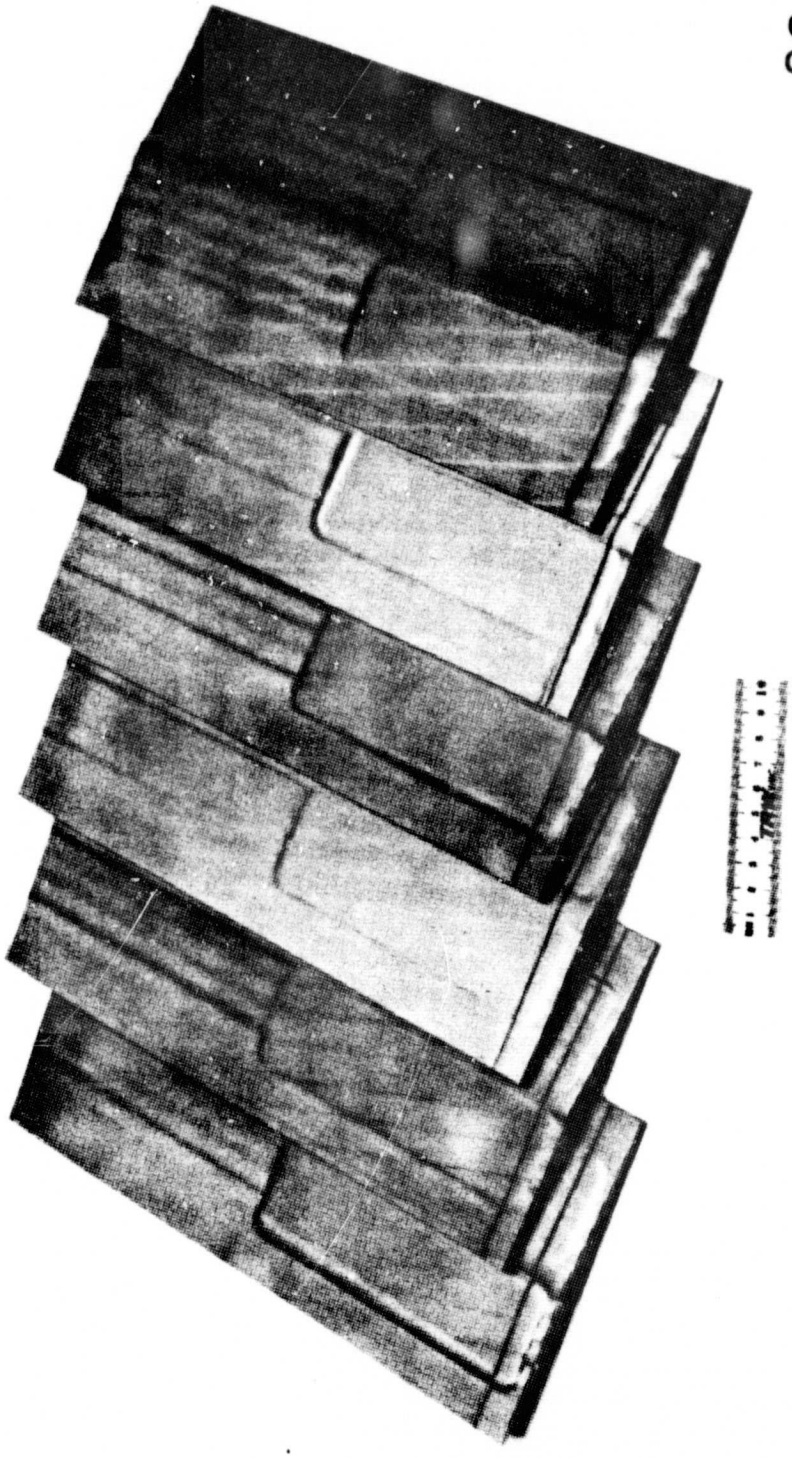

Figure 78. Six Machined and Core Leached Diamond Specimens.

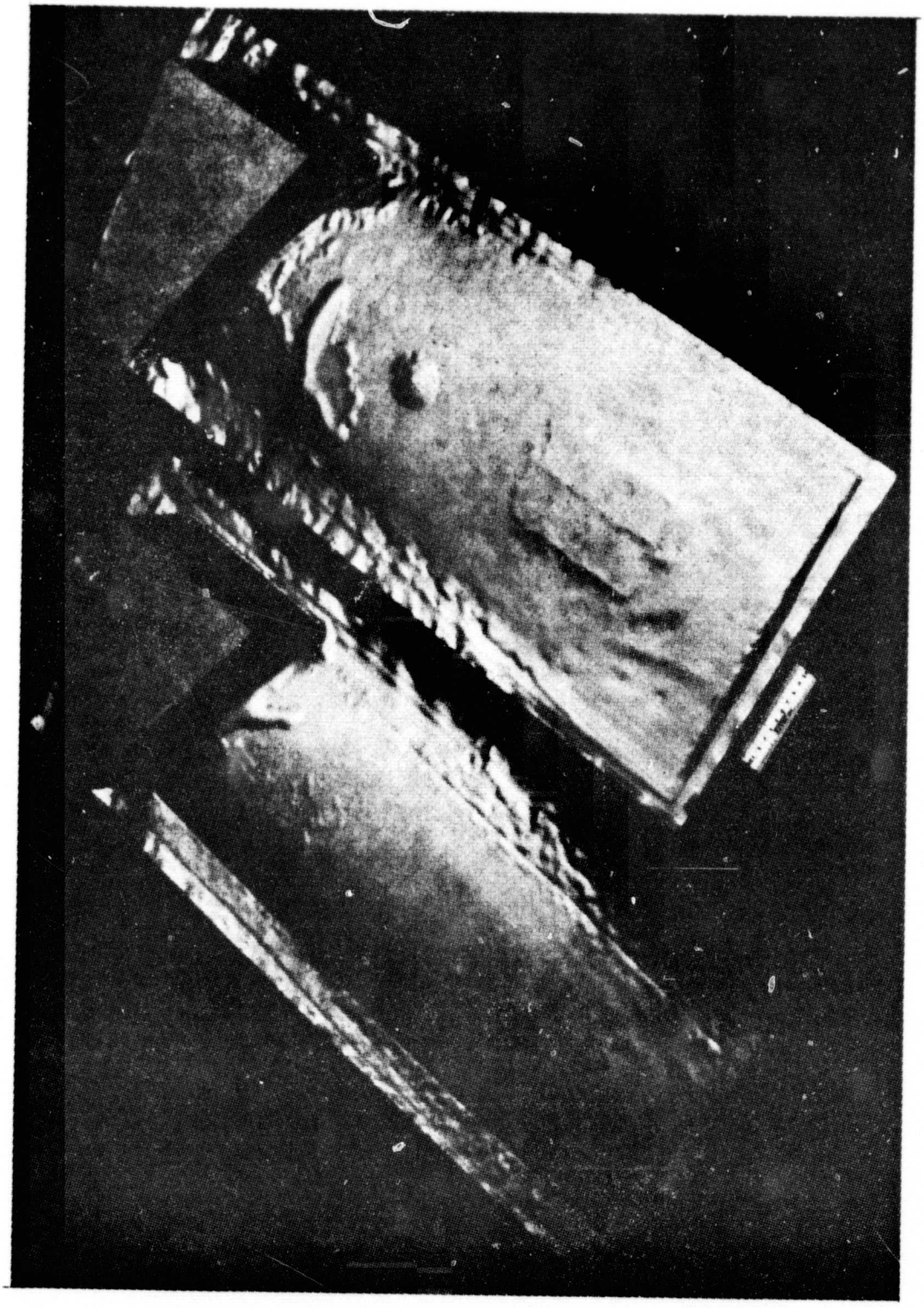

Figure 79. First Iteration Blades After HIP.

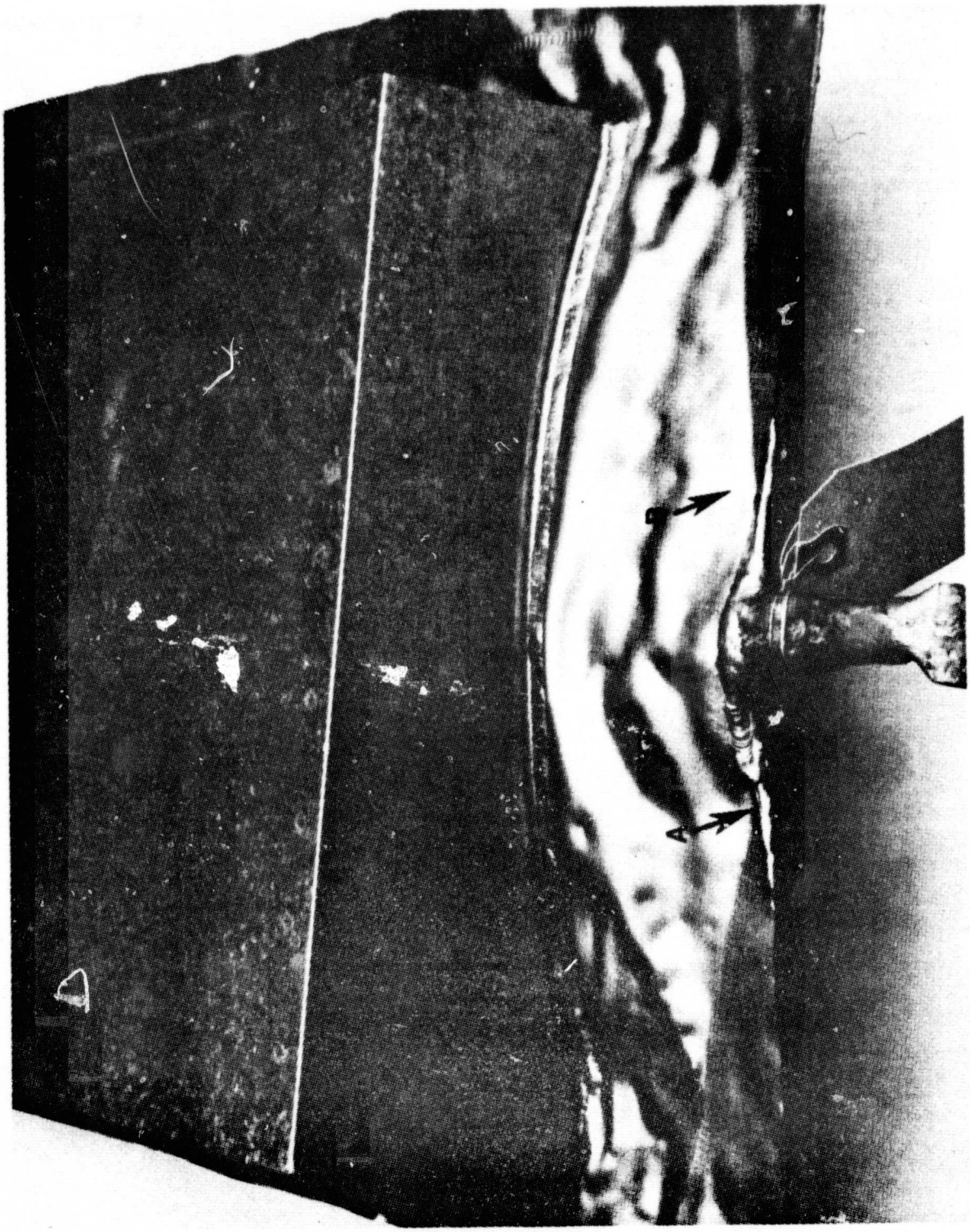

Figure 80. Closeup of Root End of HIP Blade Illustrating Location of Weld Failures.
A. TIG Weld Failure. B. Spot Weld Failure.

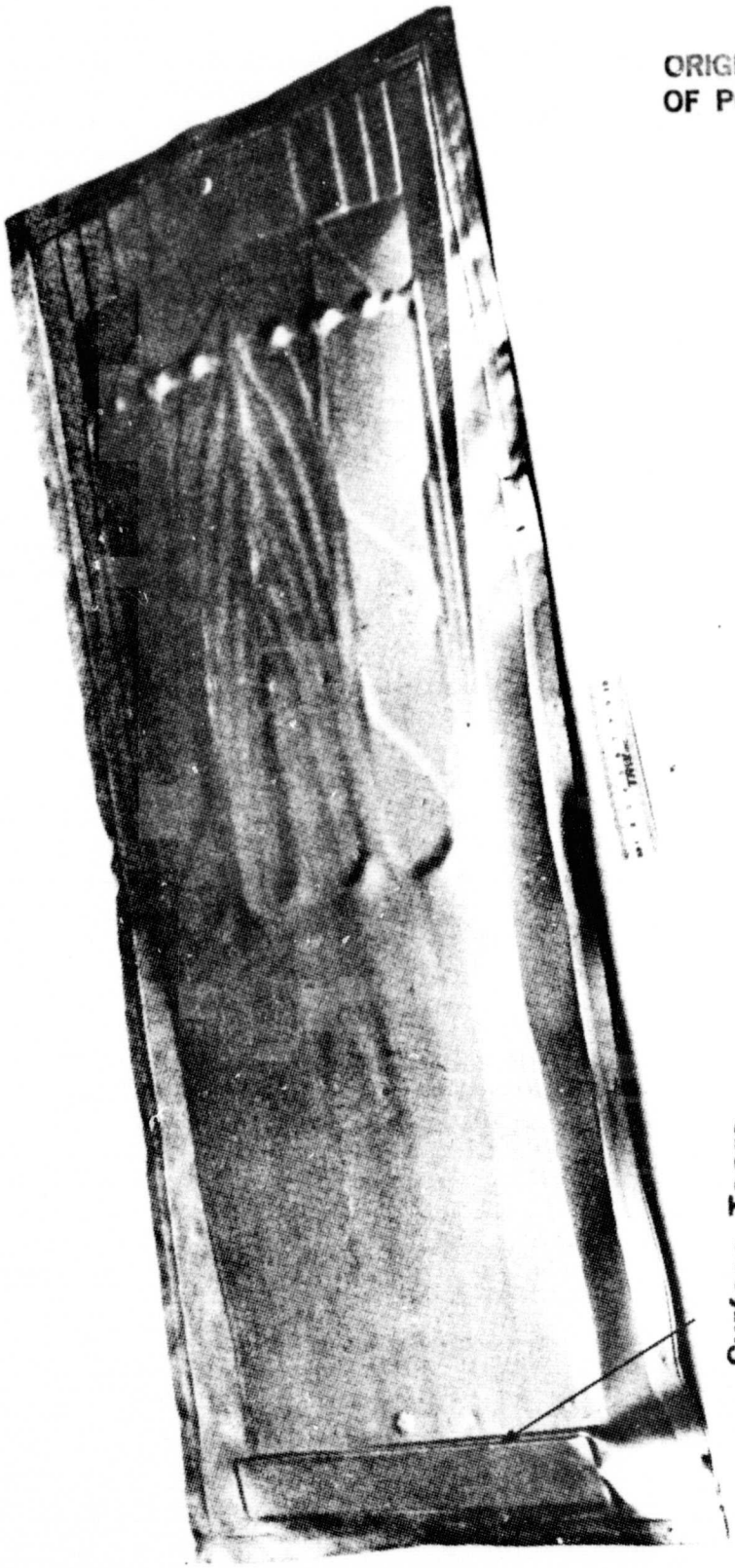

Figure 81. As-HIP Blade 3. Surface Tears Were Found Along the Edge Noted in the Figure.

cores remained in place during shipping and HIP. Attempts were made to disassemble the blade after HIP but a considerable amount of bonding had occurred. The Figure 82 photomicrograph shows the bond lines with the porosity due to argon. Note also the ply ending which indicates a lack of titanium ply flow. These observations appeared to be typical of blade 3.

c. Third Iteration

The HIP cycle used at IMT was, again, the 4.5 hours at 1750°F temperature cycle previously used. Visual observations of both blades after HIP indicated that 4 appeared to be a good, well-bonded blade while 5 leaked during HIP. Blades 4 and 5 are shown after HIP in Figures 83 and 84. As shown in Figure 83, there is considerable surface detail due to ply endings, cores, etc. The blade also "rings" when tapped with a metallic object, which is an indication of bonding. X-rays of the blade indicated goood core location with no evidence of ply endings (sharp lines in the X-ray film would indicate a lack of a good bond). However, there does appear to be some deformation of the "pins" located at the edge of the cores. The Figure 85 X-ray indicates these observations. These "pins" were added for passageways for acid core leaching. There appears also to be a relationship between the "pins" and "bumps" on the surface as shown in Figure 83. The bumps are excess titanium from the central plies.

Inspection of blade 5 with the root indicated leaks in several areas, the more prominent being in the canning sheet-root block interface towards the tip which were either seam or spot welded. Other leaks in the blade were observed, but found to be inconclusive due to lack of reproducibility. It appears that the leaks in the canning sheet-root interface were quite large leading to excessive helium in the area. This excessive helium discharge makes leak detection difficult. Based on the above observations, it appears that there was too much can collapsing in the canning sheet-root block area. High shear stresses and thin cover sheets contribute to these weld failures. It is doubtful that this canning approach can work with the current ply and root designs.

d. Fourth Iteration

Visual and X-ray results of blades 6 through 9 indicated that the four blades were successfully bonded by HIP (see Figure 86). To measure the amount of can collapse after sealing and HIP, the thicknesses at eight points were measured along the length of the blades at a distance of 4-inches from the edges. These results are shown in Table IV. The measurements were made using hand micrometers and were only intended to give some indication as to the amount of can collapse and debulking that occurs. After sealing an average can collapse of 0.15-inch was observed with more collapsing being observed at the root end. An average debulk of 0.10-inch was observed as a result of the HIP operation, and again more debulk was observed at the root end.

Metallographic evaluations of the blades were performed after isothermal forging and are discussed later.

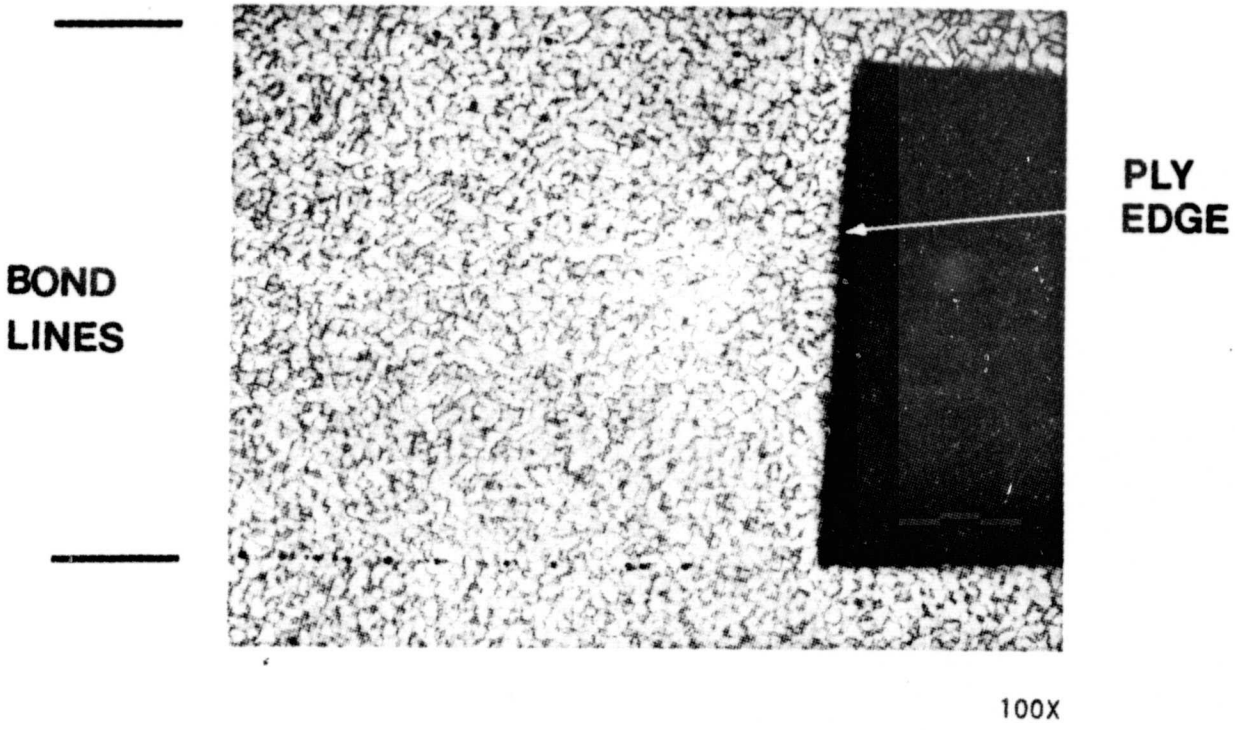

Figure 82. Typical Microstructure and Bonding Conditions Found in Blade 3.

Figure 83. AS-HIP Blade 4.

ORIGINAL PAGE IS
OF POOR QUALITY

Figure 84. AS-HIP Blade 5.

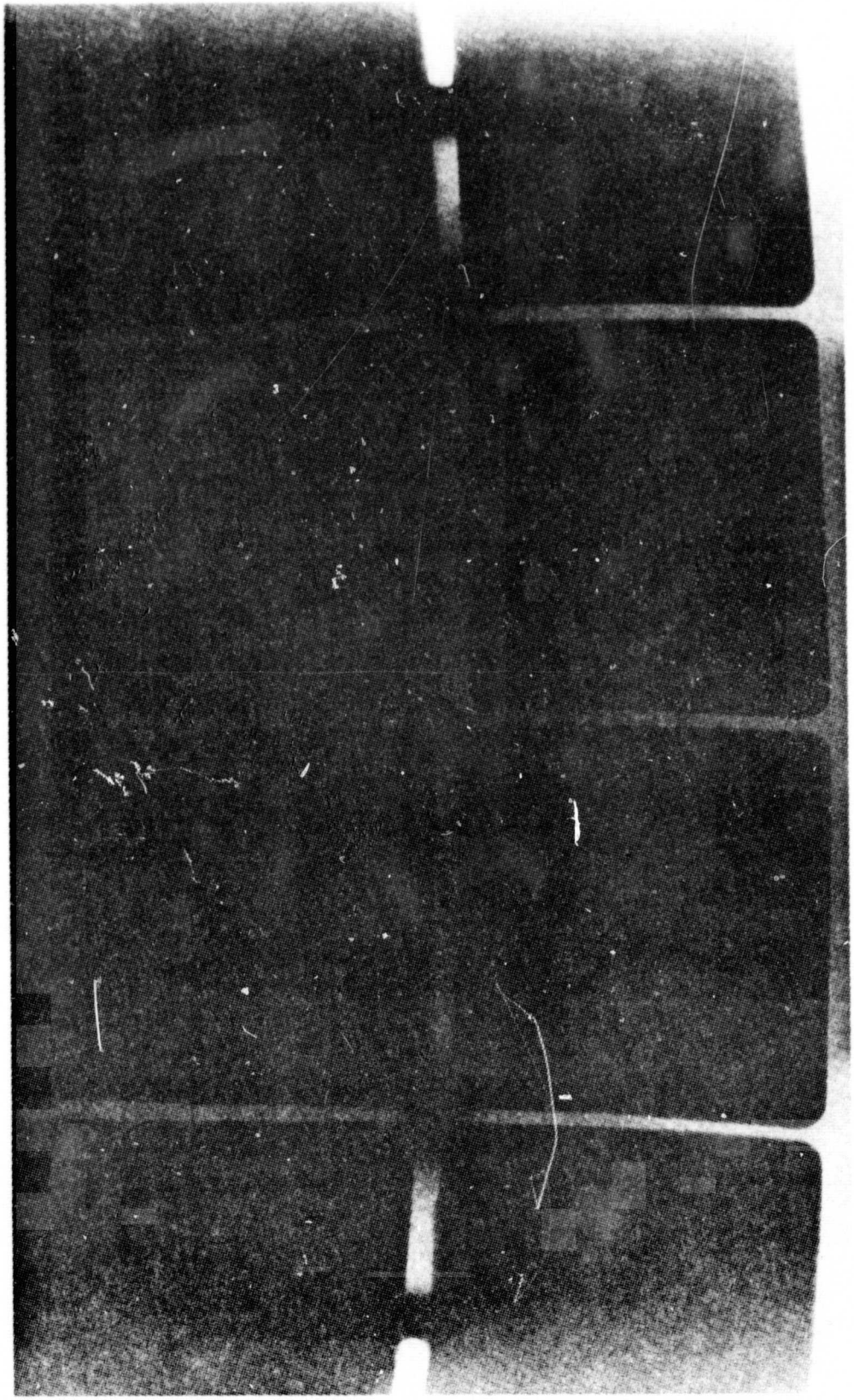

Figure 85. X-Ray of Tip Area of Blade 4.

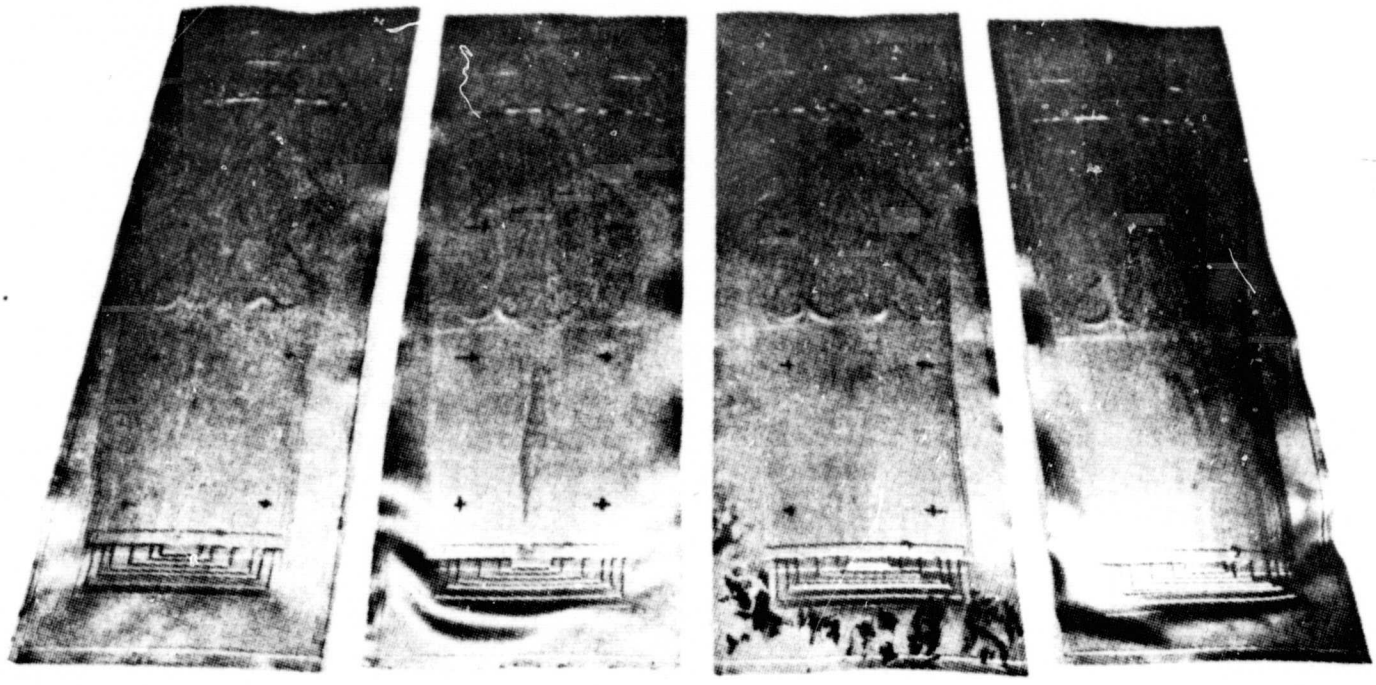

Figure 86. Blades 6 Through 9 Shown After HIP.

TABLE V

Dimensional Measurements of Canned Blades

Blade No.	Position A	B	C	D	E	F	G	H
	Before EB Sealing							
6	0.865	0.868	0.761	0.661	0.818	0.820	0.758	0.662
7	0.852	0.848	0.754	0.675	0.775	0.830	0.750	0.627
8	0.862	0.837	0.673	0.642	0.852	0.865	0.769	0.610
9	0.840	0.861	0.778	0.621	0.863	0.875	0.751	0.625
	After EB Sealing							
6	0.629	0.694	0.566	0.563	0.608	0.729	0.541	0.571
7	0.651	0.706	0.579	0.584	0.570	0.739	0.527	0.533
8	0.652	0.737	0.578	0.566	0.622	0.748	0.539	0.523
9	0.614	0.705	0.580	0.577	0.663	0.788	0.591	0.574
	After HIP							
6	0.580	0.616	0.555	0.425	0.433	0.534	0.526	0.420
7	0.516	0.627	0.552	0.447	0.520	0.580	0.509	0.418
8	0.519	0.606	0.566	0.430	0.468	0.558	0.524	0.409
9	0.561	0.639	0.563	0.436	0.459	0.588	0.566	0.431

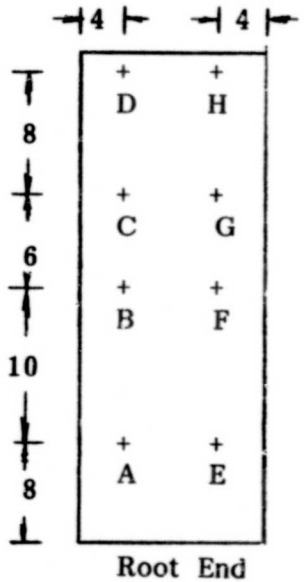

Previous results on blade 4 described what appeared to be deformation of the connecting pins of the cores as a result of the HIP operation. These observations were based on X-rays of blade 4 and were again observed for blades 6 through 9 even though excess titanium was removed from this area prior to assembly. There was some thought that the image observed in these areas on the X-ray film may be the excess titanium ("bumps") on the surface that can be seen after HIP. These "bumps" were removed from blade 4 by grinding and the blade was resubmitted for X-ray. The new X-rays revealed evidence of pin deformation. To alleviate this problem in the future, it appears that the pins between cores will have to be placed at greater distances apart than for the current design.

2. Post-HIP Processing of Hollow Fan Blades

a. Camber Trials

Blade 2 is shown after cambering in Figure 87(a). Basically, the concept of cambering a flat blade layup after HIP appears very promising. There was some severe tearing observed at the leading and trailing edge areas of the airfoil-root interface as shown in Figure 87(b). The tearing occurred because the die and punch made contact with the airfoil prior to making contact with the root. Tooling rework was performed in this area.

After rework blade 4 was cambered. The cambering process for blade 4 resulted in severe tearing near the leading and trailing edges at the intended root/airfoil interface area as shown in Figure 88. The tearing was still attributed to an early contact problem in this area and also to long transfer times causing excessive blade chilling. The upper punch was removed from the press for rework and some modifications.

Blades 6 through 9 were cambered after the second tooling rework using a two-step approach that was described previously. This approach was very successful in cambering the blades. The cambered blades are shown in Figure 89. Cambering a flat layup appears to be easily performed and cost effective if one considers the individual cambering of plies. It was noted that cambering also removed some of the surface undulations due to ply endings just from the clamping operation.

b. Twist Trials

The twist trials were performed with no problems. Total time to load blade into die and conduct twist operation for each section was of the order of 10 to 15 seconds. Inspection of the blades was not performed with a gage to measure the amount of twist; however, visual appearances of the blades after twisting (Figure 90) indicated that the blades looked similar, that is, the process appeared reproducible. A twisted blade was layed in the bottom die of the isothermal forge tooling (neither blade nor die were heated) and observed to be close to the required twist. No location problems were foreseen in isothermal forging the twisted blades.

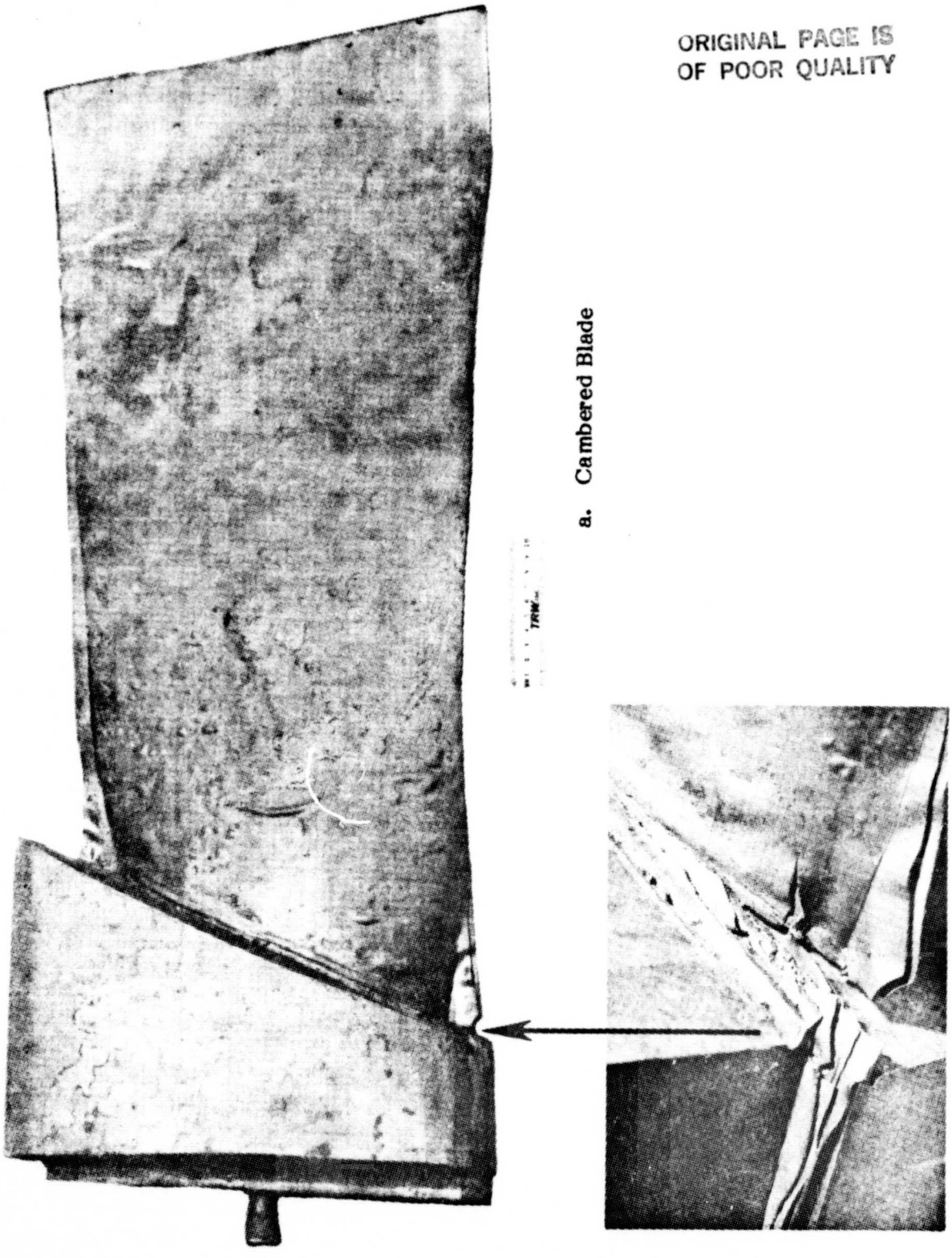

a. Cambered Blade

b. Airfoil Root Tearing

Figure 87. Blade 2 After Cambering.

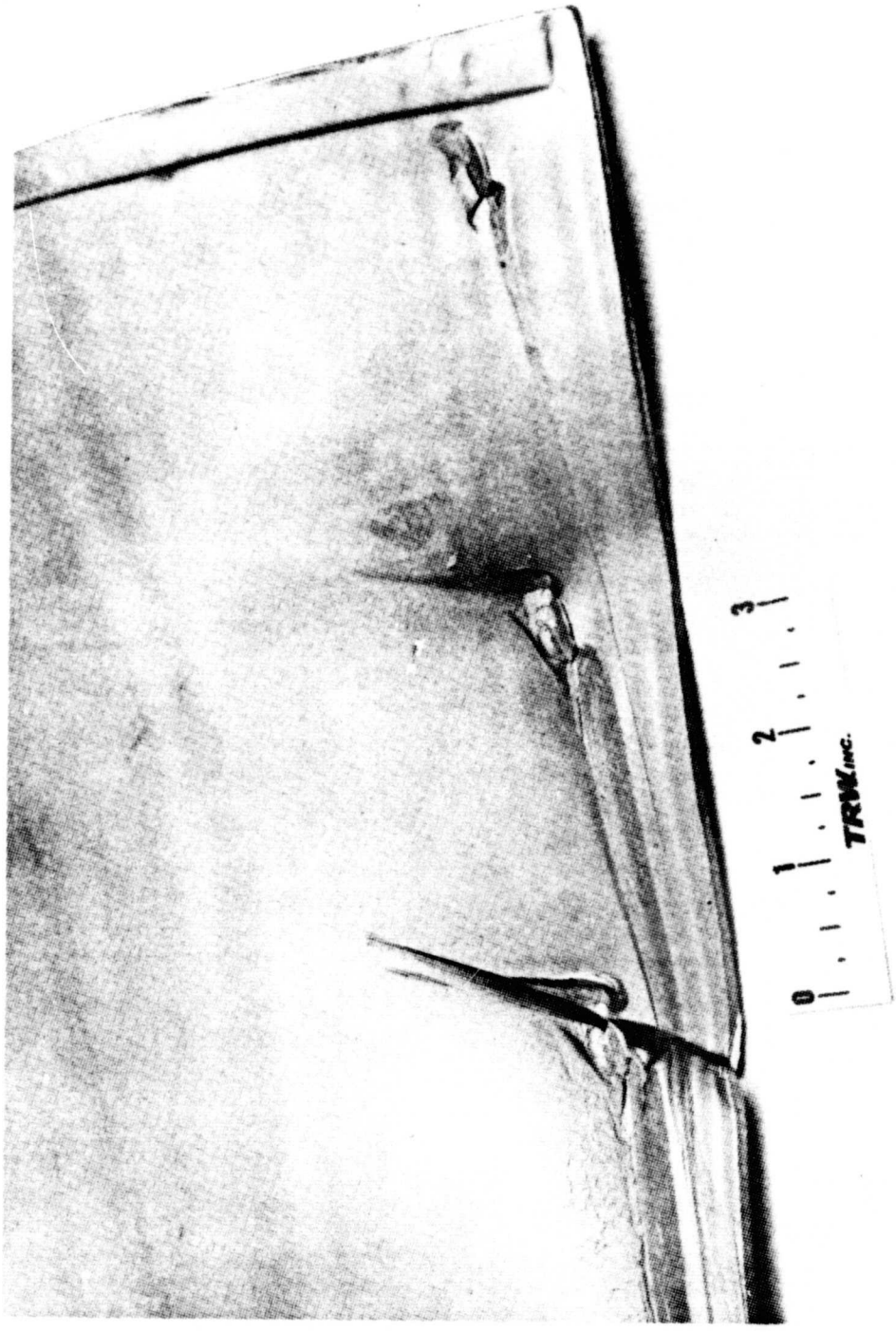

Figure 88. Shear Area as a Result of Cambering for Blade 4.

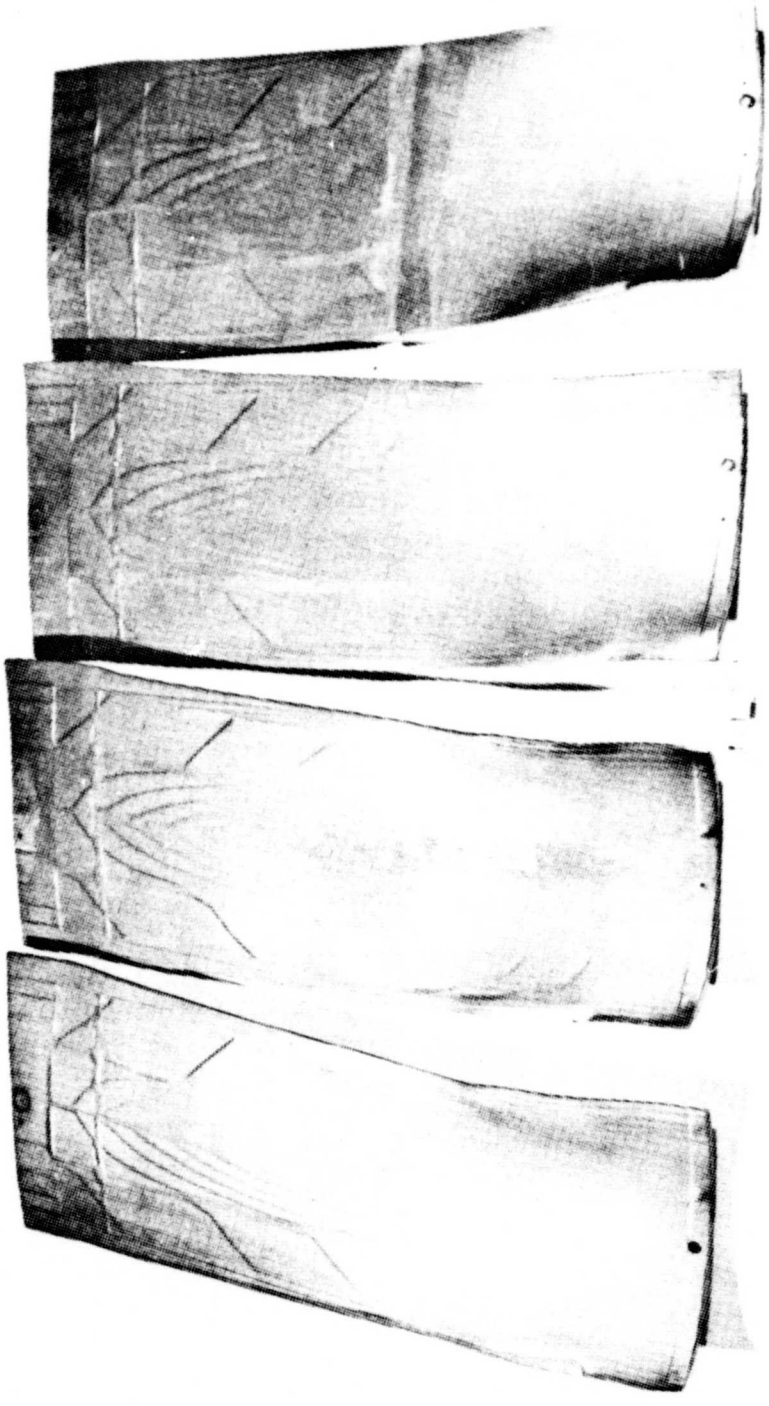

Figure 89. Blades 6 Through 9 After Cambering.

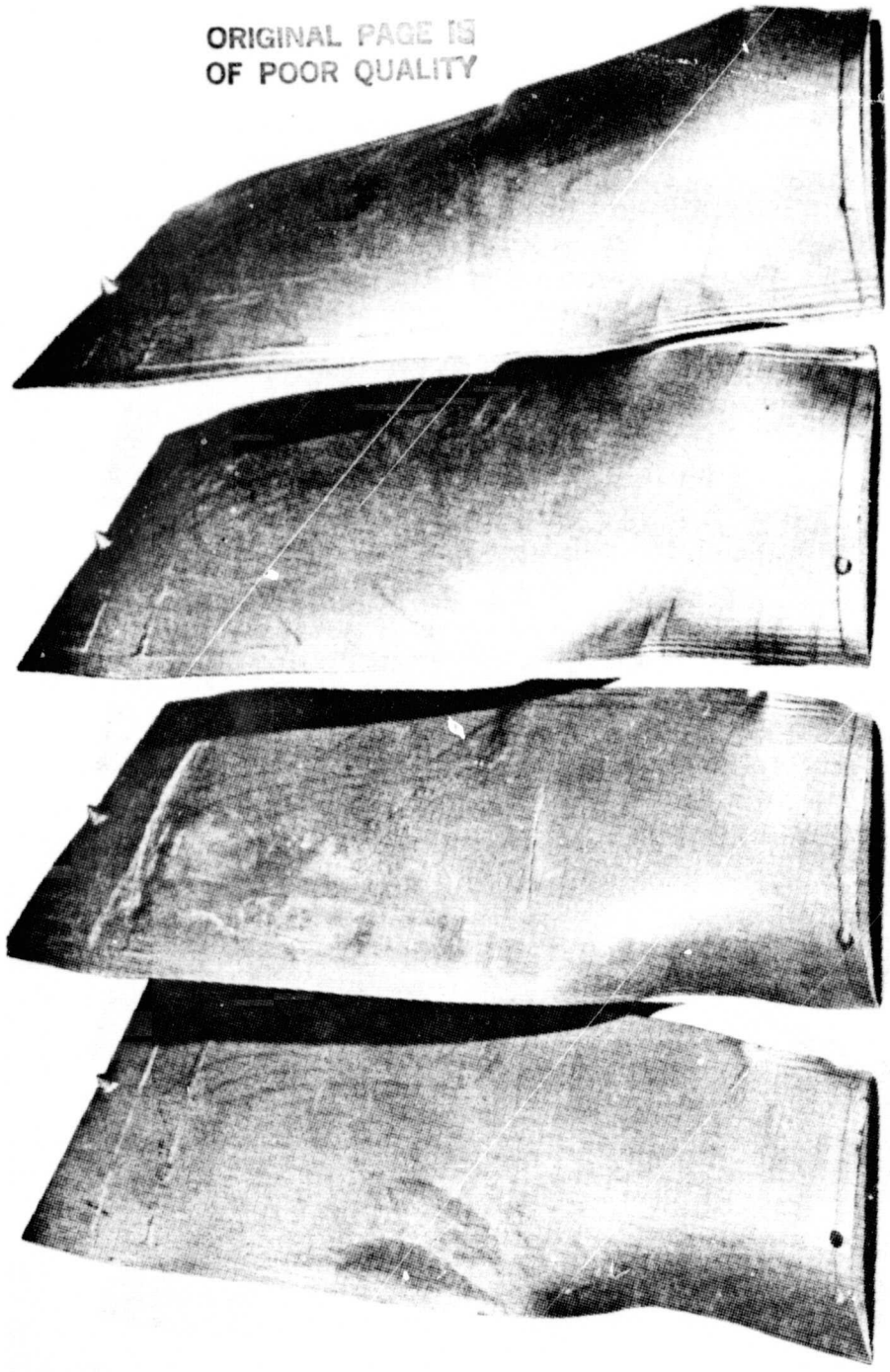

Figure 90. Blades 6 Through 9 After Twisting on Ajax Crankpress Twister.

c. Isothermal Forging

Isothermal forging of five blades was conducted without any technical problems with respect to the processing aspects; however, there were problems associated with making full blade contact near the tip end of the blade. Blades 6 and 9, forged three times, and blades 7 and 8, forged once, are shown in Figure 91. Blades 4, 6 and 9 were used to achieve setup for blades 7 and 8. Since only one press setup was now planned for this program blades 7 and 8 were forged with what was considered the best setup even though blade tip contact during forging was minimal. The dimensional changes as the result of forging are summarized in Tables VI through VIII. The blades were forged in the order of blade 4, 9 and 6 respectively. Reviewing the data it was obvious that the pitch thicknesses could be achieved for all sections except the tip, section AM-AM. The dimensional data on restrikes does not become too meaningful because in practice there would not be a restrike. The value of the restrikes was to determine whether tip contact could be made during the isothermal forge cycle. Figure 92 shows blade 9 immediately after forging, while blade 6 and 9 are shown in Figure 91 after the third restrike. For the final forging effort on blades 7 and 8 the temperature of the die and punch was kept about $1700^{o}F + 50^{o}F$ except at the root where the temperature was closer to $1600^{o}F$.

Blades 7 and 8 were isothermally forged with what was considered the best setup with the constraints of having no blades available for additional forging trials. The blades were forged without incident. Dimensional analyses of the forged blades are shown in Table IX. The pitch thicknesses measured for both blades either meet or are very close in meeting the blueprint requirements. Only the last section inspected indicates a very large oversize condition. This was expected because of the lack of contact at the tip section. This is shown in Figure 93. In general the leading and trailing edges were found to be heavy in thickness except for one section. The heavy condition is attributed to the thermal expansion of the dies during heating. The dies want to bow outward along the width. Currently die rework is the solution; however, thermal expansion data are being accumulated to better predict this type of behavior in order to incorporate these changes in the initial die design. The wider the chord the more significant the problem, and for the hollow blade the chord width is significantly larger than commercially produced blades. The one set of data at section J-J indicates that the material is probably being "pinched" in this area during forging leading to very thin edges.

Since the program effort was being terminated after one forging iteration, there was little that could be done to produce an airfoil closer to blueprint requirements at the leading and trailing edges without a significant die rework effort.

Other evaluations of the blade included X-ray analyses. All five blades were X-rayed. There was no evidence of disbond areas within the blade based on experience in interpreting X-ray film for diamond specimens. A typical X-ray is shown in Figure 94 for the core section of blade 7. It was found that the cores at the leading and trailing edges flowed during forging following the flash pattern. That is areas where more material flashing occurred resulted in more core flow in these areas. This phenomena can be observed in the Figure 94 X-ray. The X-rays also indicated that the cores had increased in length as a result of the forging operation. It was noted that the overall blade length was increasing during forging by approximately 1-inch. Core length changes are shown in

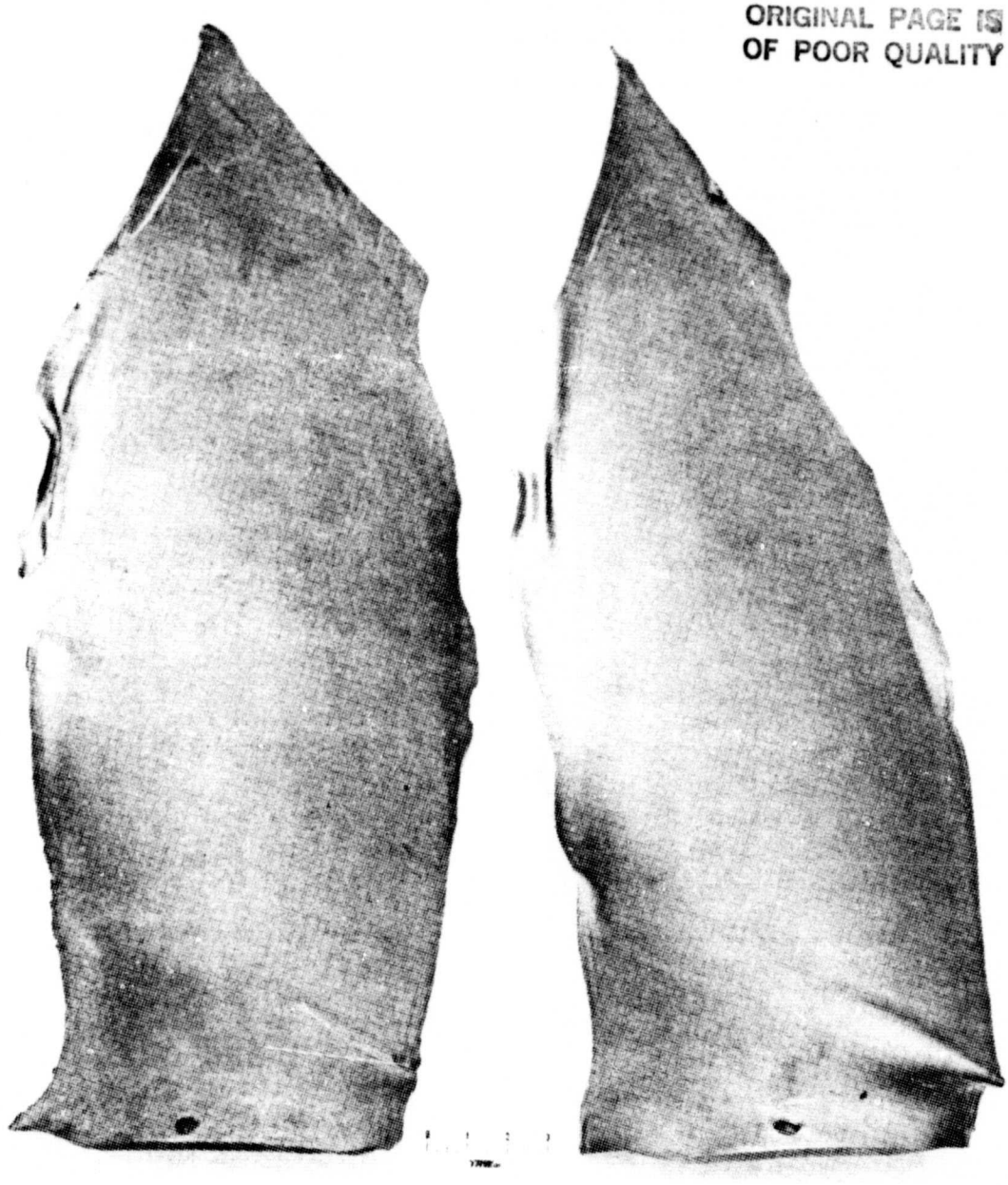

Figure 91 (a). Blades 6 Through 9 Are Shown After Isothermal Forging.

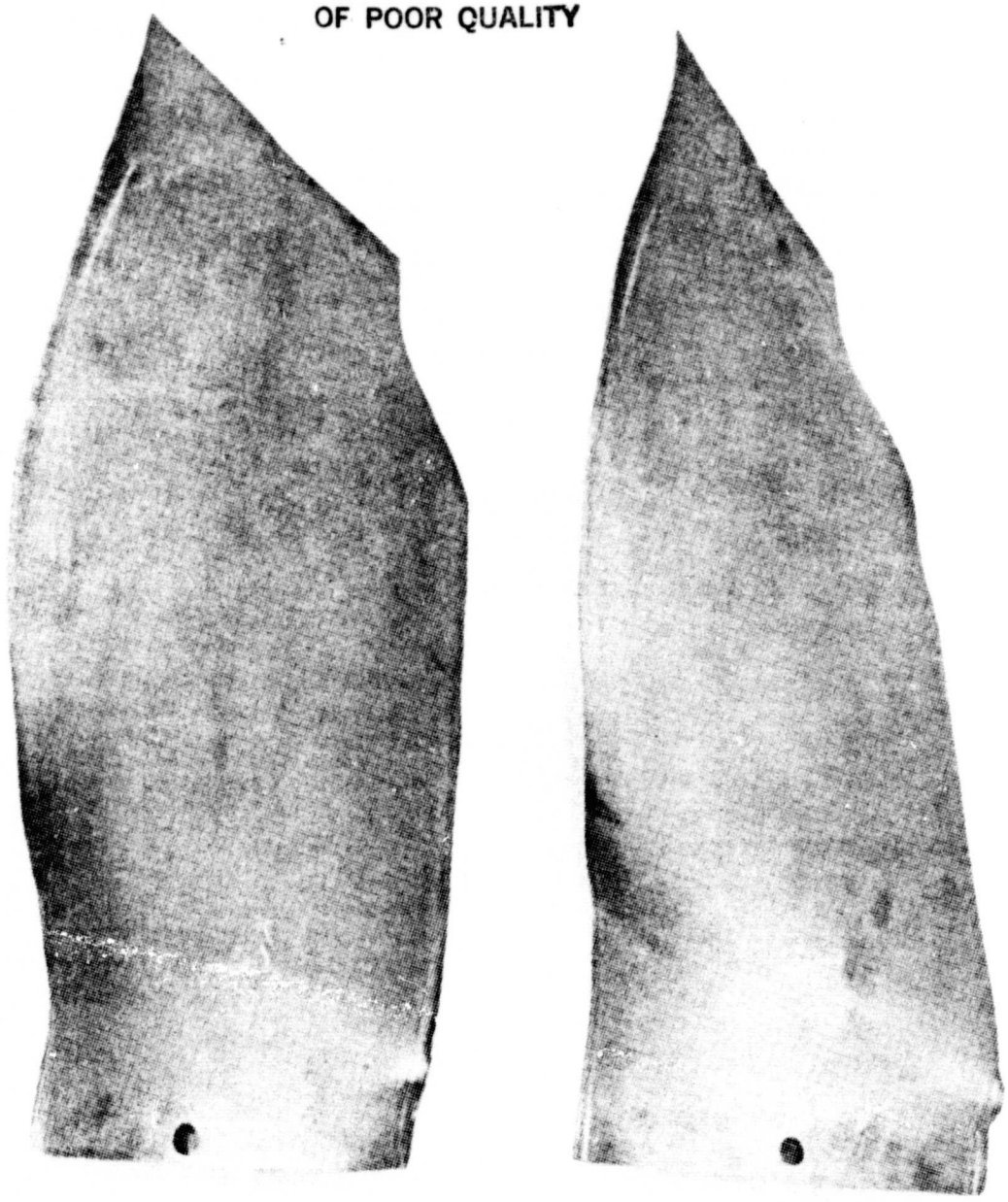

Figure 91 (b). Blades 7 and 8 Are Shown After Isothermal Forging.

TABLE VI

Pitch Thickness Measurements for Blade 4

Section	BP	First Strike	Second Strike	Third Strike
J-J	0.852	0.876	0.836	0.841
T-T	0.828	0.872	0.796	0.802
X-X	0.755	0.788	0.717	0.719
AA-AA	0.652	0.702	0.635	0.609
AG-AG	0.461	0.534	0.506	0.495
AM-AM	0.345	0.407	0.407	0.407

TABLE VII

Pitch Thickness Measurements for Blade 6

Section	BP	First Strike	Second Strike	Third Strike
J-J	0.852	0.852	0.820	0.819
T-T	0.828	0.830	0.795	0.772
X-X	0.755	0.757	0.688	0.674
AA-AA	0.652	0.641	0.585	0.572
AG-AG	0.461	0.489	0.450	0.436
AM-AM	0.345	0.390	0.395	0.394

TABLE VIII

Pitch Thickness Measurements for Blade 9

Section	BP	First Strike	Second Strike	Third Strike
J-J	0.852	0.860	0.863	0.864
T-T	0.828	0.820	0.804	0.784
X-X	0.755	0.736	0.704	0.694
AA-AA	0.652	0.635	0.605	0.592
AG-AG	0.461	0.491	0.462	0.448
AM-AM	0.345	0.404	0.408	0.408

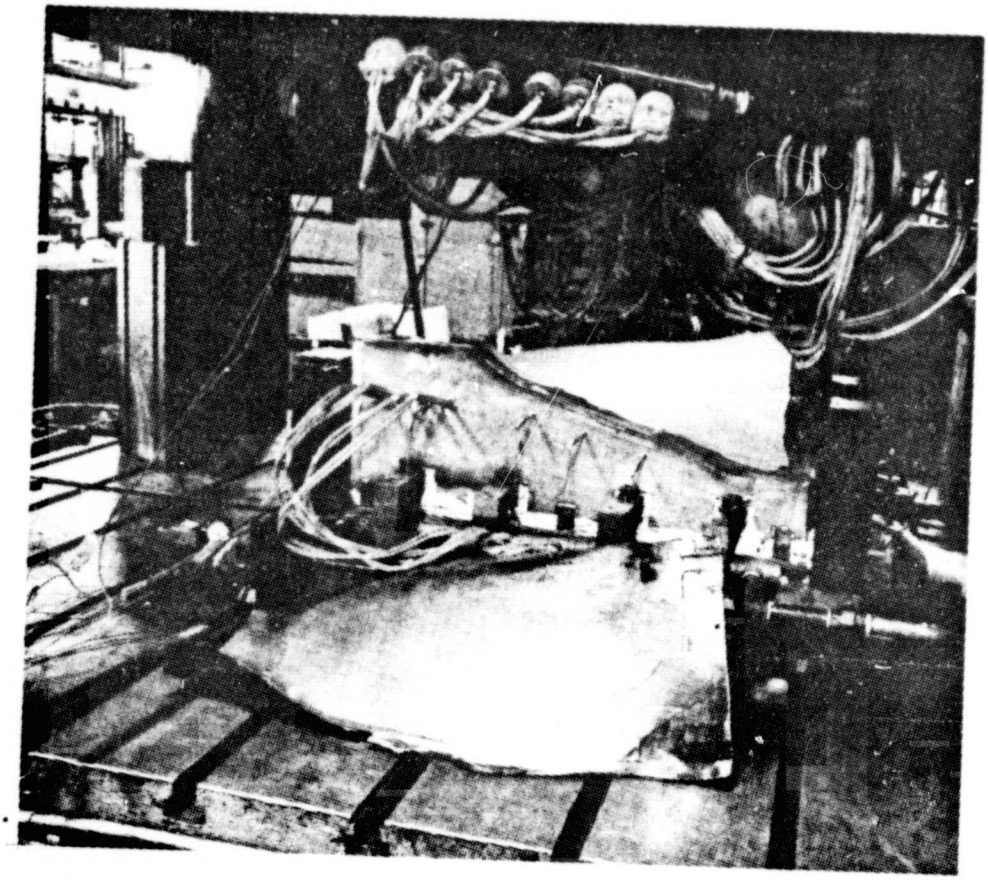

Figure 92. Blade 9 Shown Immediately After Removal From Isothermal Forging Die.

TABLE IX

Dimensional Analyses of Blade 7 and 8

Section	Pitch			LE			TE		
	BP*	Actual Blade 7	Actual Blade 8	BP*	Actual Blade 7	Actual Blade 8	BP*	Actual Blade 7	Actual Blade 8
J-J	0.852	0.866	0.865	0.081	0.184	0.161	0.089	0.037	0.018
T-T	0.828	0.833	0.832	0.079	0.201	0.195	0.089	0.105	0.094
X-X	0.755	0.746	0.742	0.073	0.146	0.147	0.079	0.118	0.118
AA-AA	0.652	0.642	0.639	0.063	0.121	0.122	0.069	0.100	0.094
AG-AG	0.461	0.467	0.469	0.047	0.071	0.070	0.049	0.104	0.096
AM-AM	0.345	0.392	0.390	0.046	0.115	0.112	0.038	0.113	0.109

* Tolerance of $\pm$0.008-inch allowed.

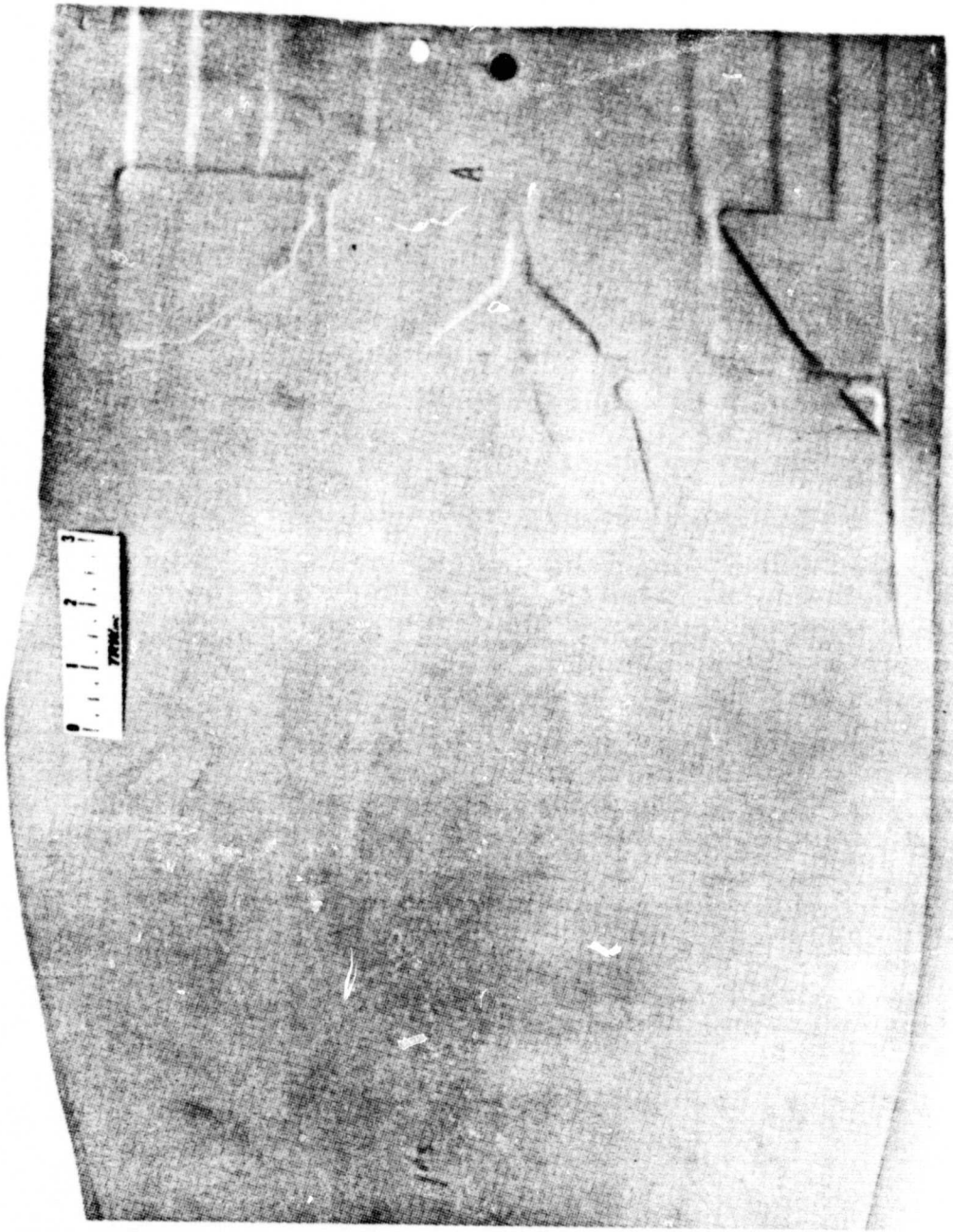

Figure 93. Tip Section of Blade 7 After Isothermal Forging Showing Lack of Contact During Forging in This Area as Indicated by Ply Endings Present on Surface.

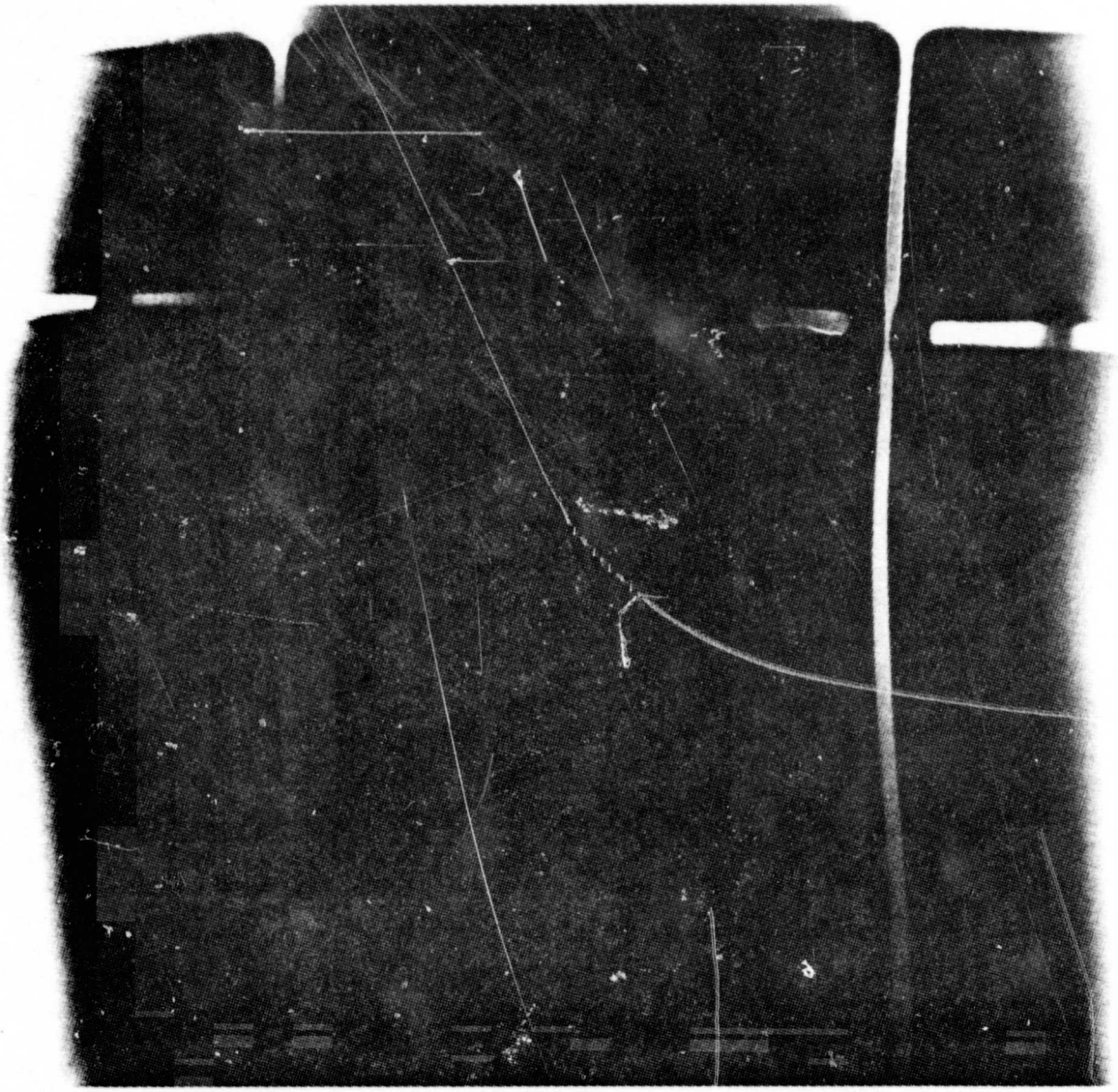

Figure 94. X-Ray Showing Lateral Core Movement Due to Isothermal Forging.

Table X. For some reason the change in length was not identical for the two blades. The edge cores seemed to elongate more than those in the central portion of the blade. The forging reductions were selected because of the need to "iron out" the surface undulations from the plies; however, based on the camber trials not much more than a "squeezing" operation may be required to eliminate the surface undulations. Thus the core deformation can be reduced by programming less blade deformation.

Blades 7, 8 and 9 were saved for machining while blades 4 and 6 were sectioned for core cavity and metallographic evaluations. Blade 4 was cut at approximately section AM-AM, AG-AG and AF-AF. Section AM-AM is near the tip and is oversize in thickness. This section, Figure 95, shows what the surface of the core end looks like internally. What is obvious are ridges from each individual ply. Section AG-AG, Figure 96, shows a typical view of a section that meets pitch thickness tolerance. The wall thickness was measured for this section and the data are presented in Table XI. It was found that the wall thicknesses met blueprint requirements. This result would lead one to suggest that, when properly designed with respect to volume distribution, wall thickness requirements can be maintained. Figure 97, section AF-AF, shows the typical internal surface condition. There are 0.030-inch steps internally as a result of ply endings on the core surfaces. Figure 98 are photos of typical longitudinal sections through blade 6. Similar surface and edge conditions exist.

Figure 99 is a series of photomacrographs and photomicrographs illustrating various surface conditions at the core edges for blade 4. Figure 99(a) shows that the connecting pin between the upper core section and lower core section experienced substantial deformation during HIP. The pin was deformed approximately 25%. This area is at the tip which saw no deformation during isothermal forging. Figure 99(b) shows an area through both core sections and the pin. While 99(c) shows an area between the two core sections. The nature of the steps indicates both core flow and ply indentation occurred during HIP. Figure 99(d) depicts a condition at the core end at the root. At this area it appears that rather severe core indentation occurred. Figure 99(e) and (f) are sections between cores (transverse sections) illustrating typical surface condition at the radii. These areas appeared to be more uniformly indented rather than a condition shown in 99(d) for the core end. Figure 99(g) shows the condition at the edge of a core at the blade edge. Figures 99(d) through (g) are from a heavily deformed area of blade 4. For all the sections evaluated there was no evidence of voids due to lack of fill. The gaps shown in Figure 99 between core and HIP laminates are the result of shrinkage during cooling. One of the obvious conclusions from the above series of photomicrographs was that core indentation was more severe for the blades than it was for the diamond specimens. In order to solve this problem a stronger core material will have to be used, but one that has a better thermal expansion match than the TRW VMS-478 alloy in order to prevent crack problems due to high stress conditions.

Sections of blade 4 were also examined metallographically for disbonds and/or contaminates at the bond lines. No evidence of either was found on the sections evaluated. Figure 100 shows the typical microstructure observed for blade 4. Material for this photomicrograph was taken from the root. No evidence of "micropores" was found

TABLE X

Core Length Changes for Blades 7 and 8

Core	Blade 7 Change	Blade 8 Change
B	+ 22/16	+22/16
C	+ 18/16	+18/16
D	+ 18/16	+ 14/16
E	+ 21/16	+ 15/16

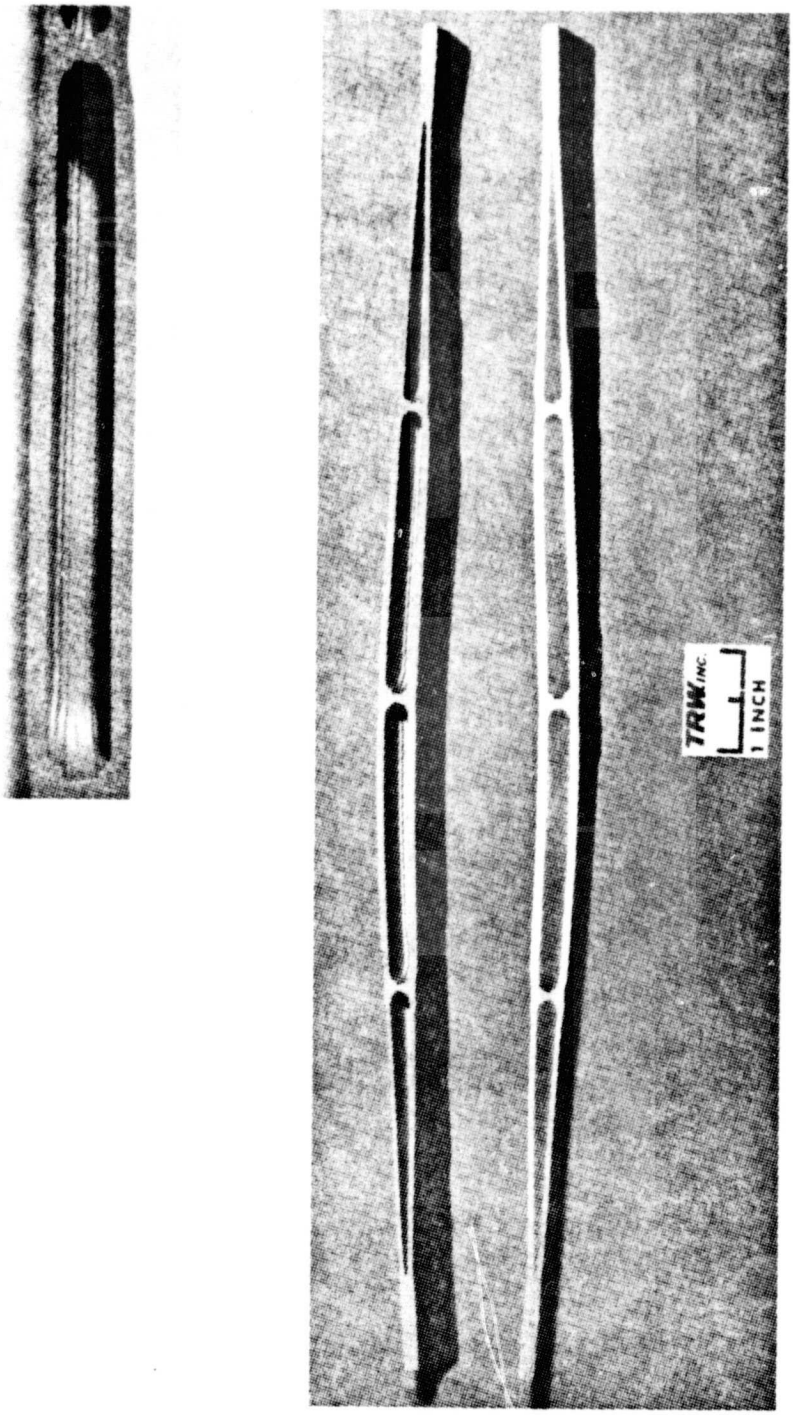

Figure 95. Section AM-AM of Blade 4. Top Piece Shown Has Core Removed.

Figure 96. Section AG-AG of Blade 4. Top Piece Shown Has Core Removed.

TABLE XI

Wall Thickness Measurements for Section AG-AG - Blade 4

Surface AU				Surface AY			
BP*		Actual		BP*		Actual	
Y	AA	Y	AA	Y	AA	Y	AA
0.055	0.055	0.070	0.068	0.055	0.055	0.069	0.058
0.060	0.136	0.068	0.131	0.060	0.136	0.062	0.148
0.136	0.061	0.134	0.069	0.136	0.061	0.145	0.065
0.055	0.055	0.066	0.059	0.055	0.055	0.060	0.055

* Tolerance of ±0.016-inch allowable.

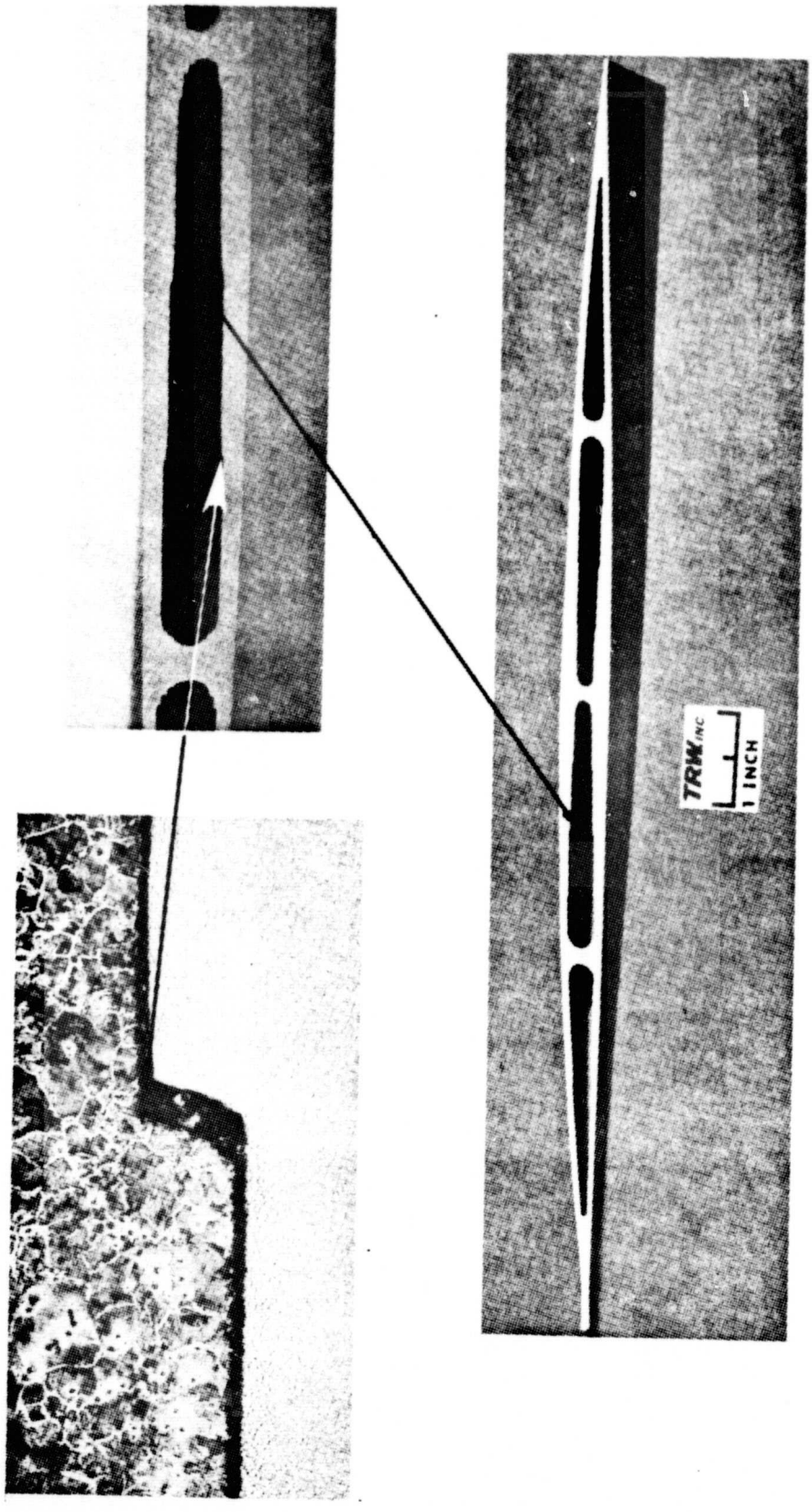

Figure 97. Section AF-AF of Blade 4 With Core Removed and Typical Internal Wall Surface Condition.

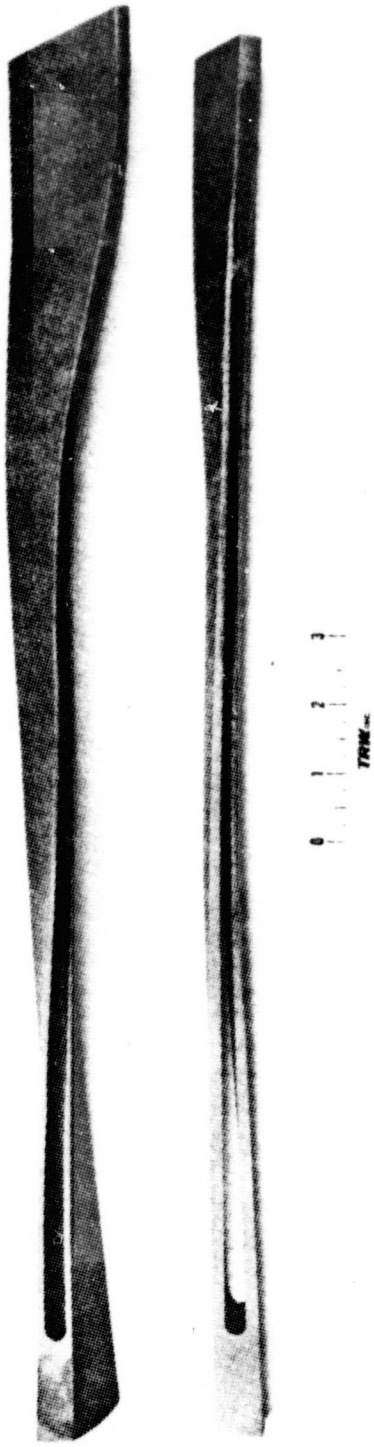

Figure 98. Typical Longitudinal Sections From Blade 6.

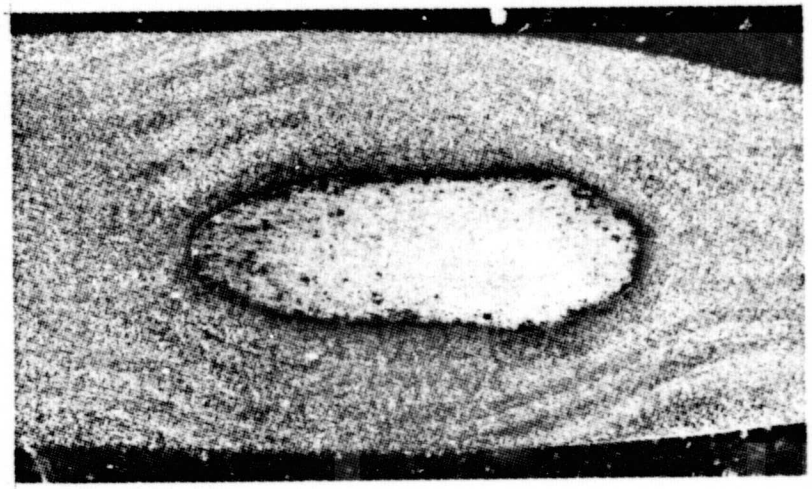

7X

a. Connecting Pin Between Upper and Lower Core Sections

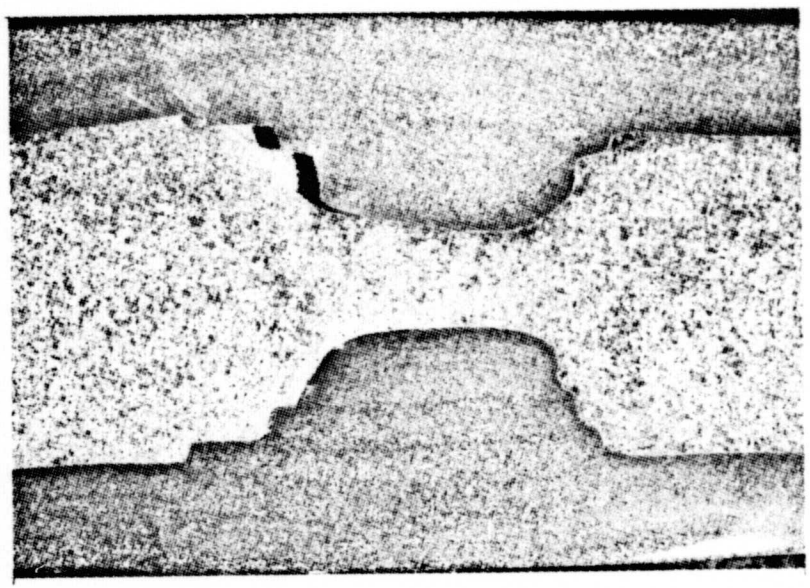

7X

30X

b. Area Between Upper and Lower Core Sections and Pins

Figure 99. Photomacrographs and Photomicrographs Illustrating Various Surface Conditions at the Core Edges for Blade 4.

30X

7X

30X

c. Area Between Upper and Lower Core Sections

Figure 99. (cont'd) Photomacrographs and Photomicrographs Illustrating Various Surface Conditions at the Core Edges for Blade 4.

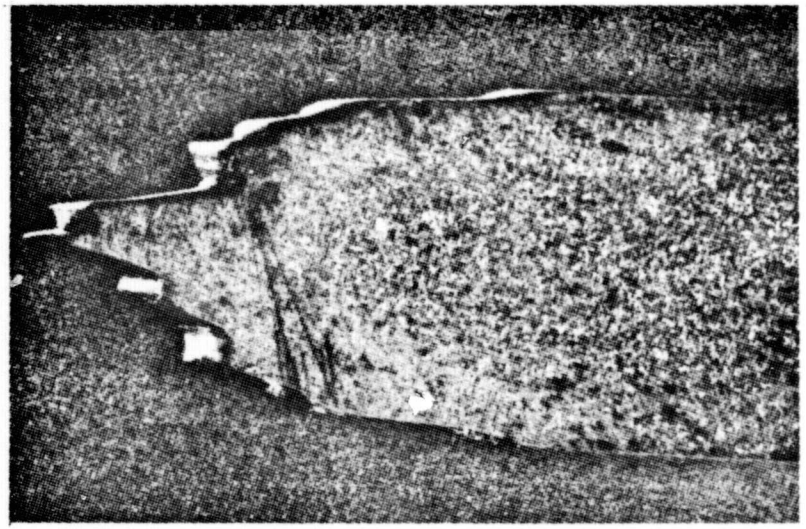

7X

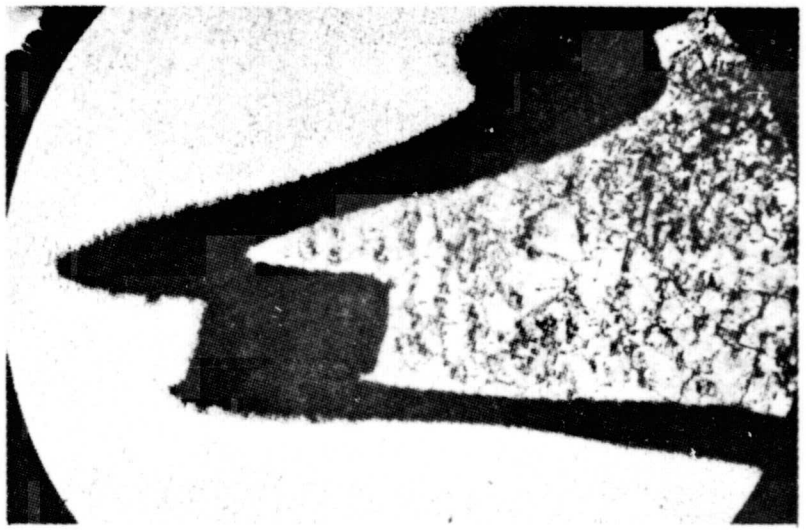

30X

d. Core Root End Cross Section

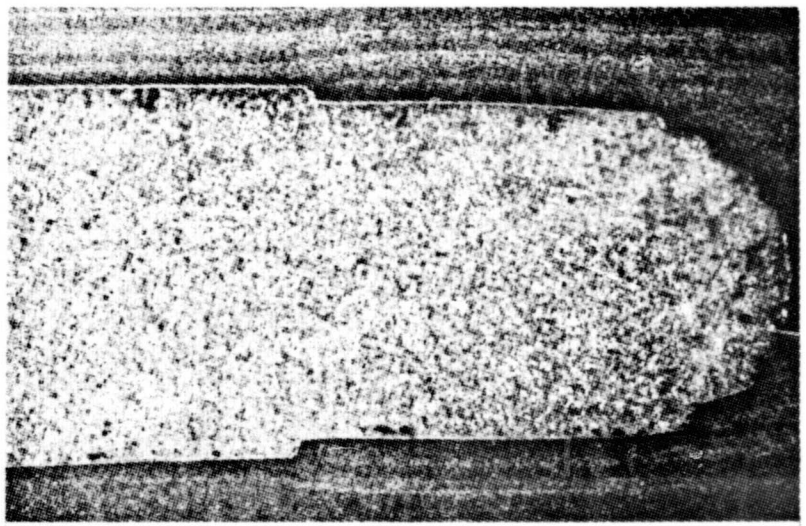

7X

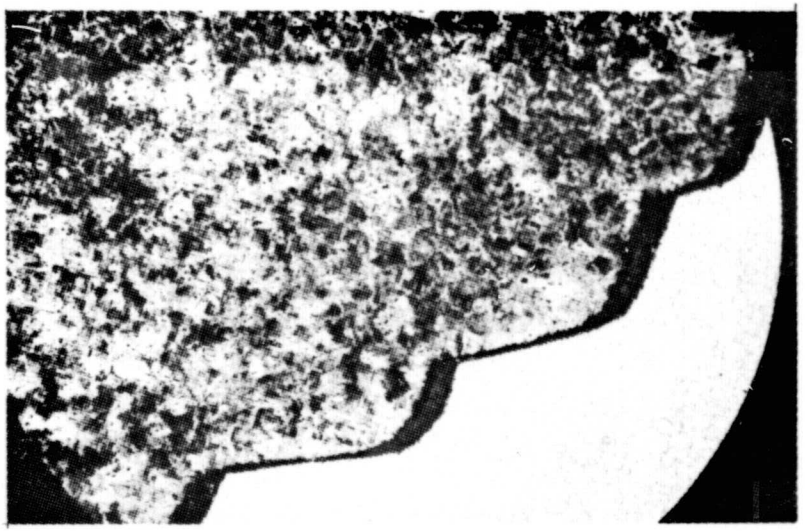

30X

e. Surface Condition Between Cores

Figure 99. (cont'd) Photomacrographs and Photomicrographs Illustrating Various Surface Conditions at the Core Edges for Blade 4.

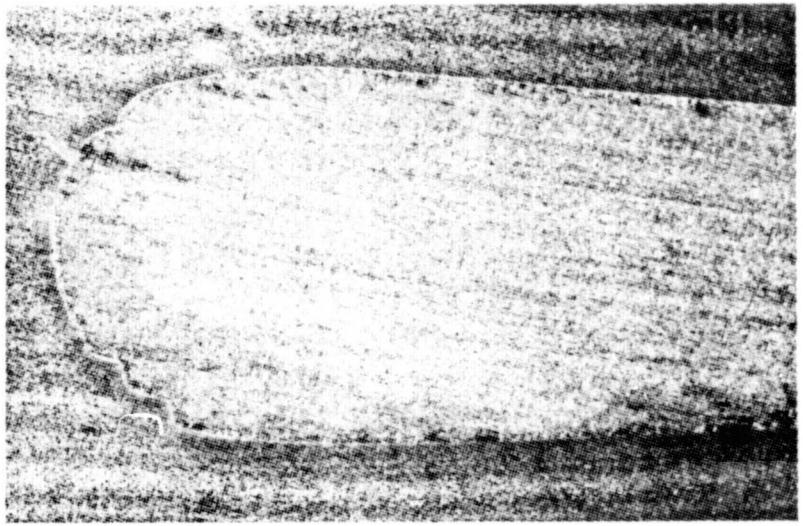

7X

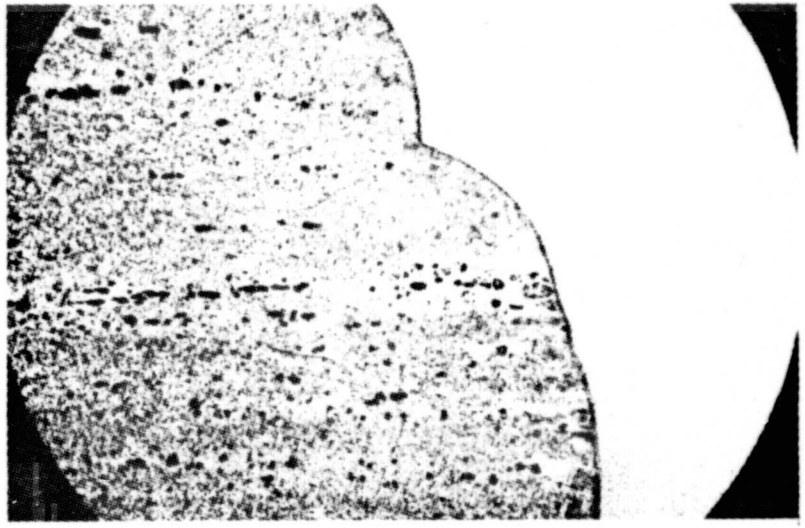

30X

f. Surface Condition Between Cores

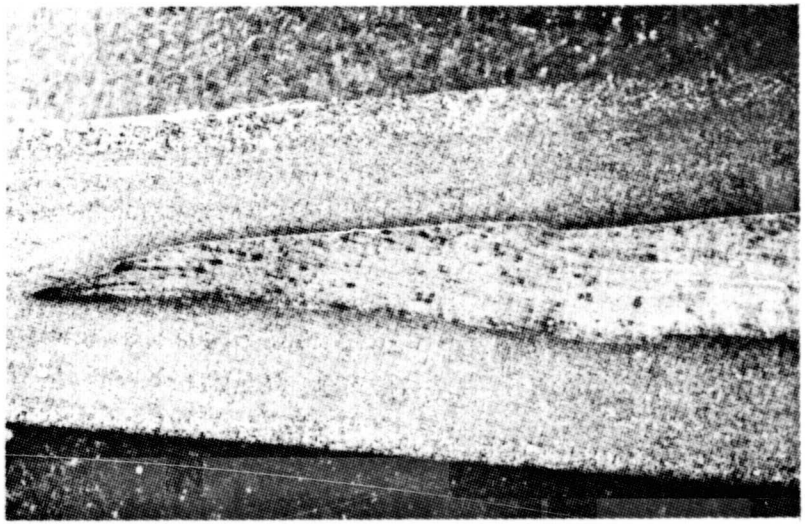

7X

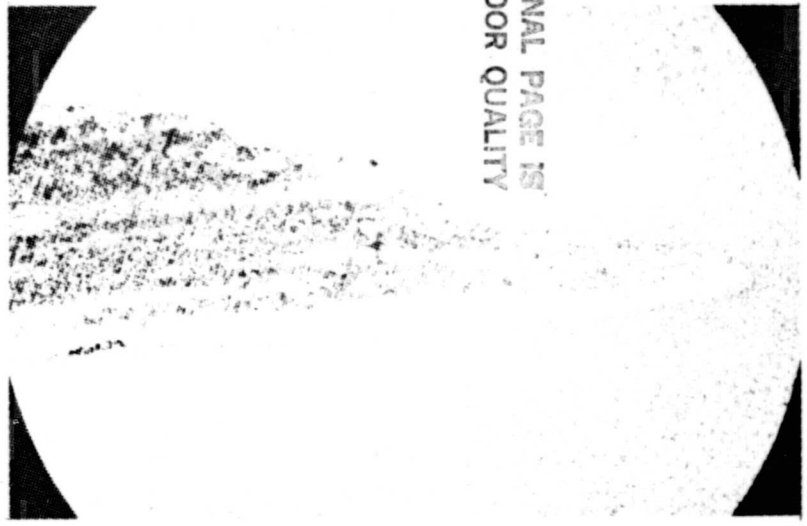

30X

g. Leading/Trailing Edge Core Condition

Figure 99. (cont'd) Photomacrographs and Photomicrographs Illustrating Various Surface Conditions at the Core Edges for Blade 4.

Etch

96 H_2O
2 HNO_3
2 HF

200X

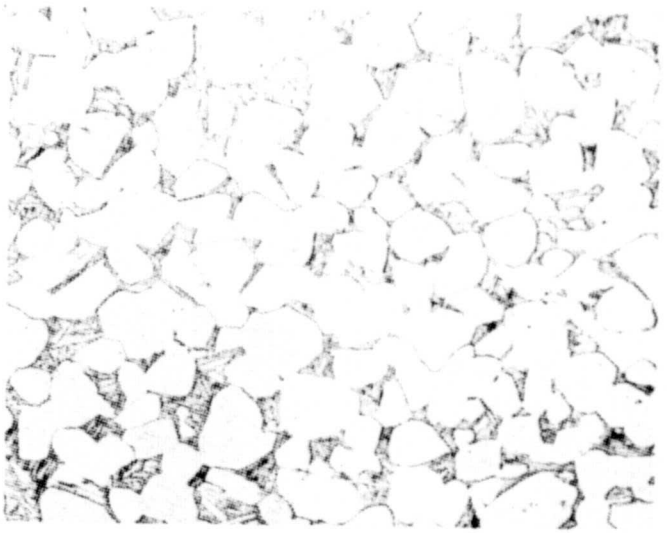

Bond Line

500X

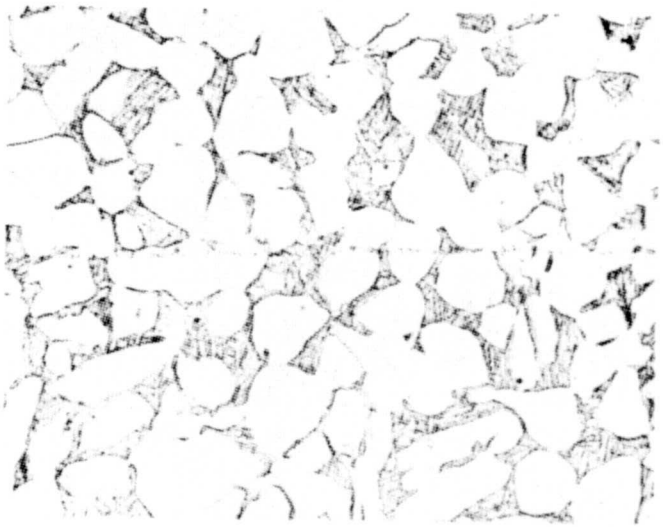

Etch

60 H_2O
35 HNO_3
5 HF

Bond Line

500X

Figure 100. Microstructure Observed for Blade 4.

at the bond lines using standard etching. The material was given a heavy etch and some evidence of "micropores" was found as shown in Figure 100; however, this condition was observed in less than 5% of the possible bond lines examined.

d. Blade Machining and Leaching

Machining of the blade primarily consisted of cutting the blade to length and width, blend in leading and trailing edge radii and polishing airfoil (removal of only 0.001-0.002-inch maximum except near tip area where the ply endings were still visible). Blades 7, 8 and 9 were finish machined. The blades were machined to the correct chord widths where possible. Due to the flow of the cores during forging, chord widths where increased between sections T-T through AA-AA up to about 0.3-inch. The width was added to the leading edge side only.

After machining racetrack holes were machined in the end of each blade as shown in Figure 101. Holes were 0.250-inch long by either 0.125-inch (inner cores) or 0.100-inch (outer cores) wide. Distance between holes within a core was 0.150-inch.

The steel cores were leached out in a water-nitric acid (2:1 ratio) bath operating at 180°F. The blades were then chem milled to remove about 0.001-inch and vapor blasted. The finish blades are shown in Figure 102. Blade 7 was shipped to NASA-Lewis, blade 8 was shipped to P&WA, and blade 9 was retained by TRW.

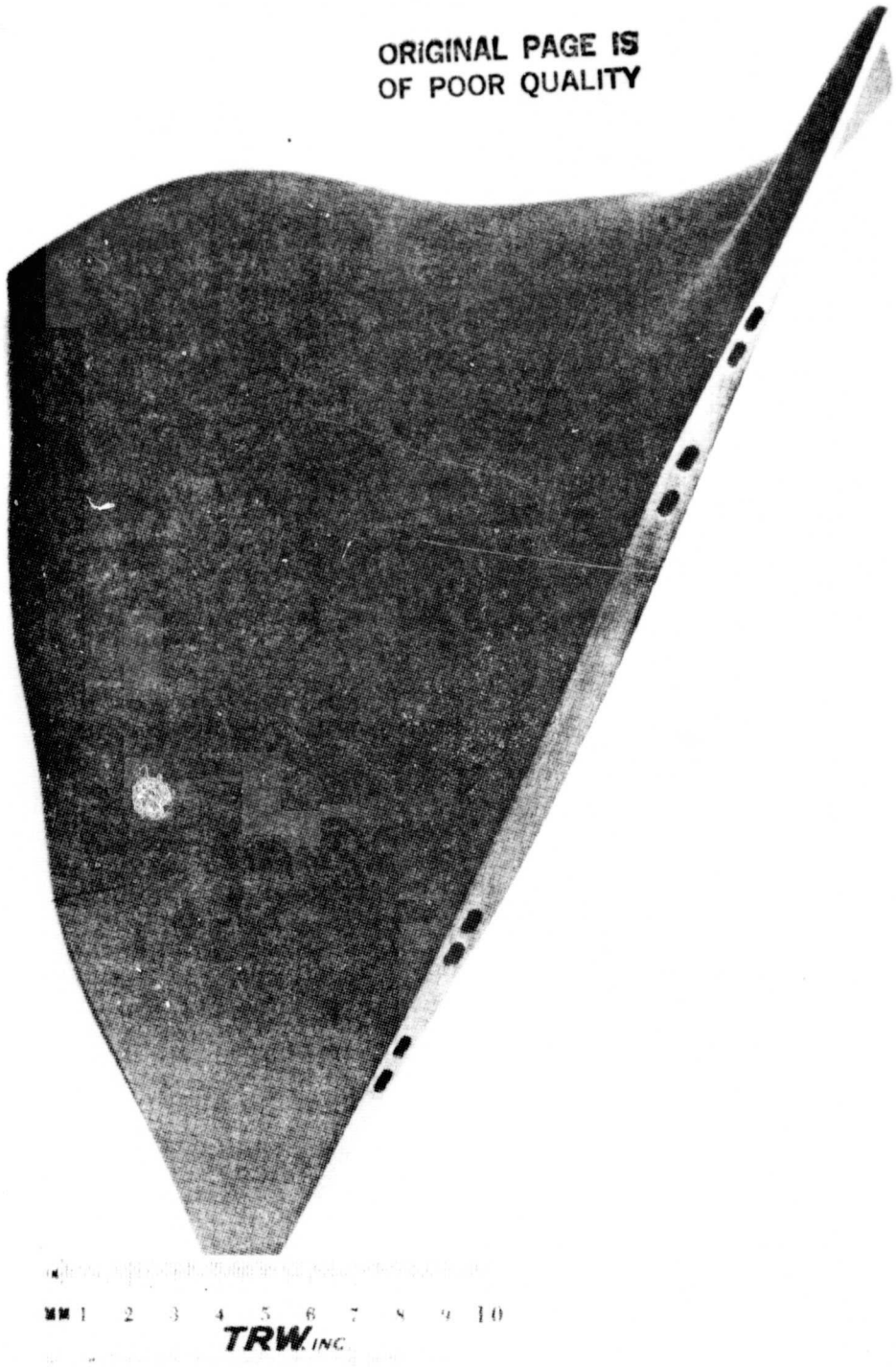

Figure 101. Racetrack Holes in Blade Tip.

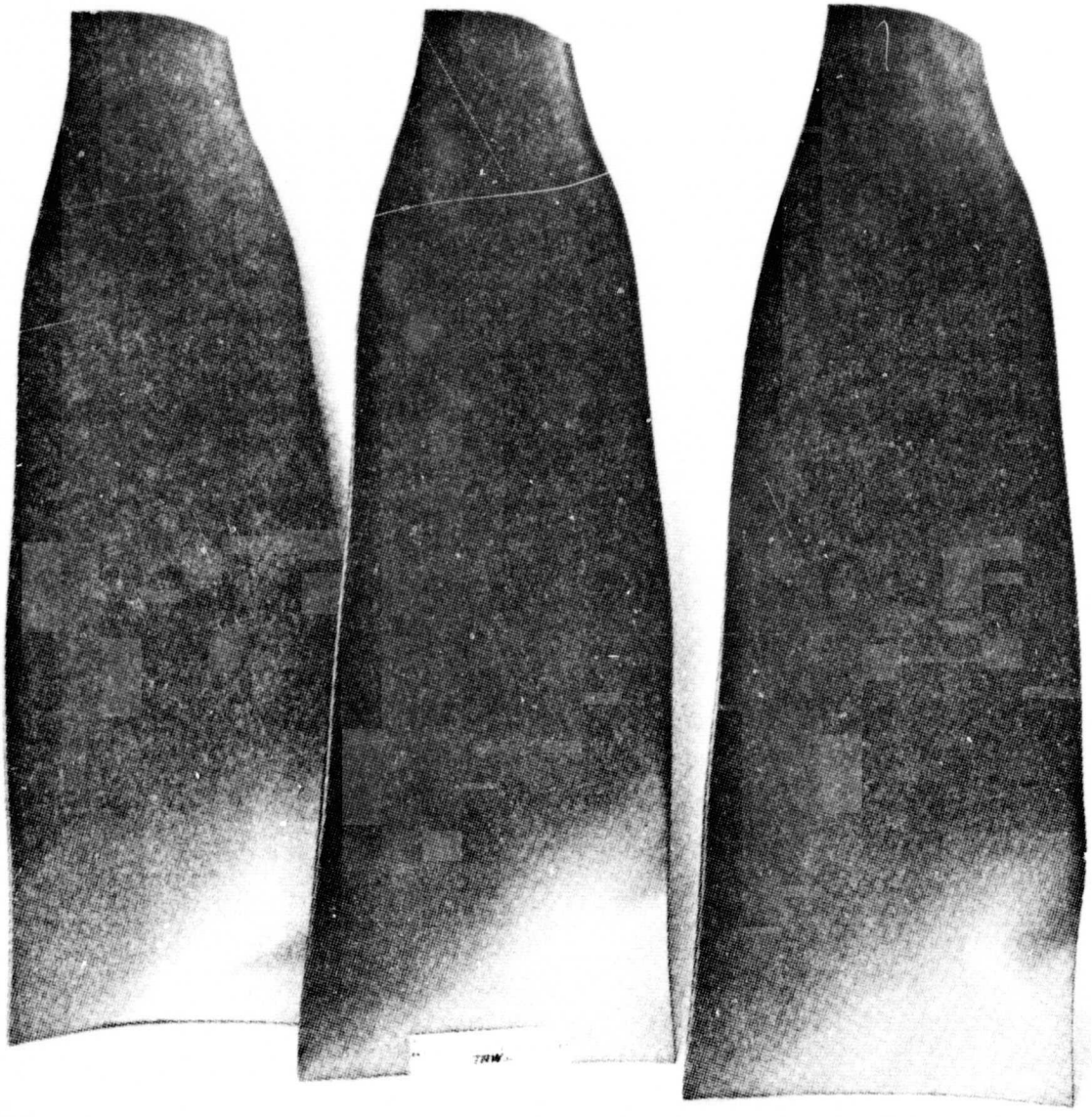

Figure 102. Blades 7, 8 and 9 After Finish Machining and Core Leaching.

V CONCLUSIONS AND RECOMMENDATIONS

This Energy Efficient Engine hollow blade program has been successful in establishing a process that can produce large airfoil structures. There are many accomplishments, conclusions and recommendations that can be drawn from this effort. These accomplishments, conclusions and recommendations are presented below:

- Feasibility of fabricating hollow blades has been successfully demonstrated using a laminated leachable core/HIP bonding approach.

- Demonstrated the developed HIP cycle (1750°F/4.5 hours/15 ksi) produces metallurgically bonded structure with grain growth across bond lines in sheet material laminate construction and no evidence of voids due to lack of material flow.

- Demonstrated that core materials having a carbon content equivalent to AISI 1045 successfully avoid any core/laminate interactions.

- Problem with "micropores" at the laminate interface was observed. Whether these "micropores" are the result of cleaning procedures, contaminants, preferential etching or are possibly related to the fact that the process is conducted in a static vacuum is probably still not understood. It is recommended that an extensive effort in material preparation on test samples be considered to define the problem.

- A considerable amount of effort was expended in welding of HIP cans. Welding and HIP can designs are critical in successfully fabricating blades. Seam welding has been demonstrated to be a very economical and successful approach to welding cans. Sheet thicknesses of cans are very important in design considerations.

- CAD and CAM for cores has been demonstrated. NC machining of cores is very expensive even in large quantities. The shape and size of the cores virtually eliminates processes such as powder metal and casting to produce the cores. Forging is viable and less costly than NC machining; however, blade designers should consider more "manufacturable" designs. Producing the cores is equivalent to producing four different solid blades.

- Consideration must be given to a different core material. Minimal core indentation using AISI 1045 was observed in fabricating diamond speicmens; however, severe core indentation were observed in fabricating hollow fan blades. The differences are probably attributable to using 0.030-inch thick sheet versus 0.010- and 0.030-inch sheet for the diamond specimens and also to ply designs. Stronger core materials (TRW VMS 478) were successful in eliminating core indentations; however, the larger thermal expansion mismatch caused cracking problems. The core material selected should have

substantially higher flow stress than titanium at 1750°F, good thermal expansion match with titanium, no reaction problems with titanium, easy to fabricate, and leachable.

- o CAD and CAM for ply generation and machining has been successfully shown. The NC approach, however, is costly if required for production quantities. The stamping approach used successfully for the diamond specimens is the obvious lost cost manufacturing method that should be selected for producing plies.

- o It is TRW's belief that the concerns for selecting a flat layup approach are no longer warranted. Use of camber and twist tooling were very successful in forming the blade prior to isothermal forging. The flat layup is least costly and easiest to accomplish while still maintaining core locations.

- o Isothermal forging was successfully demonstrated in producing a smooth airfoil finish. Although a blade meeting blueprint dimensions was not achieved, this was attributed to the fact that additional tooling rework was terminated for this effort. Experience in this type of proceesing has shown that a blade meeting blueprint dimensions can be achieved.

- o Leaching of the steel cores, although time consuming, is not labor intensive and is accomplished using hot water/nitric acid baths.

Considerations must be given as to whether or not to continue to develop the technology using the current approach. Obviously a new core material must be selected and secondly the post HIP processing conditions must be changed to avoid core movement during forging. To accomplish the latter it is TRW's belief that core movement can be eliminated by minimizing material flow. If the blade will be produced using an approach that requires diffusion bonding of a root segment later, then the root pocket in the isoforge tooling must be eliminated and dams built into the tooling at the root and tips ends. Based on the results observed during cambering that the ply undulations on the surface disappeared during clamping of the blade, it is also recommended that the plies be designed to allow for virtually no metal movement during isothermal forging. This approach along with a stiffer core material can eliminate core movement.

"If the program were to start today what approach would be recommended for producing a hollow fan blade?" This question has been asked many times. When the program was initiated titanium alloy costs were just beginning to rise. Costs have since at least doubled. Titanium bar now costs between $15 and $20 per pound. While 0.030-inch sheet costs are in excess of $40 per pound. These high sheet costs have substantially added to the blade cost. The laminate/core approach was selected based on the potential for automation and the capability to be able to reinforce the blade if necessary. Based on experience with the laminate/core approach, TRW Materials Technology believes this is a feasible process; however, it would not be the approach selected today. The approach selected would require the forging of two blade halves, machine (EDM/ECM) the required core cavities in each half, and diffusion-bond (press or HIP) with cores these halves

together. It is TRW's belief that this approach would be more cost effective, have better cavity definition and would be easier to inspect with respect to bonding. If reinforcement would be required, then a forging could be produced and the reinforcement added similarly by bonding a laminate to the surface by either press diffusion bonding or HIP.

VI REFERENCES

1. Saunders, N. T., Colladay, R. S., and Macioce, L. E., "Design Approaches to More Energy Efficient Engines," Paper 78-931, AIAA/SME 14 Joint Propulsion Conference, July 25-27, 1978.

APPENDIX A - PLY DESIGN

The availability of computer aided design background at TRW for blade forging and for composite blades facilitated the designing of the plies for the E^3 blade. It was necessary to extend the progamming capability to include the definition of the areas within the plies which were to be removed for the insertion of the cores to form the hollow sections. These program modifications were extensive. Each core area definition essentially required the generation of another airfoil.

The blade definition was transmitted to TRW on magnetic tape (coordinate data) and on drawings (EMD's) of the various cross-sections. To test the transformation of P&WA coordinates to TRW coordinates, plots of the airfoil sections using the new TRW coordinate system were compared to the EMD's of the sections received from P&WA. A problem was encountered when comparing airfoil section plots drawn using TRW's airfoil design system and the EMD's supplied by P&WA. The differences observed were as large as 0.020-inch in airfoil thickness. The source of this problem was that the point spacing used to define the airfoil section was too sparse in the high camber areas for the E^3 blade. In particular, points at 85 to 95% of the chord length were not provided. The differences between TRW's plots and the EMD's reflect the difference between the Aitken-Lagrange interpolation algorithm that is used by TRW and the cubic spline algorithm used by P&WA. To solve this problem TRW used a cubic spline interpolation program to add points at approximatley 55, 65, 75, 85 and 95% of the chord length. A comparison plot using this new data set demonstrated excellent agreement with the EMD's.

Some of the assumptions used in the ply generation were as follows: the plies would be 0.030-inch thick; there will be a full ply located along the mean camber line; there will be full plies on the concave and convex surfaces of the airfoil; a maximum of 10% deformation by isothermal forging was planned; and a chemical milling envelope of 0.0025-inch was added. There were a total of thirty-one plies that defined the airfoil. These ply designs with the core cavity definitions were quite complex as expected because of the core geometry. The computer, although defining the core cavity geometry in the ply, did not define the radii of core corners in the ply. This was accomplished manually because definition by computer would take several months. In addition, the computer plots were modified for additional stock in the root and in the tip (for full length plies only of which there are eleven).

The TRW Ply Generation System is composed of a library of stand-alone programs that offer the user various data manipulation capabilities. Some were in existence prior to this project; and some, in particular those related to core geometry, were developed for this project. Used in correct combination, they generate a final ply shape from standard airfoil digital input data. Correct use of this system calls for the user to verify each step in the sequence by checking computer-printed output and computer plots.

A stepwise description follows:

1. Airfoil digital data on P&WA magnetic tape is read into memory, formatted, and written to a disk file.

2. The digital data is plotted and compared to customer charts before any processing is performed.

3. A mean camber line for each section is computed.

4. Each section is oversized by .0025-inch.

5. Each section is additionally oversized by a 10% increase in local thickness across the blade.

6. The center ply is computed by generating parallels to the mean camber line at plus and minus one-half ply thickness for each section.

7. Plies are generated in the planes of all sections by generating parallels from ID and OD toward the mean camber line, and finding the intersections of these parallels with the center ply. Plies are now defined radially.

8. Compute ply boundaries in the axial direction as a function of blade thickness.

9. At each section, compute intersections of plies with core geometry.

10. Compute core boundaries in the axial direction.

11. Flatten each ply by removing its curvature and twist.

12. Fit a quadratic curve to tip end of ply axial boundaries.

13. Plot Final results.

The ply designs are shown in Figure 103.

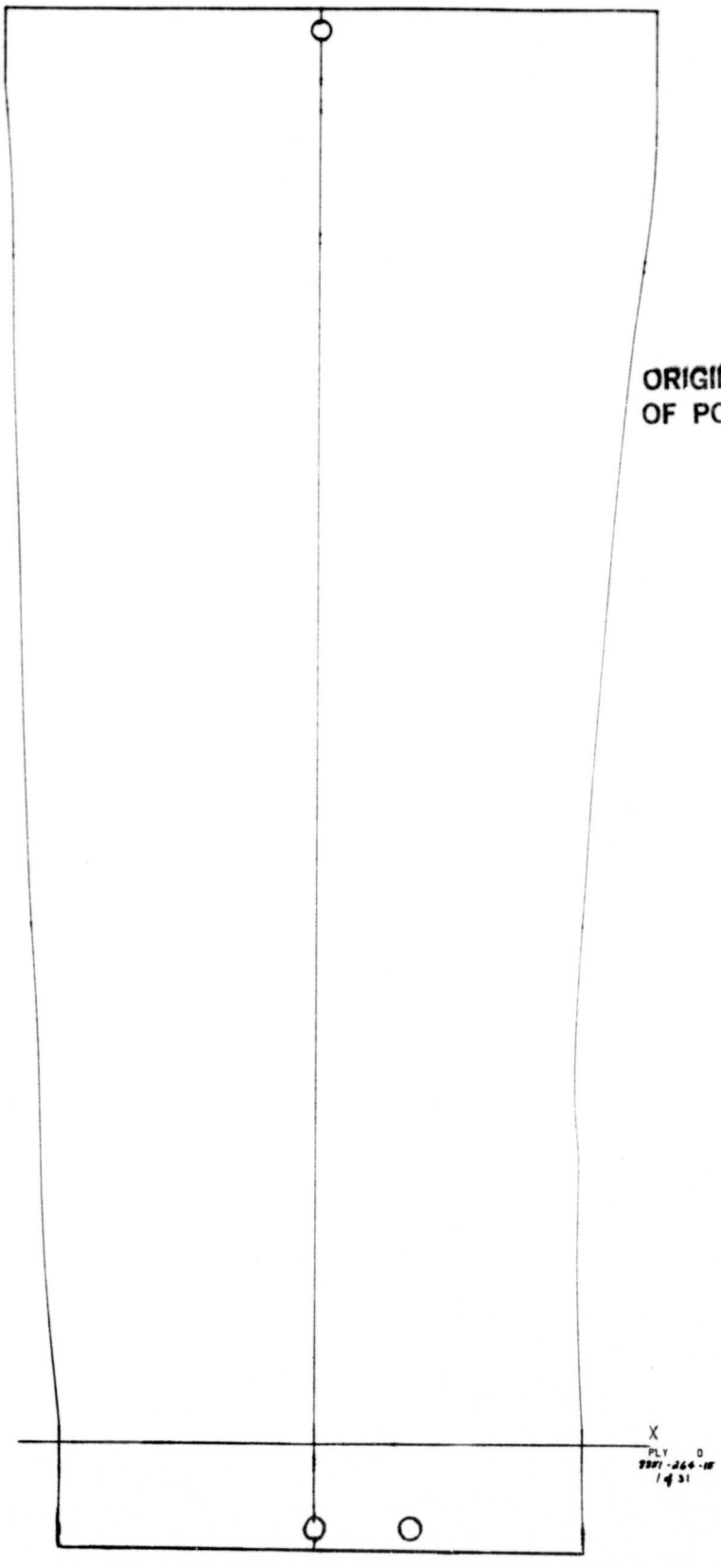

Figure 103. Ply Designs.

Figure 103. (cont'd) Ply Designs.

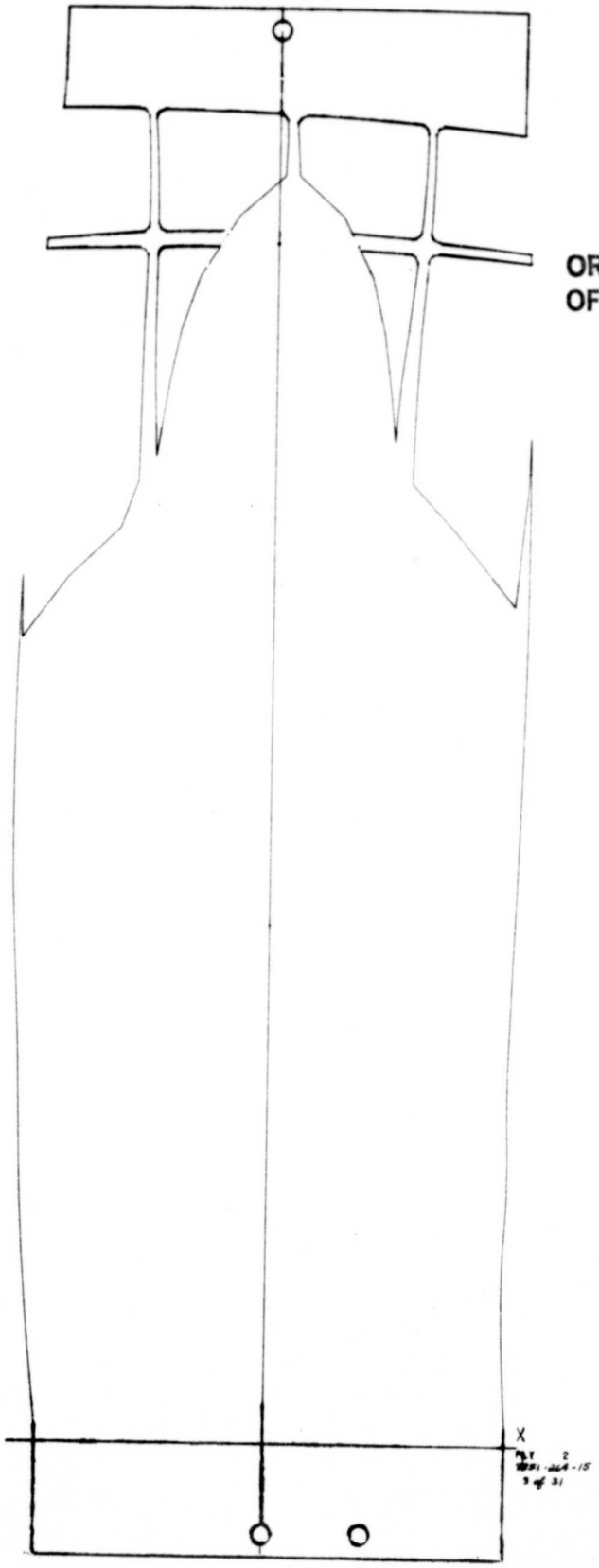

Figure 103. (cont'd) Ply Designs.

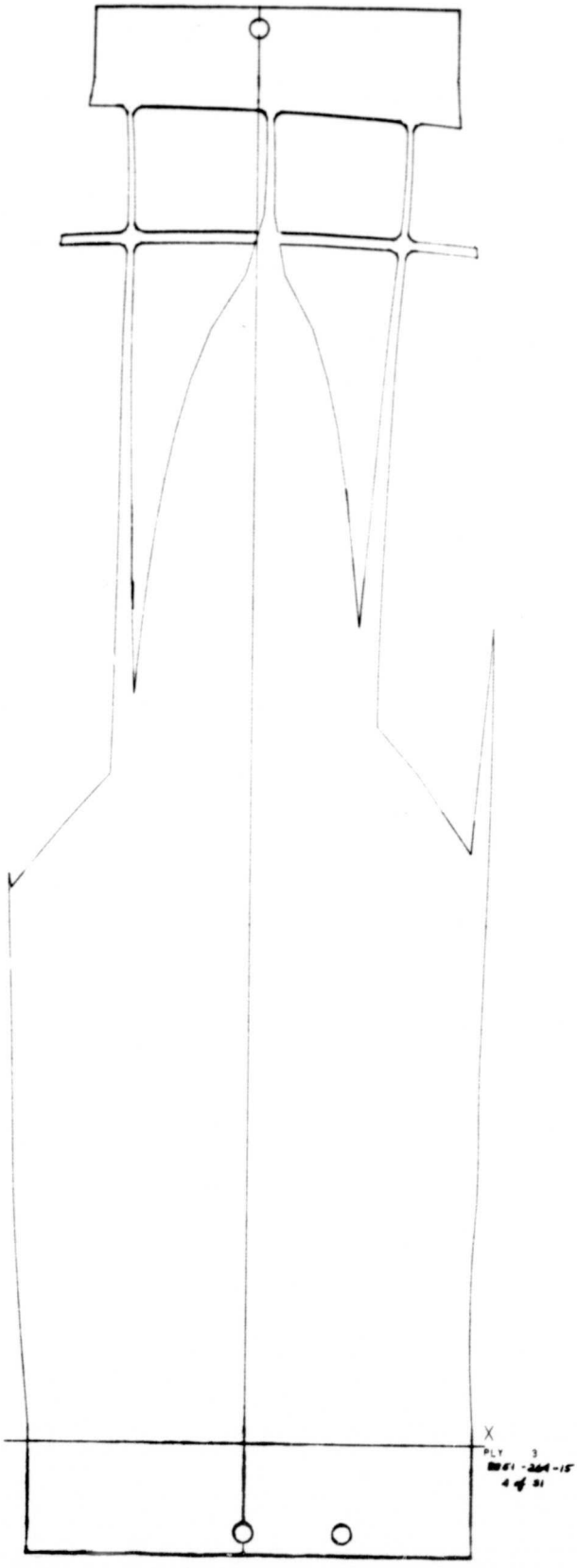

Figure 103. (cont'd) Ply Designs.

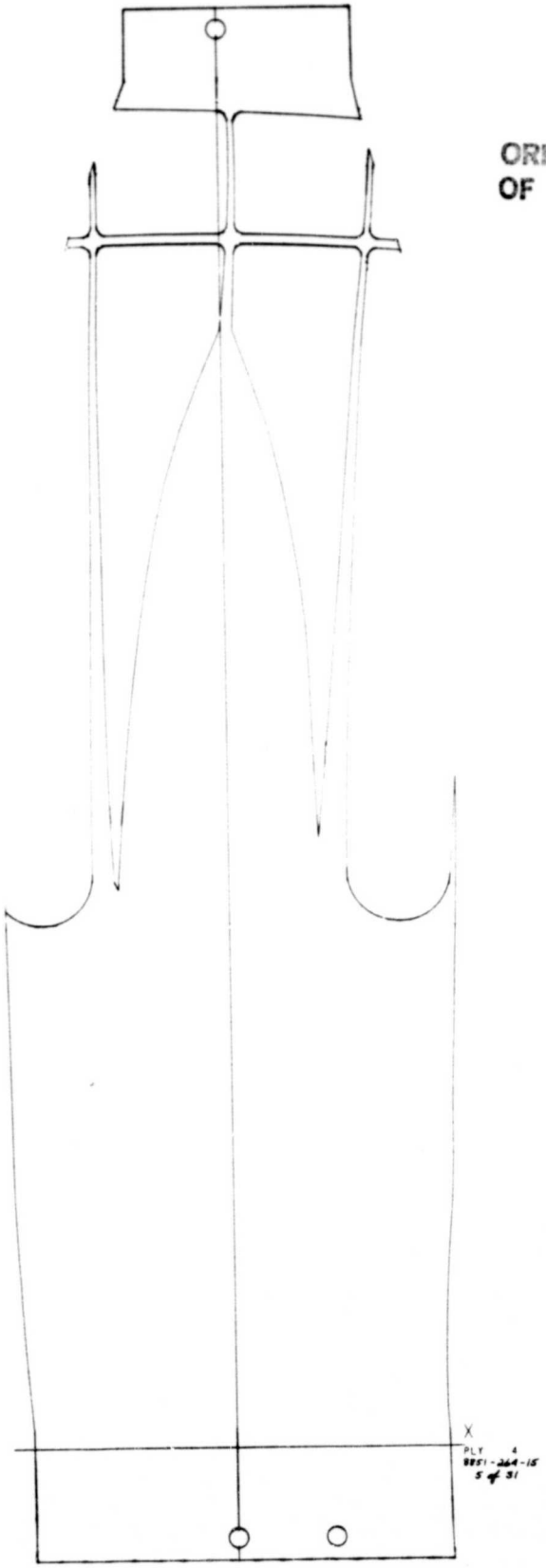

Figure 103. (cont'd) Ply Designs.

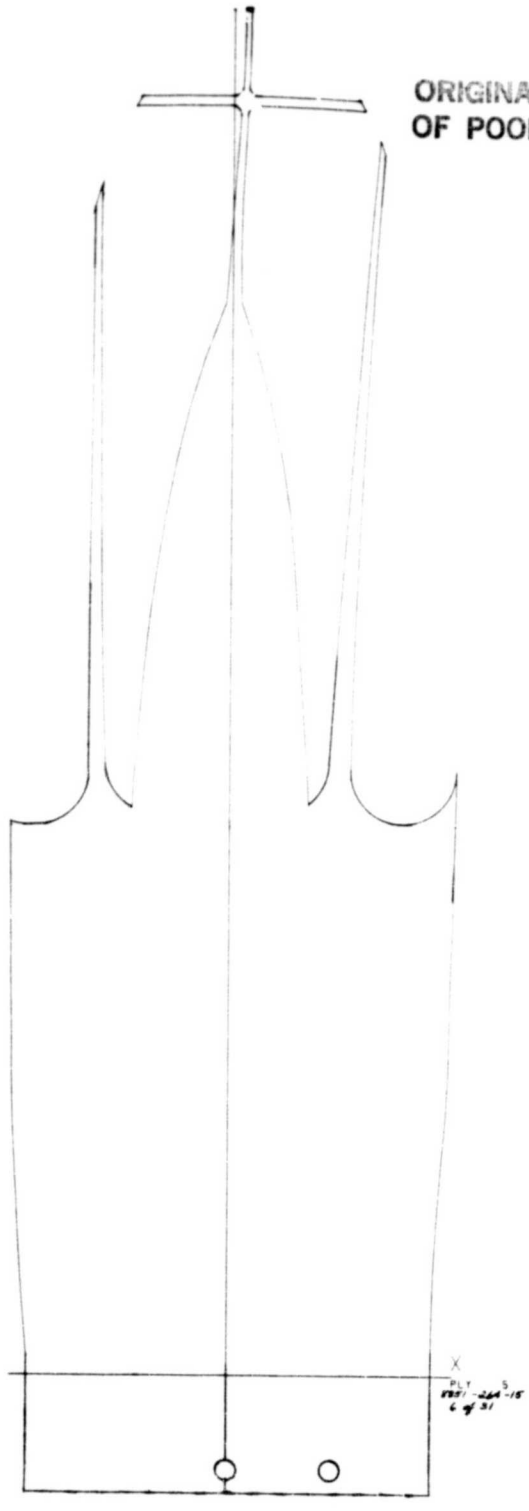

Figure 103. (cont'd) Ply Designs.

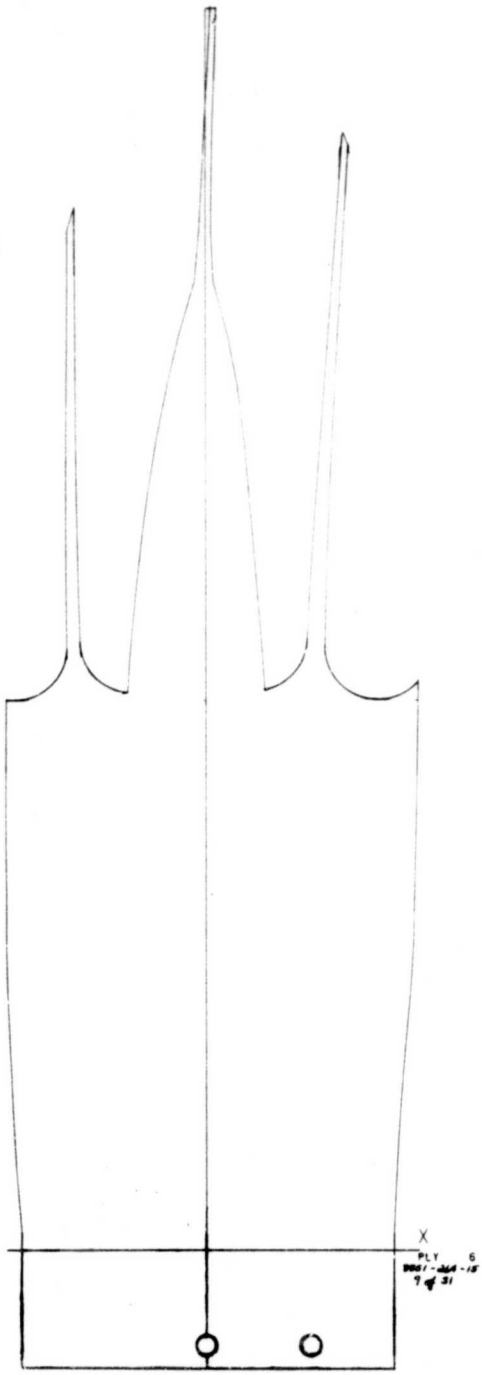

Figure 103. (cont'd) Ply Designs.

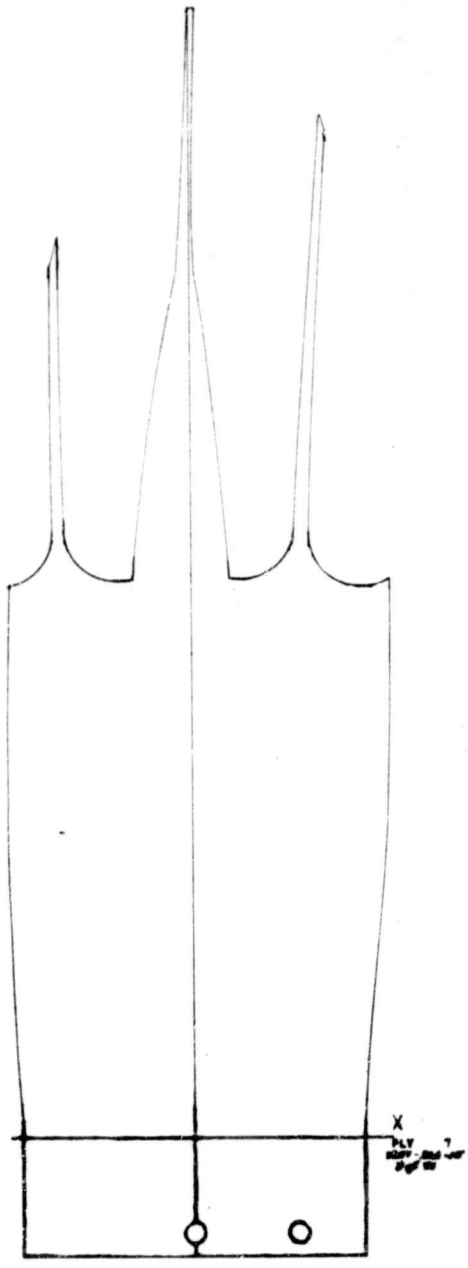

Figure 103. (cont'd) Ply Designs.

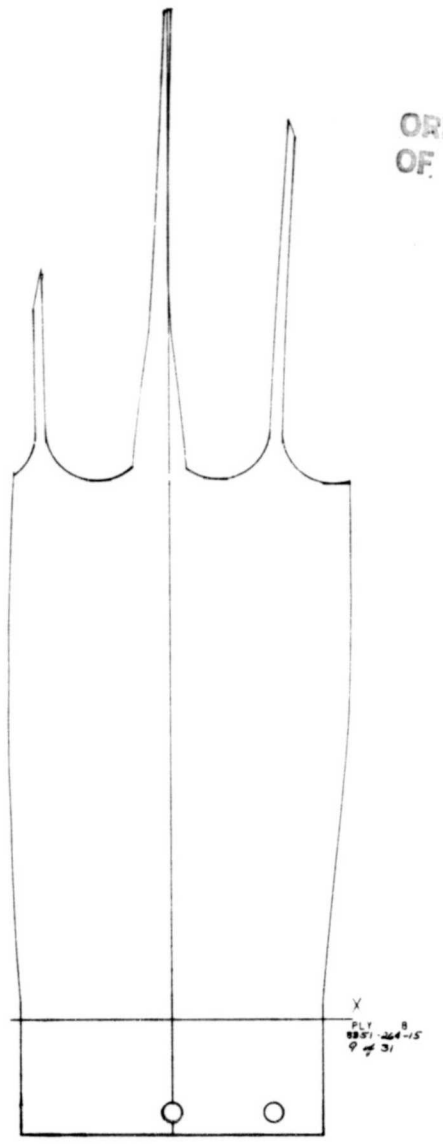

Figure 103. (cont'd) Ply Designs.

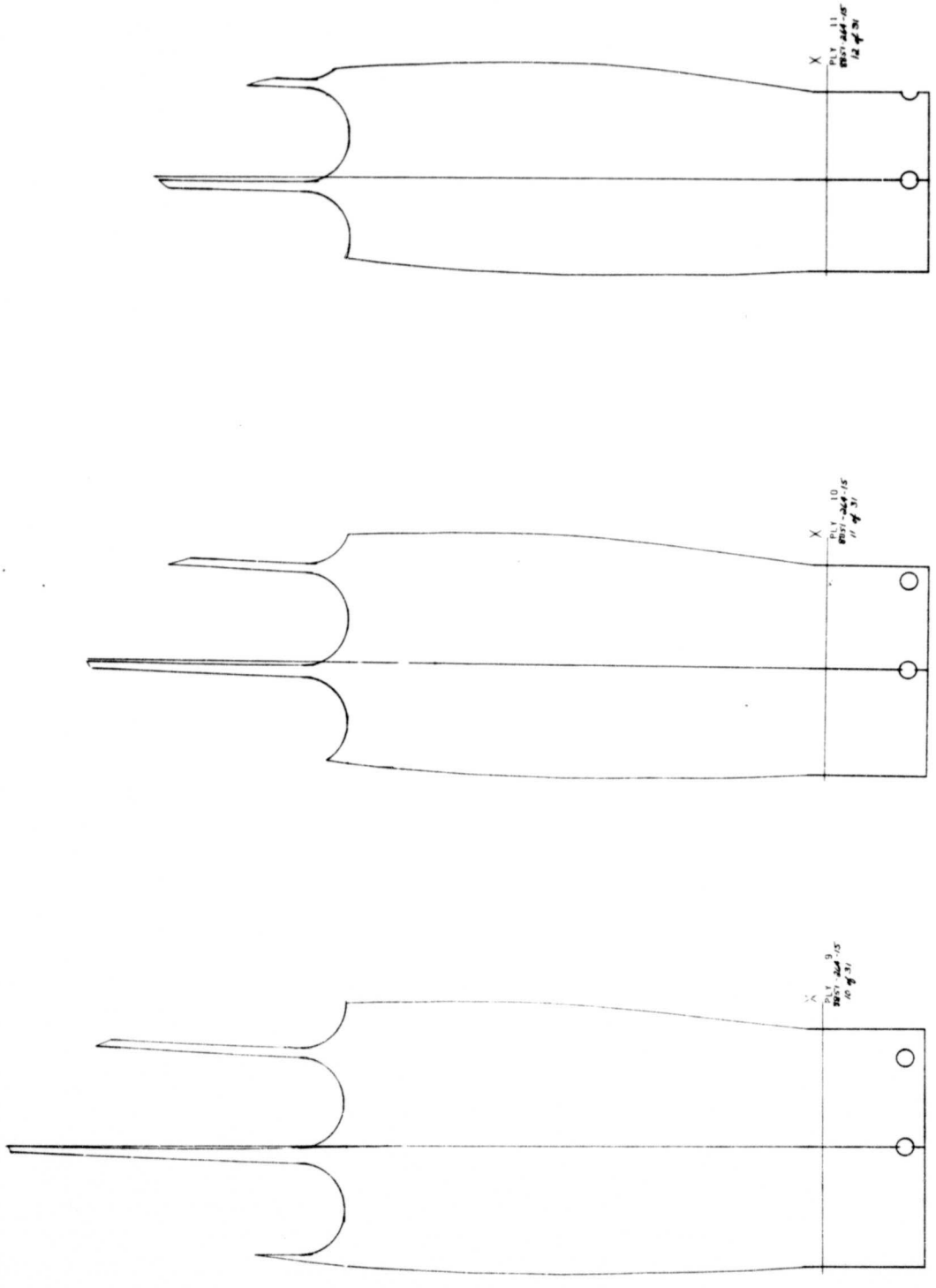

Figure 103. (cont'd) Ply Designs.

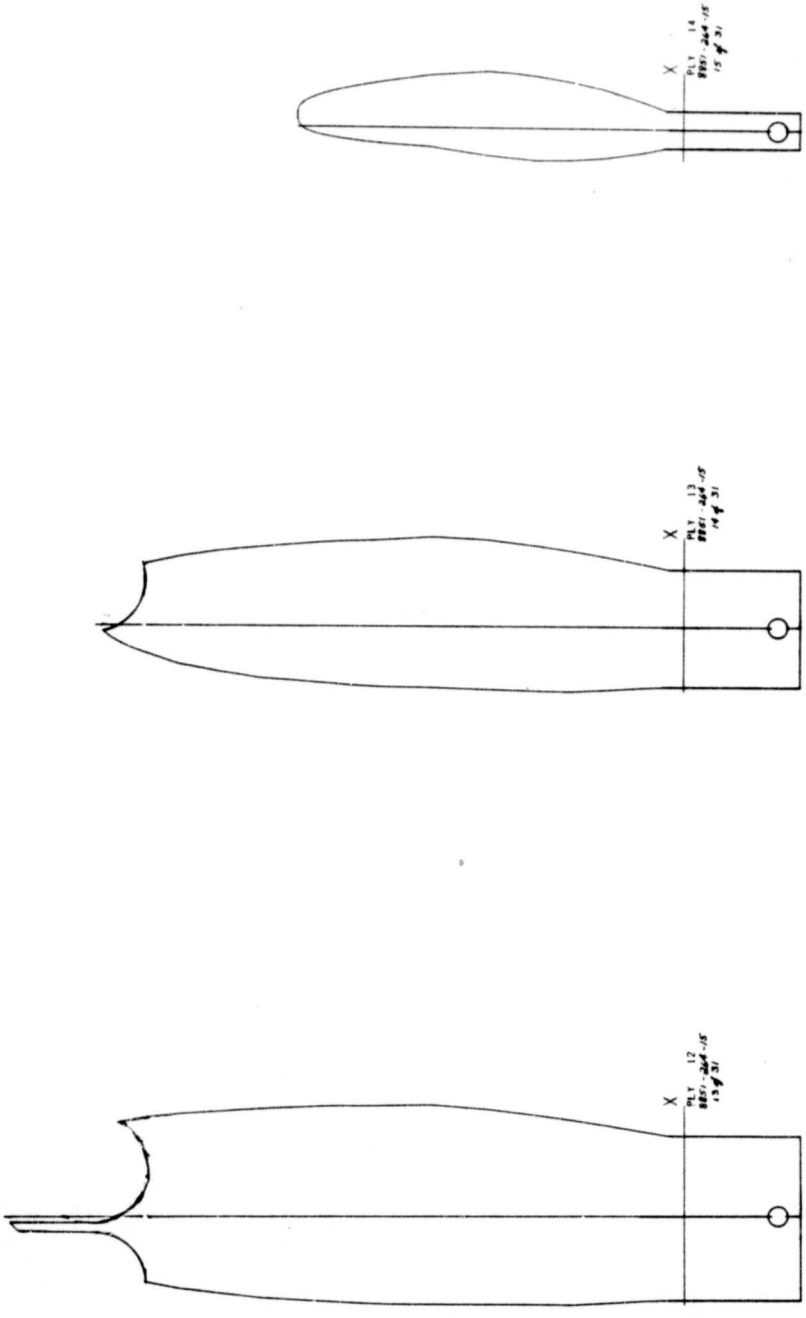

Figure 103. (cont'd) Ply Designs.

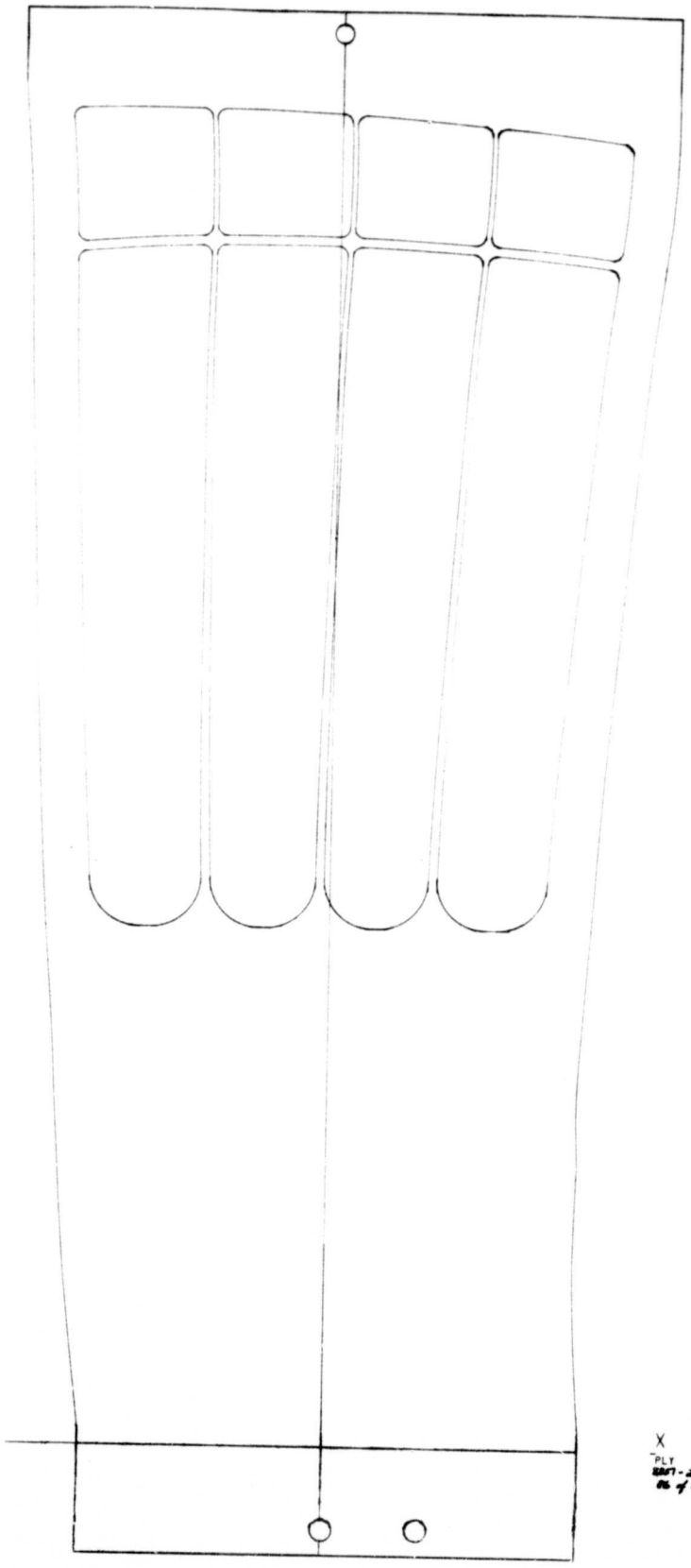

Figure 103. (cont'd) Ply Designs.

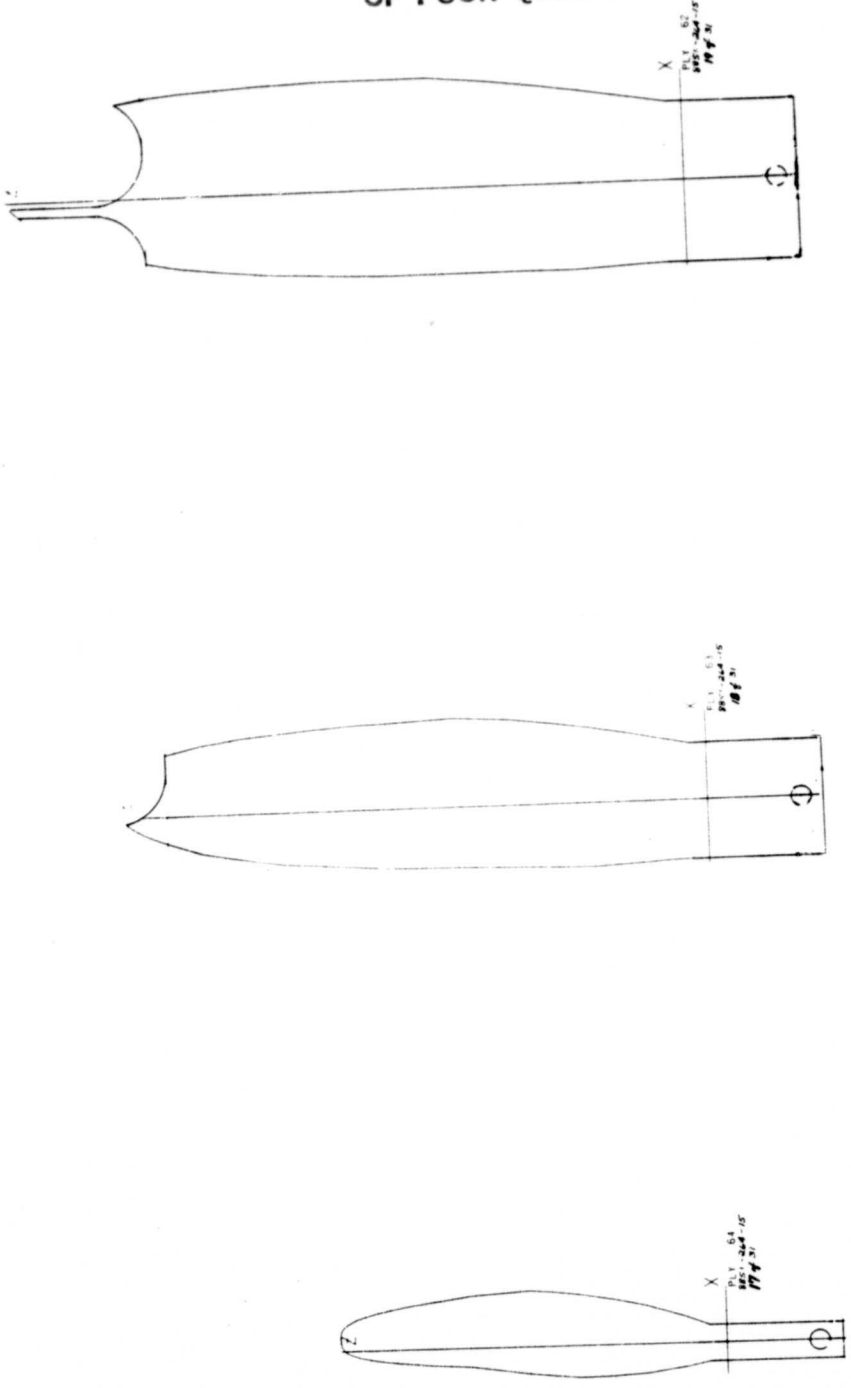

Figure 103. (cont'd) Ply Designs.

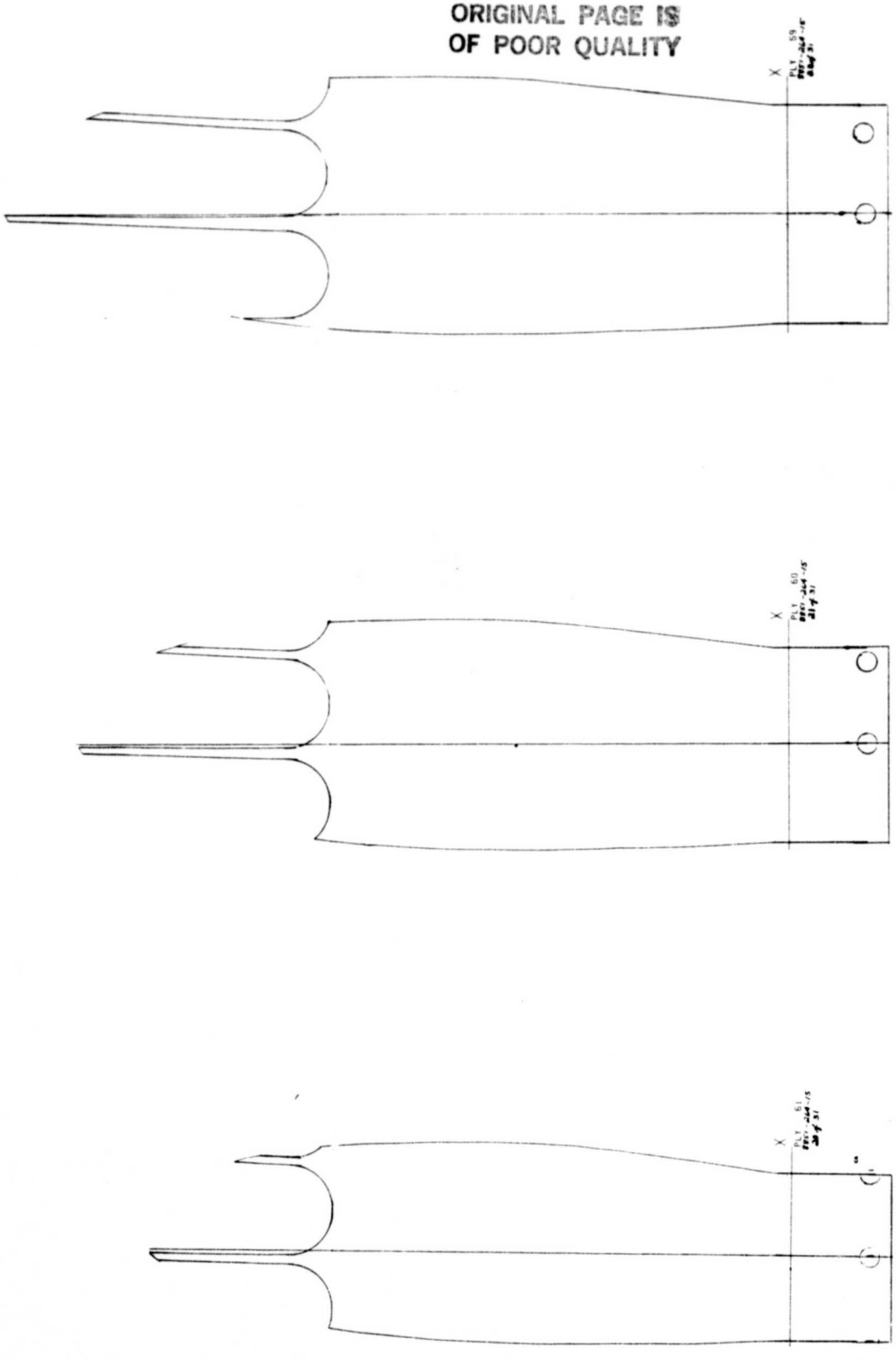

Figure 103. (cont'd) Ply Designs.

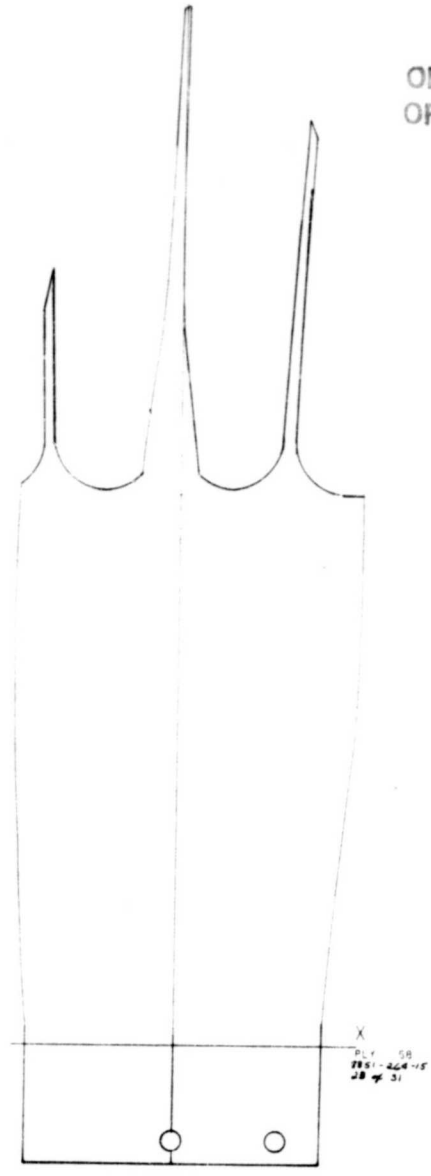

Figure 103. (cont'd) Ply Designs.

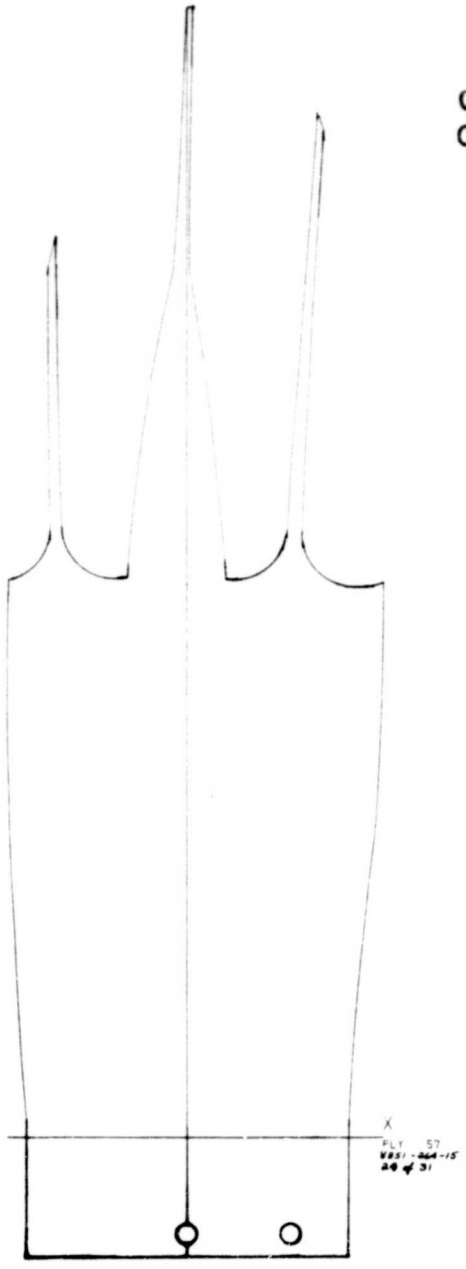

Figure 103. (cont'd) Ply Designs.

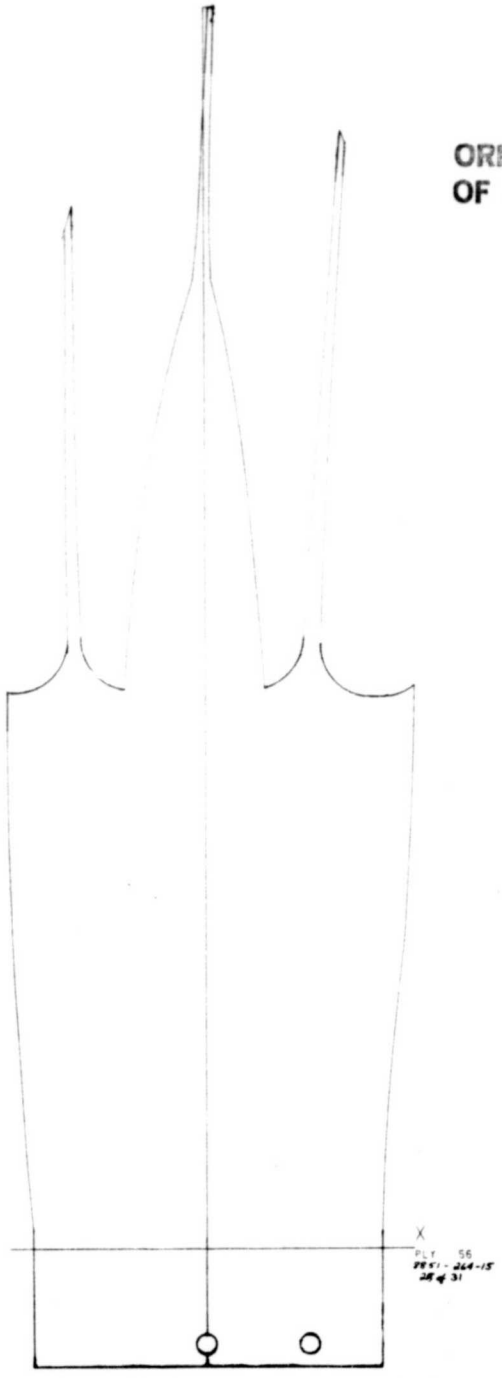

Figure 103. (cont'd) Ply Designs.

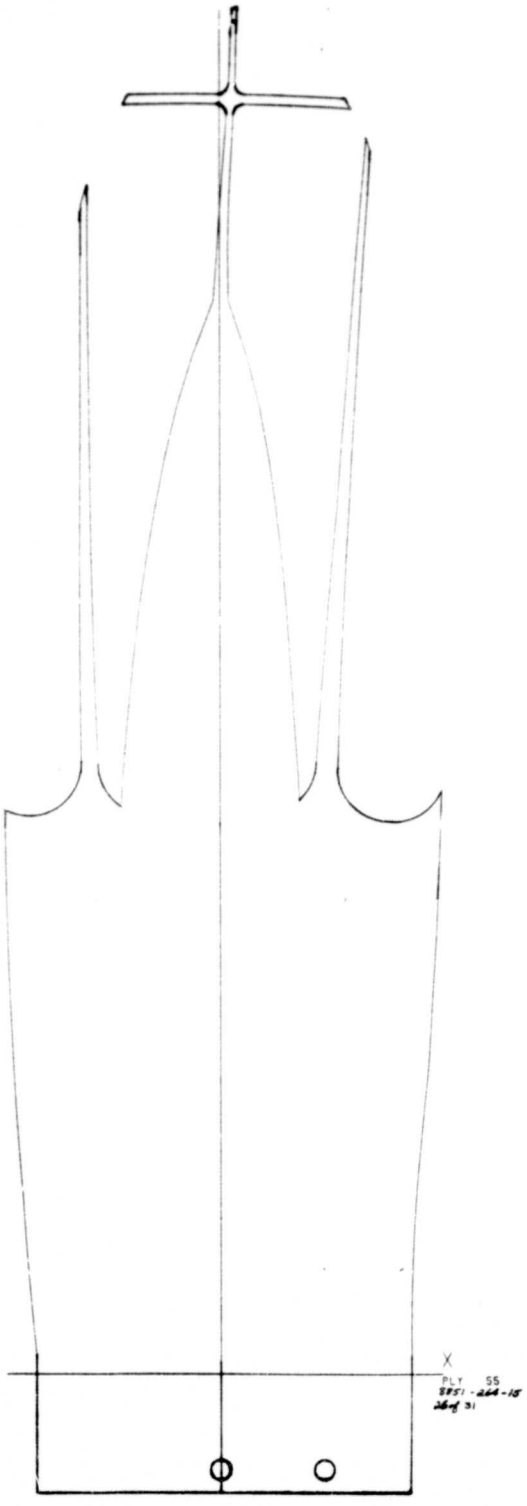

Figure 103. (cont'd) Ply Designs.

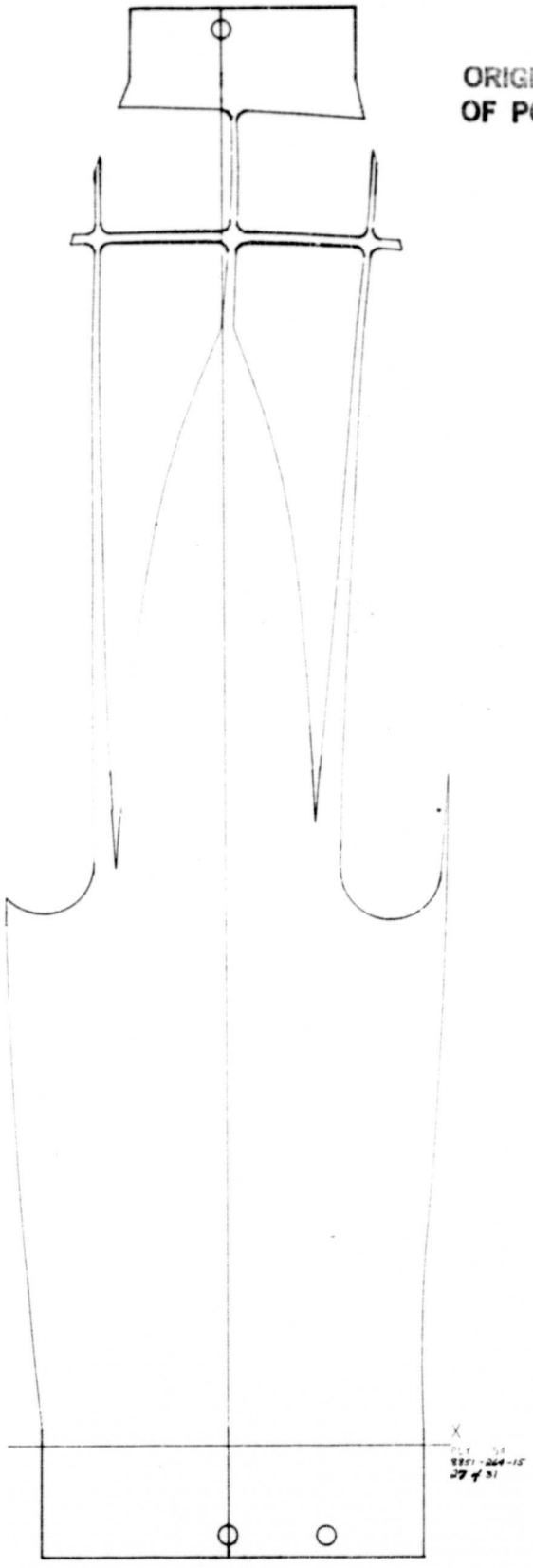

Figure 103. (cont'd) Ply Designs.

Figure 103. (cont'd) Ply Designs.

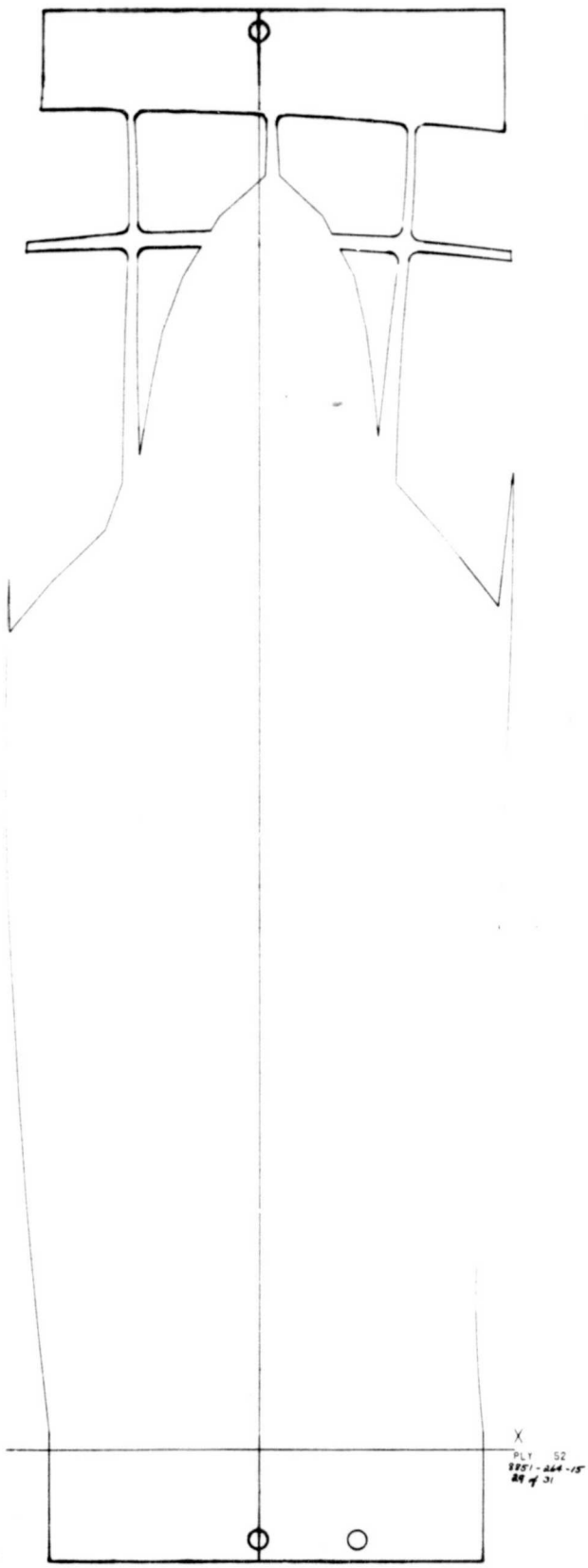

Figure 103. (cont'd) Ply Designs.

C-3

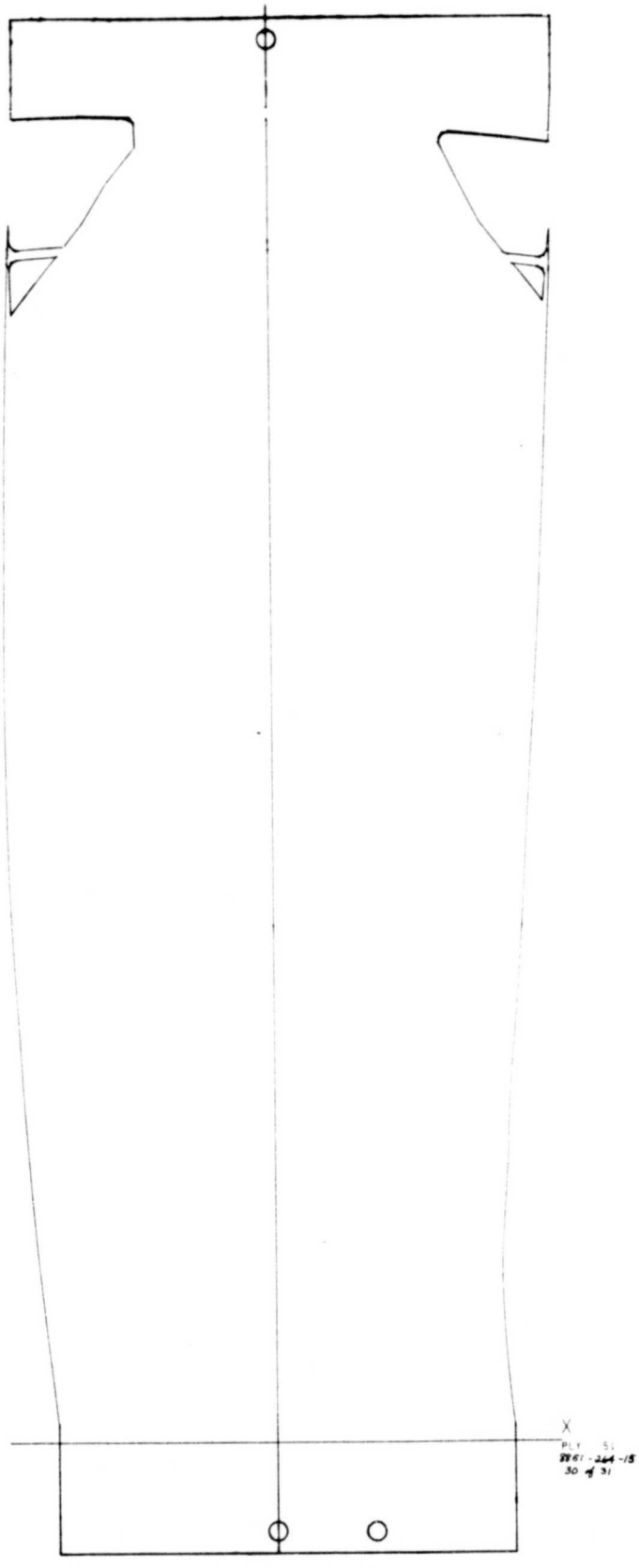

Figure 103. (cont'd) Ply Designs.

Figure 103. (cont'd) Ply Designs.

APPENDIX B - TEXTURE

The stall and aeroelastic flutter resistance of an airfoil is governed by the geometry of the airfoil and a factor derived from the airfoil material properties:

$$\sqrt{e/\rho}$$

e - Elastic Modulus
ρ - Density

Titanium alloys are used for the fan and low pressure compressor airfoils in modern gas turbine engines. For a given selected alloy, the density is fixed, however, the elastic modulus can be manipulated. Through proper processing, close-packed hexagonal crystals of alpha-titanium can be given a preferred orientation (texture). Since the (0001) crystallographic direction has a modulus of 21×10^6 in titanium, whereas the (1120) direction has a 14.0×10^6 psi modulus, alignment of the c-axes in a desired direction can result in a modulus which is substantially higher than the 16.0×10^6 psi which is found in isotropic Ti 6Al-4V. A program was therefore undertaken in order to evaluate the effect of texture rolling on the modulus Ti 6Al-4V sheet for possible use in fabricating hollow Ti 6Al-4V fan blades.

Texture rolled sheet was received from RMI in the mill annealed condition. The sheet thickness was .055-inch as received. Five sheet tensile test specimens were machined for testing parallel to the rolling direction, and five were machined for testing 90° to the rolling direction. The specimens were descaled in an HNO_3-HF solution to remove any surface contamination. Strain gages indicating longitudinal and transverse strain were attached to both faces of the tensile specimens. The use of two strain gages eliminated any inaccuracy due to bending. Tests were conducted at room temperature. Load was applied to achieve a predetermined level and the strains in the longitudinal and transverse directions measured. The specimen was then unloaded. After duplicate measurements at a given load were made, the procedure was repeated at the next load level. This procedure provides a secant modulus, rather than a true Young's modulus. However, the procedure for drawing an elastic stress-strain curve has inherent deficiencies in terms of line-fitting and in the limitation of one modulus measurement for each specimen. The use of the secant modulus provides one data point for each load level in each specimen and does not require any line fitting. For titanium, the secant modulus and Young's modulus should be equivalent. The load levels used produced stresses in the range of 10 to 70 ksi. No plastic behavior was expected and none was found. The results for the ten specimens which were tested are presented below. The results are the average of 12 data points for each specimen.

Specimens Orientation(1)	(x 10^6 psi) Young's Modulus	Poisson's Ratio
Transverse	17.59	.304
	21.20	.293
	20.70	.240
	17.70	.380
	18.51	.306
Average	19.14	.307
Longitudinal	15.11	.245
	15.20	.243
	15.55	.250
	15.95	.252
	14.40	.250
Average	15.24	.248

The scatter found in any one specimen was small, with the total range of value varying $\pm.5 \times 10^6$ in the most extreme cases. The reproducibility within any single specimen was therefore good, whereas large variations were found between specimens. For specimens tested transverse to the rolling direction, the average value of 19.14×10^6 psi was the average of a band ranging from 17.59 to 21.2×10^6 psi. Therefore the values are seen to range by $\pm 1.8 \times 10^6$ psi. There was considerably less scatter in the longitudinal direction, with the average value of 15.24×10^6 psi lying within a range of $\pm .78 \times 10^6$ psi. It is apparent, therefore, that although on average the modulus of specimens transverse to the rolling direction have a modulus approximately 3×10^6 psi greater than the isotropic value, scatter may act to effectively reduce this advantage. The scatter associated with nominally isotropic sheet was not determined in this work, but is presumed to be on the order of $\pm 1 \times 10^6$ psi.

The values of Poisson's ratio for the transverse, high modulus direction specimens varied between .240 and .380, with an average value of 0.307. The values were significantly greater than those for the longitudinal specimens which averaged .248, with values varying between .243 and .252.

RMI data has shown similar trends for the modulus of texture rolled sheet. Greater scatter is reported in the transverse direction than in the longitudinal direction and the value of modulus scatter in the transverse direction is 1.9×10^6. Boeing Vertol tests on RMI supplied sheet confirms RMI's findings. It is therefore concluded that our test technique is at least as accurate as that commonly used in industry.

(1) Orientation is with respect to rolling direction.

Effort must be undertaken to reduce the scatter by thermal processing, if this is at all possible. The modulus of 19.0×10^6 psi for transverse material should provide a usable flutter margin increase for Ti 6Al-4V blades and further work is therefore warranted. Both Timet and RMI have provided data indicating that processing procedures can be developed which can establish higher modulus properties (for example exceeding 17×10^6 psi in both directions in Ti 6Al-4V sheet) in commercially available material.